MEDICAL UNIVERSITY OF VIENNA

Engineering next-generation T cell therapy through genetic screens

Doctoral thesis at the Medical University of Vienna
for obtaining the academic degree
Doctor of Philosophy

Submitted by
Evgeniia Pankevich (Eugenia V Pankevich), MSc

Supervisor:
Univ.-Prof. Dr. Christoph Bock

CeMM Research Center for Molecular Medicine
Lazarettgasse 14, AKH BT 25.3, 1090 Vienna, Austria

Vienna, May 2025

Table of Contents

Declaration

This doctoral thesis is written in a cumulative format. Evgeniia Pankevich (published academically as Eugenia V Pankevich) is a co-first author of the included manuscript, “Systematic discovery of CRISPR-boosted CAR T cell immunotherapies”, submitted to *Nature* in a revised version upon editor’s invitation, based on favorable initial peer-reviews. The author wrote the remainder of this thesis and prepared the figures, with input from Paul Datlinger and Christoph Bock. A detailed author contributions statement is included in the manuscript in the section “Author Contributions”. Eugenia Pankevich is named as an inventor on a patent application related to the technology platform and findings that were developed during the course of the presented doctoral research. The thesis does not contain any artificial intelligence-generated text. DeepL was used to assist in translating the abstract into German prior to the refinement by Cosmas Arnold and proofreading by Eugenia Pankevich. Unless stated otherwise, the experiments and analyses by Eugenia Pankevich were performed in the laboratory of Christoph Bock at the CeMM Research Center for Molecular Medicine of the Austrian Academy of Sciences in Vienna, Austria.

Publications arising from this thesis

1. Systematic discovery of CRISPR-boosted CAR T cell immunotherapies. Datlinger P*#, Pankevich EV*, Arnold C*, Pranckevicius N, Lin J, Romanovskaia D, Schäfer M, Piras F, Orts AC, Nemc A, Biesaga P, Chan M, Neuwirth T, Artemov AV, Li W, Ladstätter S, Krausgruber T, Bock C*#. *Manuscript resubmitted to Nature in revised form*
* – shared first authors, # – corresponding authors

2. Datlinger P, Pankevich E, Bock C. Methods for single-cell CRISPR screening in vivo. World Intellectual Property Organization (WIPO), 2024. WO2024121426A1. *International patent application*

3. Pankevich EV, Bock C. Single-cell CRISPR screening in mouse brain. *Nature Protocols*, 2025. https://doi.org/10.1038/s41596-024-01128-2. *Invited News&Views article accompanying a paper co-reviewed by Eugenia Pankevich with Christoph Bock*

Abstract

T cell-based therapies have revolutionized immunotherapy and show great promise for a wide range of indications, including cancer and autoimmune disorders. As the first clinically approved T cell-based therapy, chimeric antigen receptor (CAR) T cells have demonstrated remarkable success in treating certain hematologic malignancies over the past decade. However, their broader impact remains constrained by modest remission rates, frequent relapses, and poor efficacy against multiple diseases, in particular solid tumors. These limitations are often driven by intrinsic T cell dysfunction. As CAR T cells are engineered cell products, additional genetic modifications represent a promising strategy to overcome these barriers and enhance therapeutic efficacy. Functional genetic screens enable high-throughput assessment of genetic perturbations and can thus accelerate the development of next-generation T cell-based therapies.

In this study, we present a discovery platform for CAR T cell optimization through high-content CRISPR screens. At its technological core, we developed a modular system enabling lentiviral co-delivery of a CAR and CRISPR library and a highly scalable mRNA-based delivery of CRISPR editors. We performed systematic genome-wide CRISPR screens in human primary CAR T cells, assessing T cell fitness, tumor cell recognition, activation, apoptosis, and exhaustion. Through these screens, we rediscovered established immunotherapy targets and uncovered novel regulators of CAR T cell function. To efficiently validate identified hits, we extended our platform to *in vivo* screens in a murine xenograft leukemia model, which accurately pinpointed genetic modifications that boosted CAR T cell anti-tumor responses. Among them, RHOG ablation emerged as a potent and unexpected enhancer of CAR T cell proliferative capacity. RHOG knockout, individually and in combination with FAS knockout, enhanced CAR T cell performance across multiple tumor models and CAR designs, indicating the broad applicability of these genetic perturbations. Demonstrating the versatility of our platform, we conducted combinatorial screens to identify gene knockout pairs that enhance CAR T cell performance and established tiling base editing screens to prioritize functional RHOG variants as targets for generating CRISPR-boosted CAR T cells.

In summary, we discovered, validated, and functionally characterized genetic modifications that confer enhanced efficacy to CAR T cells in diverse preclinical models. Our technology platform enables discovery of functional gene targets in primary human cells at an unprecedented scale and provides a foundation for advancing next-generation immunotherapies.

Zusammenfassung

T-Zell-basierte Therapien haben die Immuntherapie revolutioniert und sind ein vielversprechender Ansatz für ein breites Spektrum von Krankheiten, darunter Krebs und Autoimmunerkrankungen. Als erste klinisch zugelassene T-Zell-Therapie haben chimäre Antigenrezeptor (CAR)-T-Zellen in den letzten zehn Jahren bemerkenswerte Erfolge bei der Behandlung bestimmter hämatologischer Malignome gezeigt. Allerdings bremsen bescheidene Remissionsraten, häufige Rückfälle und eine geringe Wirksamkeit bei verschiedenen Krankheiten, insbesondere bei soliden Tumoren, eine breit-gefächerte Anwendung. Diese Einschränkungen sind häufig auf eine intrinsische Dysfunktion der T-Zellen zurückzuführen. Da es sich bei CAR-T-Zellen um gentechnisch veränderte Zellprodukte handelt, stellen zusätzliche genetische Modifikationen eine vielversprechende Strategie dar, um diese Hindernisse zu überwinden und die therapeutische Wirksamkeit zu verbessern. Funktionelle genetische Screens ermöglichen eine Hochdurchsatzbewertung genetischer Perturbationen und können so die Entwicklung von T-Zell-basierten Therapien der nächsten Generation beschleunigen.

In dieser Arbeit beschreiben wir eine neuartige Plattform, die auf Hochdurchsatz-CRISPR Screening basiert und so die Optimierung von CAR-T-Zellen ermöglicht. Als technologische Basis haben wir ein modulares System entwickelt, das mittels Lentiviren die simultane gentechnische Veränderung der Zellen mit verschiedenen CARs und gleichzeitig einer CRISPR-Bibliothek ermöglicht, gefolgt von einer hochskalierbaren mRNA-basierte Einbringung von CRISPR-Editoren in die Zellen. Dadurch schafft diese Arbeit die Voraussetzung die Auswirkungen dieser Genänderungen oder Stummschaltungen auf das Zellverhalten zu beobachten.

Wir haben systematische genomweite CRISPR-Screens in menschlichen primären CAR-T-Zellen durchgeführt und dabei die Fitness der T-Zellen, deren Erkennung von Tumorzellen, deren Aktivierung, Zelltod und sogenannte Erschöpfung untersucht. Durch diese CRISPR Screens haben wir bereits bekannte Zielgene der Immuntherapie wiederentdeckt und neue Regulatoren der CAR-T-Zellfunktion entdeckt. Um die identifizierten Zielgene effizient zu validieren, haben wir unsere Plattform auf In-vivo-Screens in einem Maus-Xenograft-Leukämiemodell ausgeweitet, mit denen wir genetische Veränderungen, die die Antitumorreaktion von CAR-T-Zellen verstärken, genau bestimmen konnten. Unter ihnen erwies sich die RHOG-Ablation als wirksamer und unerwarteter Verstärker der proliferativen Kapazität von CAR-T-Zellen. Die RHOG-Ablation, einzeln und in Kombination mit der FAS-Ablation, steigerte die Leistung von CAR-T-Zellen in verschiedenen Tumormodellen und CAR-Designs, was auf die breite Anwendbarkeit dieser genetischen Stummstellung hinweist. Um die Vielseitigkeit unserer Plattform zu demonstrieren, haben wir kombinatorische CRISPR Screenings durchgeführt, um Gen-Ablations-Paare zu identifizieren, die die Leistung von CAR-T-Zellen

verbessern, und Sättigungs-Basen-Editierung-Screens etabliert, um funktionale RHOG-Varianten für CRISPR-optimierte CAR-T-Zellen zu priorisieren.

Zusammenfassend lässt sich sagen, dass wir genetische Veränderungen entdeckt, validiert und funktionell charakterisiert haben, die CAR-T-Zellen in verschiedenen präklinischen Modellen eine erhöhte Wirksamkeit verleihen. Unsere Technologieplattform ermöglicht die Entdeckung funktioneller Geninterventionen in primären menschlichen Zellen in einem noch nie dagewesenen Umfang und bildet die Grundlage für die Entwicklung von Immuntherapien der nächsten Generation.

Acknowledgements

I would like to start by acknowledging the entire T Cell Screening Team in the group of Christoph Bock at CeMM. Christoph, thank you for the opportunity to lead such an ambitious project, for providing exceptional freedom and support, for your inspiring research vision and for the environment to realize it. Paul, I am especially thankful for your visionary idea to use genetic screens to enhance T cell immunotherapies, which kept me inspired and fully committed every day. Thank you for your drive to innovate and push the limits, for the excellent mentorship, and for our friendship – it has been an intense but adventurous journey, and I would do it again. Thanks, Cosmas, for your determination and support needed to bring this project to completion. Finally, I thank all the co-authors for their numerous contributions – the success of this project was ultimately the result of our teamwork.

Thanks to everyone who supported me throughout my scientific journey and made my PhD a great experience. I am grateful to the Faculty of Bioengineering and Bioinformatics at Lomonosov Moscow State University for the outstanding preparation for challenging scientific projects. I thank Giulio Superti-Furga for creating the unique CeMM environment, where serious science can feel like art, and for his inspiring words and personal belief in me. Many thanks to all my colleagues and friends, especially Paul, Zsofia, Hana, and everyone who contributed to our unforgettable terrace music sessions. Thanks to Sanya and Alibek for sharing our path through university and PhD studies and all the fun adventures.

My deepest gratitude goes to my family. First and foremost, I thank my life partner and best friend, Artem, for always supporting me and our wonderful family, for being an inspiring example of a scientist driven by curiosity and innovative research ideas, and for his invaluable scientific advice and encouragement throughout all my projects. I am also grateful to my parents and grandparents for their continuous support – especially my mother, Natalia, who encouraged me to pursue science and has been an excellent example of a strong, independent woman and researcher, passing this inspiration on to the next generations.

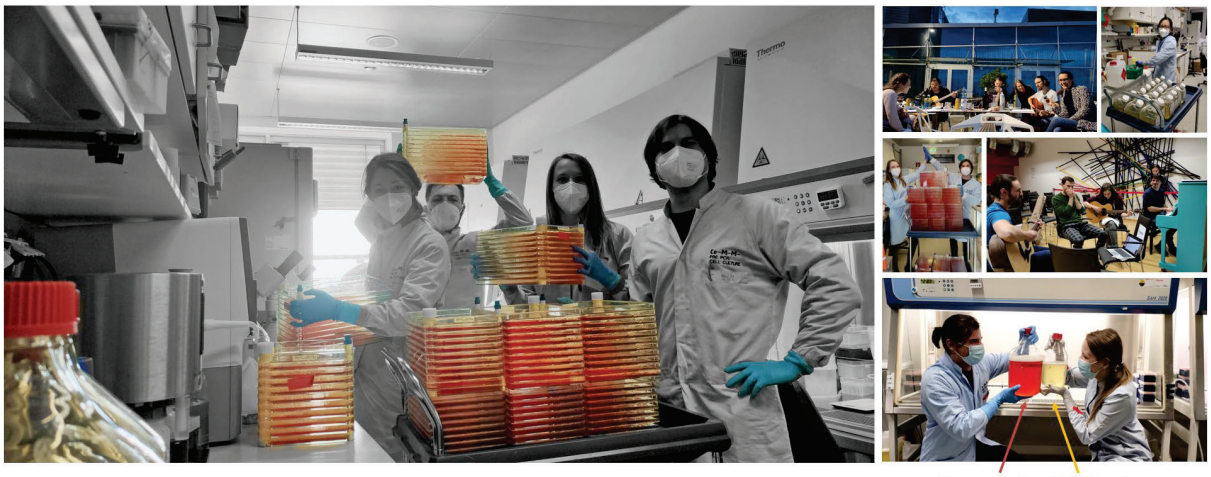

List of abbreviations

ABE	Adenine-guanine base editors	IL2	Interleukin 2
ALL	Acute lymphoblastic leukemia	ITAM	Immunoreceptor tyrosine activation motifs
APC	Antigen-presenting cell	LBCL	Large B-cell lymphoma
CAR	Chimeric antigen receptor	LoF	Loss-of-function
CBE	Cytosine-thymine base editors	MM	Multiple myeloma
CD3ζ	CD3 zeta	mRNA	Messenger RNA
CDX	Cell line-derived xenografts	nCas9	Nickase Cas9
CFSE	Carboxyfluorescein succinimidyl ester	NGS	Next-generation sequencing
CLL	Chronic lymphocytic leukemia	NHEJ	Non-homologous end joining
CRISPR	Clustered regularly interspaced short palindromic repeats	NK cell	Natural killer cells
CROP-seq	CRISPR droplet sequencing	NSG mouse	NOD/SCID/γ-chain knockout mouse
CRS	Cytokine release syndrome	PAM	Protospacer adjacent motif
dCas9	Dead Cas9	PDX	Patient-derived xenografts
DNA	Deoxyribonucleic acid	r/r	Relapse or refractory
DSB	Double-strand break	RHOG	Ras Homolog Family Member G
FACS	Fluorescence-activated cell sorting	RNA	Ribonucleic acid
FAS	Fas Cell Surface Death Receptor	RNAi	RNA interference
FDA	Food and Drug Administration	RNP	Ribonucleoproteins
FL	Follicular lymphoma	SAM	Synergistic activation mediator
GDP	Guanosine diphosphate	scFv	Single-chain variable fragment
GMP	Good manufacturing practice	shRNAs	Short hairpin RNAs
GoF	Gain-of-function	siRNAs	Small interfering RNA
gRNA	Guide RNA	TALEN	Transcription activator-like effector nucleases
GTP	Guanosine triphosphate	TCR	T cell receptor
HDR	Homologous directed repair	TIL	Tumor-infiltrating lymphocytes
HLA	Human leukocyte antigen		

List of figures and tables

List of figures:

Figures in this thesis have been prepared by Eugenia V Pankevich, the author of this thesis, utilizing certain graphical elements created by Paul Datlinger.

List of tables:

1 Introduction

1.1 Chimeric antigen receptor (CAR) T cell therapy

1.1.1 T cell therapies in the landscape of immunotherapy

Cancer is one of the leading causes of mortality worldwide, necessitating continuous innovation in therapeutic strategies to improve patient outcomes. Cancer immunotherapy has rapidly evolved in the last decades and now includes multiple modalities that are designed to harness the immune system's capacity to treat malignancies (Waldman, Fritz, and Lenardo 2020). Among these, therapies such as well-established immune checkpoint inhibitors, cytokine therapies, cancer vaccines, and oncolytic viruses have emerged, each modulating the immune response to through distinct mechanisms (Figure 1). Additionally, direct T cell-mediated anti-cancer therapies, such as tumor-infiltrating lymphocyte (TIL) therapies, bispecific antibodies as T cell engagers, and chimeric antigen receptor (CAR) T cell therapies, represent a cutting-edge approach that employs T cells to eliminate the tumor.

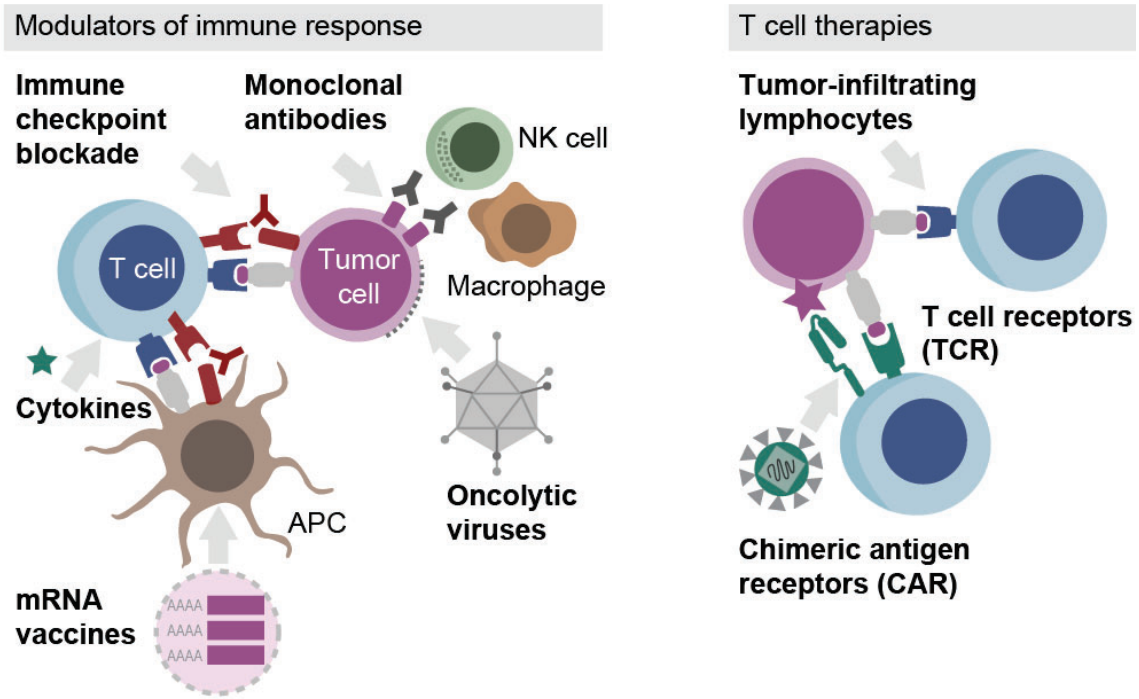

of immune cells, particularly T cells and natural killer (NK) cells, enhancing the immune system's capacity to target and destroy cancer cells. *Cancer vaccines*, such as mRNA or dendritic vaccines, encode antigens that are produced by host cells, leading to an immune response against these antigens. *Oncolytic viruses* directly infect and lyse cancer cells and act by releasing tumor antigens in a context that promotes immune activation. **(Right) Therapies directly utilizing natural or modified T cells to mediate anti-cancer effects**. *Tumor-infiltrating lymphocyte (TILs)* therapy leverages the natural tumor-reactive T cells for their anti-cancer properties by introducing large number of *ex vivo* expanded TILs into patients. *Chimeric antigen receptor (CAR) and T cell receptor (TCR) T cells* are genetically engineered *ex vivo* to specifically recognize cancer antigens leading to tumor cell killing.

The ability of T cells to recognize and specifically kill cancer cells led to the concept of adoptive cell therapy, or cellular immunotherapy, where T cells are isolated from a human for expansion or engineering purposes and are then reinfused into a patient to leverage T cell cytotoxicity to eradicate tumors (Steven A. Rosenberg and Restifo 2015).

The immune cell transfer from a donor to patient as a form of therapy initially emerged from great successes of bone marrow transplantation (Copelan 2006). A pioneering study in the 1950s showed the remission of an end-stage leukemia patient, who was infused with the twin's bone marrow after a total-body irradiation (Thomas et al. 1957). Since then, this approach became a critical milestone in hematologic cancers such as leukemia, lymphoma, and multiple myeloma, and other indications. It has demonstrated significant success in treating these diseases, paving the way for allogeneic transplantation and becoming a foundation for the development of advanced immune cell transfer therapies.

While bone marrow transplantation is used to replace and regenerate patient's immune system, adoptive cell transfer directly employes immune cells that are taken either from a donor (for allogeneic transfer) or from a patient (for autologous transfer), which perform specific functions such as cancer cell recognition and killing (Steven A. Rosenberg and Restifo 2015). The first successful clinical application of adoptive cell therapy against cancer was demonstrated in the 1980s. It followed the discovery showing that tumor-infiltrating lymphocytes (TILs) obtained from melanoma samples could specifically recognize the tumor cells from the same patient *in vitro* (S. A. Rosenberg, Spiess, and Lafreniere 1986). These TILs were further successfully expanded *in vitro* by supplementing medium with IL2. Upon reinfusion back into the patient, pre-expanded TILs led to tumor regression in patients with metastatic melanoma (S. A. Rosenberg et al. 1988). Several decades of follow-up studies, clinical trials, and therapy development led to the approval of lifileucel, the first cancer treatment by TILs against metastatic melanoma, by Food and Drug Administration (FDA) in 2024 (FDA 2024), making this product the first approved adoptive cell therapy for solid tumors.

Despite the groundbreaking successes of TILs, their lack of specificity and the challenges associated with obtaining TILs from most cancer types have restricted their therapeutic potential. To address these challenges, the concept of chimeric antigen receptors (CARs)

emerged in the late 1980s (June and Sadelain 2018). In a CAR, the extracellular domain of a TCR is replaced with an antibody fragment, which can specifically recognize a protein antigen on the surface of a tumor cell. While T cell recognition via TCRs is restricted to HLA-displayed antigenic peptide fragments, CARs can bind to any given tumor antigen independently of the patient's HLA background, greatly facilitating their use in the clinic. Moreover, the intracellular domain of modern CAR T cells is designed to provide appropriate T cell activation for its cytotoxic effect (Sadelain, Brentjens, and Rivière 2013). Thus, human T cells genetically engineered to express the CAR can be directed against cancer cells once reinfused into the body (Figure 2).

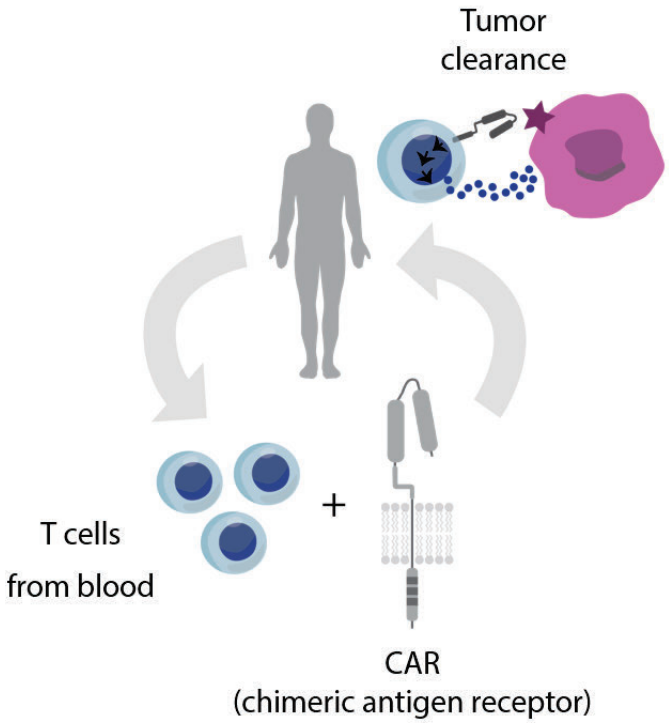

Figure 2. The concept of CAR T cell therapy. T cells from a patient are genetically engineered to express CAR enabling specific cancer cell recognition and killing upon infusion into the body.

The dramatic efficacy of CAR T cell therapy in certain hematopoietic cancers has established CAR T cells as the most widely used class of adoptive cell therapy. Given the focus of this study on CAR T cells, subsequent sections will review the generation and clinical application of CAR T cells, as well as their current limitations and strategies to overcome them.

1.1.2 CAR architecture

CARs are artificial, genetically engineered receptors that combine the antigen-binding properties of monoclonal antibodies with the signaling properties of the TCR/CD3 complex and costimulatory receptors. CARs are a primary example of how basic biology insights into T cell antigen recognition led to the design of T cell products with anti-tumor activity

(Srivastava and Riddell 2015). Following this rationale, CARs typically consist of an extracellular domain that is a single-chain variable antibody fragment (scFv), fused to a spacer/hinge and transmembrane domain as well as intracellular signaling modules derived from the TCR-associated CD3 zeta (CD3ζ) signaling chain and co-stimulatory receptors (Figure 3).

The internal domain of the first-generation CARs contained only the cytoplasmic CD3ζ signaling domain. CD3ζ contains immunoreceptor tyrosine-based activation motifs (ITAMs), which drive downstream signaling known as the signal 1 of physiological T cell activation (Lindner et al. 2020) (Figure 4). The tyrosine kinase Lck is responsible for the initial activation of the TCR signaling cascade by phosphorylating ITAMs (Rudd et al. 1988; Barber et al. 1989), providing a docking site to recruit and activate the tyrosine kinase ZAP70, which is critical for the downstream T cell activation pathway (W. Zhang et al. 1998). This pathway is mediated by numerous kinases, such as p38 MAP kinase (Salvador et al. 2005), ERK (A. M. Fischer et al. 2005) or PLCγ (Smith-Garvin, Koretzky, and Jordan 2009), and multiple transcription factors, including NF-kB (Hayden and Ghosh 2008), NFAT (Crabtree and Olson 2002), and AP-1 (Karin 1995). Initial studies showed that T cells engineered with the first-generation CARs could be activated *in vitro* in the presence of target cells (Kuwana et al. 1987; Gross, Waks, and Eshhar 1989), providing the first proof of concept that the CAR triggers a cellular immune response. However, the first-generation CARs without additional costimulatory domains were not efficient enough for eradicating cancer *in vivo*.

Second-generation CARs were extended by linking costimulatory signaling endodomains of CD28 (Maher et al. 2002), 41BB (Imai et al. 2004), or OX40 (Hombach et al. 2012) to CD3ζ. This led to additional costimulation, known as signal 2 for T cell stimulation, which is required for full physiological T cell activation and cytotoxicity and which is normally provided by antigen presenting cells upon TCR recognition. In a T cell, costimulation is provided through elaborated mechanisms, which include multiple protein players and pathways, including PI3K signaling initiated by CD28 (Ward and Cantrell 2001) and TRAF1/2 and MAPK signaling in case of 41BB-mediated costimulation (Chester, Ambulkar, and Kohrt 2016), which ultimately lead to the induction of T cell activation, proliferation and cytotoxicity (Figure 4). These costimulatory domains introduced in the second-generation CARs activate their corresponding pathways, resulting in successful anti-tumor activity of CAR T cells, first shown in preclinical models and later in clinical trials and subsequent application in medical practice (Lindner et al. 2020), as reviewed in the following sections.

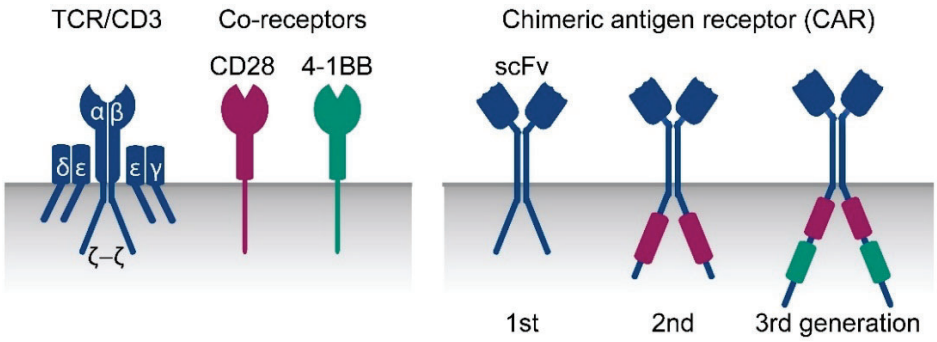

Figure 3. Schematic of 1st, 2nd, and 3rd-generation CARs. In contrast to TCR (left), CARs of different generations (right) are designed to express an antigen-binding scFv domain on the cell surface fused to one or more co-stimulatory domains along with the CD3ζ chain in a single receptor.

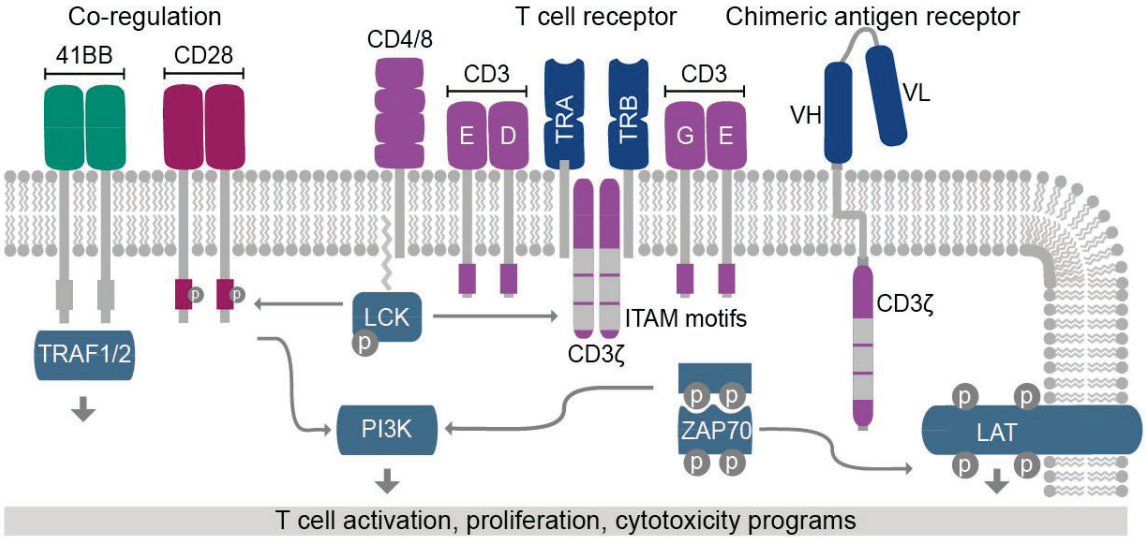

Figure 4. Schematic of the TCR and CAR signaling pathways. *TCR signaling*: Phosphorylation of ITAMS within CD3ζ domain by Lck provides a scaffold for ZAP70, which then phosphorylates LAT, which in turn induces downstream T cell activation signaling. Lck also facilitates CD4/CD8 coreceptor recruitment, strengthening the TCR interaction with the MHC-peptide complex and creating a positive feedback loop to recruit more Lck (Rudd et al. 1988; Barber et al. 1989). Costimulatory proteins provide an additional signal for T cell activation, for example CD28 costimulation via PI3K signaling and 41BB via TRAF signaling. *CAR signaling*: Phosphorylated CD3ζ recruits ZAP70. Additional domains, depending on the CAR design, recruit other proteins corresponding to their original function.

In search of additional ways to enhance CAR T cells, further next generations of CARs have been engineered. Third-generation CARs contain expanded intracellular domains, consisting of combinations of CD28, 41BB, or OX40 (Figure 4) (Tokarew et al. 2019). Later generations of CARs have been developed to contain other protein domains, which activate specific signaling pathways known as signal 3 of T cell activation (Lindner et al. 2020), such as JAK/STAT3 via an IL2 receptor β-chain domain (Kagoya et al. 2018).

All seven CAR T cell therapies approved by FDA by 2025 are based on the second-generation CARs containing either 41BB or CD28 costimulatory domains, in five and two products, respectively (Mitra et al. 2023) (Table 1). These CAR T cells target CD19 for the treatment of certain types of B cell lymphoma and leukemia and BCMA for multiple myeloma indications. The first two approved and most well-studied CARs contain an scFv antibody binding CD19 and additional costimulatory CD28 or 41BB domains, corresponding to tisagenlecleucel (Kymriah, Novartis) and axicabtagene ciloleucel (Yescarta, Kite). These two products both demonstrate high efficacy in clinical trials, and neither has been consistently proven superior to the other (Cappell and Kochenderfer 2021).

The design of intracellular signaling domains determines various functional features of CAR T cells. For example, CAR T cells with 41BB or CD28 costimulatory domains possess differences in various phenotypes and functional properties. The biological mechanism of action and signaling pathways corresponding to these domains are responsible for the success of CAR T cell stimulation itself, as well as for persistence, T cell memory formation, metabolic requirements, and antigen density threshold and potency (Lindner et al. 2020; Cappell and Kochenderfer 2021; Labanieh and Mackall 2023; 2023).

Other parts of the CAR can also play a key role in determining the effectiveness and behavior of CAR T cells. Differences in scFv structures and modifications in the hinge region or in transmembrane domains can all contribute to the modulation of CAR T cell antigen sensitivity, persistence and potency (Labanieh and Mackall 2023). This complicates the side-by-side comparisons of different CARs, because the designs of established CARs usually differ in the sequences of each domain (Cappell and Kochenderfer 2021). A recent study compared 36 representative CAR designs in a pooled fashion using single-cell RNA-seq, which revealed different phenotypes driven by CARs in a direct comparison both *in vitro* and *in vivo* (Perez et al. 2024). However, further studies are required to investigate how the CAR structure affects its function, and it remains challenging to assess and predict which CAR architectures lead to the best performance. Additionally, research on new CAR designs is actively ongoing.

In this work, we focused primarily on the anti-CD19 CAR containing the trans-membrane domain of CD8, the intracellular co-stimulatory domain of 41BB, and the CD3ζ chain, which closely resembles tisagenlecleucel. However, our technology platform for engineering CRISPR-boosted CAR T cells was designed for flexible switching between different CARs and other synthetic receptors that can be used for T cell therapies in the future, which also enabled testing different CARs in this study.

1.1.3 CAR T cell treatment workflow

CAR T cell therapy is currently used for patients with relapsed and refractory cancers. Following the clinical decision to treat a cancer patient with CAR T cells, the typical procedure

is as follows (Figure 5) (X. Wang and Rivière 2016; June and Sadelain 2018; Blache et al. 2022). Leukocytes are collected by leukapheresis from the patient's peripheral blood and shipped to a cell engineering facility. There, a T cell population is isolated and transduced with a CAR-expressing viral vector. Typically, T cells are stimulated with anti-CD3/CD8 reagents to prime for lentivirus transduction, and the culture medium is supplemented with IL2 to enable T cell growth. Genetically modified T cells are expanded, quality-controlled, and shipped back to the hospital. CAR T cell production takes several weeks, during which the patient is treated with bridging therapy. In addition, the patient receives chemotherapy for lymphodepletion several days prior to CAR T cell infusion, which improves CAR T cell engraftment and therapeutic response (Amini et al. 2022). Following CAR T cell infusion, each patient is closely monitored for the signs of cytokine release syndrome, neurotoxicity, and other side effects of CAR T cell therapy, which may require pharmacological treatment (e.g., using IL6 receptor antagonists) and intensive care.

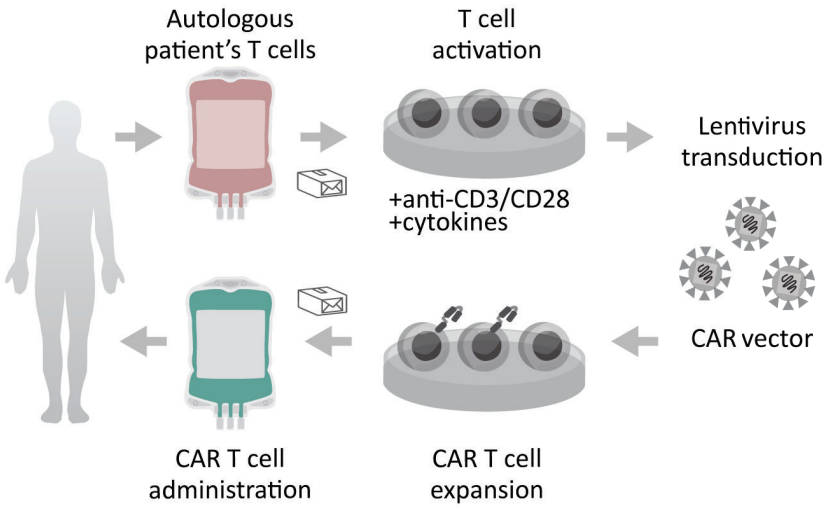

Figure 5. CAR T cell manufacturing. For currently approved CAR T cell immunotherapies, patient's own T cells are extracted, genetically modified *ex vivo*, and then reinfused into the same patient. This process is performed under Good Manufacturing Practice (GMP) guidelines and includes cryopreservation and shipment of patient's leukapheresis material to the manufacturing facility and of the final product back to the hospital.

Lentivirus transduction is a standard method for the stable expression and permanent integration of genetic constructs into the genome. In the context of T cell-based immunotherapies, lentiviral vectors are used to deliver synthetic immune receptors that enable the recognition of specific antigens, for example a CAR (June and Sadelain 2018) or TCR (Tsimberidou et al. 2021). However, multiple challenges are associated with lentiviral delivery (Milone and O'Doherty 2018). First, lentivirus vectors integrate genetic constructs randomly into the genome, posing a safety concern due to insertional mutagenesis. Second, the production of

GMP (Good Manufacturing Practice) grade lentivirus is expensive due to the complexity of manufacturing process following stringent regulatory requirements, which contributes to the high cost of CAR T cell therapy. Therefore, alternative delivery methods have been developed. For example, the Sleeping Beauty transposon system offers a non-viral precise integration method is currently used to produce CAR T cells for clinical trials (Prommersberger et al. 2021). In addition, CRISPR/Cas9 system can be used to precisely insert CAR constructs into specific genomic loci (Eyquem et al. 2017). Another emerging approach focuses on *in vivo* generation of CAR T cells using targeted viral vectors or lipid nanoparticles containing nucleic acids carrying the genetic material (Short et al. 2024). These techniques can substantially improve the logistics of CAR T cell manufacturing but require further development to ensure efficiency and safety. In addition to the methods for synthetic receptor integration, ongoing research focuses on optimizing culture conditions to enhance the efficacy of produced CAR T cells, including the use of different supplements and the reduction of manufacturing time from weeks to days.

Currently approved CAR T cell therapies involve the production of autologous CAR T cells using patient's own T cells as starting material. The use of autologous cells results in several challenges. First, the production for individual patients is associated with complex logistics, as T cells need to be collected, transferred to a manufacturing facility, modified and expanded, and sent back to the hospital. Second, previous treatment and chemotherapy can lead to reduced initial T cell fitness resulting in suboptimal final product or even a production failure (June et al. 2018). Therefore, substantial efforts are aimed at developing off-the-shelf CAR T cells, which are produced from donor T cells, typically using gene editing techniques to disrupt the expression of TCR and B2M genes to prevent graft-versus-host disease and avoid host immune rejection (Depil et al. 2020). Allogeneic T cells have multiple advantages over autologous products, including immediate availability, higher standardization, flexibility in treatment doses, and decreased cost, but their clinical efficacy has so far been inferior.

In summary, major efforts are focused on addressing current challenges in CAR T cell production to improve product quality, efficacy, safety, and availability. In the context of this thesis, optimizing CAR T cells using genetic modifications requires taking manufacturing protocols into account for several reasons. First, the identified genetic modifications need to be introduced into cells, which will ultimately require adjustments in production methods. Second, different manufacturing protocols may result in producing CAR T cells with distinct properties, which would require testing the applicability of further modifications. Therefore, an important goal is to identify genetic modifications that are universally applicable, regardless of the specific production method.

1.1.4 Clinical indications for CAR T cell therapy

Building on foundational work from the 1990s and early 2000s, CAR T cell therapy recently demonstrated remarkable clinical efficacy for certain hematopoietic cancers, culminating in the first regulatory approvals for specific types of relapsed and refractory B cell leukemia and lymphoma in 2017 (June and Sadelain 2018).

CAR T cell therapy has achieved broadly reproducible clinical success, leading to the FDA approval of seven CAR T cell therapies from 2017 until 2025 (Table 1). All of them are approved for the treatment of blood cancers, including certain types of lymphomas and leukemia, and, most recently, multiple myeloma (Cappell and Kochenderfer 2023). CAR T cell therapies targeting the B cell-specific CD19 antigen yielded complete response rates of over 40% in patients with relapse or refractory (r/r) aggressive B cell lymphomas and over 70% in r/r B cell acute lymphoblastic leukemia (ALL) (Neelapu et al. 2017; Maude et al. 2018; Schuster et al. 2019; Abramson et al. 2020; B. D. Shah et al. 2021). CAR T cells targeting B-cell maturation antigen (BCMA), which is uniquely expressed on plasma cells, including malignant plasma cells, have also shown remarkable successes in patients with r/r multiple myeloma, with complete response rates of 30-80% (Munshi et al. 2021a; Martin et al. 2023a). Long-term data have revealed that CAR T cells can maintain over a decade-long remission in patients, who were previously left with no more available treatment options (Cappell and Kochenderfer 2023). Currently, CAR T cell therapy is offered to patients with relapsed or refractory diseases, although there is the prospect of moving CAR T cells toward first-line therapy (June and Sadelain 2018). Moreover, the spectrum of indications may be further expanded by using CAR T cells in combination with immune checkpoint inhibitors (Grosser et al. 2019) and other innovative treatments such as CAR-amplifying mRNA-vaccines encoding the CAR's target antigen (Mackensen et al. 2023).

Company	Brand name	Generic name	Target antigen	Co-stimulation	Clinical indication	Patient population with relapsed/ refractory disease	Study	First approval
Novartis	Kymriah	tisagenlecleucel	CD19	41BB	B-ALL, LBCL	Children/young adults (B-ALL); Adults (LBCL)	1,2	2017-08
Gilead Kite	Yescarta	axicabtagene ciloleucel	CD19	CD28	LBCL, FL	Adults	3	2017-10
	Tecartus	brexucabtagene autoleucel	CD19	CD28	MCL, B-ALL	Adults	4	2020-07
Bristol Mayers Squibb	Breyanzi	lisocabtagene maraleucel	CD19	CD28	LBCL	Adults	5	2021-02
Bluebird Bio	Abecma	idecabtagene vicleucel	BCMA	41BB	MM	Adults	6	2021-03
Legend Biotech	Carvykti	ciltacabtagene autoleucel	BCMA	41BB	MM	Adults	7	2022-02
Autolus	Aucatzyl	obecabtagene autoleucel	CD19	41BB	B-ALL	Adults	8	2024-11

Table 1. FDA-approved CAR T cell products. Products are listed in chronological order, until April 2025. Abbreviations: B-ALL, B-cell acute lymphoblastic leukemia; LBCL, large B-cell lymphoma; MCL, Mantle cell lymphoma; FL, follicular lymphoma; MM, multiple myeloma. References used in the column "Study": (1) (Maude et al. 2018), (2) (Schuster et al. 2019), (3)

(Neelapu et al. 2017), (4) (B. D. Shah et al. 2021), (5) (Abramson et al. 2020), (6) (Munshi et al. 2021b), (7) (Martin et al. 2023b), (8) (Roddie et al. 2024).

Following the successes in hematology, the field is working to achieve clinical impact in a broader range of cancers. In addition to approved therapies, there are currently over 1000 clinical trials running for a wide range of indications (MacKay et al. 2020; V. Wang et al. 2023a). Among them, more than 250 clinical trials investigate the use of CAR T cells against solid tumors (Drougkas et al. 2023). For that, multiple CARs have been developed to target over 30 different tumor-associated antigens. However, few patients achieved complete responses in non-hematologic malignancies and the duration of response has been in the range of months (Yong et al. 2017), highlighting existing limitations of CAR T cell therapy, which will be reviewed below. Despite some discouraging clinical experience, there are also positive results, including patients achieving complete response, for instance after CAR T cell treatment of refractory glioblastoma (Brown et al. 2016). Additionally, recent studies show encouraging responses for CAR T cells in a subset of patients with neuroblastoma (Del Bufalo et al. 2023), gastrointestinal cancer (Qi et al. 2022), and other types of cancer. Moreover, FDA has recently granted accelerated approvals for two T cell-based therapies: a tumor-infiltrating lymphocyte therapy lifileucel (Amtagvi, IOVANCE Biotherapeutics) against melanoma in February 2024, and a TCR T cell therapy afamitresgene autoleucel (Tecelra, Adaptimmune) against synovial cancer in August 2024. These approvals followed clinical trials with more than 30% overall response rates and some patients achieving complete responses lasting over 6 months, providing the first proof-of-concept that T cell therapies have the potential to be curative for solid cancers.

Beyond cancer treatment, promising initial results illustrate the future potential of CAR T cell therapy for non-cancer indications (Guedan, Ruella, and June 2019). Anti-CD19 CAR T cells that were initially used against blood cancers have recently demonstrated a remarkable breakthrough in the treatment of autoimmune diseases, including systemic lupus erythematosus, idiopathic inflammatory myositis, and systemic sclerosis (Mougiakakos et al. 2021; Mackensen et al. 2022; Müller et al. 2024). In patients with these indications, the median duration of B cell aplasia following the CAR T cell treatment was over a year. In multiple cases, B cells came back but were not autoreactive anymore, which was not the case after the treatment with anti-CD19 antibodies, indicating that the cell-based therapies have an advantage in eradicating their cellular targets. In addition, clinical trials are running to assess CAR T cell therapy against HIV infection, although so far the efficacy in patients has not been demonstrated (Carvalho 2023). Promising preclinical results have also been obtained for CAR T cells against cardiac fibrosis when targeting the fibroblast activation protein (FAP) (Aghajanian et al. 2019; Rurik et al. 2022). Moreover, CAR T cells targeting urokinase plasminogen receptor (uPAR), which is specifically expressed on senescent cells in the liver, fat tissue and pancreas

of aging mice, have been demonstrated to safely eliminate these senescent cells *in vivo* and to improve physiological aging (Amor et al. 2024).

In summary, CAR T cell therapy not only establishes new treatment options for deadly cancers but also leads a trend toward programmed cell-based therapies for diverse clinical indications in cancer and beyond (Karsten et al. 2023).

1.1.5 Challenges and limitations of CAR T cell therapy

Despite the remarkable clinical efficacy of CAR T cell therapy against previously incurable blood cancers, numerous challenges and limitations need to be addressed to expand its treatment landscape and improve patient outcomes. Antigen selection, CAR T cell manufacturing, response and relapse rates, and toxicity are critical areas that influence the overall success of CAR T cell therapy (Figure 6).

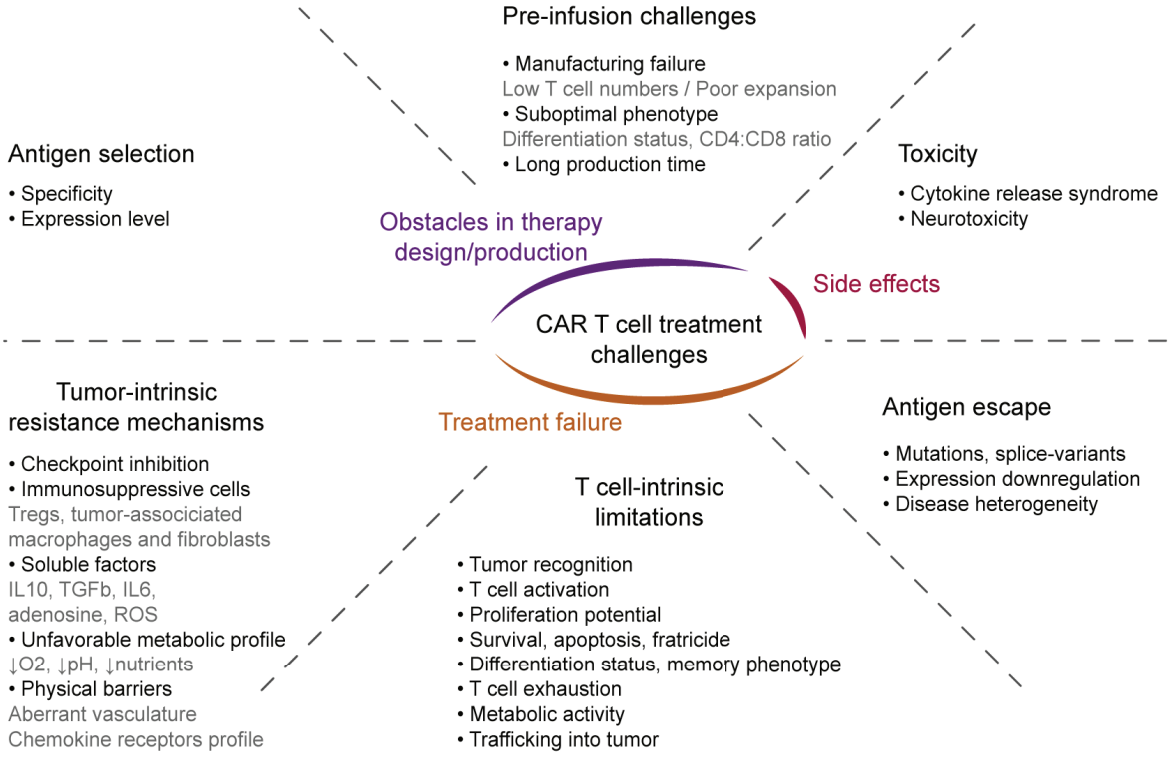

Figure 6. Challenges and limitations of CAR T cell therapy.

Impressive clinical responses to CAR T cell therapy have so far been achieved mainly for hematopoietic malignancies, most notably targeting B cell markers such as CD19, CD20, CD22 (leukemia, lymphoma) and BCMA (myeloma). However, a significant limitation for other indications is the difficulty in identifying suitable antigens for CAR T cell therapy (Flugel et al. 2023). The selection of an appropriate surface antigen is crucial for minimizing on-target off-tumor toxicity, while ensuring that the CAR T cells can effectively recognize cancer cells. Thus,

two key factors in the selection are the level and the specificity of surface protein expression. While publicly available gene and protein expression atlases aid the selection, the landscape of available targets stays limited. Therefore, synthetic biology approaches are important in designing CARs with tuned affinity and built-in logic circuits.

When a suitable CAR is available for a selected antigen, the next significant challenge lies in the manufacturing process of CAR T cells (June et al. 2018). Causes of treatment failure include failure to produce high-quality CAR T cells from patients with a compromised immune system due to low total lymphocyte counts or suboptimal phenotype, which limit T cell expansion. Moreover, due to long production time, some patients face the disease progressing before the treatment reaches them. In addition, the overall availability of CAR T cell therapy is currently limited due to the complex process and logistics of production and distribution as well as the overall cost.

Despite the high efficacy observed in clinical trials and in routine practice, a subset of patients do not respond to CAR T cell therapy, and many patients that initially respond will ultimately relapse (June and Sadelain 2018; N. N. Shah and Fry 2019). One of the prevalent causes of relapse is antigen downregulation or mutation, which leads to antigen-negative tumor escape; however, a large proportion of relapse cases have antigen-positive tumors, indicating CAR T cell failure (Figure 7). Relapse and non-response can be attributed to various factors including intrinsic resistance mechanisms within the cancer cells and poor T cell-mediated cytotoxicity. For solid cancers, the situation is even more challenging, given the physical barriers limiting T cell trafficking, aberrant vasculature, and hostile tumor microenvironment with immunosuppressive cells and unfavorable metabolic profile.

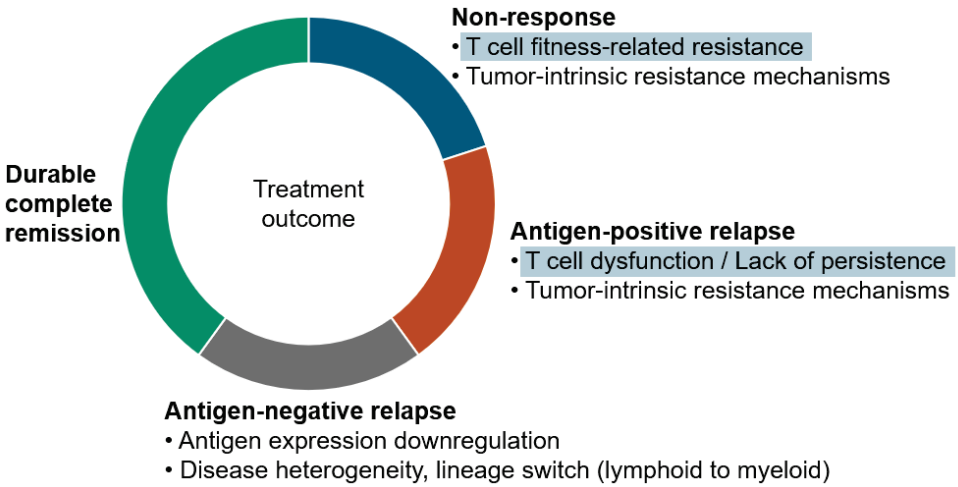

Figure 7. Outcomes of CAR T cell therapy and mechanisms of resistance. The example of approximate proportions of different outcomes is based on the use of axicabtagene ciloleucel in diffuse large B-cell lymphoma (Neelapu et al. 2017; Locke et al. 2022; Lamble et al. 2023). Blue blocks highlight the outcomes associated with T cell-intrinsic limitations, which could be addressed by further CAR T cells optimization.

Clinical outcomes provide valuable insights into the factors predicting better responses to CAR T cell therapy, which could highlight the most important challenges of this treatment. In the context of blood cancers, one of the key predictors is the early expansion of CAR T cells within the first few weeks after treatment (Figure 8) (Neelapu et al. 2017). Another critical predictor is the presence of CAR T cells with a less differentiated status and memory phenotype (Fraietta, Lacey, et al. 2018; Deng et al. 2020; López-Cantillo et al. 2022), which is associated with enhanced cellular fitness and extended proliferation capacity of T cells. These observations underscore the importance of T cell fitness as a determinant of therapeutic success. T cell fitness constitutes the ability of T cells to proliferate and survive, and multiple factors influence this ability and the overall CAR T cell efficacy, as extensively discussed in numerous scientific reviews (Rafiq, Hackett, and Brentjens 2020; Hou, Chen, and Chen 2021; López-Cantillo et al. 2022; Drougkas et al. 2023; Labanieh and Mackall 2023; 2023; Albelda 2024). The key factors include the degree of T cell differentiation, the activation of T cells upon tumor recognition, their proliferative potential, and metabolic status. Additionally, fratricide poses a significant challenge, where CAR T cells attack and kill each other. This is caused either by the expression of the target antigen on the T cell surface (Chiesa et al. 2023) or through trogocytosis, a process where T cells uptake molecules from target cells and present them on their own surface (Hamieh et al. 2019), making CAR T cells susceptible to the attack by other CAR T cells. In addition, T cell exhaustion, characterized by a decline in function due to chronic antigen exposure, leads to reduced CAR T cell fitness (Delgoffe et al. 2021). Therefore, optimizing these and other parameters is crucial for enhancing the therapy outcomes.

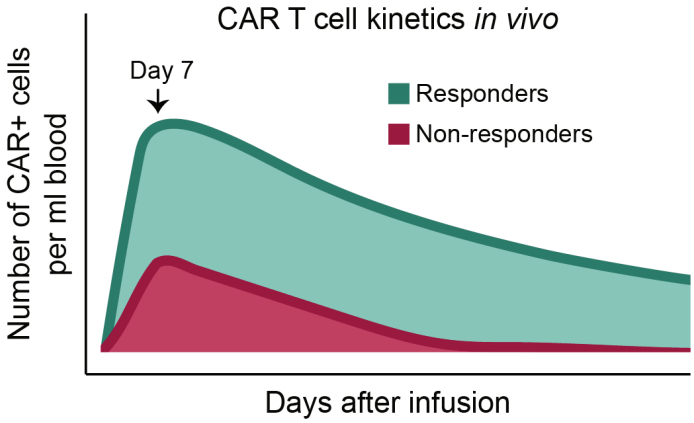

Figure 8. Early CAR T cell expansion associated with durable responses. Graphical presentation is based on the clinical data for axicabtagene ciloleucel in diffuse large B-cell lymphoma (Neelapu et al. 2017).

In addition to overall fitness, the mechanisms by which CAR T cells mediate their cytotoxic function (Figure 9) are equally important. CAR T cells mediate tumor killing through three main mechanisms (Benmebarek et al. 2019). Frist, perforin- and granzyme-mediated

killing involves the exocytosis of cytotoxic granules containing these proteins, which induce apoptosis in target cells. Second, CAR T cells utilize the Fas receptor-ligand (FasL) interaction with Fas to induce apoptosis in both antigen-positive and antigen-negative cells in the tumor, potentially targeting heterogeneous tumor populations. As a side effect, this mechanism mediates apoptosis in CAR T cells affected by fratricide due to the expression of Fas on the T cell surface (Yi et al. 2024). Third, the secretion of cytokines, such as IFNγ, stimulates the immune and stroma cells in the tumor microenvironment to mediate antitumor responses. Fine-tuning these processes in CAR T cells is crucial for the development of next-generation CAR T cells.

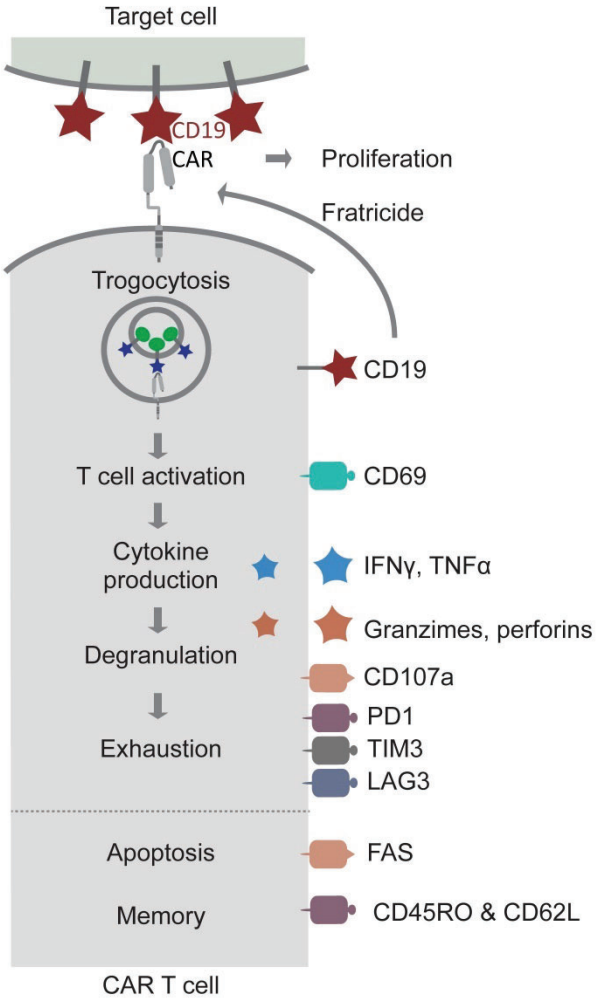

Figure 9. Key CAR T cell processes targeted for optimization.

Toxicity has been one of the key challenges in the application of CAR T cells. Therefore, the therapeutic efficacy of CAR T cells needs to be balanced against the risk of side effects. Cytokine release syndrome (CRS) is one of the common adverse effects, which results from the rapid activation and proliferation of CAR T cells, leading to a massive release of inflammatory cytokines, which sometimes causes life-threatening conditions in patients.

Managing CRS often requires treatment with corticosteroids and IL6 receptor blockers as immunosuppressive agents, and other medical procedures. Thus, the development of safety switches in CAR T cells (such as incorporation of suicidal genes) or tuning their stimulation and activation level is an area of active research. Another side effect of currently applied CAR T cells is neurotoxicity, which can lead to temporal or permanent brain damage. The analysis of the single-cell transcriptomic atlas revealed the on-target neurotoxic effect of anti-CD19 CAR T cells therapies targeting human brain mural cells expressing CD19 (Parker et al. 2020). This highlights the importance of the antigen selection and incorporation of logical circuits into CARs for more specific cancer recognition.

In conclusion, while CAR T cell therapy has significantly advanced the treatment of certain hematopoietic cancers, its broader application requires addressing a number of limitations, which are the focus of extensive ongoing research. Given that CAR T cells are engineered cellular products, additional modifications using genetic engineering and synthetic biology approaches could further enhance their efficacy and safety. These approaches will be reviewed in the next section and are the primary focus of the work presented in this thesis.

1.2 Genetic engineering to enhance CAR T cells

1.2.1 Approaches to enhance CAR T cells

Intense efforts are ongoing to address the challenges of CAR T cell therapy, with various approaches being employed to overcome known limitations and improve CAR T cell designs for a wide range of applications. Firstly, major efforts focus on the manufacturing processes, including the choice of the starting cell population (e.g., preferentially memory T cell subsets), T cell activation methods and cytokine supplements (e.g., not only IL2, but additionally IL7/IL15 to support T cell expansion), and the overall duration of the manufacturing (i.e., shorter *in vitro* culture) (Ayala Ceja et al. 2024). Recent reports suggest inosine supplementation (Klysz et al. 2024) or culture in high-salt medium (Tiriveedhi et al. 2021) as novel strategies to improve CAR T cell manufacturing, and other approaches are being constantly developed.

In addition to advances in manufacturing, synthetic biology and cell engineering provide new ways to enhance CAR T cells (Rafiq et al. 2018). CAR T cells are a cell product that is already subjected to genetic engineering, thus making them an ideal candidate for additional genetic modifications that could improve their therapeutic properties, with a relatively straightforward path for clinical translation once such modifications are discovered.

Genetic engineering to enhance CAR T cells can be done on two different levels: (1) the CAR structure and the regulation of CAR expression, and (2) the modulation of T cell processes. The development of novel CARs covers the design of external and internal

domains with enhanced properties (such as increased sensitivity or signal transduction via endodomains, as reviewed above) and the incorporation of additional features via synthetic biology approaches. The latter include smart switches to induce controllable CAR expression, which enable the incorporation of the logical AND/NOT gates. Such gates have been developed (1) to recognize cancer cells expressing more than one specific antigen (Roybal et al. 2016; Choi et al. 2019), (2) to reduce exhaustion by temporarily switching off CAR expression, which leads to reduced tonic signaling and T cell exhaustion (Weber et al. 2021), and (3) to completely switch off the CAR expression by an “off-switch” or even activate apoptosis upon a trigger such as the addition of a drug (Jones et al. 2014), to provide a safety mechanism in case a treated patient develops severe side effects such as CRS (Sterner and Sterner 2021).

While CAR engineering is crucial for therapy development, modulation of T cell processes provides a complementary path for enhancing different T cell therapies, often applicable across multiple CARs or other synthetic receptors. Multiple challenges in CAR T cell therapy, such as T cell dysfunction, could be addressed by directly targeting the T cell regulatory programs. Consequently, the identification of targets for genetic modifications to enhance CAR T cells has become the goal of multiple studies in the last few years. While the field is still relatively new, multiple beneficial modifications have been identified (Figure 10). Key processes targeted for enhancement include proliferative and metabolic potential, T cell differentiation status, transcriptomic or epigenetic profiles, cytotoxicity, cytokine production, persistence, *in vivo* efficacy in various mouse tumor models, or clinical efficacy in the ongoing trials (De Castro et al. 2024). The approaches used to identify genetic modifications that enhance these parameters can be classified in three groups: (1) serendipity, (2) knowledge-based findings, (3) systems-level search through genetic screens.

The first ground-breaking report published in 2018 showed that the disruption of an epigenetic regulator TET2 promoted the therapeutic efficacy of CD19-targeted CAR T cells (Fraietta, Nobles, et al. 2018). In this study, patients were followed over the course of CAR T cell treatment of r/r CLL. TCR sequencing revealed that a single CAR T cells clone dominated the response. The subsequent in-depth investigation showed that the CAR delivered by a lentivirus was integrated into the TET2 locus leading to gene disruption. At the same time, the second copy of TET2 in this patient was already disrupted. Thus, TET2 was fully inactivated in this CAR T cell clone. This coincidence highlights the importance of *serendipity* in biological studies. The authors further showed that TET2 inactivation led to improved expansion and central memory phenotype of CAR T cells, benefiting the patient and the therapy. Thus, this work provided the ground for the concept of enhancing CAR T cells via permanent genetic modifications in T cells.

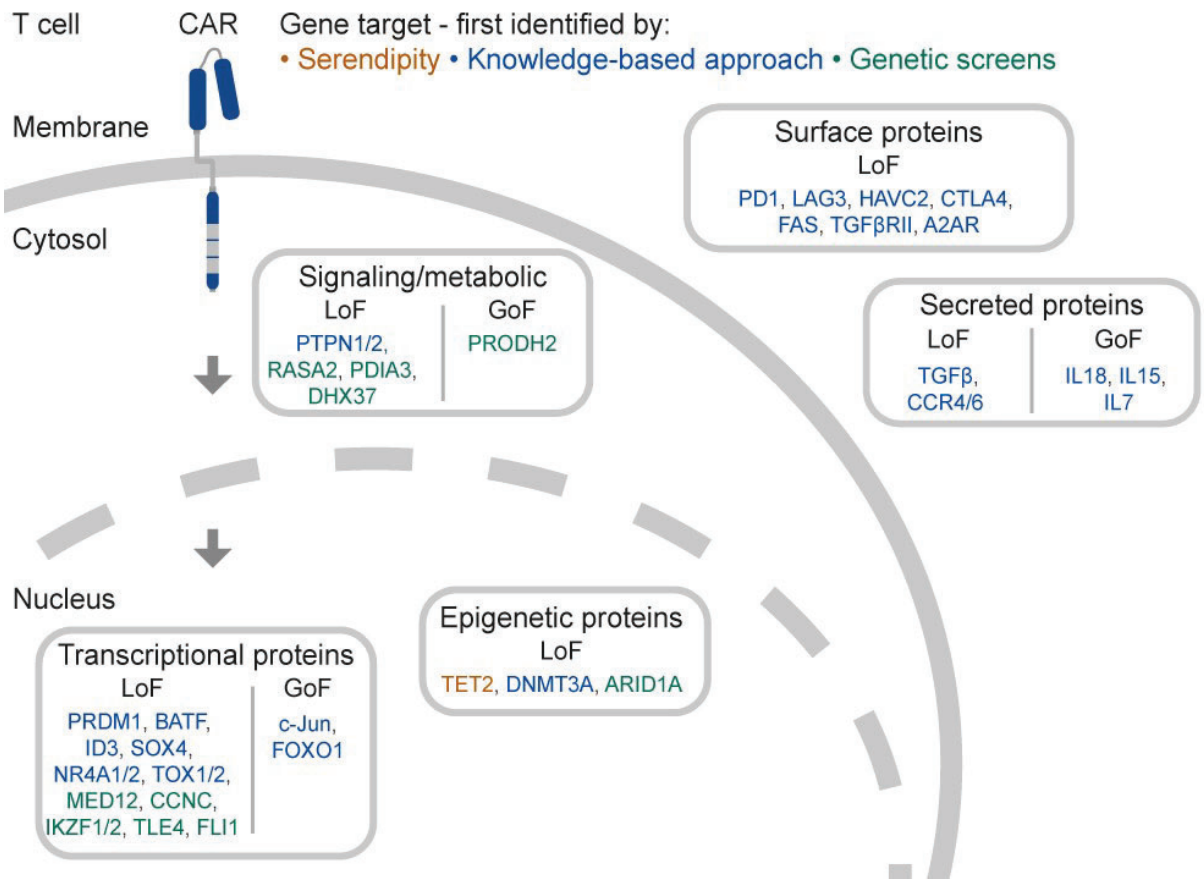

Figure 10. Targets identified to improve CAR T cell functions via genetic modifications. Abbreviations: LoF – loss-of-function (knockdown, knockout, inhibition, point mutations by base editing), GoF – gain-of-function (overexpression, expression activation).

The *knowledge-based approach* combines deep understanding of immunology and T cell biology in cancer with technological advances, such as multi-omics profiling of patient-derived T cells. A number of targets have been identified by a "good guess", such as inactivation of well-studied immune checkpoints (e.g., PD1 (Stadtmauer et al. 2020), LAG3 (Y. Zhang et al. 2017), HAVC2 (TIM3) (Zou et al. 2019), CTLA4 (Shi et al. 2017), and their combinations (Zou et al. 2019)) or immune receptors (e.g., A2AR (Giuffrida et al. 2021) and TGF-β receptor II (Tang et al. 2020) as negative regulators of T cell effector responses, or FAS (Ren et al. 2017) as a mediator of apoptosis). Overexpression of cytokines, chemokines and their receptors has been utilized to enhance the efficacy of CAR T cells (Ghahri-Saremi et al. 2021), illustrated by an example of the currently ongoing clinical trial investigating CAR T cells with IL18 overexpression (NCT04684563).

In addition, transcriptomic and epigenomic profiling studies have emerged as the strategy to gain insights into complex processes leading to T cell dysfunction in cancer (Hong et al. 2020), which could be used to generate biology-driven hypotheses on genetic modifications to improve CAR T cells. For example, Lynn et al. used multi-omics profiling in a model of CAR

T cell tonic signaling and exhaustion to demonstrate the epigenomic dysregulation of AP-1 transcription factor-binding motifs and the increased expression of transcription factors bZIP and IRF being involved in exhaustion (Lynn et al. 2019). Subsequently, this group tested the hypothesis that T cell dysfunction resulted from the imbalance between activating and immunoregulatory function of AP-1 and IRF complexes and proposed the overexpression of c-Jun, an AP-1 family transcription factor, to compensate for this imbalance. Indeed, c-Jun overexpression made CAR T cells more resistant to exhaustion and increased their proliferation, both *in vitro* and in multiple *in vivo* tumor models. Another example is the overexpression of a transcription FOXO1, which was shown to enhance CAR T cell memory potential and metabolic, as recently reported independently by two groups (Chan et al. 2024; Doan et al. 2024). To suggest the hypothesis of FOXO1 overexpression, Chan et al. explored epigenome and transcriptome of CAR T cells cultured in the presence of IL15, and revealed the enrichment of FOXO1 gene signature in memory CAR T cells (Chan et al. 2024), and Doan et al. analyzed the profiles of CAR T cells with memory phenotype to also show the increased chromatin accessibility at FOXO1 motifs (Doan et al. 2024). In a similar manner, Jung et al. had previously employed single-cell RNA-sequencing profiles of CAR T cell infusion products administered to patients, and found elevated expression of PRDM1 (Blimp-1) in non-responders (Jung et al. 2022), leading to the hypothesis that targeting PRDM1 could improve CAR T cells. Indeed, Yoshikawa et al. observed that the ablation of PRDM1 led to a lower degree of T cell differentiation and a higher number of memory CAR T cells as well as to prolonged survival in mouse tumor leukemia model (Yoshikawa et al. 2022). Going a step further, Jung et al. found that PRDM1-deficient CAR T cells displayed a negative epigenetic feedback program nuclear factor of activated T cells (NFAT)-driven T cell dysfunction, driven in particular by NR4A3 expression (Jung et al. 2022). Therefore, the group tested PRDM1 and NR4A3 double knockout and showed that CAR T cells showed less exhausted phenotype and improved antitumor responses (Jung et al. 2022). In another study, by profiling CAR T cells in a hypofunctional model, BATF was identified as transcription factor involved in T cell exhaustion, and subsequent BATF deletion enhanced antitumor activity of CAR T cells against solid tumors (X. Zhang et al. 2022). These and other studies led to the identification of multiple additional targets such as ID3 and SOX2 (Good et al. 2021), PTPN1 (M. Liu et al. 2023), PTPN2 (Wiede et al. 2020), NR4A1/2 (J. Chen et al. 2019), DNMT3A (Prinzing et al. 2021). A review by De Castro et al. provides a comprehensive summary of gene targets for inactivation in CAR T cells to enhance their function, that have been identified through the knowledge-based approach, as well as the functional readouts and *in vivo* tumor models utilized in these studies to test modified CAR T cells (De Castro et al. 2024).

Additional common targets have been determined in a biology-driven way aiming to facilitate allogeneic transfer and prevent fratricide. To this end, TRAC/TCRB (TCR genes) and

B2M (beta-2 microglobulin, an essential component of the MHC class I molecules) knockouts are frequently included in CRISPR-modified CAR T cells produced in currently ongoing clinical trials (De Castro et al. 2024) to enhance safety and specificity and to prevent immune rejection, respectively. To prevent fratricide, CRISPR-mediated knockouts and base editing have been used to delete surface markers such as CD7 (Georgiadis et al. 2021; Chiesa et al. 2023), CD5 or CD139 (Ureña-Bailén et al. 2020), which are selected as tumor targets but also expressed in T cells, leading to CAR T cell self-recognition and fratricide when the expression remains unaltered.

The modulation of the expression of above-mentioned proteins has been demonstrated to boost the efficacy of engineered CAR and TCR T cells in hematologic and solid tumor models, and clinical trials with CRISPR-edited T cells containing some of these modifications are currently ongoing (De Castro et al. 2024; Rafiq, Hackett, and Brentjens 2020; Ureña-Bailén et al. 2020; Labanieh and Mackall 2023). For example, the first clinical study of CRISPR-edited T cells was set up to evaluate NY-ESO-1-directed transgenic TCR T cells with CRISPR-Cas9 edits to remove endogenous TCR and PD1 (NCT03399448) (Stadtmauer et al. 2020). These examples highlight how scrutiny can unveil promising candidates for genetic modifications to enhance CAR T cells.

As evident from the examples above, different modes of genetic modifications can be employed to modulate CAR T cell functions, including loss-of-function (knockdown, knockout, inhibition, point mutations by base editing) and gain-of-function (overexpression, expression activation). Given that human genome contains about 20,000 genes, each of which could be targeted with multiple editing modes, knowledge-based approach may miss some of the most impactful modifications, since only a handful of targets can be tested experimentally in a low-throughput way.

Genetic screening provides an alternative for high-throughput testing of candidate modifications genome-wide. In brief, in pooled screens, various genetically encoded perturbations (gene modifications) are introduced into pools of cells, from which cells with desired properties are selected based on functional readouts (e.g., the enhancement of a particular function of CAR T cells), and the perturbation-induced effects are evaluated through quantification of these perturbations identified by sequencing. To date, several studies have conducted genetic screens in human T and CAR T cells, and a number of gene modifications have been found to enhance CAR T cells (Figure 10). In this work, we established a platform for genetic screens in CAR T cells, and therefore the progress in this field will be reviewed in detail below. However, to engage with genetic screens, we first need to review the methods used for genetic engineering in human primary T cells and understand the experimental challenges associated with it.

1.2.2 Genetic engineering in human primary T cells

As reviewed above, various approaches have been utilized to genetically engineer CAR T cells with enhanced functionality. Historically, loss-of-function modifications have been more commonly used, owing to well-established experimental methods and tools such as meganucleases, zing finger nucleases, transcription activator-like effector nucleases (TALEN) or CRISPR-Cas system (Mirzaei et al. 2018; De Castro et al. 2024). In particular, CRISPR-Cas tools offer precision, flexibility and simplicity to implement, and therefore have emerged as the most widely used strategy for genome editing in human cells (Pacesa, Pelea, and Jinek 2024). Moreover, the safety and feasibility of using CRISPR-edited T cells have already been demonstrated in clinical trials (Stadtmauer et al. 2020; Lu et al. 2020; Khan and Sarkar 2022), thus showing the translational potential of CRISPR technology for the next-generation CAR T cell therapies. Additionally, CRISPR offers an opportunity to conduct genetic screens with flexible modes of perturbations (Bock et al. 2022) including gene activation, repression and base editing. Below, we will discuss CRISPR editing tools and their implementation in human primary cells.

CRISPR, an acronym for “clustered regularly interspaced short palindromic repeats”, has revolutionized molecular biology since the pioneering work published in 2012 and conducted at the University of Vienna and later at the University of California (Jinek et al. 2012) by the groups of Emmanuelle Charpentier and Jennifer Doudna, who were awarded the Nobel Prize for this discovery already in 2020. This work showed that CRISPR-Cas9 system could be programmed to cut specific DNA sequences defined by synthetic guide RNAs (gRNAs), establishing a simple and efficient method for targeted DNA editing. Following this discovery in bacterial cells, CRISPR editing was demonstrated in mammalian cells, highlighting its potential for a wide range of applications (Cong et al. 2013; Mali et al. 2013).

Various Cas proteins have been identified for CRISPR-Cas gene editing. In the CRISPR-Cas9 gene knockout approach, the Cas9 protein introduces a double-strand break (DSB) at a genomic locus specified by a gRNA, which gets repaired by non-homologous end joining (NHEJ) or homologous directed repair (HDR) if a template is provided (Figure 11). The error-prone NHEJ results in indels and deletions leading to premature STOP codons or frame shifts causing the disruption of gene expression, which is widely used for functional genomic studies (Cong et al. 2013).

The CRISPR editing modes have been further expanded by multiple tools. For example, CRISPR base editing emerged as a technology enabling precise nucleotide conversions (Figure 11). Two main types of currently established base editors allow adenine-to-guanine (A-G) and cytosine-thymine (C-T) substitutions (Huang, Newby, and Liu 2021). These editors are designed as fusions of a catalytically inactive Cas9 (dCas9, an acronym for dead Cas9)

or a Cas9 nickase (nCas9) with specific deaminases, which convert either adenine to inosine or cytosine to uracil, which are then recognized as guanine or thymine by DNA polymerase during DNA replication or repair, which leads to A:T-G:C or C:G-T:A conversions, respectively (Figure 11). A standard Cas9 protein and its versions require a protospacer adjacent motif (PAM) NGG to be present directly downstream of DNA sequence targeted by the 20-base-pair-long gRNA. The abundance of NGG sites in the genome makes the gRNA design for gene knockout a straightforward process. However, the strict NGG requirement limits the number of point mutations that can be introduced by base editors. To expand the editing space, near-PAMless base editors, such as SpRY (R. T. Walton et al. 2020), have been designed.

Beyond DNA-level editing, CRISPR tools have been developed to influence transcriptional and epigenetic status of gene expression. For instance, CRISPR activation systems complement the gene knockout approach by providing a possibility to introduce gain-of-function modifications. As such, Synergistic Activation Mediator (SAM) system utilizes dCas9 fused with transcriptional activators such as VP64, further linked to additional activation domains like p65 and HSF1, which together enable the specific recruitment of these activators to the promoter regions of target genes leading to enhanced transcription without altering the genomic sequence (Konermann et al. 2015) (Figure 11). On the other side, a fusion of dCas9 with an inhibitory KRAB domain in the CRISPRoff system enables highly efficient and heritable transcriptional repression via epigenome editing (Nuñez et al. 2021). Other recent advances include prime editing, which combines a reverse transcriptase and a pegRNA to directly write new genetic sequences into targeted sites without relying on HDR or double-strand breaks (Anzalone et al. 2019).

Overall, CRISPR tools are rightfully compared with a Swiss knife (Doench 2018) offering a variety of gene editing modes. In summary, CRISPR has revolutionized the landscape of genetic engineering by providing an exceptionally flexible toolbox enabling multiple editing modes, including multiple approaches to introduce loss- and gain-of-function perturbations.

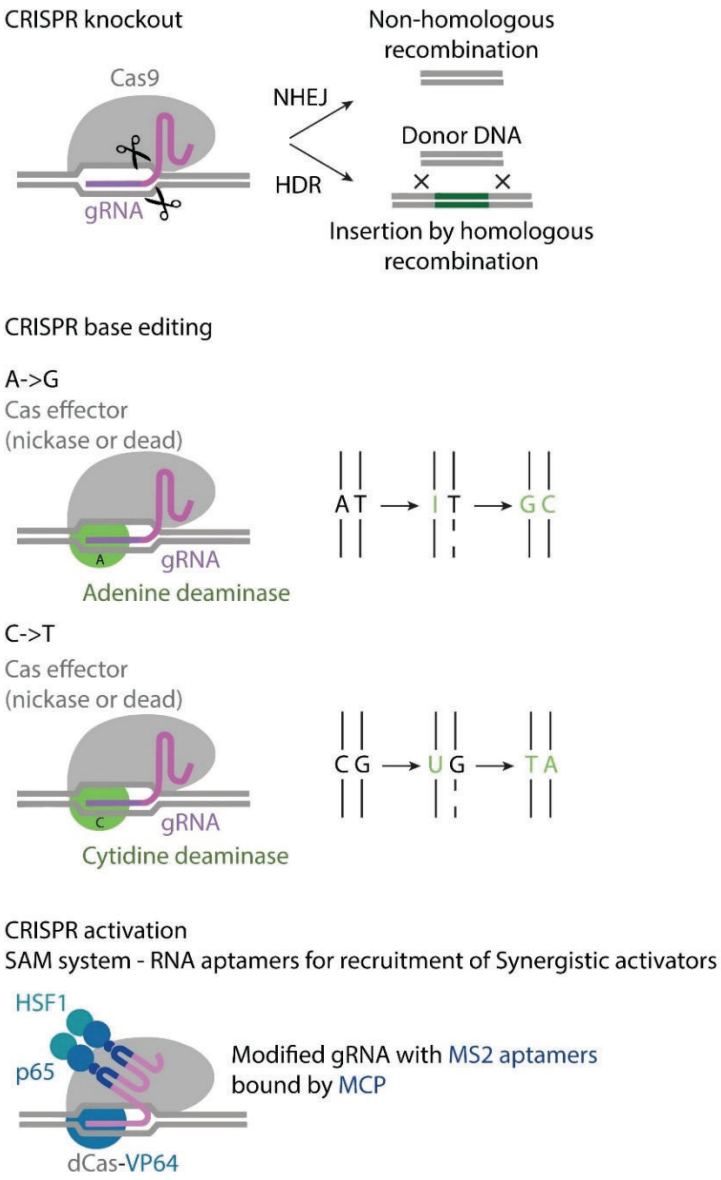

Figure 11. Examples of CRISPR-Cas applications. CRISPR-Cas9 knockout. Cas9 introduces double-strand breaks (DSBs) at the genomic locus targeted by gRNA. DSBs are repaired either by non-homologous end joining (NHEJ) repair, or by homology-directed (HDR) repair if a homologous DNA template is provided, enabling targeted insertion of specific DNA sequences. The error-prone NHEJ repair system leads to insertions or deletions that can disrupt the gene function, which is used for gene knockouts. **CRISPR base editing**. dCas9 enables targeting the locus specified by gRNA, with typical editing window in the range of positions 3-7 of the gRNA. A-G base editors (ABEs): the enzymatic domain deaminates adenine to inosine, which is interpreted as guanine by DNA polymerase, resulting in an A:T-G:C conversion. C-G base editors (CBEs): the enzymatic domain converts cytosine to uracil, which is interpreted as thymine by DNA polymerase, resulting in a C:G-T:A conversion. After a DNA base is modified, the mismatch is targeted by DNA repair system leading to base substitution. Using a Cas9 nickase (nCas9) leads to nicking the non-deaminated strand, which leads to preferential DNA repair based on the strand with the deaminated nucleotide, resulting in the conversion of both DNA strands to the desired base pair with increased efficiency. **CRISPR activation – SAM system.** dCas9 is fused with a transcriptional activator domain VP64. In addition, the modified gRNA contains aptamer sequences, which recruit additional transcriptional activators p65 and HSF1. The recruitment of activators to promoter regions allows precise upregulation of gene expression.

CRISPR tools have been widely adopted for various applications including gene editing in human primary cells, which offers translational perspective for engineered cell therapies (Pacesa, Pelea, and Jinek 2024). However, applying CRISPR technology to primary cells, including human primary T cells, presents certain constraints. In particular, while immortalized cell lines can be engineered to stably express Cas proteins, whose DNA sequence contains several kilobases, and can be selected over multiple cell passages, efficient delivery of these large proteins and their corresponding DNA into primary cells is more challenging. Viral vectors, and particularly lentiviruses, have been widely used for delivering CRISPR components into cell lines. Lentiviruses can carry CRISPR components and integrate them into the host genome, ensuring stable expression. However, the simultaneous delivery of the Cas9 protein (more than 4000 bp) together with gRNA expressing unit (around 350 bp) and other genetic constructs (for example, CARs containing over 1000 bp) is limited by the packaging capacity of lentiviral vectors, necessitating the use of subsequent virus infections to deliver different components. Moreover, transduction rates in primary cells are notoriously low in comparison to cell lines with typically high efficacy of virus vector integrations. Electroporation is another widely used technique that temporarily disrupts the cell membrane with an electrical field, allowing the CRISPR components to enter the cell. The initial protocols for CRISPR knockout in human primary T cells used Cas9:single-guide RNA ribonucleoproteins (Cas9 RNPs) (Schumann et al. 2015). By electroporating RNPs into T cells, high cell viability and gene editing can be achieved. However, electroporation enables only temporary expression, while stable integration of gRNAs is essential for tracing genetic perturbations by sequencing in genetic screens. Moreover, the use of RNPs relies on the optimized protein production for each CRISPR application, limiting the versatility of this technique.

In summary, successful CRISPR editing in human primary cells is often limited by multiple factors such as variability in transduction efficiency and transgene expression. Addressing these challenges in the context of genetic screens requires the development of novel delivery systems and optimization of existing protocols.

1.2.3 Overview of pooled genetic screening

Functional genetic screens offer a comprehensive assessment of the effects of genetic modifications at scale, which can greatly accelerate the development of enhanced T cell-based therapies. In particular, pooled CRISPR screens have emerged as a widely used technology, building on previous successes of arrayed and pooled RNA interference (RNAi) screens using small interfering RNAs (siRNAs) or short hairpin RNAs (shRNAs) (Echeverri and Perrimon 2006).

Genetic engineering techniques provide the essential basis for genetic screens. The CRISPR-Cas9 tools possess several key properties for successful knockout screens. First, the CRISPR-Cas9 system typically achieves a high knockout efficiency, despite the fact that NHEJ repair often results in indels with no frameshift (in about 30% of cases) retaining protein functionality. Second, CRISPR-Cas9 offers high specificity with relatively low levels of off-target rates. Third, the knockouts are directly and permanently installed into the genome, in contract to repression (for example by RNAi), which needs to be maintained throughout the screen and could be affected by gene expression and other factors. Additionally, as discussed above, CRISPR offers a unique advantage over other techniques by providing a variety of editing modes, expanding the space of possible genetic screens from CRISPR knockout to CRISPR base and prime editing or activation screens. A number of reviews provide an overview of strengths, applications, and technological advancements of CRISPR screens, as well as the techniques used to perform them (T. Wang et al. 2014; Shalem, Sanjana, and Zhang 2015; Doench 2018; Bock et al. 2022), which will be also discussed below in the context of screens in human primary T cells.

In addition to efficient CRISPR editing techniques, which are essential for engineering the screening cell population, every genetic screen has a functional readout at its core. The choice and optimization of a functional readout is key for the screen quality, because the readout determines how well the cell populations with a desired phenotype can be separated from other cells. Existing readout strategies can be classified into three categories (Doench 2018) (Figure 12). First, proliferation-based screens identify genetic perturbations that influence cell fitness based on over- or under-representation of cells carrying specific gRNAs over time. Second, FACS-based screens physically separate cells by the protein marker expression, enabling CRISPR screening with more complex phenotypes. Third, single-cell CRISPR screens combine pooled screening with a single-cell transcriptome (Datlinger et al. 2017a; Adamson et al. 2016; Dixit et al. 2016; Jaitin et al. 2016) or epigenome readout (Pierce, Granja, and Greenleaf 2021; Liscovitch-Brauer et al. 2021). Each of these screening types can be performed *in vitro*, when the population of screening cells is cultured in a dish, or *in vivo*, in which case the screening population is injected or established in a model animal and is later isolated for profiling. Each readout type assesses various cell phenotypes and, as we will see below, can be employed in genetic screens to identify targets for improving T cell-based therapies.

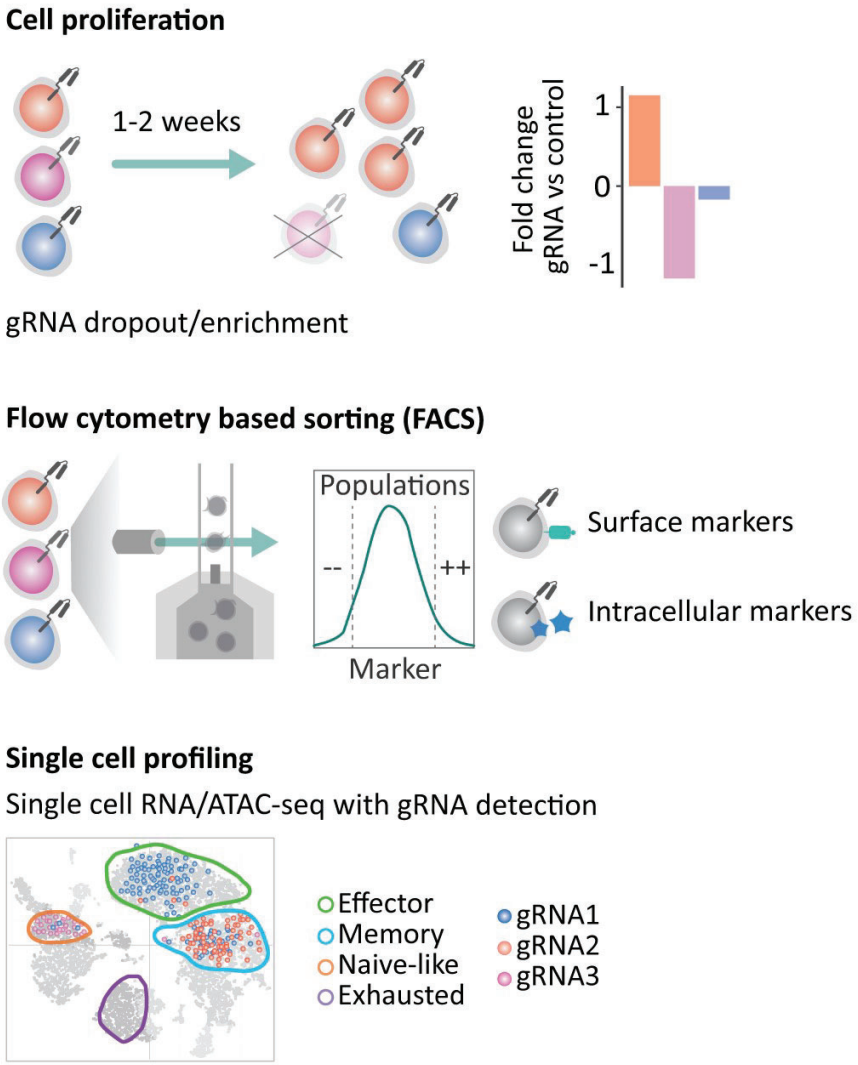

Figure 12. Pooled CRISPR screens classified by functional readouts: cell proliferation-based dropout or enrichment screens, FACS-based screens, and single-cell screens.

1.2.4 Genetic screens in human T and CAR T cells

CAR T cells are a genetically engineered cell product, infused into patients to fight their cancer. This makes them particularly attractive for genetic screening, because hit genes can be directly translated to the clinic, using the existing modification pipeline and regulatory framework. Currently, there is great interest in developing next-generation CAR T cell therapies that harbor additional genetic modifications, such as CRISPR-mediated knockouts or gene overexpression. Genome-wide screens offer an opportunity to discover modifications in a high-throughput manner and find unexpected hits, going beyond the targets found by serendipity or knowledge-based approach.

Each study utilizing genetic screens to enhance CAR T cells contains three key parts: CAR T cell engineering for screening, functional readout, and hit validation (Figure 13). To enable pooled CRISPR screens in CAR T cells, human primary T cells have to be modified

with the following three components: (1) a chimeric antigen receptor (CAR) (2) a library of CRISPR gRNAs, integrated into the genome to make perturbations genetically traceable (3) CRISPR editors that perform genome engineering, as directed by the gRNA. Once the engineered cells are produced, pooled screens rely on phenotypic readouts to physically separate cell populations of interest. Following the screening analysis, the genetic modifications predicted to induce a desired cell phenotype are validated using *in vitro* and *in vivo* models and assays. Below, we summarize the current state of the art in the following areas: the techniques and bottlenecks in genetic screens in human primary (CAR) T cells, and in particular the progress in genome-scale screens; the functional assays to measure CAR T cell phenotypes and performance as screening readouts; and the targets for genetic modifications to enhance CAR T cells identified using CRISPR screens in primary T cells.

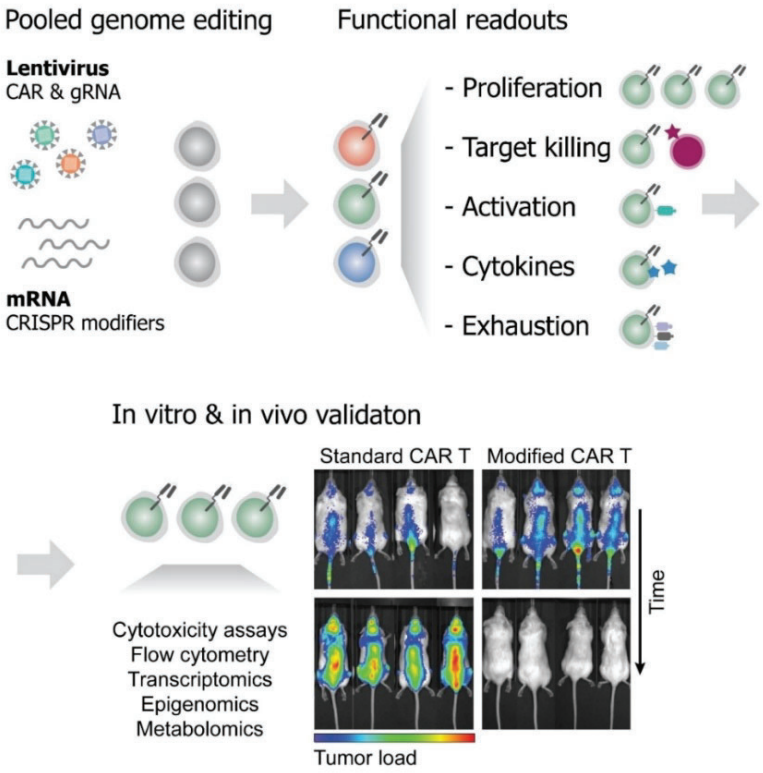

Figure 13. Stages of a genetic screening study in CAR T cells: cell engineering, functional readouts, and validation. Approaches used in the present study are shown as examples.

While knockout screens conducted in tumor cell lines (Patel et al. 2017; Manguso et al. 2017; Pan et al. 2018) and mouse primary T cells (Belk et al. 2022; Dong et al. 2019) have identified important regulators of T cell signaling, performing screens directly in human primary T cells is crucial for more clinically relevant translation, as immortalized cell lines or mouse cells may not fully capture their critical biological functions. Several studies have applied

genome-wide CRISPR screens to investigate regulators and enhance the functionality of T cells and CAR T cells. Among them, six studies reported genome-scale CRISPR screens (Table 2) (Shifrut et al. 2018; D. Wang et al. 2021; Carnevale et al. 2022; Freitas et al. 2022; Schmidt et al. 2022; 2023) – the scale which ultimately enables the unbiased discovery of targets that would not be predicted in a knowledge-based approach or found in small-scale focused screens.

In a seminal paper originated from the Alexander Marson lab at UCSF in 2018, Shifrut, Carnevale et al. first demonstrated genome-wide screens in CD8 human primary T cells using lentiviral transduction to deliver the gRNA library and electroporation to deliver the Cas9 protein (the SLICE method (Shifrut et al. 2018)). The resulting genome-edited T cells were stimulated with anti-CD3/CD28 beads, and cell divisions were tracked by cell staining with carboxyfluorescein succinimidyl ester (CFSE). FACS was used to isolate cells with high and low proliferation rates. The analysis of gRNAs in these populations uncovered regulators of *in vitro* proliferation and antitumor activity of anti-NY-ESO TCR T cells. In this study, the incorporation of Cas9 delivery by electroporation was key to solve the challenge of inefficient delivery of Cas9 and gRNAs in the same lentiviral vector. The SLICE method was successfully applied to perform further screens in T cells that identified RASA2 knockout as a strategy to enhance CAR T cells in the study by Carnevale, Shifrut et al. (Carnevale et al. 2022). However, SLICE uses protein delivery, which relies on the established commercial reagents that are currently available mainly for Cas9 or on optimizing protein production for each CRISPR protein of interest, limiting the number of possible CRISPR applications.

Building up on the SLICE technique, the first genome-wide screens in human CAR T cells were reported by Wang, Prager et al., where the gRNA library and the CAR construct were incorporated into T cells in subsequent transduction rounds, and Cas9 was delivered via protein electroporation (D. Wang et al. 2021). The authors used a prolonged co-culture of CAR T cells with tumor cells and performed FACS to screen for CAR T cells with a reduced PD1 level, using PD1 as the marker of T cell exhaustion. Interestingly, although expected, no PD1 gRNA enrichment (inducing PD1 knockout) was observed in the PD1-negative cell population, which could indicate a high level of noise, potentially caused by low gRNA coverage or other factors. Nevertheless, the study identified and validated TLE4 and IKZF2 as targets for enhancing CAR T cell efficiency in a glioblastoma tumor model.

Freitas, Belk et al. reported another set of genome-wide screens in human CAR T cells and discovered MED12 and CCNC knockouts as a strategy to boost therapeutic response in leukemia models (Freitas et al. 2022). This study used a similar cell engineering approach for screens: the gRNA library and CAR were introduced by subsequent lentivirus and retrovirus transductions, while Cas9 was delivered by protein electroporation. The authors expanded the number of functional readouts by performing a proliferation-based screen using a prolonged

co-culture of CAR T and tumor cells, and FACS-based screens by sorting CAR T cells with high levels of IFNγ and IL2. However, given the limited transduction rates in human primary T cells, the subsequent transductions inherently lead to inefficiencies and massive loss in the number of edited cells that can be produced, which consequently limits the number of functional readouts that can be performed.

In addition to loss-of-function screens, Schmidt, Steinhart et al. demonstrated the possibility of CRISPR activation and interference screens in CD4 and CD8 T cells (Schmidt et al. 2022). The authors used FACS to separate CD4 or CD8 T cells with high and low levels of IFNγ or IL2, to identify genetic perturbations that affect cytokine production. Later, in the paper by Schmidt, Ward et al. from the same group presented CRISPR base editing screens targeting multiple proteins implicated in T cell function with genome-scale gRNA libraries (Schmidt et al. 2023). CRISPR modifiers and gRNA libraries were introduced one-by-one using different lentiviral constructs. Similar to delivering the CAR and gRNA components in two viral vectors, subsequent transduction rounds introduce inefficiencies, thus limiting the screening power and potentially restricting the ability to introduce further components into cells (e.g., to perform CRISPR activation or interference screens in CAR T cells, and not in T cells lacking additional synthetic receptors).

To sum up the T cell engineering strategies for CRISPR screens, virus transduction is a standard method for the stable expression and permanent integration of genetic constructs in a cell, which is also widely used for CAR T cell manufacturing for approved therapy and for CRISPR applications in T cells. In the context of pooled genetic screens, viral vectors are typically used to deliver the gRNA library as well as the synthetic receptor in the case of CAR T cells. CRISPR modifiers are usually delivered via the electroporation of Cas9 protein (SLICE method) or by two successive transductions with different lentiviral constructs, where one encodes a CRISPR modifier, and the other a gRNA library (Schmidt et al. 2022; D. Wang et al. 2021). Among the challenges associated with these techniques, multiple transduction rounds limit the numbers of transduced cells and therefore the screening capacity, and the dependency on protein restricts the number of possible CRISPR applications. Our technology platform developed as part of this thesis addresses these challenges by transducing T cells with a single lentiviral vector containing CAR and the gRNA library, and by delivering CRISPR modifiers via mRNA electroporation. Meanwhile, a screening study by Dai, Park, Du, Na, Lam et al. employed a similar strategy by using adeno-associated virus-based delivery of CAR and gRNAs and mRNA electroporation of Cas12a/Cpf1 (CLASH protocol) (Dai et al. 2023). Although the CLASH method was only demonstrated for focused gRNA libraries, the co-delivery of CAR and gRNA increases the cell engineering efficiency in comparison to subsequent transduction rounds. Additionally, the mRNA delivery of CRISPR modifiers provides a simple strategy to flexibly switch between the editing modes, thus expanding the screening

capabilities. This advantage has been employed in a screening study by Walsh, Shah et al., using mRNA for delivery of CRISPR base editors to study single-nucleotide variants in T cells and identify gain-of-function mutations boosting CAR T cells (Walsh et al. 2024).

Complementing cell engineering technologies, functional readouts are key to perform genetic screens. The selection of ideal gene modifications involves a thorough analysis of multiple readouts to assess the impact on various aspects of T cell function. Cell proliferation and survival have emerged as the key characteristics reflecting the T cell efficacy. Widely used models to assess these and other properties of T cells include T cell activation by anti-CD3/CD28 reagents or co-culture of T cells with target cells. Prolonged culture is suitable to perform screens to identify genetic modifications that improve the overall cell fitness, assessed by the gRNA enrichment in culture (Freitas et al. 2022) or in cells sorted based on the number of cell divisions (Shifrut et al. 2018). Multiple other parameters can be assessed in FACS-based screens, such as differentiation status and memory phenotype, expression of activation and inhibitory molecules, cytokine production, degranulation, and exhaustion markers. These and other characteristics have been assessed in screens *in vitro* and *in vivo*, in the genome-scale screens discussed above and in a number of focused screens in T and CAR T cells, comprehensively summarized in dedicated reviews (Xiang et al. 2024; De Castro et al. 2024). In addition, transcriptomic analysis has been used in single-cell CRISPR screens in primary human T cells to characterize the effect of genetic perturbations on distinct T cell phenotypes (Belk et al. 2022; McCutcheon et al. 2023; Zhou et al. 2023; Alda-Catalinas et al. 2024).

Cell engineering techniques for genome-scale screens in human primary cells open the opportunity to discover targets to enhance CAR T cells, which would be otherwise overlooked in screens with focused libraries, which typically target only the genes that are already known in connection to immune cell functions. Multiple functional readouts have been established to discover strategies to modulate various CAR T cell phenotypes. While we primarily focused on reviewing genome-scale screens in human primary (CAR) T cells, both genome-wide and smaller-scaler screens, performed in human and in mouse T cells, enabled the discovery of genetic modifications that enhance immunotherapy (Figure 10). In addition to above-mentioned targets found in genome-wide screens in human T cells, genes such as PDIA3 (Ye et al. 2019), DHX37 (Dong et al. 2019), ARID1A (Belk et al. 2022), FLI1 (Z. Chen et al. 2021), IKZF1 (Zhou et al. 2023), SOCS1 (Sutra Del Galy et al. 2021), and PRDM1 (Dai et al. 2023) have been identified in focused screens in both human and mouse T cells. These targets have been validated as functional regulators of T cells, presenting promising knockout targets to optimize T cell immunotherapies. CRISPR activation screens have further identified gain-of-function modifications, such as overexpression of PRODH2 (Ye et al. 2022) or BATF3 (McCutcheon et al. 2023), to enhance CAR T cell properties. Beyond single genetic perturbations, the field is actively working to develop screens with multiplexed genetic modifications.

As the first example in CAR T cells, Tieu et al. established CRISPR knockdown screens and identified beneficial dual targets, such as CBLB (an E3 ubiquitin-protein ligase) and FAS (Tieu et al. 2024). The high throughput of genetic screens is particularly important for multiplexed screens due to the massive space of combinatorial modifications. Genome-wide screens provide a foundation to preselect targets for follow-up screens combining perturbations that may enhance CAR T cells through orthogonal pathways.

While screening readouts are usually carefully selected to reflect T cell phenotypes desired for their therapeutic efficacy, the majority of screens are performed *in vitro*. In this controlled environment, (CAR) T cells are stimulated in the culture medium containing high levels of IL2 and other supplements, which may not mirror the physiological conditions but could affect CAR T cell phenotypes and therefore the screening results. Although the co-culture model of CAR T and tumor cells mimics certain clinically relevant aspects of CAR T cell functionality, only *in vivo* studies can bridge the gap between *in vitro* findings and clinical application. The next section will focus on the strategies and models for *in vivo* validation of enhanced CAR T cell properties. In addition to validation studies, techniques to perform genetic screens directly *in vivo* are being actively developed, and some of them have been successfully applied to CAR T cells (Dai et al. 2023; Korell et al. 2024), despite remaining technical challenges, such as engraftment rates and clonal biases. Addressing these limitations, our screening technology was designed to be compatible with *in vivo* screens and was successfully applied to screen for CRISPR-boosted CAR T cells directly in a mouse tumor model.

In summary, genetic screens serve as a powerful tool for high-throughput analysis of genetic perturbations. A number of targets have been found to modulate distinct CAR T cell features. However, multiple technological challenges remain to expand the screening capabilities, in particular in terms of scale and editing modes. Thus, the field requires constant innovation in the tools to optimize CAR T cell therapy systematically and at scale, directly in human primary cells, both *in vitro* and *in vivo*.

1.2.5 Preclinical testing of T cell therapies

Numerous parameters of CAR T cells can be optimized to broaden their therapeutic performance and treatment outcomes, as discussed in the sections above. Key aspects that can benefit from further optimization include overall fitness and cytotoxic functionality, which are characterized by multiple processes including target recognition, proliferation, differentiation status, T cell activation, cytokine production, exhaustion, apoptosis, and fratricide. Each of these features can be assessed during preclinical testing of engineered CAR T cells. Moreover, while CAR T cell functionality is key to predict their therapeutic efficacy, it is equally important to assess the risks of potential toxicities and side effects, in particular when CAR T cells are designed to have boosted cytotoxic signaling. The recent reports regarding the

potential for malignant transformations of CAR T cells (FDA 2023) additionally emphasize the need to evaluate this risk, especially for CAR T cells with enhanced proliferation and persistence properties. A variety of preclinical models have been developed to systematically assess the efficacy and safety of CAR T cells both *in vitro* and *in vivo*.

In the first stage of preclinical testing, *in vitro* systems can be used to assess whether CAR T cells proliferate, kill target cells, and perform essential functions, and whether modified CAR T cells outperform the standard design in any of these aspects. Common methods for *in vitro* evaluation include co-culture with target cells, plate coating with antigens, and the use of antigen-coated beads. These approaches serve as CAR-stimulation techniques, which can be used to profile CAR T cell response to the antigen, including the target recognition, killing efficiency, or activation of CAR signaling, by assessing the expression of protein markers using flow cytometry or multi-omics approaches. *In vitro* culture can model various challenges of CAR T cell therapy. For example, in a chronic stimulation model, CAR T cells are continuously or repeatedly stimulated with the target antigen, which leads to reduced killing efficiency and T cell exhaustion (Carnevale et al. 2022; D. Wang et al. 2021; Freitas et al. 2022). The plate-based approaches can provide the means to carefully assess CAR T cell sensitivity to different levels of antigens and fine-tune it to avoid tumor escape by antigen downregulation (Gudipati et al. 2020). Importantly, *in vitro* models are also cost-effective and easy to scale, which allows testing multiple CAR T cell designs. Consequently, these models have been widely used for CRISPR screens to optimize CAR T cells, as previously discussed. However, the culture conditions, such as the use of medium supplements, differ significantly from the physiological environment, limiting the translation of *in vitro* findings. Moreover, cell culture models do not account for tumor heterogeneity and cell-cell interactions. To better model tumor microenvironment, *in vitro* systems like organoids have been developed (Dekkers et al. 2023). However, organoids also depend on *in vitro* culture and so far have been developed only for certain cell types, thus not fully recapitulating the tumor heterogeneity.

For the clinical translation of CAR T cell therapies, *in vivo* models are ultimately required to assess their efficacy and safety. Several types of murine models have become widely accepted for the evaluation of CAR T cells, which are discussed in detail in focused reviews (Si et al. 2022; Duncan, Dunbar, and Ishii 2022).

Immune-compromised mouse models are commonly used to evaluate the performance of human CAR T cells against human tumors. Most *in vivo* studies rely on injecting human cancer cell lines into NOD/SCID/γ-chain knockout (NSG) mice, lacking T, B, NK, and dendritic cells. Mice with established xenografts are then treated with human CAR T cells. This setup is used to model both blood cancers (following intravenous injections of cancer cells) and solid tumors (typically established via subcutaneous injections). These models are used to assess the ability of CAR T cells to recognize and kill tumor cells under *in vivo*

conditions. In addition to cell line-derived xenografts (CDX), patient-derived xenografts (PDXs) can be used to further model the heterogeneity observed in clinical tumor samples, which are used as starting material for injection into immune-deficient mice (Y. Liu et al. 2023a).

While xenograft models are widely used to evaluate novel CAR T cells designs, they do not recapitulate the interactions between CAR T cells and the host immune system. Humanized mouse models can address this issue. For that, immune-compromised mice are implanted with human CD34-positive hematopoietic stem cells leading to the development of human immune cells in the mice. Thus, humanized mice help to evaluate human CAR T cells in the context of an intact immune system. However, establishing this model is time-consuming and requires obtaining human stem cells, while the mice still lack human stromal cells.

Syngeneic tumor models allow studying CAR T cells within an intact immune system as well as stromal cells. In addition, transgenic mouse models, in which mice are genetically engineered to express a specific human antigen, further offer a possibility to study the exact same CAR receptor, intended for targeting human cells, in the immune-competent mice. However, both syngeneic and transgenic models require the use of murine instead of human CAR T cells, which can limit the clinical relevance of the findings.

Non-murine models for studying CAR T cells involve dogs and non-human primates (Duncan, Dunbar, and Ishii 2022) and are particularly important for assessing CAR T cells against new antigens to assess on-target off-tumor toxicity. However, the use of these animals involves extremely high costs as well as additional ethical concerns.

In summary, multiple preclinical models have been developed to assess both the potential and challenges of CAR T cell therapy, some offering easier access and scalability (*in vitro* models and cell line xenografts) and others better mimicking the tumor environment (organoids, PDX, and immune-competent models). Although the results in preclinical models do not always translate to clinical outcomes, these models are essential for testing the performance of novel CAR T cell designs and for investigating biological mechanisms by which CAR T cell modifications enhance their functions.

1.3 Thesis aims

Summary. CAR T cells are pioneering the vast potential of synthetic cell therapies. They are already saving lives of numerous patients with certain blood cancers and are on track to become first-line therapy. There is also great hope that CAR T cells will revolutionize the treatment of solid cancers and autoimmune diseases. But numerous challenges remain, and the field requires the tools to develop and optimize CAR T cells systematically and at scale.

Rationale. Certain T cell intrinsic processes could limit CAR T cell therapy. An important goal for understanding CAR T cell biology and improving their therapeutic efficacy across various applications will thus be the identification and removal of these barriers. Given that CAR T cells are already genetically engineered, additional genetic modifications constitute a natural approach to remove such biological roadblocks. Thus, CRISPR screens could be employed for systematic optimization of CAR T cells.

Aims. The objectives of the present doctoral study were as follows:

1. Develop a technology platform for CAR T cell optimization through genetic screens.
2. Create a comprehensive dataset of genome-wide CRISPR screens in human CAR T cells.
3. Discover and validate genetic perturbations to enhance CAR T cells.

2 Results

The manuscript included below follows the aims outlined for this thesis, including:

1) Technology development for screens in human primary CAR T cells (Fig. 1, S1);

2) Data from genome-wide fitness and FACS-based screens (Fig. 1-2, S2-6);

3) Hit prioritization through *in vivo* screens (Fig. 3, S7-8);

4) Individual validation of genetic perturbations in mouse tumor models, identifying RHOG knockout as a potent booster of CAR T cells (Fig. 4, S8);

5) Mechanistic investigation of RHOG knockout effects in CAR T cells (Fig. 5, S9);

6) Combinatorial screens and tiling base editing screens for further identification and characterization of beneficial genetic modifications in CAR T cells (Fig. 6, S10-11).

The supplementary tables can be found in a shared folder Supplementary Tables[1] (encrypted with the following file password: CarTScreening!2025) and will be published along with the presented manuscript.

The author of this thesis, Eugenia V Pankevich, contributed as a shared first author by conceptualizing, designing, planning, executing, and supervising experiments and analyses conducted by multiple team members, as well as preparing the draft and revised versions of the manuscript and figures.

[1]Full web-link: https://1drv.ms/f/s!AgQVlfawXAOYguQiZi2vbXh4E_PuMg?e=ey8wtB

Systematic discovery of CRISPR-boosted CAR T cell immunotherapies

Paul Datlinger[1,3,4*], Eugenia V. Pankevich[1,4], Cosmas Arnold[1,4], Nicole Pranckevicius[1], Jenny Lin[1], Daria Romanovskaia[1], Moritz Schäfer[1,2], Francesco Piras[1,2], Anne-Christine Orts[1], Amelie Nemc[1], Paulina Biesaga[1], Michelle Chan[1], Teresa Neuwirth[1], Artem V. Artemov[2], Wentao Li[1], Sabrina Ladstätter[1], Thomas Krausgruber[1,2], and Christoph Bock[1,2*]

[1] CeMM Research Center for Molecular Medicine of the Austrian Academy of Sciences, Vienna, Austria
[2] Medical University of Vienna, Institute of Artificial Intelligence, Center for Medical Data Science, Vienna, Austria
[3] Present address: Arc Institute, Palo Alto, USA
[4] These authors contributed equally: Paul Datlinger, Eugenia V. Pankevich, Cosmas Arnold

[*] Correspondence: Paul Datlinger (paul.datlinger@outlook.com), Christoph Bock (cbock@cemm.oeaw.ac.at)

Abstract

CAR T cell therapy has shown remarkable success in treating blood cancers, but therapies often fail due to intrinsic T cell dysfunction. Here we present CELLFIE, a CRISPR screening platform for enhancing CAR T cells across multiple clinical objectives. We performed genome-wide screens in human primary CAR T cells, with readouts capturing different aspects of T cell biology, including proliferation, target cell recognition, activation, apoptosis and fratricide, and exhaustion. Top hits were validated and prioritized using a novel pooled *in vivo* screening method in a xenograft model of human leukemia, establishing several gene knockouts that boost CAR T efficacy. Among these, RHOG knockout emerged as a potent and unexpected CAR T cell enhancer, both individually and together with FAS knockout, which we validated in multiple *in vivo* models, CAR designs, and patient-derived cells. Demonstrating the versatility of the CELLFIE platform, we performed combinatorial screens to identify target gene pairs, and tiling base editing screens to further characterize RHOG variants. In summary, we discovered, validated, and biologically characterized CRISPR-boosted CAR T cells that outperform standard CAR T cells in widely used benchmarks, and established a foundational resource for optimizing and enhancing cell-based immunotherapies.

Keywords: Cancer immunotherapy, human primary cell engineering, next-generation cell therapy, CAR T cells, CRISPR screens, mRNA technology, *in vivo* screens, CROP-seq, high-throughput biology, systems immunology

Introduction

CAR T cell therapy constitutes a groundbreaking advance in cancer treatment, and the first example of genetically engineered cells as widely used therapeutics. Beyond clinically approved and routinely prescribed CAR T cell products for certain blood cancers[1,2], CAR T cells hold great potential for solid tumors[3,4], autoimmune diseases[5], tissue regeneration[6], and other applications. It is a grand challenge of cell-based immunotherapy to optimize and validate CAR T cells for their many potential uses.

Important obstacles to CAR T cell efficacy have surfaced from clinical trials and preclinical studies[7]: (1) T cell fitness and proliferation are often insufficient for sustained treatment efficacy. (2) Heavily pre-treated patients with a compromised immune system may not provide sufficient T cells for CAR T cell production. (3) Chronic stimulation of the CAR can lead to T cell dysfunction and exhaustion. (4) The *in vivo* cellular environment is often immunosuppressive and devoid of key nutrients, which can induce CAR T cell inhibition and apoptosis. (5) CAR T cells have a tendency to kill each other (fratricide), following the uptake of target antigen by trogocytosis, which weakens the anti-cancer response and may help cancer cells avoid detection by removing antigen from their cell surface[8].

This study is based on the premise that roadblocks of CAR T cell therapy may be overcome by disabling biological functions that evolved to prevent T cell autoimmunity but impede CAR T cell performance. As products of cell

engineering, CAR T cells have not been optimized by evolution, and certain genes that are important for normal T cell function may not only be dispensable but actively detrimental for the anti-cancer effect of CAR T cells. This hypothesis is supported by the serendipitous finding that deletion of TET2 rendered a single CAR T cell clone highly effective in a patient with leukemia[9]; by studies that demonstrated improved CAR T cell efficacy upon knockout of immune checkpoints PD1[10] and CTLA4[11], epigenetic regulator PRDM1[12], signaling protein RASA2[13], and mediator complex subunits MED12 and CCNC[14]; and by studies that enhanced CAR T cell function through the overexpression of transcription factors with a regulatory role in T cells including c-Jun[15] and FOXO1[16,17].

Given that CAR T cells are genetically modified cell products, CRISPR gene editing and genetic screening constitutes a natural, clinically translatable approach for their systematic optimization and customization to a broad range of applications[14,18,19], building on similar screens in human primary T cells[13,20–22]. Genome-wide screens with clinically relevant readouts thus provide a scalable method of "artificial evolution" to select perturbations that enhance CAR T function, and effective screening in CAR T cells may facilitate the development of new therapies.

Here we introduce CELLFIE, a discovery platform for developing CRISPR-boosted CAR T cell therapies with high-content genetic screening, and we demonstrate our platform's utility by engineering CAR T cells that strongly outperform standard CAR T cells in widely used *in vivo* models. CELLFIE addresses several challenges that have held back CRISPR screening in human primary CAR T cells, including efficient co-delivery of three components (CAR, gRNA library, CRISPR editor), the difficulty of condensing clinical limitations of CAR T cell therapy into screenable readouts, and the limiting factors of cost and throughput for genome-wide screens. We further demonstrate *in vivo* CRISPR screening in a mouse model of CAR T cell therapy by adapting our CROP-seq method[23], and we identified RHOG, PRDM1, and FAS knockouts as boosters of CAR T cell efficacy *in vivo*. Moreover, our combinatorial screens and individual validations discovered and confirmed double knockouts that further enhance CAR T cell performance, including the RHOG-FAS combination, which strongly enhanced anti-tumor activity.

RHOG in particular is an unexpected discovery given that RHOG deficiency in humans causes a monogenic form of immunodeficiency[24]. We characterized the effect of RHOG knockout on CAR T cells and observed enhanced proliferative capacity, explaining the improved efficacy of RHOG knockout CAR T cells. We further established tiling base editing screens in human primary CAR T cells and used this method to quantify the biological effects of mutating individual amino acids throughout the RHOG protein, and to identify functional missense mutations in RHOG for safe clinical translation without inducing double-strand breaks.

In summary, we present the first integrated platform for CRISPR screening in primary immune cells, supporting all phases of CAR T cell screening, including genome-wide discovery screens, *in vivo* pooled screens for hit validation, combinatorial screens for identifying gene knockout pairs with enhanced efficacy, and preclinical development with tiling base editing screens. The CELLFIE platform enabled us to create the most comprehensive resource of CAR T cell perturbation screens to date, based on which we systematically identified gene edits that enhance CAR T cell performance, including the discovery of RHOG knockout as CAR T cell booster.

Results

A versatile and highly scalable discovery platform for genetic screens in CAR T cells

Our CELLFIE platform ("cell engineering for immunotherapy enhancement") uses human peripheral blood or patient-derived apheresis product as starting material and introduces three components to create CAR T cells for high-content CRISPR screening: (1) a chimeric antigen receptor, (2) a CRISPR editor for genome engineering, and (3) a library of CRISPR gRNAs encoding genetic perturbations (Fig. 1a). Both the CAR and the gRNA need to be stably retained to enable CRISPR screening in CAR T cells. We co-deliver them on a single lentiviral vector that integrates into the genome, providing high expression of the CAR for effective cancer cell killing and enabling a sequencing-

based readout of the gRNA-encoded perturbations. In contrast, CRISPR nucleases or base editors need to be induced only briefly, and we provide them as synthetic mRNAs, prepared by flexible and cost-effective *in vitro* transcription.

Lentiviral delivery of the CAR and gRNA employs our CROP-seq technology[23], which provides built-in support for pooled, arrayed, single-cell, and spatial CRISPR screening. Specifically, we designed a CROP-seq-CAR lentiviral transfer plasmid that uses the EF1α promoter to transcribe the CAR, followed by a P2A self-cleaving peptide and a puromycin resistance gene. In CROP-seq, the gRNA is placed inside the lentiviral 3' LTR, just before the vector's polyadenylation signal. There, it becomes part of the highly expressed CAR-P2A-Puro transcript and is readily detected by bulk and single-cell RNA-seq assays. The gRNA cassette is also duplicated to the 5' LTR during lentiviral integration and transcribed from a polymerase III promoter for effective genome editing. This way, our vector simultaneously achieves high genome editing performance and efficient sequencing-based readout of the gRNA.

We used a 19-BBz CAR composed of a leader peptide, a single-chain variable fragment (scFv) antibody binding CD19 (clone FMC63), the trans-membrane domain of CD8, the intracellular co-stimulatory domain of 41BB, and the CD3ζ chain (Table S1a). This CAR closely resembles tisagenlecleucel (Kymriah), which is approved for treating certain types of B cell leukemia and lymphoma. Importantly, our vector was designed for flexibility and modularity, enabling straightforward exchange for other CARs or TCRs.

CELLFIE employs mRNA technology[25] to deliver the CRISPR editors, which avoids the inefficiencies of lentivirus production and delivery of large transgenes into primary T cells. At the same time, mRNA delivery is more versatile than the use of recombinant proteins, especially given the limited commercial availability of CRISPR editors other than Cas9 and high setup cost for custom purified proteins. Inspired by mRNA vaccine technologies[25], we developed an optimized workflow to produce any CRISPR editor as electroporation-ready mRNA with standard laboratory equipment (Fig. S1a). Specifically, the CRISPR editors are cloned into our mRNA production vector, which contains 5' and 3' untranslated regions to stabilize the mRNA, and the mRNAs are produced by *in vitro* transcription from a T7 promoter with co-transcriptional capping, and terminated by a hardcoded A-tail of 55 bases. Optionally, modified bases such as 5-methoxy-U can be incorporated to optimize mRNA properties[26]; however, this increases the cost of mRNA production and was not necessary in our screens. We designed mRNAs for a broad range of CRISPR editors and selection markers, establishing a versatile toolbox for gene engineering in CAR T cells (Fig. S1b-c, Table S1b).

To quantify the efficiency of CRISPR knockout using our platform, we transduced human primary T cells with a single gRNA targeting the IL2RA gene (which codes for CD25) and electroporated Cas9 mRNA. Genome editing efficiency exceeded 80% across multiple blood donors, as measured on the DNA level by amplicon sequencing and on the protein level by flow cytometry (Fig. S1d). Our custom-made mRNA achieved consistent editing efficiency comparable to commercially available Trilink Cas9 mRNA, at a tenfold lower cost (Fig. S1e, S2a-b).

Our CELLFIE platform also provides support for various CRISPR modalities including knockout, base editing, and activation, facilitated by our flexible mRNA production and delivery workflow. For base editing, we tested the A-to-G editor ABEmax and the C-to-T editor AncBE4max[27], as well as their near-PAMless variants based on SpRY, which provide greatly extended targeting space[28]. We tested multiple genomic loci and observed base editing efficiencies above 75% for the A-to-G editors and up to 50% for the C-to-T editors (Fig. S1f), introducing precise mutations within a narrow editing window (Fig. S1g). This performance is similar to the original studies, which is remarkableas our experiments tackled the harder task of editing primary cells, compared to cell lines in the original publications. While knockouts and base edits are established once and stably retained in DNA, our platform is also compatible with CRISPR-based epigenetic editing and modulation of gene regulation. In particular, we tested the efficiency of CRISPR activation (CRISPRa) using the Synergistic Activation Mediator (SAM) system[29], and we achieved strong activation of CD34 at the protein level in up to 50% of CAR T cells (Fig. S1h).

To enable genome-wide, multi-readout CRISPR screens, we performed extensive optimization experiments (summarized in Supplementary Note 1), which established highly efficient CAR T cell culture, cell stimulation, lentiviral

transduction, gRNA integration, mRNA electroporation, and cell selection (Fig. S2). We also confirmed that CAR T cells generated with our optimized discovery platform expressed the anti-CD19 CAR on their surface (Fig. S2p) and achieved highly effective and specific killing of CD19-positive cancer cell lines (Fig. S2q).

In summary, we developed a platform for flexible and efficient production and genome editing of human primary CAR T cells, which supports genome-wide genetic screening with a broad range of CRISPR-based perturbations.

Genome-wide CRISPR knockout screens of CAR T cell fitness

Treatment failure in CAR T therapies is often associated with impaired cell fitness, affecting cellular phenotypes such as proliferation, persistence, exhaustion, and dysfunction. We sought to address these challenges using the CELLFIE platform, in a series of CRISPR screens with cell proliferation and survival readouts (Fig. 1b).

Freshly isolated human primary T cells were stimulated with anti-CD3 and anti-CD28 antibodies and expanded for 7 to 10 days, followed by restimulation, lentiviral transduction, and electroporation of Cas9 mRNA together with mRNA conferring blasticidin resistance. Cells were then subjected to puromycin and blasticidin to select for successful lentiviral transduction and mRNA electroporation. We validated the feasibility of proliferation-based screens in a pilot experiment using a library of positive controls (gRNAs targeting the puromycin resistance gene PAC) and negative controls (gRNAs targeting a safe harbor locus). Reassuringly, we observed strong and selective depletion of the positive control gRNAs during culture with puromycin, in both CD4 and CD8 CAR T cells (Fig. S3a).

For genome-wide CRISPR knockout screening, we cloned the widely used Brunello gRNA library[30] into the CROP-seq-CAR vector, confirmed a balanced gRNA representation by amplicon sequencing (Fig. S3b), and conducted genome-wide screens in CAR T cells derived from four blood donors (Fig. S3c). After expansion and genome editing, the CAR T cells were stimulated either via their endogenous TCR using anti-CD3/CD28 beads or via their transduced CAR through repeated exposure to CD19-positive K562 cancer cells (Fig. 1b, S3c, Table S2).

Our screens recapitulate important cell-intrinsic limitations of CAR T cells. First, we observed slower expansion upon CAR stimulation than upon TCR stimulation (Fig. S3d), consistent with the lower effectiveness of CAR signaling[31]. Second, we detected high levels of CD19 antigen on the CAR T cells, which can be explained by acquisition of membrane components from their target cells through trogocytosis (Fig. S3e). The resulting CD19 antigen on CAR T cells prompts killing by other CAR T cells (fratricide), a known challenge in T cell immunotherapies[8]. Third, the CAR T cells upregulated certain markers of T cell exhaustion including PD1, LAG3, TIM3 and TIGIT (Fig. S3f), which has been linked to poor clinical performance[32]. These characteristics suggest that CRISPR screens using our setup may be able to identity gene knockouts that enhance CAR T cell function across multiple dimensions.

The technical quality of our genome-wide CRISPR screens was consistently high, with strong depletion of known essential genes compared to non-essential genes (Fig. S3h), outperforming comparable screens in primary human T cells that used the Brunello library[13,18,20] (Fig. S4a-f). Together with the dataset by Freitas et al.[14], our screens are approaching the quality of screens in the Jurkat cell line[33], despite the challenges of screening in human primary cells rather than in a cancer cell line. Our screening hits were enriched for immune cell functions including T cell activation, differentiation, and apoptosis, and for general cell functions such as cell cycle, splicing, RNA transport, and translation (Fig. 1c-d, S3i). Focusing on the T cell receptor pathway, both TCR and CAR stimulation required signaling through the IL2 receptor, including IL2RG, JAK3, and the co-receptor CD4 (Fig. 1e). Our screens also captured more subtle aspects of TCR signaling, including positive and negative regulation. For example, the positive co-receptor CD28 was strongly depleted, while its negative counterpart CTLA4 was enriched (Fig. 1e). As expected, the TCR subunits CD3E and CD3D were essential only in TCR-stimulated samples, where they are activated by the bead-bound anti-CD3 antibody. Our screens thus identified many expected and biologically plausible genes and processes, validating the dataset as a promising resource for studying TCR and CAR signaling.

To identify potential boosters of T cell or CAR T cell therapies, we analyzed our screening data with the MAGeCK MLE algorithm and selected knockouts with strong enrichment upon stimulation of the CAR, or of both CAR and TCR (Fig. 1f-g, in green). Supporting the quality of our dataset, this analysis re-discovered CTLA4, a well-established immune checkpoint inhibitor, and PRDM1, an epigenetic factor implicated in terminal T cell differentiation and a known suppressor of T cell activity; both knockouts have been reported to enhance CAR T cell efficacy[11,12].

In summary, we demonstrated genome-wide screening in human primary CAR T cells exposed to an *in vitro* model of cancer cell killing over a three-week time course that recapitulates important challenges of CAR T cell immunotherapy, and we identified both known and novel targets for the genetic enhancement of CAR T cell therapy.

Genome-wide screening with FACS readouts of CAR T cell biology

Complementing the cell proliferation and survival readout of our genome-wide fitness screens (Fig. 1), we established FACS-based readouts for six cellular markers and four biological processes that constitute established clinical limitations of CAR T cell therapy (Fig. 2a): (1) We exploited the above-mentioned phenomenon of trogocytosis to devise a marker of cumulative target cell recognition, by measuring the amount of CD19 that individual CAR T cells have taken up from their target cells. (2) We used CD69 expression as a marker of T cell activation, allowing us to select for T cells with elevated signaling or reduced negative co-regulation. (3) We sorted for expression of the cell death receptor FAS, which is markedly upregulated upon TCR stimulation, to identify knockouts that reduce the detrimental effect of apoptosis and fratricide in CAR T cell therapy. (4) Given the elevated expression of several T cell exhaustion markers in our co-culture system, we used a combined PD1, LAG3, and TIM3 readout to screen for modulators of these early exhaustion indicators. While these markers cannot capture the full complexity of CAR T cell function *in vivo*, they allow us to assay specific aspects of CAR T cell biology through genome-wide screens.

To establish robust genome-wide screening for each of these FACS readouts, we measured the surface protein expression on CAR T cells by flow cytometry and defined sorting thresholds for marker-positive and marker-negative cells (Fig. 2b, left). We observed strong uptake of CD19, induction of CD69, and FAS expression for all CAR T cells, as well as upregulation of PD1, LAG3, and TIM3 in a subset of CAR T cells. We further validated these markers across three CARs with different antigen recognition and intracellular domains (Fig. S5a-d) and observed consistent results supporting the broad utility of these FACS readouts for identifying modulators of CAR T cell function, except for CD19 uptake (which is affected by CAR affinity and target antigen expression). We validated our sorting strategy in a series of mini-screens with a gRNA library targeting each marker gene with 20 gRNAs. We observed strong enrichment of targeting gRNAs in the marker-negative population and depletion in the marker-positive population (Fig. 2b, right), thus confirming the utility of these markers as screenable readouts.

Using our optimized FACS-based screening platform (Supplementary Note 1, S5e-i, S6c-d), we performed 45 genome-wide CRISPR screens, with four readouts, twelve sorted cell populations, two cell types (CD4 and CD8 CAR T cells), and cells derived from multiple blood donors (Fig. 2c, S5j, S6a-b, Table S3). Data quality was consistently high, as illustrated by the strong enrichment of gRNAs targeting the FACS markers in the marker-negative populations (Fig. 2d). We conducted a statistical analysis focusing on four CAR T cell populations with potentially beneficial properties: ‘CD19 high’ (increased target cell recognition), ‘CD69 high’ (strong CAR T cell activation), ‘FAS very low or absent’ (reduced apoptosis/fratricide), and ‘PD1 / LAG3 / TIM3 triple-negative' (low early exhaustion indicators) (Fig. 2e), aiming to identify gene knockouts that modulate these complementary aspects of CAR T cell biology. We also incorporated the data from our genome-wide fitness screens in this integrated analysis (Fig. 1).

Using stringent statistical thresholds, we selected 43 gene knockouts from our 58 *in vitro* screens, 25 of which were shared across several screens (Fig. 2e-f, S4g). In addition to new targets that we investigated further, our analysis re-discovered known modulators of T cell and CAR T cell function, including the immune checkpoint regulators

PD1 (PDCD1), CTLA4, TIM3 (HAVCR2), and TIGIT, solely based on genome-wide CRISPR screening and without any prior biological knowledge going into the experimental or computational analyses. These are all clinically validated targets of immunotherapeutic drugs, which underscores the discovery power of the CELLFIE platform.

In summary, we conducted genome-wide fitness screens and genome-wide FACS-based screens at unprecedented scale, addressing key challenges of CAR T cell therapies. These screens uncovered gene knockouts that enhance CAR T cell performance, and they provide a rich dataset for studying regulators of T cell and CAR T cell biology.

In vivo CROP-seq screening to validate and prioritize CAR T boosters in mice

To validate the hits from our *in vitro* screens, we extended the CELLFIE platform to support pooled *in vivo* screening in xenograft mice (Fig. 3a), which offer a more physiologically relevant model and remain the gold standard for preclinical CAR T cell evaluation. We injected 0.5 million human CD19-positive NALM6 cells into immunodeficient NSG mice, which induced systemic leukemia that the mice succumbed to after three weeks when left untreated (Fig. S8a-b). To evaluate our CRISPR-boosted CAR T cells, we injected 1 million anti-CD19 CAR T cells on day 5 of the leukemia model. These CAR T cells were prepared as for the *in vitro* screens, with lentiviral co-delivery of the CAR and a gRNA library. The CAR T cell dose was chosen to induce a suboptimal response with initial leukemic cell clearance followed by swift relapse (Fig. S8a-b). While higher doses can be curative in this model, our dose leaves room to screen for knockouts that enhance the therapeutic response. We collected spleen and bone marrow on day 9 (initial treatment) and day 21 (prolonged treatment) after CAR T cell injection, dissociated the organs, and sequenced the gRNAs to determine which gene knockouts enhanced CAR T cell survival and proliferation (Fig. 3a).

To enable robust *in vivo* screening with the CELLFIE platform, we needed to overcome major technical hurdles that have so far prevented the broad adoption of *in vivo* screens in cancer immunology. First, the low frequency of CAR T cells in the collected organs led to extremely poor gRNA amplification efficiency from genomic DNA in our pilot experiments, with near-zero gRNA alignment rates (Fig. 3c). A nested primer design for genomic DNA yielded only marginal improvements. We thus developed a new method for *in vivo* screening in primary cells based on the CROP-seq technology[23], exploiting the method's incorporation of the gRNA into a highly expressed mRNA transcript. *In vivo* CROP-seq thus replaces the conventional DNA readout of gRNA sequences by an mRNA readout, profiting from the high copy number of gRNA-containing mRNAs (Fig. 3b, S7a-b). We amplified gRNAs from reverse-transcribed mRNA using nested PCR and routinely reached over 90% gRNA alignments in pooled *in vivo* screens (Fig. 3c, S8c). Second, *in vivo* screens are affected by strong cell population bottlenecks, clonal competition, and random drift, which can obscure biological signals if not carefully controlled for. Therefore, we equipped the CROP-seq-CAR construct with unique molecular identifiers (UMIs) and developed a sequencing strategy to read the UMI along with the gRNA (Fig. 3b, S7b). Third, while UMIs are critical for *in vivo* screening, it is difficult to maintain plasmids with high-complexity UMIs over time. We thus devised a cloning method that combines a high complexity UMI on a constant oligonucleotide with the gRNA library to maximize UMI diversity (Fig. S7a).

We used our *in vivo* CROP-seq method to validate the identified boosters of CAR T cell performance (Table S5), which we selected from the fitness screens (Fig. 1) and FACS-based screens (Fig. 2) using strict statistical thresholds (normalized MAGeCK MLE $\beta > 0.99$ for the fitness screens and $\log_2FC > 2$, FDR < 0.05 for the FACS-based screens), and we filtered for genes that are robustly expressed in CAR T cells (Fig. S6e, Table S7). Each gene was targeted with eight gRNAs, and we included gRNAs targeting known essential genes and non-essential olfactory receptor genes as controls. We performed the screen for all 39 target genes in 20 mice (5 mice per T cell donor and per time point), reducing the animal numbers by ~20-fold in comparison to individual knockout validation.

Supporting the high quality of our *in vivo* screens, we observed strong depletion of the essential genes (POLR2L, PSMB4, RPL8) across organs and time points, and neutral fold changes with low noise for the non-essential genes (OR4C6, OR10G4, OR14J1) (Fig. 3d, S8d). Using the UMIs for clonal analysis, we detected thousands of individual

CAR T cell clones for each donor, indicating strong engraftment and adequate screening coverage (Fig. 3e-f). We also used the UMIs to create internal replicates within each screen[34], which substantially improved sensitivity (Fig. S8d-f). With stringent statistical thresholds ($log_2FC > 1.5$ and FDR < 0.01), our *in vivo* CROP-seq screens consistently identified three gene knockouts as boosters of CAR T performance for both spleen and bone marrow: FAS, PRDM1, and RHOG; and a fourth gene knockout (CDKN2A) was specifically enriched in bone marrow (Fig. 3d, right, Table S5). Notably, these genes would have been missed by standard analysis without internal replicates (Fig. 3d, left), highlighting the importance of UMIs for successful *in vivo* screening.

FAS is a cell death receptor highly expressed in CAR T cells and linked to FasL-induced apoptosis, and its expression has been shown to limit CAR T cell efficacy, driven at least partially by FAS interaction with FasL on the CAR T cells themselves[35]. PRDM1 is an epigenetic regulator whose knockout is known to enhance CAR T cell persistence, likely because of altered T cell differentiation in PRDM1 knockouts[12,19]. Our screen supports the positive *in vivo* effect of PRDM1 knockout in CAR T cells. The third gene, which codes for the GTPase, RHOG, is a novel and unexpected hit emerging from both our *in vitro* and *in vivo* screens. RHOG has previously been linked to a monogenic form of immunodeficiency[24], where its knockout appears to be detrimental to normal immune function. In contrast, we observed a strong beneficial effect of RHOG knockout in CAR T cells. The knockouts of FAS, PRDM1, and RHOG dominated the CAR T cell response and collectively accounted for 25% of all CAR T cells on day 21 post injection, with a clear upward trend (Fig. 3g). We thus focused on the FAS, PRDM1, and RHOG knockouts to further investigate the effect of these promising boosters of CAR T cell therapy.

RHOG, FAS, and PRDM1 knockouts enhance CAR T cell therapy in vivo

To validate and quantify the therapeutic benefit of RHOG, FAS, and PRDM1 knockout in CAR T cells, we treated NALM6 tumor-bearing mice with a further reduced dose of 0.6 million CAR T cells, which led to an initial therapeutic response followed by early relapse for standard (safe harbor locus-edited) CAR T cells (Fig. 4a, S8a-b).

We first produced knockout CAR T cells with each gene targeted by all 8 gRNAs from our *in vivo* screens (Fig. 4b, left, Fig. S9a) and compared CAR T cells with individual knockouts for RHOG and PRDM1 against standard CAR T cells (Fig. 4c-e). Leukemic cell load and therapeutic response were monitored by frequent *in vivo* imaging of the luciferase-expressing leukemia cells. PRDM1 knockout CAR T cells achieved better initial leukemic cell clearance than the control CAR T cells, peaking at a ~20-fold reduction of leukemic cell load. The positive effect of PRDM1 knockout CAR T cells aligns with previous reports[12,19]. However, PRDM1 knockout CAR T cells could not significantly delay relapse and death of the treated mice in this model (Fig. 4f). In contrast, RHOG knockout CAR T cells achieved striking leukemic cell clearance and a sustained response, which significantly extended the survival compared to both PRDM1 knockout and standard CAR T cells (Fig. 4f-g).

Encouraged by the ability of RHOG knockout CAR T cells to boost the therapeutic response above and beyond the well-validated PRDM1 knockout, we performed a second set of experiments with RHOG and FAS knockouts as well as standard CAR T cells (Fig. 4h-j). We chose the top-performing gRNA from our focused screen (Fig. S9b, Table S1) and delivered the gRNA in complex with the Cas9 protein by ribonucleoprotein (RNP) electroporation (Fig. 4b, right), while the anti-CD19 CAR was separately delivered with a lentiviral vector, following an approach previously used for CRISPR knockout in clinical CAR T cell production[10]. RHOG and FAS knockout CAR T cells clearly outperformed standard CAR T cells also in these experiments (Fig. 4h-j).

The beneficial effect of FAS knockout in CAR T cells is consistent with previous reports[35–38] and with the use of FAS knockdown in CAR T cells against ovarian cancer in an ongoing clinical trial (NCT05617755). RHOG knockout CAR T cells achieved a similar or even better reduction of the leukemic cell load compared to FAS knockout and had a similar effect on overall survival. Moreover, we discovered a strong combined effect when knocking out RHOG and FAS (Fig. 4h-i, in blue), greatly extending survival compared to both single knockouts (Fig. 4j). Notably,

this was also observed when using CAR T cells produced from a cancer patient scheduled to receive CAR T cell therapy (Fig. S8i). Treatment with RHOG-FAS knockout CAR T cells was curative in two mice with over 200 days of remission (Table S6), while the leukemia was rapidly and universally fatal in mice treated with standard CAR T cells (Fig. S8j). When the CAR T cell dose was doubled, RHOG knockout alone was also curative (Fig. S8k). Supporting the safety of the RHOG and RHOG-FAS knockout CAR T cells, long-term surviving mice were followed up to 392 days after CAR T cell treatment without evidence of malignant transformation (Fig. S8l).

Finally, we tested the effect of RHOG knockout in CAR T cells across several CAR designs. We found that RHOG knockout led to elevated expansion of both T cells and CAR T cells *in vitro* (Fig. S8m) and improved leukemia clearance *in vivo* not only for 19-BBz but also for 19-28z and GD2-BBz CAR T cells (Fig. S8n-o), underlining the beneficial effects of RHOG knockout across CARs targeting different antigens or containing different intracellular signaling domains. The RHOG and FAS knockout combination also led to improved tumor clearance in a solid tumor model of subcutaneously injected Huh7 cancer cells treated with GPC3-BBz CAR T cells (Fig. S8p).

In summary, all three top hits (RHOG, FAS, PRDM1) of our *in vivo* screens were successfully validated, underlining our method's reliability. We confirmed the strong and surprising effect of RHOG knockout in multiple independent experiments, nine sample donors including a patient scheduled for CAR T cell therapy, two CAR T cell production protocols, and multiple RHOG gRNAs, with highly consistent results (Fig. 4, S8g-p, S9a-c, Table S6). Finally, we established the combined knockout of RHOG and FAS as an attractive strategy to enhance CAR T cell performance.

RHOG knockout enhances proliferation and persistence of CAR T cells

These promising results prompted us to investigate the biological roles of RHOG in CAR T cells, which remain entirely unexplored. RHOG is known to play a role in normal T cells in the context of immune synapse formation, cytoskeleton modulation, TCR stimulation, T cell proliferation, and T cell anergy[39]. RHOG deficiency can cause inborn errors of immunity with abrogated cytotoxic function of T lymphocytes in humans[24], and reduced T cell signaling[40]. These observations make RHOG an unexpected target for enhancing CAR T cell performance. At the same time, RHOG aligns remarkably well with the foundational hypothesis of our study, that CAR T cells are handicapped by genes with critical roles in normal T cells, but with detrimental effects on CAR T cell function.

We characterized RHOG knockout CAR T cells in terms of their molecular and cellular properties (Fig. 5, S9). We conducted a time series experiment where RHOG knockout CAR T cells and standard (safe harbor locus edited) CAR T cells were repeatedly exposed to CD19-positive cancer cells over 10 days (Fig. 5a). CD4 and CD8 CAR T cells were profiled by flow cytometry and RNA-seq at time points corresponding to acute stimulation (day 1 and day 3 after first target cell encounter) as well as chronic stimulation (day 7 and day 10, following 2 and 3 rounds of target cell stimulation, respectively). We first investigated the effect of the RHOG knockout on CAR T cell differentiation status, which has emerged as a predictor of long-term expansion capacity and CAR T cell performance in the clinic[41]. We measured the T cell differentiation markers CD62L and CD45RO using flow cytometry over 10 days of CAR T cell co-culture with cancer cells and observed an increased fraction of $CD62L^+$ $CD45RO^+$ cells in RHOG knockout CAR T cells (Fig. 5b, S9g). These results suggest that RHOG knockout may shift CAR T cells toward a central memory phenotype, which could contribute to their observed proliferation advantage.

The RNA-seq profiles consistently clustered by time point (day 0, 1, 3, 7, 10), rather than by cell type (CD4, CD8) or donor, and differential expression analysis uncovered widespread differences between RHOG knockout and control CAR T cells (Fig. S9j-l, Table S7). We aggregated the differential gene expression on the level of biological processes using gene set enrichment analysis (Fig. 5c, S9m-n). RHOG knockout CAR T cells showed increased expression of genes associated with DNA replication and cell cycle, ribosome metabolism, and protein translation (Fig. 5c-d, S9m-n). These results support an elevated proliferative and biogenic capacity of RHOG knockout CAR T cells compared to standard CAR T cells. For the day-7 and day-10 samples, we further observed a strong increase

in the expression of S phase marker genes (Fig. 5e), suggesting a proliferative advantage of RHOG knockout CAR T cells that is maintained in the phase of chronic stimulation. This effect was observed in both CD4 and CD8 CAR T cells, indicating that RHOG knockout might be broadly beneficial across different CAR T cell subsets.

To further investigate the functional roles of the RHOG knockout in CAR T cells *in vivo,* we tested them in the NALM6 xenograft leukemia model, isolated spleen and bone marrow at day 15 after injection, and profiled CD4 and CD8 CAR T cells using flow cytometry (Fig. 5f). We found that the number of CAR T cells in both organs was strongly increased (sixfold for CD4 and tenfold for CD8 cells, Fig. 5g) and the expression of important markers of T cell exhaustion (LAG3, TIM3, TIGIT) was reduced (Fig. 5h), indicating that the RHOG knockout has a combined effect of increased CAR T cell persistence and reduced exhaustion in this *in vivo* model.

We also investigated the effect of RHOG knockout on other CAR T cell properties including cytotoxicity and T cell signaling. To that end, we profiled CAR T cell responses to *in vitro* stimulation with CD19-positive K562 cells using flow cytometry, but we did not observe statistically significant changes for any of the investigated markers including CD69 for T cell activation, CD107a for degranulation, IL2 production, and IFNγ production (Fig. S9h), suggesting that RHOG knockout does not alter these processes. The observations that RHOG knockout CAR T cells maintain their full killing ability (Fig. S9d) and their T cell signaling dynamics strengthen RHOG knockout as a strategy for boosting for CAR T cell therapy. Moreover, only FAS but not RHOG knockout led to decreased apoptosis levels (Fig. S9i), indicating that RHOG knockout acts through enhancing proliferation rather than survival.

In summary, we found that the strong positive effect of RHOG knockout on CAR T cell performance is driven by these cells' enhanced proliferative capacity, supported by a shift toward a central memory phenotype and reduced T cell exhaustion of the RHOG knockout CAR T cells *in vitro* and *in vivo* (Fig. 5i). Moreover, our results indicate that the RHOG and FAS knockouts have an additive positive effect on CAR T cells by acting through complementary mechanisms (increased proliferation by the RHOG knockout and increased survival by the FAS knockout).

Combinatorial screens identify double gene perturbations enhancing multiple CAR T cell designs

The high efficacy of RHOG-FAS double knockout CAR T cells highlights that targeting complementary aspects of CAR T biology can lead to strong combined effects. This finding prompted us to incorporate combinatorial screening as an additional feature into the CELLFIE platform. Leveraging the CROPseq-multi technology[42], we established a dedicated delivery vector that enables CAR T cell screens with defined combinations of two gene knockouts in the same cell (Fig. S10a). This is achieved through a single transcript containing two gRNAs, which are separated by tRNA sequences and cleaved into separate gRNAs by the endogenous tRNA processing system.

We selected the top gene knockouts identified by our *in vivo* screens (RHOG, FAS, PRDM1, CDKN2A, HAVCR2, CTLA4), along with three essential genes and safe harbor locus controls, and we designed a gRNA library with all combinations of two gRNAs per gene, resulting in a total of 238 knockout combinations (Fig. 6a-b). We cloned this gRNA library into our newly developed CROP-seq-CAR-multi vector, using three alternative versions with three CARs containing different antigen recognition (anti-CD19 FMC63 versus anti-GD2 14g2a scFV) and intracellular domains (41BB versus CD28). Performing *in vitro* fitness screens using these vectors, we confirmed efficient detection of gRNA combinations and recombination rates of 12.5%, which is close to previously reported numbers (Fig. S10b-c). Consistent with previous research, we noted a positional effect on gRNA efficiency, with stronger depletion of essential genes when targeted by the second gRNA in the array (Fig. 6c, S10d).

These screens validated the strong performance of RHOG-FAS double knockout CAR T cells across all three CAR designs (Fig. 6c-d, S10e), confirming the beneficial effect of this dual perturbation for several CAR T cell designs. Moreover, we identified new knockout combinations with the potential to further enhance CAR T cells (Fig. 6c-d,

S10f). In summary, we successfully established combinatorial screens as another feature of the CELLFIE platform, underlining its versatility and expanding its utility to the discovery of combined gene perturbations in CAR T cells.

Tiling base editing screens functionally characterize RHOG and prioritize gene edits for clinical translation

Through multiple screens and validation experiments, we established RHOG knockout as a promising way to enhance CAR T cell performance, both alone and together with FAS knockout. While CRISPR nucleases are effective discovery tools, their reliance on double-strand breaks pose safety risks for clinical translation. CRISPR base editing, where individual bases in the DNA are enzymatically modified[43], may provide a safer alternative. Moreover, tiling base editing screens enable protein function characterization with a "biochemistry by sequencing" approach[22,44–47]. Exploiting our platform's support for various CRISPR base editors, we thus performed tiling base editing screens with mutational scanning of RHOG to characterize gene function and evaluate gRNAs for future clinical translation.

We designed a gRNA library with 3,756 base editing gRNAs (Fig. 6e), tiling the gene body of RHOG with 1,169 gRNAs. We also included 1,140 gRNA tiling the antibiotic resistance gene puromycin N-acetyltransferase (PAC), positive control gRNAs that induce nonsense and splice-site mutations in genes we identified as essential in CAR T cells, and negative control gRNAs targeting a safe harbor locus. We cloned this gRNA library into our CROP-seq-CAR vector, transduced CD4 T cells from two blood donors, and electroporated synthetic mRNAs for four base editors with different specificities in separate experiments: the A-to-G editor ABEmax[27], the C-to-T editor AncBE4max, and their near PAM-less variants[28], which enabled dense tiling of the target genes (Fig. 6f). As an additional control for our screen and library, we electroporated standard Cas9 mRNA into CAR T cells transduced with the base editing gRNA library, which generates frameshift mutations at various positions in the gene body.

After 12 days of CAR stimulation with CD19-expressing cancer cells, the CAR T cells that received standard Cas9 mRNA showed a strong enrichment of gRNAs targeting RHOG, and a strong depletion of gRNAs targeting essential genes as well as PAC (Fig. S11a). This observation validates our screening setup and confirms that Cas9 edits can disrupt protein function largely independent of the gRNA position within the target gene. For the base editors, we can expect that only a subset of mutations disrupts protein function, while others are well tolerated. Nevertheless, in the screens for any of the four base editors, we observed a clear separation of gRNAs targeting RHOG (enriched), PAC (depleted), and essential genes (depleted), relative to gRNAs targeting a safe harbor locus (Fig. S11b-e), which confirms that tiling base editing screens for CAR T cell fitness are feasible using the CELLFIE platform.

We mapped the enrichment or depletion of base editing gRNAs along the protein sequence (Fig. S6g-h, S11f-g) and identified the most affected amino acids. We validated this approach for the puromycin resistance gene PAC and found several highly depleted amino acids co-localized around the known puromycin binding site (Fig. S11f-g). For RHOG, we observed enrichment of multiple gRNAs, including gRNAs predicted to introduce missense mutations into the GTP-binding pocket (e.g., Lys-16 and Cys-18, which form hydrogen bonds with GTP) (Fig. 6g-h). This screen not only prioritizes base editing gRNAs for future clinical translation but also suggests and informs pharmacological inhibition of RHOG as an alternative strategy for enhancing CAR T cell performance by interfering with RHOG function. We further confirmed our base editing screen by targeted sequencing of the RHOG locus in focused screens, which identified specific missense mutations that conferred a strong proliferative advantage to CAR T cells (Fig. S11h-i). We selected the corresponding base editing gRNAs and validated the individual effects (Fig. S11j-k).

These experiments establish tiling base editing screens as an additional feature of CELLFIE, which is useful both for the functional characterization of screening hits (including potential drug binding sites) and the empirical selection of base editing gRNAs for clinical translation of CRISPR-boosted CAR T cells without double-strand breaks.

Discussion

CAR T cells constitute the first broadly successful demonstration of genetically engineered cells as therapies, with strong future potential for a wide range of purposes and diseases. Our study builds on the biological premise that CAR T cells are products of engineering which are not evolutionarily optimized to their therapeutic tasks, and that certain mechanisms of homeostasis and regulation they inherit from T cells are detrimental to the performance of CAR T cell therapies. Given that CAR T cells are created by genetic engineering, optimizing their properties with genetic screens provides a natural approach to compensate for their lack of evolutionary optimization, and is directly translatable into new therapies given accumulating evidence that CRISPR (base editing in particular) is safe and effective in patients. In this study we established a discovery platform for CRISPR-boosted immunotherapies, employing the concept of high-content CRISPR screens[48] for the genetic systematic optimization of CAR T cells.

Our CELLFIE platform provides an integrated approach for CAR T cell optimization, with genome-wide discovery screens, *in vivo* pooled screens for hit validation, and in-depth hit characterization by combinatorial screens and tiling base editing screens. The core of this technology is a CROP-seq vector for co-delivery and readout of the CAR and CRISPR library, and mRNA-based delivery of CRISPR editors. To provide flexibility (including support for various CRISPR base editors), scalability, and cost-effectiveness, we established *in vitro* transcription of mRNA for essentially any CRISPR editor, requiring only standard molecular biology techniques. Moreover, we optimized genome-wide screens with fitness and FACS-based readouts to study regulators of CAR T cells and to address limitations of current CAR T cells. We provide comprehensive open-source reagents and detailed protocols that will make such screens realistic for many laboratories. While this study focuses on screens in human primary CAR T cells, many aspects of our platform are readily transferable to other cell types and other cell-based therapies.

Demonstrating the practical utility of the CELLFIE platform, we conducted a series of different and complementary screens to enhance anti-CD19 CAR T cells, which are in wide clinical use but fail for a substantial proportion of patients. We established a large resource of CRISPR screens in human primary CAR T cells, comprising 58 genome-wide screens for six biological processes (CAR T cell fitness and proliferation upon CAR or TCR stimulation, target cell recognition, activation, apoptosis and fratricide, and expression of inhibitory receptors), providing the most comprehensive functional genomics characterization of CAR T cell biology to date.

We also present pooled *in vivo* screening as an attractive alternative to one-by-one hit validation. In this study, we tested 39 genes in 20 mice (a 20-fold reduction in animal use) while enabling UMI-based clonal tracking and head-to-head comparisons of knockout CAR T cells. Although our focus was on validating hits rather than on *de novo* discovery, the CELLFIE platform is readily scalable for larger *in vivo* screens. By reducing gRNA coverage from eight to four per gene, and leveraging our dual-gRNA vector for combinatorial delivery, up to 156 genes can be tested in just five animals. Scaling to 50 mice (which is still a manageable number) would support over 1,500 genes, and allowing two or more perturbations per cell would expand coverage beyond 3,000 genes. In summary, our platform enables broad adoption of *in vivo* screening with full UMI-based clone tracking.

We found that RHOG and FAS knockout CAR T cells significantly improved tumor control and survival *in vivo*. Our validations covered four CAR designs (CD19-BBz, CD19-28z, GD2-BBz, GPC3-BBz), leukemia (NALM6), a solid tumor model (Huh7), and patient-derived T cells. RHOG in particular is a fascinating discovery, with a beneficial effect that appears impossible to guess from prior knowledge. RHOG deficiency in humans is linked to impaired immunity, yet its knockout in CAR T cells enhances proliferative capacity, DNA replication, memory-like differentiation, and reduces exhaustion. This supports our hypothesis that genes essential in normal immune cells can become roadblocks in CAR T cell therapy. FAS knockout provides a complementary effect by promoting CAR T cell survival and reducing apoptosis. Together, the double knockout yielded markedly improved outcomes, including two long-term remissions in this intentionally non-curative model. These findings exemplify a modular approach to CAR T cell engineering, where distinct perturbations are combined to improve therapeutic performance.

To support the discovery and characterization of beneficial CAR T cell modifications, we expanded CELLFIE with two advanced screening capabilities. First, combinatorial knockout screening confirmed the benefit of RHOG-FAS double knockout CAR T cells and revealed additional combinations with enhanced CAR T cell proliferation. Second, we used base editing for tiling screens of RHOG ("biochemistry by sequencing"), enabling precise variant mapping. This established a strategy for introducing functional RHOG mutations without double-strand breaks.

In summary, we created an open-source discovery platform for CRISPR-boosted CAR T cell therapies, demonstrated the versatility of high-content CRISPR screening for optimizing cell-based immunotherapies, established a major resource of functional genomics data for human primary CAR T cells, and proposed RHOG and FAS double knockout as a therapeutically promising and biologically interesting strategy to enhance CAR T cell performance.

Supplementary Note 1. Scaling the CELLFIE platform for genome-wide multi-readout screens

For genome-wide CRISPR screening in primary CAR T cells with multiple parallel readouts, we have to achieve a high and balanced representation of gRNAs throughout the screen. This requires a large number of gene-edited CAR T cells to be maintained with minimal non-intentional selective pressures or genetic drift, which needs careful optimization of cell culture, lentiviral transduction, mRNA electroporation, cell selection, and screening readouts.

We made several observations and optimizations that helped achieve robust genome-wide screens in CAR T cells. First, CD8 T cells required presence of CD4 T cells for effective proliferation (Fig. S2c), while CD4 T cells proliferated better alone than in co-culture (Fig. S2c-d). Expectedly, both CD4 and CD8 cells differentiated into effector and memory cells during T cell culture (Fig. S3g). Second, we carefully optimized antibiotic selection for cells that were successfully transduced with lentivirus (Fig. S2e) and electroporated with synthetic mRNA (Fig. S2f). This reduced cell culture costs and enhanced the signal-to-noise ratio in our screen. Third, we scaled our electroporation workflow from small pilot experiments (1.5 million cells per cuvette) to billions of cells with consistent editing efficiency and high cell viability (Fig. S2g-h). Fourth, successful lentiviral transduction depended on the stimulation status of T cells, and only a small subset of proliferating cells allowed viral entry. We thus tested widely used TCR stimulation reagents and obtained the best results with ImmunoCult CD3/CD28 activator at day 3 post stimulation (Fig. S2i-k). Fifth, we found that the commonly used polybrene reagent was toxic to T cells, whereas spinfection and plate coating with retronectin were well-tolerated but did not further improve T cell transduction (Fig. S2j-k).

Using our optimized conditions, transduction rates in primary T cells saturated around 50% for CD4 and 20% for CD8 cells (Fig. S2m), which is adequate for genome-wide screening. We quantified lentiviral titers (Fig. S2l) and determined lentivirus amounts needed to transduce T cells at a multiplicity of infection of 0.3 (Fig. S2m), to avoid multiple lentiviral integrations with different gRNAs in the same cell. To accurately quantify the number of gRNA integrations per cell and confirm our choice of lentiviral amounts, we developed a next generation sequencing (NGS) assay that is based on single-cell expansion and gRNA amplicon sequencing (Fig. S2n). Analyzing 62 T cell clones, we determined an average of 1.5 gRNAs per cell (Fig. S2o). This is an ideal value to maximize the number of usable cells in genome-wide screens where most gRNAs do not impact the phenotype. Cell numbers for transduction and electroporation were chosen to achieve at least 1000x gRNA coverage in the genome-wide screens (Table S2l, S3p).

We made several additional improvements for genome-wide FACS-based screening in CAR T cells. First, we developed a sorting strategy to effectively isolate viable CD4 or CD8 CAR T cells following exposure to CD19-positive cancer cells (Fig. S5e), with pre-selection for those CAR T cells that successfully engaged cancer cells (as evident from trogocytosis-acquired CD19 on their cell surface). Second, we devised a reliable cell fixation protocol that allows prolonged cell sorting without compromising marker staining or cell integrity (Fig. S5f-i). This was a critical step, as the total sorting time across all FACS-based screens exceeded 100 hours and sorting unfixed cells would have been infeasible. Third, complex FACS readouts can result in low numbers of sorted cells, but we demonstrated that the fully optimized workflow can yield high data quality data across multiple genome-wide screens (Fig. S6a-b) and in a series of focused validation screen with as few as 1000 sorted cells (Fig. S6c-d, Table S3).

Methods

Cloning the CROP-seq-CAR screening vectors

CROPseq-Guide-Puro (Addgene #86708) was digested with XmaI and SalI. The resulting 7737-bp fragment was gel-extracted using the S.N.A.P. UV-Free Gel Purification Kit (Thermo Fisher Scientific #K200025), and de-phosphorylated with Shrimp Alkaline Phosphatase (rSAP, NEB #M0371S) for 1 hour at 37 ℃, followed by heat-inactivation for 20 min at 80 ℃. We ordered two IDT gBlocks encoding *EF1a-CAR* (gBlock-17) and *P2A-mCherry-WPRE* (gBlock-18), where the CAR consisted of a leader peptide, a single-chain variable fragment (scFv) antibody binding CD19 (clone FMC63), the trans-membrane domain of CD8, the intracellular co-stimulatory domain of 41BB, and the CD3ζ chain. The gBlocks were PCR-amplified using Q5 High-Fidelity 2X Master Mix (NEB #M0492L) with primers gBlock-17-FWD and gBlock-17-REV for gBlock-17, or with gBlock-18-FWD and gBlock-18-REV for gBlock-18. These primers extend the gBlocks with BsmBI type IIS restriction sites and overhangs for Golden Gate cloning. PCR-amplified and gel-purified gBlocks were digested with BsmBI-v2 (NEB #R0739S), column-purified, and ligated with the Quick Ligation Kit (NEB #M2200S). The ligation product was PCR-amplified with primers gBlock-17-FWD and gBlock-18-REV, column-purified, digested one more time with BsmBI-v2, and inserted into the CROP-seq backbone by Gibson's isothermal assembly using NEBuilder HiFi DNA Assembly Master Mix (NEB #E2621S). Sequences of the gBlocks and amplification primers are provided in Table S1. This cloning strategy yielded pPD0010_CROP-seq-CAR-mCherry2, from which all CROP-seq-CAR variants were derived.

For efficient selection of CAR positive cells, mCherry was replaced by the Puromycin acetyltransferase gene (PAC), which resulted in the pPD0039_CROP-seq-CAR-19-BBz vector, which was used for most screens. To generate CROP-seq vectors with different CARs, PD0039 was linearized by PCR using Q5 High-Fidelity 2X Master Mix (NEB #M0492L) and primers prCART0026 and prCART0028 that exclude the CD19 scFv. The scFvs for GD2 (14g2a scFv) and GPC3 were synthesized as gBlocks (IDT), PCR-amplified with primers that add overhangs that are homologous to the ends of the linearized backbone (primer and scFv sequences are provided in Table S1i) using Q5 High-Fidelity 2X Master Mix (NEB #M0492L), and cloned by Gibson's isothermal assembly using NEBuilder HiFi DNA Assembly Master Mix (NEB #E2621S). This resulted in the pCROP-seq-CAR_GD2-BBz and pCROP-seq-CAR_GPC3-BBz vectors. The pCROP-seq-CAR_CD19-28z vector was generated by replacing the intracellular 41BB co-stimulatory domain by the CD28 co-stimulatory domain ordered as a gBlock.

Cloning the CROP-seq-CAR-multi screening vectors

CROPseq-multi-v2mTagBFP2-NLS (Addgene #225754) was amplified with the primers CROPseq_FWD_016-minusACC and CROPseq-multi-v2_REV1 (Table S1) using Q5 High-Fidelity 2X Master Mix (NEB #M0492L) to generate the backbone for all CROP-seq-CAR-multi vectors (7622 bp, including 40 bp extensions), followed by DpnI digestion (NEB #R0176L) to remove the parental plasmid. The CARs were amplified from pPD0039_CROP-seq-CAR-19-BBz, pCROP-seq-CAR_CD19-28z, and pCROP-seq-CAR_GD2-BBz with the primers PD39-FWD1 and CROPseq_REV_019 (Table S1), followed by DpnI digestion. PCR products were digested with PaqCI (NEB #R0745S), heat inactivated, and cleaned up using the Monarch PCR & DNA Cleanup Kit (NEB #T1030). The purified PCR fragments were ligated using T4 DNA Ligase (NEB #M0202T) at a 3:1 ratio of insert and backbone. This resulted in the vectors pCROP-seq-CAR-19-BBz-multi, pCROP-seq-CAR-19-28z-multi, and pCROP-seq-CAR-GD2-BBz-multi. The DNA sequence of all vectors was verified by full-plasmid sequencing (Microsynth).

Cloning the mRNA expression vectors

Open reading frames (ORFs) for mRNA production were cloned into the pIVTRup vector (Addgene #101362) by Gibson assembly. The pIVTRup backbone was linearized by PCR with the primers pIVTRup_linearize_FWD and pIVTRup_linearize_REV (Table S1). ORFs for CRISPR modifiers and selection markers were amplified from existing plasmids (Table S1) with ORF-specific primers that included extensions for Gibson's isothermal assembly:

mRNA_ORF_Gibson_FWD and mRNA_ORF_Gibson_REV (Table S1). Both backbone and insert were amplified using Q5 Hot Start High-Fidelity 2x Master Mix (NEB #M0494L). Each 50 µl PCR reaction was mixed with 6 µl CutSmart Buffer, 3 µl nuclease-free H2O, and 1 µl of DpnI (NEB #R0176S) and incubated for 1 hour at 37 ˚C to digest the plasmid template, followed by heat inactivation for 20 min at 80 ˚C. PCR products were cleaned with the QIAquick PCR Purification Kit (Qiagen #28106). The final product was assembled with NEBuilder HiFi DNA Assembly Master Mix (NEB #E2621L) using a 2:1 molar ratio of insert to backbone. After incubating the mix for 15 min at 50 ˚C, the samples were stored at -20 °C or directly used for bacterial transformation. All plasmids were fully validated by Sanger sequencing.

Cloning of the gRNAs and gRNA libraries

Individual gRNAs and small-scale gRNA libraries were cloned into CROP-seq-CAR vectors as described previously[23]. To clone the genome-wide Brunello gRNA library into the CROP-seq-CAR vector, we PCR-amplified the gRNA insert from Addgene #73178[30]. We mixed Q5 Hot Start High-Fidelity 2x Master Mix (NEB #M0494L), SYBR Green, 0.5 µM of primers gRNA_library_FWD and gRNA_library_REV, and 1 µg of plasmid DNA per 50 µl reaction. The amplification was stopped at ~3000 RFU in the exponential phase to avoid library over-amplification. We treated the PCR product with DpnI (NEB #R0176L) to remove plasmid DNA and concentrated by ethanol precipitation to achieve high purity. The Brunello gRNAs were assembled into BsmBI-linearized CROP-seq-CAR vector using NEBuilder HiFi DNA Assembly Master Mix (NEB #E2621L), as described previously[23].

Cloning of the gRNA library for *in vivo* CROP-seq

To prepare the gRNA library for *in vivo* CROP-seq (Fig. S6a), a backbone fragment was PCR-amplified from the CROP-seq-CAR plasmid, using Q5 High-Fidelity 2X Master Mix (NEB #M0492L), and 0.5 µM of primers CART52_Bkbn_FWD and CART52_Bkbn_REV (Table S1). For quality control, we ran 1 µl of PCR reaction on a 0.8% agarose gel containing SYBR Safe stain and verified the product size of 9783 bp. Template plasmid was removed by DpnI digestion (NEB #R0176L) for 1 hour at 37 ℃, followed by inactivation of the enzyme for 20 min at 80 ℃, cleaning with the QIAquick PCR Purification Kit (Qiagen #28104), and quantification with the Qubit dsDNA HS assay (Thermo Fisher Scientific #Q32854). The gRNA library was obtained from IDT as an oPool. The sequences of the gRNA library libCART011, which we used for our pooled *in vivo* validation screen, are listed in Table S5. This includes all genome-wide screening hits (from Fig. 2f) for which gene expression was detected in CAR T cells by RNA-seq (Fig. S5e). A template oligonucleotide to design new libraries is provided in Table S1. CART52_const_ultra was ordered as an IDT ultramer oligonucleotide. The library oPool and constant ultramer oligo were diluted to 2 µM and annealed in T4 DNA Ligase Buffer (NEB #B0202S). The library insert cassette was extended and amplified using Q5 High-Fidelity 2X Master Mix (NEB #M0492L) with 0.5 µM primers CART52_cassette_FWD and CART52_cassette_REV (Table S1). The product size of 225 bp was confirmed on a 2% agarose gel. The backbone and library insert were assembled by Gibson's isothermal assembly, using NEBuilder HiFi DNA Assembly Master Mix (NEB #E2621L). Gibson reactions were desalted by filter dialysis (Merck #VMWP04700), and electroporated into Lucigen Endura E. coli cells (Lucigen #60242-2). The library plasmid was prepared using the Plasmid Plus Giga Kit (Qiagen #12991).

Cloning of the gRNA library for combinatorial screening

For combinatorial screening, we selected the six strongest CAR T boosters based on the pooled *in vivo* screen (FAS, RHOG, PRDM1, CDKN2A, HAVCR2, CTLA4) as well as three essential genes (RPL8, PSMB4, POLR2L). For each gene, we selected the two best-performing gRNAs (out of a total of eight). As negative controls, we selected the 15 most neutral PPP1R12C safe harbor targeting gRNAs, from which we randomly picked gRNAs for combinations with other targets (Fig. 6b, Table S8). The gRNAs that target boosters and essential genes were paired separately, yielding combinations targeting the same genes, different genes within each set, or one target gene and

the safe harbor locus. This resulted in 238 dual gRNA combinations (Fig. 6b), for which we designed a CROP-seq-multi library based on published code (https://github.com/rtwalton/CROPseq-multi)[42].

The CROP-seq-multi library inserts (238 oligos, Table S8) were obtained as an oligo pool (Twist Bioscience) and PCR-amplified using 2X KAPA HiFi HotStart Ready Mix (Roche #KK2601) with 1M Betaine (MilliporeSigma #B0300), 300 nM primers (oRW1083 and oRW1086), and 12 pg/µl template per 25 µl-PCR reaction. Thirty-three PCR reactions were performed with the following conditions: 95 ºC for 3 min, 13 cycles of (98 ºC for 20 s, 62 ºC for 15 s, 72 ºC for 15 s), 72 ºC for 1 min. Here, the low input and few amplification cycles help reduce recombination during the PCR[42]. The pooled PCR reactions were purified using the Monarch PCR & DNA Cleanup Kit (NEB #T1030), digested with BsmBI-v2 (NEB #R0739L), and purified. The CROP-seq-CAR-multi vectors (pCROP-seq-CAR-19-BBz-multi, pCROP-seq-CAR-19-28z-multi, and pCROP-seq-CAR-GD2-BBz-multi) were digested with BsmBI-v2, dephosphorylated using rSAP (NEB #0371L), and purified. In 20 µl of total volume, 20 fmol digested oligo pool and 20 fmol digested plasmid backbone were ligated using 400 U/µL of T4 DNA ligase (NEB #M0202S) at 16 ºC overnight, followed by heat inactivation and cleanup with SPRI beads (Beckman Coulter #B23317) at a 1.5x ratio. The purified ligation reaction was electroporated into Lucigen Endura *E. coli* cells (Lucigen #60242-2) on a Gene Pulser Xcell (BioRad #1652662) (settings: 1.8 kV, 600 Ohms, 10 µF), recovered for 90 minutes at 30 ºC in 1 mL of Endura recovery media, followed by 100 mL liquid culture in selection LB medium (100 µg/ml carbenicillin) at 30 ºC, shaking at 225 rpm. Library plasmids were prepared using Plasmid Plus Midi Kit (Qiagen #12943).

Production of lentiviruses

Lentivirus was produced using Lipofectamine 3000 (Invitrogen #L3000150) as described previously[23], followed by 100x concentration using Lenti-X Concentrator (Takara #631232). For large-scale lentivirus production, all reagent and cell culture volumes were scaled accordingly for Nunc EasyFill Cell Factory Systems (Thermo Fisher Scientific). Lentivirus titer was quantified by qPCR, using the Lenti-X qRT-PCR Titration Kit (Takara Bio #631235). For each lentivirus preparation, two aliquots of concentrated virus were diluted 100x with 1x PBS and used as input for quantification, and the mean titer (RNA copies/ml) was calculated.

Production of mRNA

The DNA template for mRNA production was PCR-amplified from 10 ng of pIVTRup with the cloned ORF, using Q5 Hot Start High-Fidelity 2x Master Mix (NEB #M0494L) and 0.5 µM of the primers pIVTRup_FWD_AG and pIVTRup_REV (Table S1), in a total volume of 50 µl and using 26 amplification cycles. The PCR product was cleaned using the QIAquick PCR Purification Kit (Qiagen #28106). Synthetic mRNA was produced by *in vitro* transcription with the HiScribe T7 High Yield RNA Synthesis Kit (NEB #2040S). Reactions contained 500 ng of PCR product, 10 mM of each nucleotide, and 8 mM of CleanCap Reagent AG (TriLink BioTechnologies #N-7113-10), and were incubated for 2 hours at 37 ºC, followed by DNaseI treatment (Promega #M6101) for 15 min at 37 ºC. For large-scale production, the number of reactions was scaled accordingly. Immediately after the incubation, mRNA was cleaned with the RNeasy Mini Kit (Qiagen #74104), loading 8-16 reactions per column. mRNA concentration was measured in a Qubit RNA BR Assay Kit (Invitrogen #Q33223), and mRNA integrity was assessed with the Bioanalyzer RNA 6000 Pico Kit (Agilent #5067-1513).

T cell isolation

Peripheral blood samples from healthy donors were obtained through the Austrian Red Cross as blood packs with buffered sodium citrate as anti-coagulant. Human primary T cells were isolated using RosetteSep Human T Cell, $CD4^+$ T Cell, or $CD8^+$ T Cell Enrichment Cocktail (Stemcell #15061, #15062, #15063) to isolate pan-CD3, CD4, or CD8 T cells, respectively. After incubation with the antibody cocktail, cells were centrifuged using Lymphoprep (Stemcell #7861) in SepMate-50 tubes (Stemcell #85460), washed, and treated with 1x Red Blood Cell Lysis Buffer (eBioscience #00-4333-57). Isolated T cells were immediately stimulated and cultured as described below.

Patient-derived T cells were obtained from a 57-year-old female patient diagnosed with relapsed stage III multiple myeloma, who previously receive multiple lines of chemotherapy and autologous stem cell transplantation, and who was scheduled to receive anti-BCMA CAR T cell therapy as part of routine clinical care. The apheresis product was collected using the Spectra Optia Apheresis System (Terumo BCT) with ACD-A as anticoagulant, simultaneously with the collection for clinical CAR T cell production. T cells were isolated from the apheresis product using EasySep Human T Cell Isolation Kit (Stemcell #17951) following the manufacturer's instructions for leukapheresis samples. Isolated patient T cells were immediately stimulated and cultured as described below.

The study complied with all relevant ethical regulations for working with human samples. Informed consent was obtained from all sample donors. The study was approved by the ethical committees of the contributing institutions (Austrian Red Cross, Medical University of Vienna).

T cell culture

T cell culture medium was based on CTS OpTmizer T-Cell Expansion Serum Free Medium (Thermo Fisher Scientific #A1048501), where 1000 ml of CTS OpTmizer T-Cell Expansion Basal Medium was supplemented with 26 ml of CTS OpTmizer T-Cell Expansion Supplement, 1% GlutaMAX (200 mM, 100x, Gibco #35050061), 1% Penicillin-Streptomycin (10,000 U/ml, Gibco #15140122), 2% Human AB Serum (heat-inactivated according to manufacturer's instructions, Sigma #H4522). The complete medium was supplemented with 12.1 ng/µl Human Recombinant IL-2 (Stemcell #78145.2) right before use. T cells were cultured at 37 ˚C and 5% CO2. For stimulation, T cells were seeded at 1 million/ml in T cell medium with 25 µl/ml ImmunoCult Human CD3/CD28 T Cell Activator (Stemcell #10990). After 2-3 days of stimulation, the medium was exchanged completely. For harvesting, T cells were spun at 400 RCF for 5 min. For optimization experiments, CD4 T cells were frozen after 1 week of pre-expansion in CTS OpTmizer T-Cell Expansion SFM with 20% Human AB Serum and 10% DMSO. Immediately after thawing, cells were stimulated and cultured. Cells were counted using CASY TT (Schärfe-System #3222).

T cell transduction

T cells were collected 2-3 days after stimulation and seeded in fresh T cell medium at 1 million/ml. Lentivirus was added to the medium and mixed with cells. After 24-48 hours, the medium was exchanged with a 4x larger volume. For single locus targeting, 100x concentrated virus containing a single gRNA was added to the medium at 1:10 v/v ratio. For screens, the lentivirus titer was quantified by qPCR, and lentivirus was added at 247 lentivirus RNA copies per cell for CRISPR screening in CD4 T cells and at 432 copies per cell for CRISPR screening in CD8 T cells.

T cell electroporation

For electroporation using the ExPERT ATx Electroporator (MaxCyte), cells were pelleted, washed once with room temperature 1x PBS, washed once with room temperature MaxCyte Buffer, and then resuspended in MaxCyte Buffer at a concentration of 100 million/ml. Synthetic mRNA encoding CRISPR editors was added right before electroporation at a concentration of 150-300 µg/ml. mRNA for fluorescent markers or blasticidin resistance gene (BSD) was added at a concentration of 75 µg/ml. For ribonucleoprotein (RNP) electroporation, synthetic gRNA (TrueGuide Synthetic gRNA, Synthego) and Alt-R S.p. Cas9 Nuclease V3 (IDT #1081059) were mixed at a 2:1 molar ratio, and incubated for 30 min at room temperature for RNP complex formation. Immediately before electroporation, RNP was added to cells with a final gRNA concentration of 3 µM and Cas9 concentration of 1.5 µM. Cells were mixed with mRNA or RNP and were transferred to MaxCyte cuvettes. Cuvettes were pulsed with a customized program "Optimization 3-2". For electroporation using the Amaxa Nucleofector II system, cells were pelleted, washed once with room temperature 1x PBS, and resuspended in 100 µl of Electroporation Master Mix from the Amaxa Human T Cell Nucleofector Kit (Lonza #1002) right before electroporation, at a maximum concentration of 15 million/ml and mixed with mRNA. Cells were transferred to the cuvettes and pulsed using program "X-001". In both cases

(electroporation with MaxCyte and Amaxa systems), cells were transferred to fresh pre-warmed medium without puromycin at a concentration of 1 million/ml and transferred to culture flasks immediately after electroporation.

CRISPR editing of single genomic loci

T cells were freshly isolated or thawed from samples frozen after 1 week of pre-expansion. T cells were stimulated in T cell culture medium supplemented with 25 µl/ml ImmunoCult Human CD3/CD28 T Cell Activator (Stemcell #10990). 2 to 3 days after stimulation, cells were transduced with a lentivirus encoding a locus-specific gRNA (Table S1), a fluorescent marker (mCherry) and puromycin resistance gene (PAC). 2 to 3 days after transduction, selection with 1 µg/ml of puromycin was started and maintained until the end of the experiment. 7 to 9 days after stimulation, cells were restimulated. 2 to 3 days later, cells were co-electroporated with mRNAs encoding a CRISPR editor and a fluorescent marker or blasticidin selection gene. When using GFP or BFP mRNA as co-electroporated selection marker, we gated successfully electroporated (BFP^+ or GFP^+) and transduced ($mCherry^+$) alive T cells in flow cytometry or FACS. When using the blasticidin resistance gene (BSD) as co-electroporated selection marker, cells were selected with 50 µg/ml blasticidin starting 24 hours post-electroporation, blasticidin was washed out after 1 to 2 days of selection, and cells were further expanded for an additional 3 to 7 days.

CRISPR knockout and base editing. Cells were lentivirally transduced to express a locus-specific gRNA with standard Cas9 backbone, and electroporated with mRNA encoding Cas9, ABEmax, AncBE4max, ABEmax7.10-SpRY, or CBE4max-SpRY (Table S1). Following genome editing, cells were collected, and genomic DNA was extracted. To measure the editing efficiency on the DNA level, target loci were amplified using Q5 Hot Start High-Fidelity 2x Master Mix (NEB #M0494L) with locus-specific primers (Table S1). Amplicons shorter than 300 were sequenced directly. Longer amplicons were further fragmented with the Nextera XT Library Prep Kit (Illumina #15032352). Libraries were sequenced on the Illumina MiSeq platform using MiSeq Reagent Kit v3 reagents (Illumina #MS-102-3001, or #MS-102-3003). The frequency of insertions and deletions was determined based on the aligned sequencing reads. For CRISPR base editing, reads were considered successfully edited when they had at least one expected base conversion and no insertions or deletions. To measure editing at the protein level, we measured CD25 or CD44 levels by flow cytometry. For CD25, T cells were stimulated with 25 µl/ml ImmunoCult Human CD3/CD28 T Cell Activator for 24 hours prior to flow cytometry to induce the expression of CD25. For CD44, cells were cultured normally, given that CD44 is stably expressed in human T cells without need for stimulation.

CRISPR activation. Cells were lentivirally transduced to express a gRNA targeting the CD34 promoter. The gRNA backbone contained two MS2 aptamers. T cells were further electroporated with mRNAs encoding dCas9-VP64 and MCP-p65-HSF1. The induction of CD34 protein was assessed by flow cytometry.

CRISPR screening

For genome-wide knockout screens and tiling base editing screens, T cells (either pan-CD3 or CD4-only, depending on the experiment and documented in the supplementary table s) were freshly isolated, pre-expanded for 7 to 10 days and restimulated once more. For knockout and base editing focused screens, T cells were either freshly isolated or thawed from samples frozen after 1 week of pre-expansion, and immediately used. T cells were stimulated with 25 µl/ml ImmunoCult Human CD3/CD28 T Cell Activator (Stemcell #10990). Two to three days after stimulation, cells were transduced with CROP-seq-CAR lentivirus to deliver the chimeric antigen receptor, gRNA library and puromycin resistance gene (PAC). Two days after transduction, cells were electroporated with mRNAs encoding the CRISPR editor and the blasticidin resistance gene (BSD). Twenty-four hours after electroporation, puromycin (0.5 µg/ml) and blasticidin (50 µg/ml) were added. Puromycin selection was maintained until the end of the experiment. Blasticidin was removed after 24 to 48 hours by a full exchange of cell culture medium. Cell numbers for transduction and electroporation were chosen to maintain at least 1000x gRNA coverage (Table S2l, S3p).

For combinatorial screens and *in vivo* screens, CD4 T cells were stimulated with 25 µl/ml ImmunoCult Human CD3/CD28 T Cell Activator (Stemcell #10990). Two days after stimulation, cells were transduced with CROP-seq-CAR-multi lentiviruses to deliver the CAR, the combinatorial gRNA libraries and the puromycin resistance gene (PAC). Two days after transduction cells were subjected to puromycin selection (0.5 µg/ml). Five days after transduction, selected CAR T cells were restimulated. Two days later, CAR T cells were electroporated with mRNAs encoding the CRISPR editor and BSD, and cultured as described above.

Cancer cell lines

Antigen-expressing cancer cell lines (K562-CD19-mGFP, K562-CD20-mGFP) were produced by lentivirus transduction of K562 cells with constructs pLenti-C-CD19-mGFP-P2A-Puro (Origene #RC230267L4) or pLenti-C-MS4A1-mGFP-P2A-Puro (Origene #RC221570L4). Cells were selected with 2 µg/ml Puromycin (10 mg/ml, Gibco #A1113802), which was maintained throughout cell culture. The suspension cell lines K562 and NALM6 were cultured in RPMI10 medium containing RPMI 1640 (Gibco #11875085), 10% FBS (Sigma #F7524) and 1% Penicillin-Streptomycin (10,000 U/mL, Gibco #15140122). Cells were split and culture medium was exchanged every 3 to 4 days. For genetically engineered cell lines, antibiotic selection was maintained throughout cell culture. The adherent cell line Huh7 was cultured in high glucose DMEM (Sigma #D5796) supplemented with 10% FBS (Sigma #F7524) and 1% Penicillin-Streptomycin (10,000 U/mL, Gibco #15140122). Cells were split and culture medium was replaced twice a week following standard procedures for adherent cells. For irradiation, cells were resuspended at 4 million/ml in RPMI10 and irradiated with 100 Gy using the Yxlon X-Ray System. Irradiated cells were spun down, washed once with fresh medium, and either freshly used or frozen at 20 million/ml in Freezing Medium (RPMI 1640 (Gibco #11875085) with 5% FBS (Sigma #F7524) and 5% DMSO (Sigma #D2650)).

Readouts of the fitness screens

For TCR stimulation, cells were seeded at 1 million/ml in T cell medium containing 25 µl/ml ImmunoCult Human CD3/CD28 T Cell Activator (Stemcell #10990) and cultured for 2 to 3 days before medium exchange and further culture. For CAR stimulation, cells were seeded at 1 million/ml in T cell medium containing 1 million/ml irradiated K562-CD19-mGFP target cells. The medium contained 0.5 µg/ml puromycin throughout and was exchanged every 2-4 days. On day 0 (before electroporation) and on days 7, 14 and 21 after electroporation, T cells were collected for gRNA sequencing. For screens in CD4 CAR T cells, cells were lysed for DNA isolation right away. For screens in CD8 CAR T cells, cultures containing pan-CD3 T cells were stained with live/dead stain and anti-CD8 antibody, were fixed and FACS-purified to obtain a CD8 CAR T cell population for genomic DNA isolation.

Readouts of the FACS-based screens

For flow cytometry profiling, the BD LSRFortessa cell analyzer was used. For cell sorting, the Sony SH800S cell sorter was used for optimization experiments and the BD FACSAria Fusion for genome-wide screening. Cells were stained as follows: Pellet the cells, wash with 1x PBS, stain with 1/1000 Zombie Viability Dye (Biolegend) at room temperature for 10 min, wash and pellet the cells, stain with a mix of the relevant antibodies in Cell Staining Buffer (Biolegend #420201) at 4 ˚C for 30 min, wash and pellet cells, resuspend in the desired volume, and filter through a cell strainer. For storage prior to cell sorting, cells were fixed in Fluorofix Buffer (Biolegend #422101) at room temperature for 30 min in the dark, followed by washing cells twice and storing them in Cell Staining Buffer at a concentration of 50 million/ml. For large-scale screens, staining and fixation steps were done in 50 ml tubes placed on a rotator to avoid cell pelleting and clumping. The staining reagents used in this study are listed in Table S1.

Amplification and sequencing of gRNAs

Genomic DNA was isolated using the DNeasy Blood & Tissue Kit (Qiagen #69506) or QIAamp DNA Blood Maxi Kit (Qiagen #51194) depending on the number of cells. For cell lysis, we used AL buffer for freshly collected cells

and ATL buffer for fixed and sorted cells. In both cases, cell lysates were incubated with proteinase K for 10 min at 56 °C, and fixed cells were additionally incubated for 4 to 12 hours at 65 °C for DNA decrosslinking.

Library preparation for gRNA sequencing was performed as described in the CROP-seq protocol[23]. Up to 2 µg of purified genomic DNA was amplified and indexed with primers CROPseq_libQC_i5 and CROPseq_libQC_i7 (Table S1), resulting in a sequencing-ready library. To avoid sequencing library over-amplification, we added SYBR Green for qPCR quantification, and stopped the amplification once it reached the exponential phase. For genome-wide screens, multiple PCR reactions were set up to retain 1000x coverage for the individual gRNAs of the genome-wide gRNA library. Multiple 50 µl PCR reactions for the same sample were pooled together, and a minimum of 10% of the amplified material was used for purification. For plasmid libraries, we set up 1 to 8 separate PCRs with 100 ng of input depending on the gRNA library size. We aimed for 1000 NGS reads per gRNA in the plasmid library. PCR-amplified gRNAs were cleaned by SPRI, using Mag-Bind TotalPure NGS Beads (Omega Bio-tek #M1378-01). Large gDNA fragments were removed with a 0.45x SPRI bead cleanup, followed by purification of the gRNA amplicon from the supernatant with a 1.0x bead ratio to remove primer dimers.

Desired read numbers were calculated based on cell numbers and estimated fraction of T cells with a gRNA, aiming for 4 to 10 reads per cell. DNA concentrations for sequencing libraries were measured in with the Qubit dsDNA HS assay (Thermo Fisher Scientific #Q32854), and 0.25 ng were analyzed on an Bioanalyzer High Sensitivity DNA chip (Agilent #5067-4626) to confirm the purity of the expected single band at 282 bp. Sequencing libraries were diluted to 3.5 nM with EB Buffer + 0.1% Tween and pooled according to the desired read number. Libraries were sequenced with 1% PhiX on the Illumina Novaseq 6000 platform using a 100-cycle v1.5 flow cell with a read configuration of 122 Read1 + 8 Index1 + 8 Index2.

Library preparation for *in vivo* CROP-seq

Reverse transcription. RNA was isolated using the AllPrep DNA/RNA Mini Kit (Qiagen #80204) and quantified with the Qubit RNA HS Assay Kit (Invitrogen #Q32852). For reverse transcription, 33 µl of RNA sample per reaction (maximum 15 µg) was mixed with 3 µl 10 mM dNTPs (Thermo Fisher Scientific #R0193) and 3 µl of 2 µM CART0065_RT_002 primer (Table S1). To resolve RNA secondary structures, the reaction was incubated at 65 °C for 5 min, and immediately placed on ice to prevent their re-formation. Next, a master mix of 12 µl 5x Superscript IV (SSIV) Buffer, 3 µl of 100 mM DTT (Sigma Aldrich #646563-10x.5ML), 3 µl of RNaseOUT RNase inhibitor (Invitrogen #10777019) and 3 µl of SuperScript IV Reverse Transcriptase (Thermo Fisher Scientific #18090010) was added. The reverse transcription was incubated at 55 °C for 10 min, followed by heat inactivation for 10 min at 80 °C, and then placed on ice. Template RNA was digested with 3 µl of RNase A (NEB # T3018L) for 30 min at 37 °C. Afterward, the volume was brought to 60 µl with nuclease-free H2O and cDNA was cleaned with a 1.8x SPRI cleanup using 108 µl of Mag-Bind TotalPure NGS Beads (Omega Bio-tek #M1378-01), eluting in 40 µl nuclease-free H2O. Several reactions were performed to ensure processing of the entire RNA isolated for each organ.

Nested PCR. The PCRs were set up with 19.5 µl of template DNA, 25 µl Q5 High-Fidelity 2X Master Mix (NEB #M0492L), 2.5 µl of 10 µM FWD and REV primers, and 0.5 µl 100x SYBR Green. All amplification reactions were incubated at 98 °C for 30 sec (initial denaturation), then cycled between 98 °C for 10 sec and 72 °C for 40 sec in a BioRad CFX96 qPCR cycler until the reaction reached >1500 RFU. PCRs were finished in a second cycler at 72 °C for 2 min, then cooled on ice. PCRs were cleaned with 0.8x SPRI using Mag-Bind TotalPure NGS Beads (Omega Bio-tek #M1378-01). The outer PCR used primers CART0065 FWD-001 and CART0065 REV-001 (Table S1). The inner PCR used CROPseq_libQC_i5 with different stagger lengths and i5 indices, and TruSeq_i7 with different i7 indices. All primer sequences are listed in Table S1, and a schematic overview is provided in Fig. S6.

NGS library quality control and sequencing. Sequencing libraries were quantified with the Qubit dsDNA HS assay (Thermo Fisher Scientific #Q32854). 1.5 ng of the sequencing library was run on a Bioanalyzer High Sensitivity DNA chip (Agilent #5067-4626) to verify the final size of 288 to 294 bp (depending on stagger length). Sequencing

libraries were diluted to 2.0 nM with EB + 0.1% Tween and sequenced on the Illumina Novaseq 6000 platform using 100-cycle v1.5 reagents with a read configuration of 50 Read1 + 8 Index1 + 8 Index2 + 26 Read2.

Library preparation for the combinatorial screens

Amplification of plasmid gRNA library. The amplification of the plasmid library was performed as described previously[42], using 2x NEBNext Ultra II Q5 Master Mix (NEB #M0544), 2.5 µl of 10 µM FWD and REV primers (Table S1j), and 0.5 µl 100x SYBR Green and 100 ng plasmid template with the following cycling conditions: 98 ℃ for 1 min, followed by 10 cycles of 98 ℃ for 10 sec, 67 ℃ for 10 sec and 72 ℃ for 15 sec, followed by 72 ℃ for 1 min. The PCR reactions were cleaned up with 1x Mag-Bind TotalPure NGS Beads (Omega Bio-tek #M1378-01). Quality control and dilution were performed as described above.

Amplification of genomic DNA from combinatorial screens. The amplification of the genomic DNA was performed in a BioRad CFX qPCR cycler, to monitor amplification using 2x NEBNext Ultra II Q5 Master Mix (NEB #M0544) 2.5 µl of 10 µM FWD and REV primers (Table S1), and 0.5 µl 100x SYBR Green and 2.5 µg gDNA with the following cycling conditions: 98 ℃ for 1 min, followed by 26-32 cycles of 98 ℃ for 10 sec, 67 ℃ for 10 sec and 72 ℃ for 15 sec, plate read, 72 ℃ for 10 sec, followed by 72 ℃ for 1 min. Amplification was stopped 3 cycles after SYBR green enrichment detection to avoid overamplification and unwanted recombination events. The PCR reactions were cleaned with 1x Mag-Bind TotalPure NGS Beads (Om ega Bio-tek #M1378-01). The quality control and dilution were performed as described above. The reference samples were collected on the day of electroporation (day 0). 5 days after electroporation cells were restimulated with irradiated target cells (K562-CD19-GFP or NALM6-GD2) and cultured without puromycin (as NALM6-GD2 cells are not puromycin resistant). Samples were collected for genomic DNA extraction 12 days after electroporation.

Luciferase reporter cell lines

Synthetic DNA fragments encoding firefly luciferase, a P2A self-cleaving peptide, and zeocin resistance gene (Luc-P2A-Zeo, all human codon-optimized) were ordered as IDT gBlocks. The lentiCas9-Blast plasmid (Addgene #52962) was digested with EcoRI and XbaI in order to replace the insert for Luc-P2A-Zeo. Lentivirus was produced with Lipofectamine 3000 reagents. NALM6 and K562-CD19-mGFP cells were lentivirally transduced by spinfection as described previously[23] and selected for 2 to weeks using zeocin.

Luciferase assay on microwell plates

CAR T cells were co-cultured with luciferase-expressing K562-CD19-mGFP for 18 hours. Cells were transferred to a 384-well assay plate (Corning #3707). For lysis and luciferase detection, we used the Steady-Glo Luciferase Assay System (Promega #E2510) and a Perkin Elmer Victor x3 2030 Multilabel Reader.

CAR T cell production for mouse validation experiments

Gene knockout using mRNA electroporation. Freshly isolated CD3 T cells were transduced with CROP-seq-CAR lentivirus containing a pool of 8 gRNAs for each target gene. Four gRNAs were taken from the genome-wide screen and four additional gRNA were designed using the VBC score method[49]. Two days later, selection with puromycin (0.5 µg/ml) was started. Seven days after isolation, cells were restimulated. Three days later, cells were electroporated with Cas9 and BSD mRNA. Blasticidin (50 µg/ml) was added 24 hours later. On the following day, cell culture medium was exchanged, and cells were cultured for an additional three days. Five or six days after electroporation, the cells were injected into mice.

Gene knockout using RNP electroporation. Freshly isolated CD3 T cells were stimulated with 25 µl/ml ImmunoCult Human CD3/CD28 T Cell Activator (Stemcell #10990) for 2 days before electroporation with RNPs as described above, directly followed by transduction with CROP-seq-CAR lentivirus. Two days later, puromycin selection (0.5

µg/ml) was started. Seven days after isolation, cells were restimulated with 25 µl/ml ImmunoCult Human CD3/CD28 T Cell Activator (Stemcell #10990). Three days after restimulation, cell culture medium was exchanged, and cells were cultured for an additional 3 to 4 days. Five or six days after electroporation, the cells were either directly injected into mice or frozen in Bambanker freezing medium (Nippon Genetics #BB02). CAR T cells were thawed one day before injection into mice in the presence of 0.1 mg/ml DNase I (Sigma #11284932001).

Mouse *in vivo* xenograft cancer models

Mice were bred and maintained under specific-pathogen-free conditions at the Medical University of Vienna. Experiments were performed at the Core Facility Laboratory for Animal Breeding and Husbandry, using individually ventilated cages. Experiments followed established guidelines and were approved by the institutional ethical committee at the Department for Biomedical Research of the Medical University of Vienna (BMWFW-2020-0.605.586).

Leukemia xenograft model. NOD/SCID/IL-2Rγ-null (NSG) mice at 8 to 12 weeks of age were intravenously injected with 0.5 million NALM6 cells (clone G5, ATCC #CRL-3273) or 0.5 million NALM6-GD2 cells (gift from the Crystal Mackall Lab). After 5 days, CAR T cells were administered by intravenous injection. For *in vivo* screens, we injected 1 million CAR T cells per mouse. For single knockout validation, we injected 0.6 million CAR T cells per mouse. Mice were tracked by bioluminescence imaging and weight measurements and were monitored for any signs of morbidity.

Solid tumor xenograft model. NSG mice at 8 to 12 weeks of age were subcutaneously injected (right flank) with 1 million Huh7 cells in 100 µl of 1x PBS. After 20 days and an average tumor volume of 0.3-0.4 cm^3, CAR T cells were administered by intravenous injection. Tumor size was tracked by measurement using a precision caliper.

IVIS Bioluminescence Imaging

XenoLight D-Luciferin K+ salt (PerkinElmer #122799) was dissolved at 30 mg/ml in sterile 1x PBS, and injected intraperitoneally at a concentration of 150 mg/kg body weight. Mice were anesthetized with isoflurane and bioluminescence imaging was performed 15 minutes after injection on the IVIS Spectrum In Vivo Imaging System (PerkinElmer #124262). Bioluminescence was quantified using the Living Image Analysis Software (PerkinElmer).

Organ dissociation

During extraction, organs and cells were kept on ice for the entire procedure. Spleens were rinsed with ice-cold 1x PBS + 5 mM EDTA + 0.1% BSA (PBS + EDTA + BSA), smashed through a 70 µm cell strainer, and the resulting cell suspensions were collected in 50 ml tubes. Femurs from both hind limbs were collected and soft tissue was removed with scissors. Bone marrow was flushed with PBS + EDTA + BSA. Cells were filtered through a 70 µm strainer and transferred to 50 ml tubes. Cell suspensions from both organs were centrifuged at 500 RCF for 5 min, and resuspended in 3 ml of 1x Red Blood Cell Lysis Buffer (eBioscience #00-4333-57) for 5 min to lyse red blood cells, the reaction was stopped by adding 20 ml of cold PBS + EDTA + BSA. Supernatants were filtered through a 70 µm cell strainer and counted using the CASY TT (Schärfe-System #3222) system.

RNA-seq profiling of CAR T cells

RNA-seq was performed on CAR T cells produced from CD3 T cells. To isolate CD4 or CD8 cells from T cell cultures and co-cultures with irradiated cancer cells, we used the EasySep Human CD4 Positive Selection Kit II (Stemcell #17852) and EasySep Human CD8 Positive Selection Kit II (Stemcell #17853). RNA was isolated using the Monarch Total RNA Miniprep Kit (NEB #T2010S), starting from at least 200,000 lysed cells and storing the extracted RNA at -80 ˚C in 300 µl of Protection Reagent. RNA-seq libraries were prepared with the NEBNext Ultra II Directional RNA Library Prep Kit for Illumina (NEB #E7760L) and sequenced with paired-end 50 bp reads on the Illumina NovaSeq 6000 platform.

Data pre-processing for the CRISPR screens

The sequencing data were pre-processed with a custom pipeline, starting from demultiplexed but unaligned BAM files provided by the Biomedical Sequencing Facility at CeMM. The BAM files were converted to FASTQ format using bedtools v2.30.0 bamtofastq. Reads were trimmed with cutadapt v3.4, using the -g flag to specify the 5' adapter and stagger (Table S1). For the *in vitro* CRISPR screens, raw gRNA counts were obtained with the MAGeCK package v0.5.9.4 using command mageck count, specifying the gRNA sequences for alignment with the -l option. For *in vivo* CROP-seq screens, we used MAGeCK2, cloned from Github repository davidliwei/mageck2. We used the mageck2 count command, providing the gRNA sequences with the -l flag, and defining the UMI configuration with --umi secondpair,0,26. Finally, quality control metrics were derived from MAGeCK log files, including total reads, mapped reads, gRNA alignment rate, gRNAs with count zero, Gini index, and read trimming statistics.

Analysis of the genome-wide fitness screens

MAGeCK RRA analysis. Samples obtained following TCR or CAR stimulation at days 7, 14, or 21 after electroporation were separately compared to samples collected prior to stimulation (day 0). The analysis was performed with MAGeCK package v0.5.9.4, using the mageck test command. The -k option was used to specify the raw gRNA count table in TSV format. Samples were provided with the -t and -c flags. We used --remove-zero both --remove-zero-threshold 0 to remove gRNAs with zero reads in both of the two compared samples. As normalization method, we used --norm-method control, and we used --control-gene to provide a set of previously described negative control genes for human (gene set NEGv1)[50]. Day 0 samples were selected for variance estimation with the --variance-estimation-samples option. Essential genes were defined with a stringent threshold of $\log_2$FC < -1.5 and FDR < 0.01. Gene set enrichment for Gene Ontology (GO) terms labelled BP (for Biological Process) was performed in R with the clusterProfiler package v4.0.0[51], using the function compareCluster with extra arguments fun = "enrichGO", OrgDb="org.Hs.eg.db", keyType = "SYMBOL", and ont="BP". Next, the similarity between nodes was calculated with the pairwise_termsim function from the enrichplot package, using the default Jaccard similarity coefficient method. The network graph was plotted with enrichplot::emapplot with showCategory = 100, node_scale = 10, min_edge = 0.3, cex_line = 0.5, cex_category = 10, pie = "Count", cex_label_category = 1.

MAGeCK MLE analysis. Samples obtained before (day 0) and after (day 14) TCR and CAR stimulation were compared in one joint analysis with MAGeCK package v0.5.9.4, using the command mageck mle. Raw gRNA counts in TSV format were provided with --count-table, and the experimental design was defined with the --design-matrix option. In the design matrix, the day 14 samples were modeled as TCR-stimulated or CAR-stimulated, as shown in Table S2 (tab 'S2J_GW_fitness_MLE-design'). We further used --norm-method control and provided a set of non-essential genes (gene set NEGv1)[50] via the --control-gene option. The analysis was performed with --permutation-round 2. The MAGeCK MLE gene_summary.txt output file was read with R package MAGeCKFlute v1.12.0 using function ReadBeta. Normalizing beta values against essential genes is important when samples in the screen have different proliferation rates, as it is the case for TCR and CAR-stimulated versus unstimulated T cells (Fig. 1b). We thus normalized beta values with function NormalizeBeta, specifying a set of essential genes with argument posControl (CEGv2[50]) and method = "cell_cycle". We selected candidate genes that improved the function of both T and CAR T cells, and of CAR T cells alone.

Analysis of the genome-wide FACS-based screens

The sequencing data from the genome-wide sorting screens for markers CD19, CD69, FAS, and the combination of PD1, LAG3, and TIM3 were pre-processed as described above, and filtered with quality control thresholds of gRNA alignment ≥ 62.5%, ≥ 2 mapped reads per sorted cell, and ≥ 100 mapped reads per gRNA in the library. The trimming auto determination result of MAGeCK was zero for ≥ 96% of reads, confirming correct adapter annotation and

usage. For the CD69 screens, each of the three positive populations ($CD69^{+}$, $CD69^{++}$, $CD69^{+++}$) and all their combinations were individually analyzed with MAGeCK RRA, and we selected the $CD69^{+}$ population for the main comparison as it has the most consistent signal due to higher numbers of sorted cells than for the $CD69^{++}$ and $CD69^{+++}$ populations. For the FAS screens, where three negative populations (FAS^{---}, FAS^{--}, FAS^{-}) were sorted, the FAS^{---} population showed the strongest enrichment of the screening marker and was selected for the main comparison. All analyses were performed with MAGeCK package v0.5.9.4, using the RRA algorithm with the mageck test command. We used the options --remove-zero both --remove-zero-threshold 0 to remove gRNAs with zero reads in both of the two compared samples. We specified the raw gRNA count matrix with -k, test samples with -t, and unsorted reference samples with -c. In addition, reference samples were also provided as --variance-estimation-samples. For read normalization, we used --norm-method median, and provided a set of non-essential genes (gene set NEGv1)[50] via the --control-gene option. All comparisons were run in --paired mode.

Genes were selected for inclusion in the *in vivo* CROP-seq experiment based on the results of the TCR and CAR fitness screens (normalized MAGeCK MLE $\beta > 0.99$) and the FACS-based screens ($\log_2FC > 2$, FDR < 0.05), with RNA levels in human CAR T cells serving as an additional filter (Fig. S6e, Table S7).

Analysis of the *in vivo* CROP-seq screens

The sequencing data from the *in vivo* CROP-seq screens were pre-processed as described above. Reads with UMIs containing an N were discarded. Different versions of the raw gRNA and UMI count table were prepared. For clonal tracking, the full UMI information was retained. For internal replicate analysis, only UMI bases 1 (4 internal replicates), 1-2 (16), 1-3 (64), 1-4 (256), and 1-5 (1024) were used. Finally, a table was prepared where all UMI information was discarded. All tables were further processed with mageck-ibar (https://bitbucket.org/WeiLab/mageck-ibar.git)[52]. Screening hits were defined using a stringent threshold of $\log_2FC > 1.5$ and FDR < 0.01. To determine the number of T cell clones in each sample, we plotted a "knee plot" by visualizing $\log_{10}$(rank) against $\log_{10}$(reads) for each UMI. To find the inflection point that separates T cell clones from background noise, we modeled a sigmoid curve of form $L / (1 + exp(-k * (x - x_0))) + b$ using the nls function from the R package stats. For modeling the log-transformed data, we disregarded the top-50 UMIs with highest read count as well as all UMIs with fewer than 10 reads. The coefficient x0 represents the inflection point that separates T cell clones from background noise.

RNA-seq data processing

The RNA-seq read data (unaligned BAM files) were aligned to the hg38 genome assembly using an adapted STAR pipeline[53]. The resulting count matrix was split by cell type and time point, and all downstream analyses were performed for each dataset separately. The analyses and visualizations described here were performed using a publicly available Snakemake 7.21.0[54] workflow v1.0.1[55]. Transcripts were filtered using the filterByExpr function from the R package edgeR v3.32.1[56] with the following parameters: group set to cell type and time point, min.count to 30, min.total.count to 50, large.n to 20 and min.prop to 0.8. Filtering reduced the number of analyzed transcripts from 60,676 to 15,856. The data were normalized using Conditional Quantile Normalization (CQN) from the R package cqn 1.44.0[57]. The parameters used for this normalization included gene length and GC content. The normalization results were $\log_2$-transformed for downstream analyses. Batch effects related to T cell donor were corrected for using the reComBat method[58] based on the log-transformed data. The normalization and batch correction were performed on the entire dataset for downstream visualization by PCA and visualization of pre-defined signatures.

Differential expression and gene set enrichment analysis

Differential expression analysis was performed on the quality-controlled, filtered, and normalized transcript counts using limma 3.46.0[59] to fit a linear model to find statistically significant transcripts in RHOG knockout compared to standard CAR T cells. We applied a publicly available snakemake workflow v1.0.2[60]. Briefly, we used lmFit to fit the model to the data, and limma's Bayes procedure with incorporated mean-variance trend to compute t-statistics.

For each comparison, we used topTable to determine transcript-wise average expression, effect sizes (log_2 fold change), and statistical significance (adjusted p-values based on the Benjamini-Hochberg method). Furthermore, we calculated transcript scores, for each transcript in each comparison, using the formula *-log_{10}(p-value)*sign(log_2 fold change)* for downstream ranked enrichment analyses.

Gene set enrichment analysis was performed with a publicly available snakemake workflow v0.1.1[61] using GSEA (https://www.genepattern.org/modules/docs/GSEAPreranked/1) with the prerank function from the GSEApy 1.0.3 package[62]. The "GO biological process sets" gene sets were selected (http://www.broadinstitute.org/gsea/msigdb). Enrichment scores (ES) reflect the degree to which a gene set is overrepresented at the top or bottom of a ranked list of genes, and normalized enrichment scores (NES) are ES scores normalized by mean ES across all comparisons for the dataset. The results of all queries were aggregated by method and database. Additionally, we filtered the results by retaining only the union of terms that were statistically significant (adjusted p-value < 0.05) in at least one query. The aggregated results were visualized using hierarchically clustered heatmaps and bubble plots. The union of the most significant terms per query were determined, and their effect size and significance were visualized as a hierarchically clustered bubble plot encoding both effect size (color) and statistical significance (size), with statistical significance denoted by an asterisk. All summary visualizations values were capped at an adjusted p-value of 0.0001 to minimize the visual effect of genes with very low p-values. Clustering of enriched terms was done using R clusterProfiler package v4.8.1 function emapplot[51]. Cell cycle-related genes were defined from a gene signature[63].

Analysis of the combinatorial screens

The combinatorial screening data were processed as follows: Raw reads were extracted from unaligned BAM files (*samtools view* with flag *-f 64* for read1 and *-f 128* for read2), joined by the read identifier (column1 or QNAME of the BAM), and CROP-seq-multi features (spacer1, iBAR1, spacer2, and iBAR2) were extracted based on their position. To produce a count matrix for downstream analyses (Table S8c), we matched the combination of spacer1, iBAR1, spacer2, iBAR2 to the combinatorial gRNA library (Table S8a, 0 mismatches allowed). We calculated additional quality control metrics, such as percent of perfect matches to library features, fold difference between the 10^{th} and 90^{th} percentiles of library counts, and percent recombination between spacer-iBAR pairs (Table S8b). The processed data were analyzed with MAGeCK MLE, using a design matrix modeling the 19-BBz, 19-28z, and GD2-BBz CARs (Table S8e), with options *--permutation-round 10 --max-sgrnapergene-permutation 40*. We normalized the data relative to dual safe harbor gRNAs with the *--norm-method control* and *--control-sgrna* options. We provide sample annotation (Table S8b), gRNA counts (Table S8c), and MAGeCK MLE output (Table S8f).

Comparison of screening quality with published datasets

We obtained CRISPR screening data for primary T cells from Shifrut, Carnevale et al. 2018[20], Wang, Prager et al. 2021[18], Carnevale, Shifrut et al. 2022[13], Freitas, Belk et al. 2022[14], and data for the Jurkat cell line from DepMap release 24Q4 (https://plus.figshare.com/articles/dataset/DepMap_24Q4_Public/27993248/1). Detailed information on the data sources is provided in Table S4b. For datasets where raw gRNA counts were available (Shifrut, Freitas), we calculated log_2 fold changes between day 16 (Shifrut) or 20 (Freitas) to the plasmid reference. For the Jurkat data, log_2 fold changes between day 21 and the plasmid reference were directly available (AvanaLogfoldChange.csv), and for Carnevale 2022 we obtained log_2 fold change values from the MAGeCK RRA output. For Wang 2021, only beta values but not the full MAGeCK MLE output were available, so we re-processed our own data with the same MAGeCK MLE settings. To compare the dropout of essential genes across screens while taking the variance into account, we used the strictly standardized mean difference (SSMD) metric, calculated as:

$$\mathrm{SSMD} = \frac{\overline{X}_e - \overline{X}_{ne}}{\sqrt{s_e^2 + s_{ne}^2}}$$

where $\overline{X}_e$ and $\overline{X}_{ne}$ are the mean $\log_2$ fold changes of essential and nonessential genes, and s_e and s_{ne} are the corresponding standard deviations. We used sets of 684 essential genes (CEGv2), and 928 nonessential genes (NEGv1), both from the BAGEL2 publication[50]. Screens with an SSMD < 0.5 were flagged as low quality and excluded from the downstream hit analysis.

Comparison of screening results with published datasets

We obtained MAGeCK output files for all high-quality screens (SSMD > 0.5): Shifrut 2018 (TCR fitness, CGS-21680), Carnevale 2022 (regulatory T cell, TGFβ, TCR fitness, Adenosine), Freitas 2022 (IL2/TNF, CAR fitness) and from this study (TCR fitness, CAR fitness, FAS, PD1/LAG3/TIM3, CD69, CD19). Most screens were processed with MAGeCK RRA, where we defined significant hits as z-normalized $\log_2$ fold change > 2 and FDR < 0.05. For the TCR and CAR fitness screens from this study, we used MAGeCK MLE with beta value normalization for essential genes via MAGeCKFlute, to control for the different proliferation rates between TCR and CAR stimulated T cells, with a selection threshold of normalized beta > 0.99. For the heatmap in Fig. S4g, we included all significant hits except for those from our fitness screens, where the high number of significant genes required us to limit the selection to the *in vivo* tested genes.

Base editing gRNA library design

We first designed all possible gRNAs for each target gene, including all exons and ±20 base pairs into each intron or UTR. Editing outcomes were annotated using the base-editor-design-tool (https://github.com/mhegde/base-editor-design-tool#base-editor-design-tool)[44]. We excluded gRNAs containing stretches of 4 or more Ts, which can lead to premature termination of gRNA transcription. We also exclude gRNAs with BsmBI cut sites because the PCR-amplified gRNAs were cloned with Gibson assembly, where the backbone was cut by BsmBI.

For the PAM-less tiling screens of RHOG and PAC, all possible gRNAs were used. For essential genes, we designed gRNAs introducing specific mutation types, depending on the base editor: 50 splice-site mutations for ABEmax, 50 splice-site and 50 nonsense mutations for AncBE4max, 200 splice-site mutations for ABEmax7.10-SpRY, as well as 200 splice-site and 200 nonsense mutations for CBE4max-SpRY. To that end, we filtered gRNAs introducing nonsense or splice-site mutations in the first half of the transcript, where the target base is in positions 5 to 7 (which corresponds to the central part of the editing window). We selected essential genes according to their rank in the MAGeCK RRA analysis of our genome-wide fitness screens, with a limit of 4 gRNAs per gene. For control gRNAs targeting a safe harbor locus, we designed gRNAs such that 50% of them contained ≥1 A but no C and 50% contained ≥1 C but no A in the editing window, such that they can serve as non-targeting controls for C→T and A→G editors, respectively. Each group contained 25% gRNAs with NGG PAM and 25% gRNAs with non-NGG PAM.

For the base editing validation screens, we selected gRNAs based on the z-score from the initial screen: 3.5% most enriched for RHOG and 3.5% most depleted for PAC from average z-score for two donors, and for each donor separately) with additional safe harbor-targeting control gRNAs, resulting in a library of 323 gRNAs (Table S9).

Base editing analysis

For plasmid and pre-electroporation reference samples, sequencing reads were aligned to the gRNA library. As the gRNAs are integrated into the genome, they may be susceptible to self-editing by near-PAM-less base editors upon electroporation. Therefore, we created expanded reference files separately for the A-to-G and C-to-T editors, containing all original gRNA sequences as well as sequences resulting from self-editing in the editing window (gRNA positions 4 to 8). We aligned reads from base-edited samples to these references, and produced gRNA-level count files (Table S9). $\log_2$FC values were calculated by comparing samples from day 14 (screening readout) and day 0 (pre-electroporation reference) using MAGeCK RRA with parameters --norm-method median, --remove-zero both, --remove-zero-threshold 0, --paired, and --variance-estimation-samples, pairing samples by T cell donor (two donors

for the initial screening and five donors for the base editing validation screens) and using samples from day 0 for variance estimation. For visualization, protein 3D structures were downloaded from PDB and the 15 amino acids corresponding to the most impactful base editing gRNAs were drawn as stick representation using PyMOL. Hydrogen bonds were computed between the highlighted amino acids and the small molecule reagents using the PyMOL command "distance hbonds, small_molecules, top15_aas, mode=2".

Base editing validations

Base editing validation screens. CD4 T cells were lentivirally transduced with the CROP-seq-CAR vector containing a focused gRNA library for base editing validation screens (Table S9) and cultured as described above ("CELL-FIE screening pipeline"). gRNA amplification was performed as described above for all base editors. For genomic locus sequencing, ABEmax-edited CAR T cells were collected 2 and 12 days after electroporation. A 200-bp region of the RHOG locus, harboring high-scoring gRNAs from the focused validation screens was PCR-amplified with primers containing overhangs compatible with TruSeq indexing (Table S1c) using Q5 Hot Start High-Fidelity 2x Master Mix (NEB #M0494L) followed by 1.2x SPRI bead purification using Mag-Bind TotalPure NGS Beads (Omega Bio-tek #M1378-01). The purified PCR fragments were indexed by PCR using the TruSeq indexing primers (Table S1d) to prepare them for sequencing on the Illumina NovaSeq 6000 platform.

Single gRNA validations. CD4 T cells were lentivirally transduced with CROP-seq-CAR vectors, each harboring a single base editing gRNA, targeting either the RHOG or PAC gene. After 7 days of puromycin selection including 2 days of restimulation, CAR T cells were electroporated with mRNA encoding the ABEmax base editor (Table S1b). Three days after electroporation, a portion of cells was collected for gDNA extraction and the remaining cells were restimulated with 25 µl/ml ImmunoCult Human CD3/CD28 T Cell Activator (Stemcell #10990) and further cultured in the presence of puromycin, until collection for gDNA extraction at day 12 after electroporation. To assess the editing efficiency at the target loci on the DNA level, the RHOG and PAC loci were PCR-amplified using Q5 Hot Start High-Fidelity 2x Master Mix (NEB #M0494L) with locus-specific primers (Table S1c). The resulting amplicons from samples collected at day 3 and day 12 after electroporation were Sanger sequenced and editing efficiency was analyzed using the EditR tool[64] with default parameters.

Materials availability

All plasmids generated in this study, including the CROP-seq-CAR and mRNA production vectors, have been deposited to Addgene (Table S1).

Data availability

The RNA-seq data are available from GEO (accession number: GSE266618; reviewer token: wvyjckskhhcjjst). The CRISPR screening data are provided in Table S2 (fitness screens), Table S3 (FACS screens), Table S5 (*in vivo* screens), Table S8 (combinatorial screens), and Table S9 (base editing screens).

Acknowledgements

We would like to thank the Austrian Red Cross (Robert Geretschläger, Christiane Feinböck) for providing healthy donor blood samples; Antonia Müller and Stephanie Winter at the Department of Transfusion Medicine and Cell Therapy of the Medical University of Vienna for providing a leukapheresis product from a patient scheduled to receive CAR T cell therapy; the Biomedical Sequencing Facility at CeMM for assisting with next-generation sequencing; the Core Facility Flow Cytometry of the Medical University of Vienna for providing access to cell sorting equipment; the Core Facility Laboratory Animal Breeding and Husbandry and the Preclinical Imaging Laboratory of the Medical University of Vienna for hosting the animal work and providing access to materials, services, and equipment; Crystal Mackall Lab for providing the NALM6-GD2 cell line; Niki Winhofer for feedback on illustrations; and the members of the Bock Lab for advice and discussions. This work was supported by an ERC Consolidator Grant (grant agreement no. 101001971, grantee: C.B.) of the European Union's Horizon 2020 research and innovation program, and an Austrian Science Fund (FWF) Special Research Program grant (F7001, grantee: C.B.).

Author contributions

P.D. conceived and designed the CELLFIE platform; P.D. and E.V.P. developed the CELLFIE platform and led the experiments; P.D., E.V.P., and C.A. planned and performed the experiments; J.L., N.P., A.-C.O., A.N., P.B., M.C., and T.N. assisted with the experiments; P.D. and E.V.P. led and performed the data analysis with contributions by D.R., M.S., and A.V.A.; S.L. and T.K. prepared the animal license and organized the *in vivo* experiments; F.P., W.L., and T.K. assisted with the *in vivo* experiments; T.K. provided feedback on the T cell experiments; P.D. and E.V.P. visualized the results, prepared the figures, and wrote the draft manuscript; P.D., E.V.P., and C.B. wrote the manuscript with contributions from all authors; P.D. and C.B. supervised the project.

Competing financial interests

P.D., E.V.P., and C.B. are inventors on patent applications related to the CELLFIE platform and boosters of immunotherapy. C.B. is a cofounder and scientific advisor of Myllia Biotechnology and Neurolentech. P.D. acknowledges outside interest in Xaira Therapeutics. The remaining authors declare no competing interests.

Figures

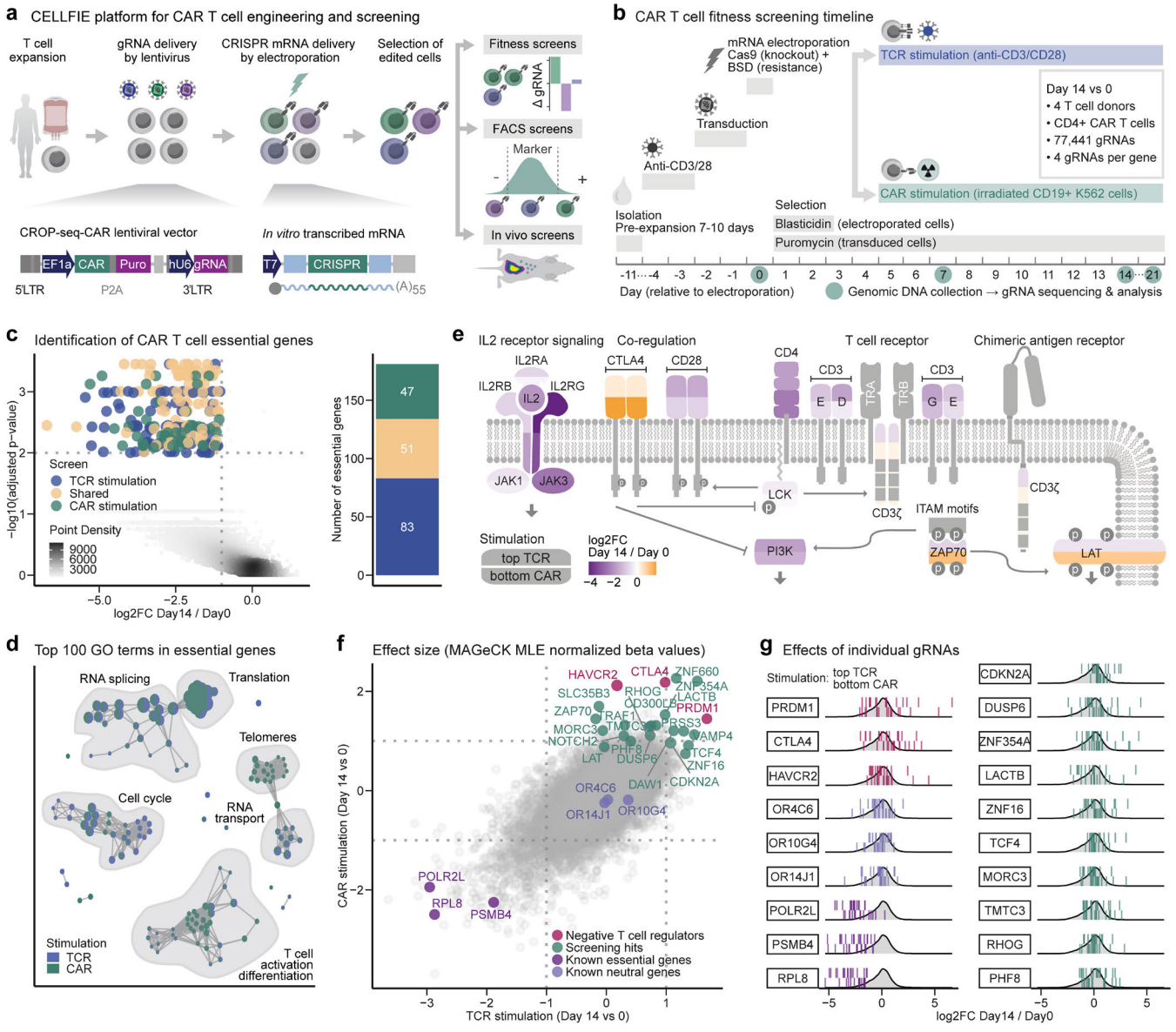

Fig. 1 | Genome-wide fitness screening in human primary CAR T cells with the CELLFIE platform.

a, Overview of the CELLFIE platform for highly scalable CAR T cell engineering and CRISPR screening. Human primary T cells are isolated, activated and expanded, transduced with a lentivirus delivering the chimeric antigen receptor (CAR) and gRNA library, and electroporated with synthetic mRNA that delivers the CRISPR editor.

b, Experimental timeline for genome-wide fitness screens. Human primary T cells were isolated from whole blood, activated, and pre-expanded for 7 to 10 days. Following a second round of activation, cells were transduced with the CROP-seq-CAR lentivirus for co-delivery of the CAR and the genome-wide gRNA library. Two days later, cells were electroporated with synthetic mRNA for Cas9 and blasticidin resistance. Antibiotic selection with puromycin selects for successful lentiviral transduction, and blasticidin selects for successful mRNA electroporation. Gene-edited CAR T cells were expanded under repeated T cell receptor (TCR) stimulation with anti-CD3/CD28 beads or repeated CAR stimulation with $CD19^{+}$ K562 cells. The gRNA representation was analyzed by sequencing on day 0, 7, 14, and 21. Comparison between day 14 and day 0 was based on 4 blood donors in two independent screens.

c, Essential genes for human CAR T cells under CAR and TCR stimulation (details in Table S2). The scatterplot shows gene-level $\log_2$ fold changes between day 14 and day 0 of the screen (x-axis) against FDR-adjusted p-values (y-axis), highlighting genes that passed stringent significance thresholds (FDR < 0.01 and $\log_2$ FC < -1.5).

d, Unsupervised clustering of the top-100 most enriched Gene Ontology (GO) terms from the Biological Process category among the essential genes (panel c).

e, Gene-level $\log_2$ fold changes between day 14 and day 0 for the fitness screens, mapped onto a schematic of the TCR and CAR signaling pathways. For each protein shape, the top-half color corresponds to the TCR stimulation screens and the bottom-half color to the CAR stimulation screens.

f, Effect sizes for fitness screens with TCR stimulation (x-axis) and CAR stimulation (y-axis). MAGeCK MLE beta values comparing day 14 and day 0 were normalized to essential genes, to account for the different proliferation rates upon TCR or CAR stimulation (Fig. S3d). Color-coded are genes with increased fitness (green), known negative T cell regulators (magenta), neutral olfactory receptors (blue), and essential genes (purple).

g, High-resolution view of gRNA $\log_2$ fold changes between day 14 and day 0 for each gRNA and each donor.

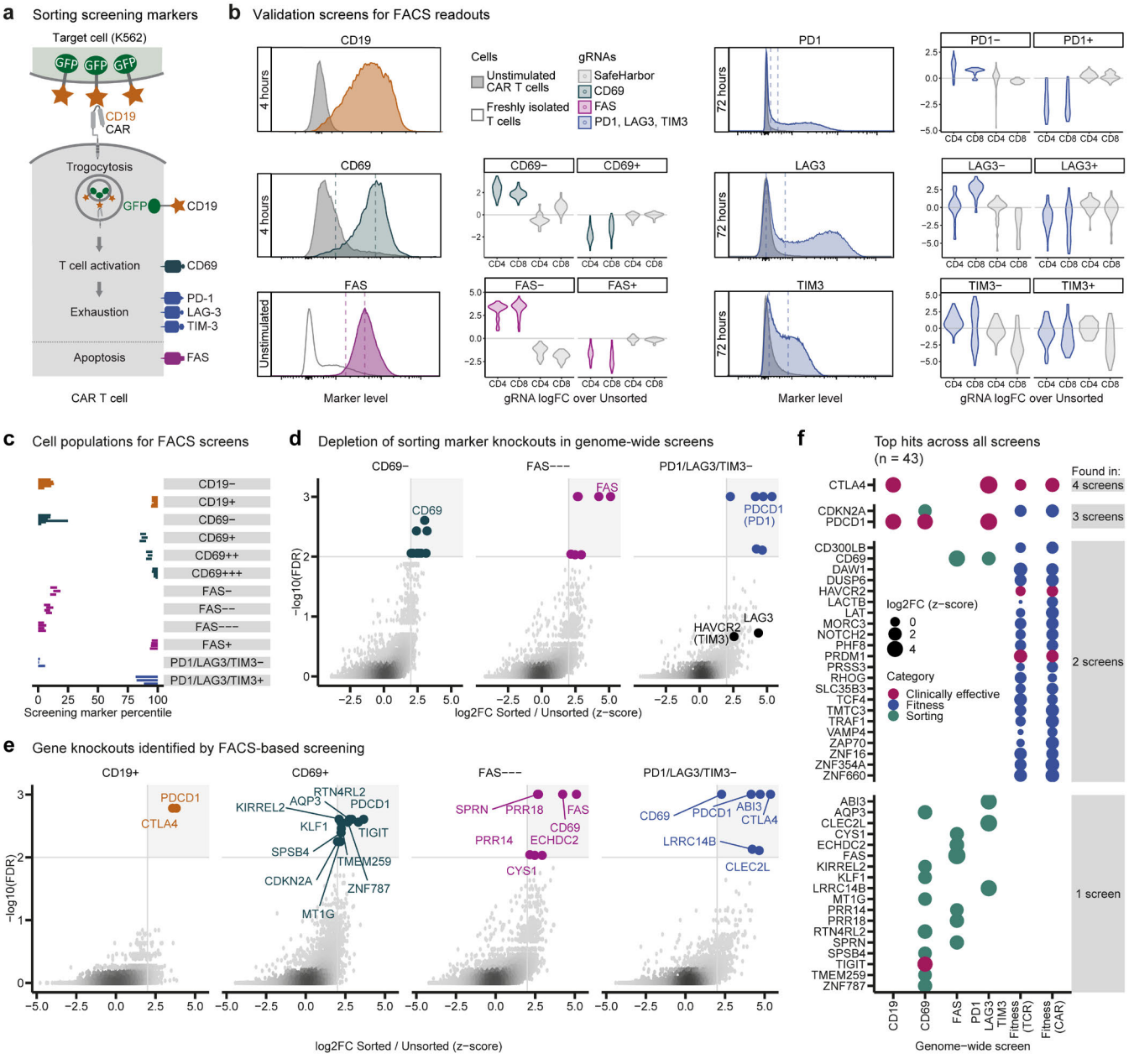

Fig. 2 | Genome-wide screens with six FACS-based markers that model clinical limitations of CAR T cells.

a, Surface proteins on CAR T cells used as FACS-based screening readouts. Antigen recognition by the CAR can transfer CD19 from the target cell to the CAR T cell surface (trogocytosis), which is used here a marker of target cell recognition; CD69 expression is used as a marker of CAR T cell activation; FAS expression as a marker of apoptosis; and combined expression of PD1, LAG3, and TIM3 as an early indicator of T cell exhaustion.

b, Optimization of marker protein gating and sampling time points by flow cytometry using unmodified CAR T cells (left, showing one representative experiment) and focused validation screens ($n \geq 3$ independent T cell donors, right) comparing distributions of $\log_2$ fold changes of gRNAs targeting the sorting marker ($n = 20$, colored) or a safe harbor locus ($n = 20$, grey), shown separately for marker-negative and marker-positive populations (for all markers except CD19, which is taken up from target cells rather than produced by the CAR T cells).

c, Sorted cell populations ($n = 45$, details in Table S3) for all genome-wide FACS-based screens. Each bar represents one independent T cell donor.

d, Validation analysis showing strong enrichment of FACS marker genes among the marker-negative cell populations. Significantly enriched genes (FDR < 0.01 and log_2FC > 1.5) are colored, and genes used as markers for FACS are labeled.

e, Identification of knockouts that improve CAR T functionality in the FACS-based screens. The scatterplots show gene-level log_2 fold changes between sorted and unsorted populations (x-axis) plotted against FDR-adjusted p-values (y-axis). Genes are highlighted that passed stringent significance thresholds (FDR < 0.01 and log_2 FC > 1.5).

f, Summary of positive screening hits (n = 43) that improved various properties of CAR T cells, derived from all genome-wide fitness screens (blue) and FACS-based screens (green). The bubble plot shows log_2 fold changes of z-scores for significant gene knockouts. Clinically proven immunotherapy target genes are highlighted in magenta.

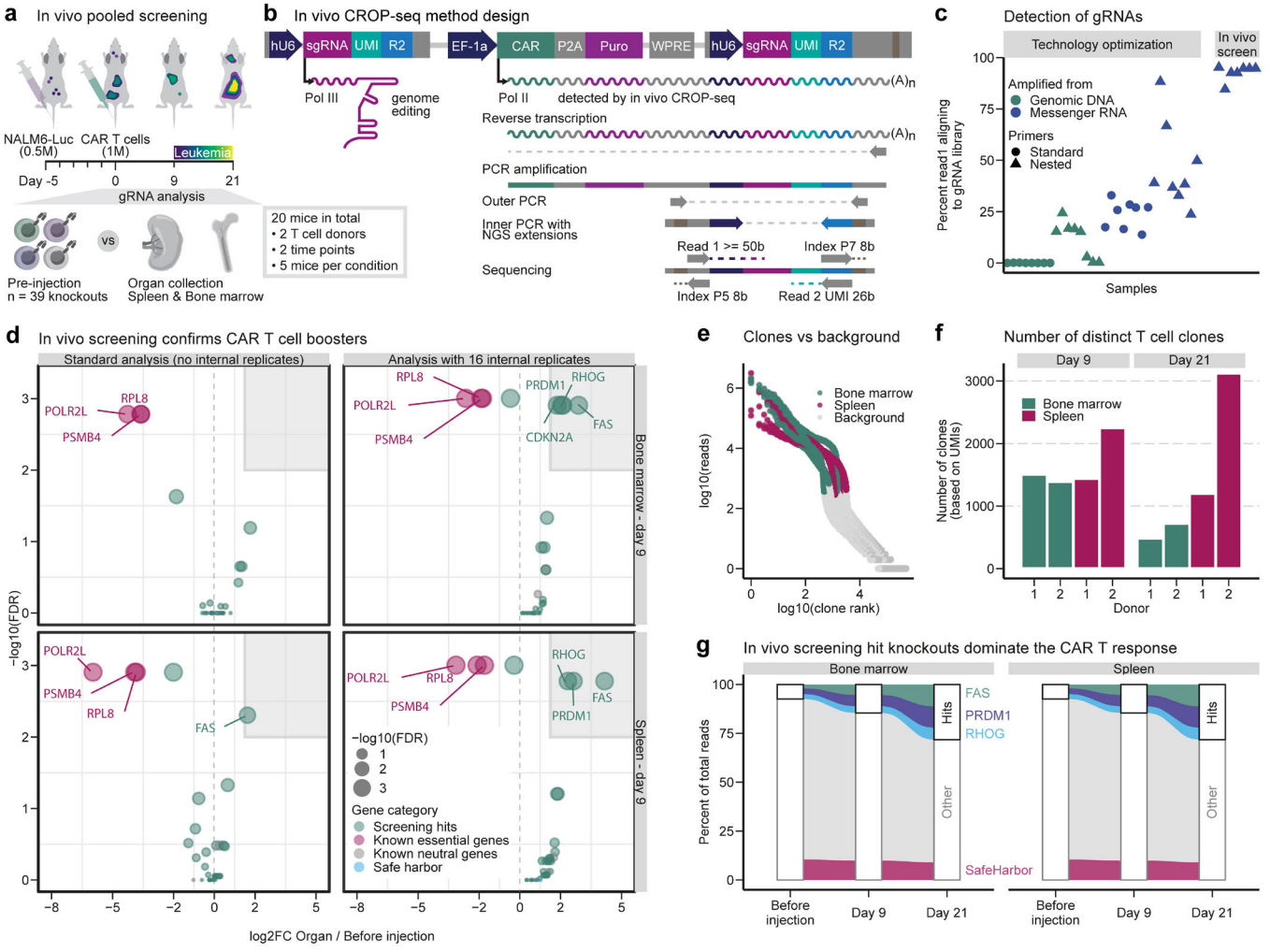

Fig. 3 | *In vivo* pooled validation screen of putative CAR T cell boosters in leukemic mice.

a, Experimental timeline for pooled *in vivo* screening. Immunodeficient NSG mice were injected with human NALM6 cells to induce systemic B cell leukemia. These mice were treated with a low (and deliberately non-curative) dose of knockout CAR T cells for the screening hits (from Fig. 2f) as well as controls. Spleen and bone marrow were collected on day 9 and 21, and the gRNA representation was compared to the pre-injection sample.

b, Vector design and technical outline of the *in vivo* CROP-seq method. The gRNA cassette, including a unique molecular identifier (UMI) and Illumina Read2 sequence, was cloned into the 3' LTR of the CROP-seq-CAR vector. The gRNA and UMI can be detected from a polymerase II transcript encoding CAR-P2A-Puro, using reverse transcription and nested PCR. The gRNA is sequenced with Read1 and the UMI with Read2 in paired-end sequencing.

c, gRNA detection for state-of-the-art pooled screening with gRNA amplification from genomic DNA, and for *in vivo* CROP-seq with gRNA amplification from mRNA, both tested with single PCR and nested PCR amplification.

d, *In vivo* CROP-seq data analyzed with standard methods (left) or with UMIs to group reads into 16 internal replicates (right). RHOG, FAS, PRDM1, and CDKN2A were identified as significant (FDR < 0.01 and $\log_2$FC > 1.5).

e, "Knee plot" showing rank versus read number for each UMI. The inflection point separates distinct CAR T cell clones identified by their unique UMIs (colored) from background noise (grey).

f, Number of CAR T cell clones detected for each organ, donor, and time point.

g, CAR T cells for the three top-ranked gene knockouts (FAS, PRDM1, and RHOG) dominate the CAR T response, collectively accounting for >25% of CAR T cell clones at day 21 after injection. In contrast, CAR T cells with gRNAs targeting a safe harbor locus (magenta) are largely unchanged in their relative frequency.

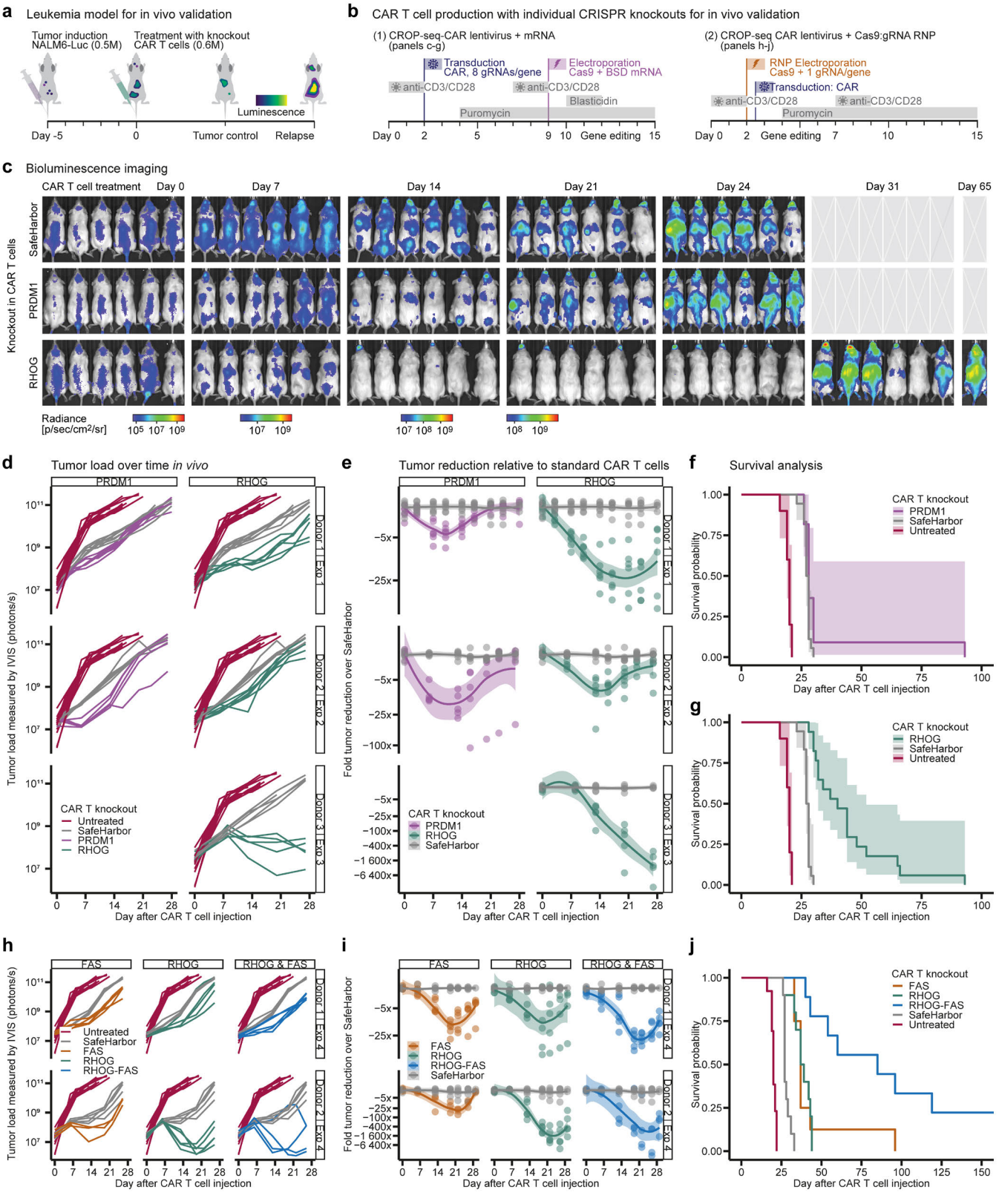

Fig. 4 | RHOG, FAS, and PRDM1 knockouts enhance leukemic cell control and survival *in vivo*.

a, Experimental timeline for the individual *in vivo* validation experiments. Immunodeficient NSG mice were injected with 0.5 million human NALM6 cells to induce systemic B cell leukemia. On day 5, mice were treated with a low

(and deliberately non-curative) dose of 0.6 million CAR T cells with knockouts for RHOG, FAS, or PRDM1 in separate experiments. NALM6 cells were engineered to express firefly luciferase for *in vivo* imaging.

b, Experimental outline for the individual *in vivo* validation experiments with CRISPR-boosted CAR T cells, which were genetically engineered either by lentiviral co-delivery of the CAR and a pool of 8 gRNAs followed by mRNA delivery of Cas9 (as in the *in vitro* and *in vivo* screens) or by electroporation of a pre-assembled RNP complex of Cas9 protein and one top-performing gRNA (as is common practice in CRISPR-edited cell therapy).

c, Representative bioluminescence images showing initial leukemic cell control and subsequent relapse for leukemic mice treated with standard (safe harbor locus-edited) CAR T cells or with PRDM1 or RHOG knockout CAR T cells.

d, Leukemic cell load over time, as measured by bioluminescence imaging, for mice that were left untreated or were treated with standard CAR T cells or with PRDM1 or RHOG knockout CAR T cells. CRISPR-edited CAR T cells for 6 independent T cell donors were prepared with mRNA delivery of Cas9 (panel b, left). Results are shown for 3 representative donors from 3 independent experiments. All data are provided in Table S6.

e, Leukemia-reducing effect of PRDM1 or RHOG knockout CAR T cells, calculated by comparing the leukemic cell load of the knockout CAR T cells to that of standard CAR T cells (results for the mice shown in panel d).

f,**g**, Survival analysis for leukemic mice that were left untreated or were treated with standard CAR T cells or PRDM1 (panel f) or RHOG (panel g) knockout CAR T cells (results for the mice shown in panel d).

h, Leukemic cell load over time, as measured by bioluminescence imaging, for mice that were left untreated or were treated with standard CAR T cells or CAR T cells with FAS knockout, RHOG knockout, or RHOG-FAS double knockout. CRISPR-edited CAR T cells for 2 independent T cell donors were prepared using electroporation of a pre-assembled RNP complex of Cas9 protein and one top-performing gRNA (panel b, right).

i, Leukemia-reducing effect of knockout CAR T cells for FAS, RHOG, or RHOG-FAS double knockout, calculated by comparing the leukemic cell load of the knockout CAR T cells to that of standard CAR T cells (results for the mice shown in panel h).

j, Survival analysis for leukemic mice that were left untreated or were treated with standard CAR T cells or with knockout CAR T cells for FAS, RHOG, or RHOG-FAS double knockout (results for the mice shown in panel h). The smoothed line in **e** and **i** indicates the mean; the shaded area in **e**, **i**, **f**, **g**, **j** shows the 95% confidence interval.

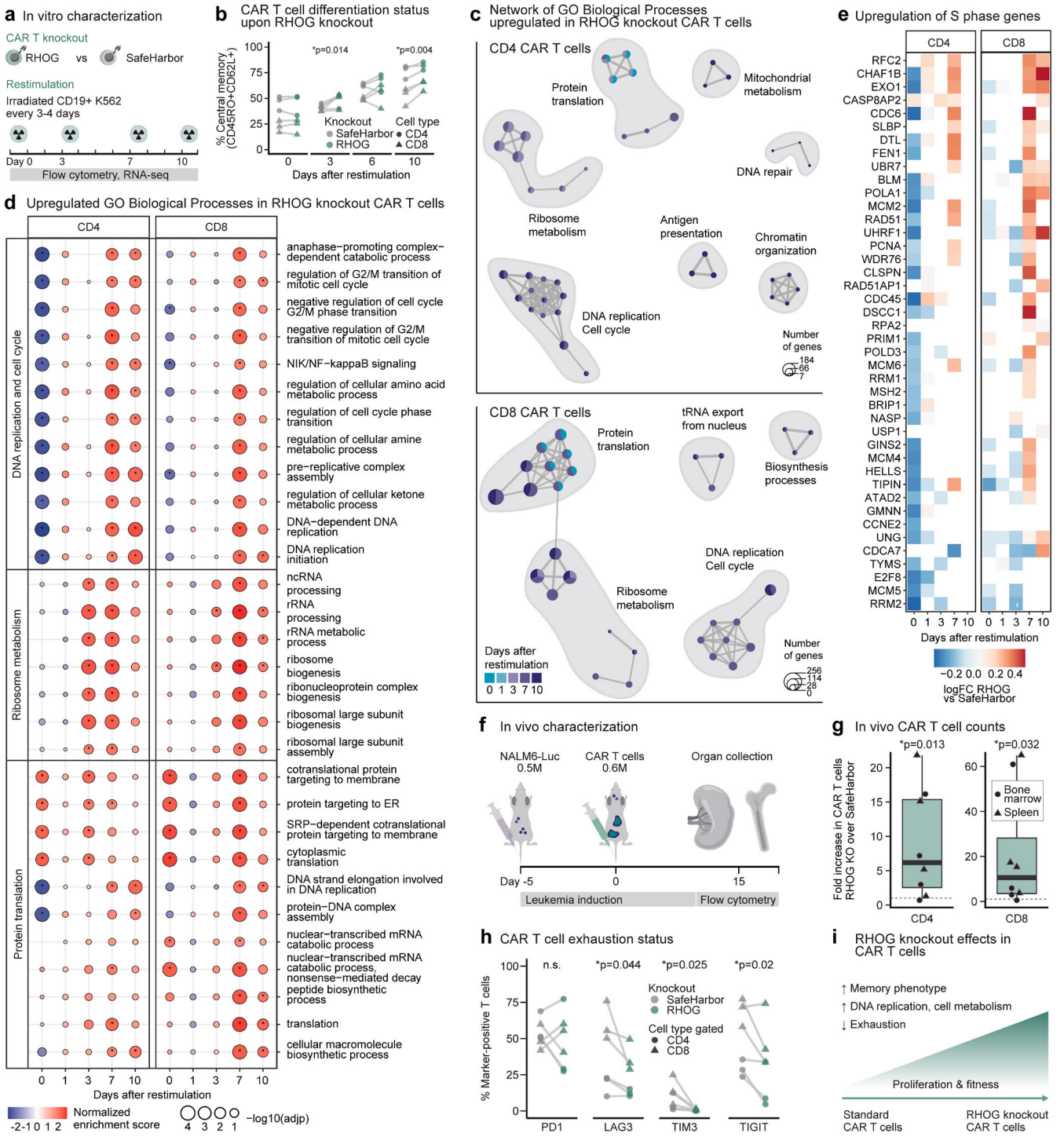

Fig. 5 | Enhanced proliferation and persistence of RHOG knockout CAR T cells.

a, Experimental timeline for comparing RHOG knockout CAR T cells to standard (safe harbor locus-edited) CAR T cells *in vitro*. CAR T cells were repeatedly stimulated with irradiated CD19$^+$ K562 cancer cells. On day 0, 3, 7, and 10, CD4 and CD8 CAR T cells were isolated and profiled by RNA-seq and flow cytometry.

b, Increase in central memory (CD45RO$^+$CD62L$^+$) CAR T cells over 10 days of repeated stimulation with cancer cells, comparing RHOG knockout to standard CAR T cells (n = 3 independent T cells donors).

c, Network visualization of upregulated GO Biological Process terms in RNA-seq data comparing RHOG knockout to standard CAR T cells, shown separately for CD4 (top) and CD8 (bottom) CAR T cells.

d, Gene set enrichment analysis of GO Biological Process terms for three clusters from panel c.

e, Differential gene expression for cell proliferation associated genes (S phase marker genes) comparing RHOG knockout to standard CAR T cells.

f, Experimental timeline for comparing RHOG knockout CAR T cells to standard (safe harbor locus-edited) CAR T cells *in vivo*. Immunodeficient NSG mice were injected with 0.5 million human NALM6 cells to induce systemic B cell leukemia. On day 5, mice were treated with 0.6 million RHOG knockout or standard CAR T cells. On day 15 after treatment, CAR T cells isolated from bone marrow and spleen were profiled by flow cytometry.

g, Fold increase in the total number of CD4 or CD8 CAR T cells in mice treated with RHOG knockout CAR T cells in comparison to standard CAR T cells. Cell counts were obtained by flow cytometry of spleen and bone marrow on day 15 after CAR T treatment. The center line is the median, the box limits are the upper and lower quartiles, and the whiskers extend to 1.5 times the interquartile range.

h, Decreased expression of exhaustion markers LAG3, TIM3, and TIGIT in RHOG knockout CAR T cells *in vivo*.

i, Schematic summary of RHOG knockout effects in CAR T cells, explaining their improved *in vivo* efficacy.

Statistical comparisons were performed using paired one-tailed Student’s t-test.

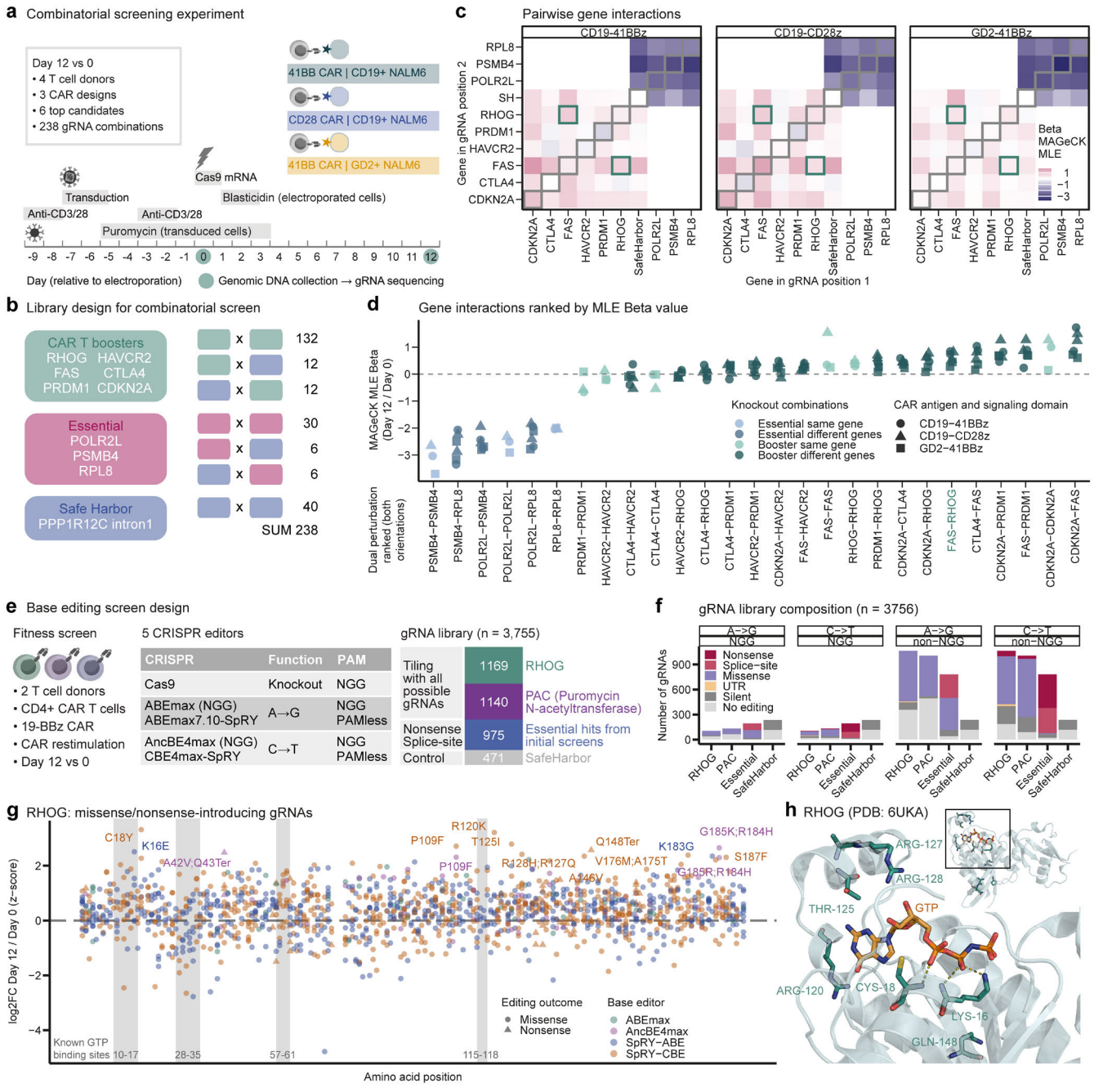

Fig. 6 | Combinatorial knockout and base editing screens with the CELLFIE platform.

a, Experimental timeline of combinatorial fitness screens with CROP-seq-CAR-multi vectors for 3 different CARs (19-BBz, 19-28z, GD2-BBz), replicated in 4 different T cell donors.

b, Library design covering 238 combinations of gRNAs targeting top hits from the *in vivo* validation screen, essential genes, and safe harbor gRNAs.

c, Heatmap of fitness effects for pairwise gene knockouts (MAGeCK MLE beta value comparing day 12 vs. day 0).

d, Ranking of fitness effects for pairwise gene knockouts (MAGeCK MLE beta value comparing day 12 vs. day 0).

e, Experimental outline of tiling base editing screens for RHOG. CD4 CAR T cells from 2 blood donors were transduced with a library of 3,756 base editing gRNAs tiling the gene body of RHOG and the antibiotic resistance gene

puromycin-N-acetyltransferase (PAC). We also included base editing gRNAs as positive controls that induce non-sense and splice-site mutations in essential genes, as well as negative controls targeting a safe harbor locus. We electroporated synthetic mRNA for standard Cas9, and four different base editors (A-to-G, C-to-T, and their near-PAM-less variants). The gRNA distribution was compared between day 12 and day 0 after CAR restimulation.

f, Number and type of mutations predicted to be introduced by each of the four CRISPR base editors.

g, Mutagenesis map for RHOG derived from the base editing screens. Log_2 fold changes of z-scores (y-axis) are shown for each gRNA throughout the gene body. The top-15 enriched gRNAs are labeled with predicted amino acid changes, and RHOG functional domains are annotated.

h, Amino acids with the strongest mutagenesis effects for RHOG highlighted on the protein structure.

Extended Data Figures

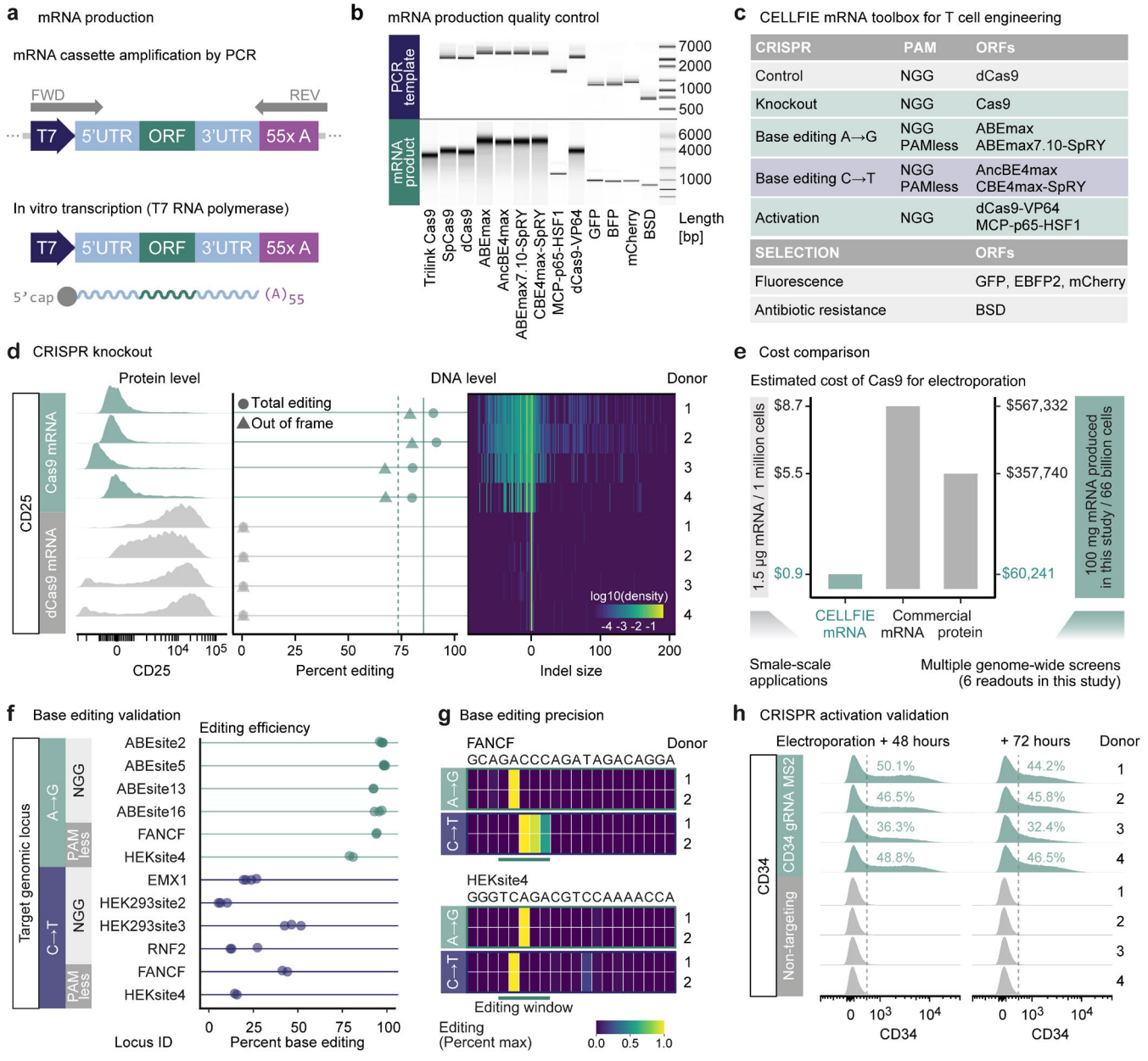

Fig. S1 | CELLFIE: a versatile platform for engineering human primary CAR T cells.

a, Schematic of the mRNA production plasmid. Open reading frames (ORFs) for CRISPR editors and selectable markers were cloned between untranslated regions (UTRs) to stabilize the mRNA. For mRNA production, we amplified a PCR template and used it as input for *in vitro* transcription (IVT) from the T7 promoter with co-transcriptional capping, terminating at a hardcoded A-tail of 55 bases.

b, Representative size profiles of PCR templates and *in vitro* transcribed mRNA for CRISPR editors and selection markers.

c, Validated synthetic mRNAs for delivery of CRISPR editors and selection markers into human primary T cells and CAR T cells.

d, Efficient knockout of IL2RA (CD25) at the DNA and protein level in CD4 T cells from four independent donors.

e, Cost of custom-made synthetic Cas9 mRNA, compared to commercial reagents. Left: Synthetic mRNA cost for a small-scale editing experiment. Right: Total cost for all mRNA produced in this study, used for delivering synthetic mRNA into 66 billion human primary (CAR) T cells and for assay development and optimization experiments.

f, CRISPR base editing efficiency (top: A-to-G, bottom: C-to-T) in CD4 T cells using standard and near-PAM-less base editors for multiple genomic loci.

g, CRISPR base editing specificity within the editing window for two genomic loci.

h, CRISPR activation of CD34 using mRNA-based delivery of the SAM system into CD4 T cells obtained from 4 independent donors.

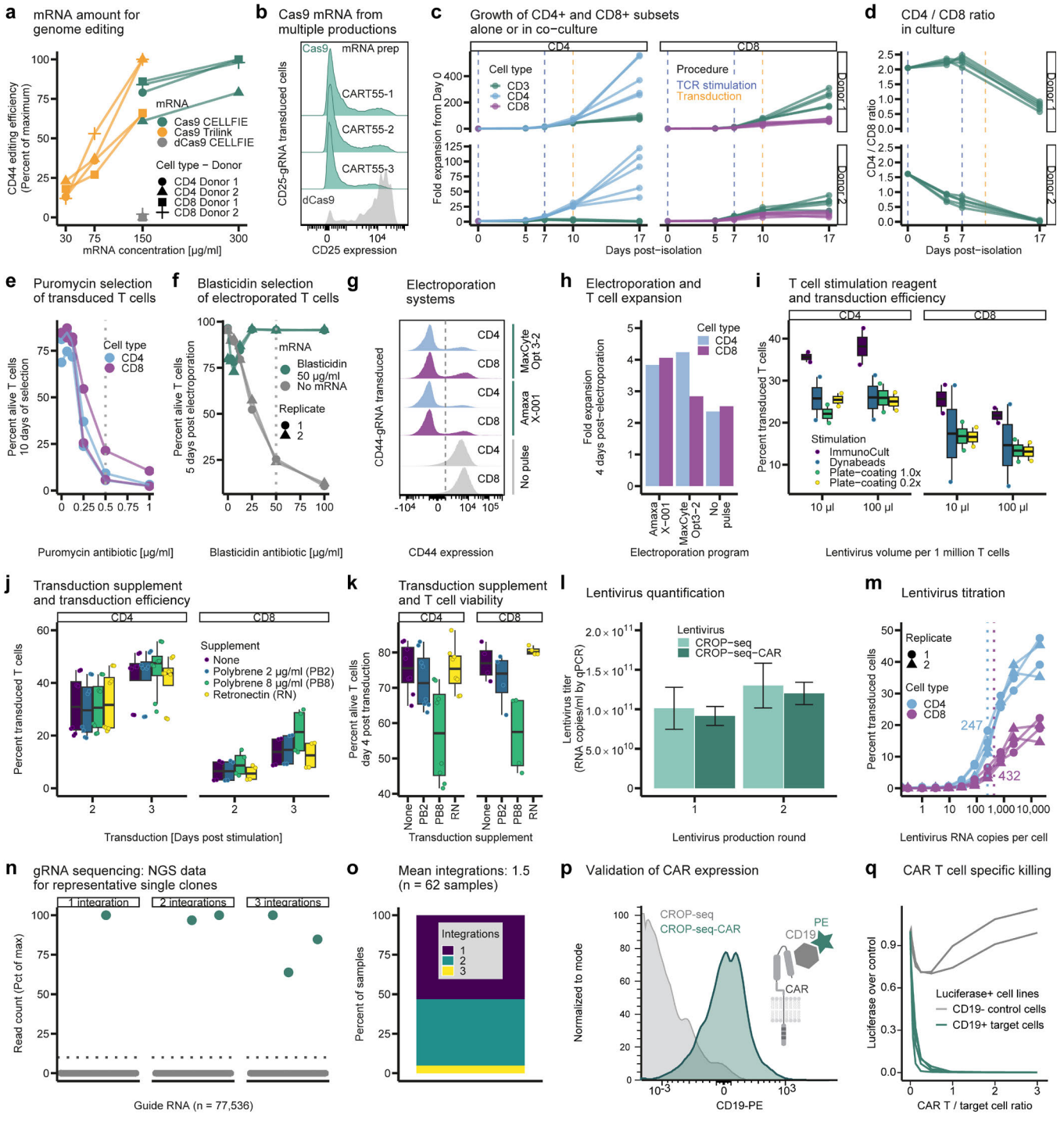

Fig. S2 | Developing and optimizing the CELLFIE platform.

a, Titration of synthetic mRNA concentration for efficient CRISPR knockout of CD44 in human primary CD4 and CD8 T cells from two independent donors. Pan-CD3 T cells were used as starting material. Comparable editing efficiencies were observed for custom-made and commercial Cas9 mRNA.

b, Consistent editing efficiencies in CD4 T cells with custom-made Cas9 mRNA from multiple production rounds.

c, Cell proliferation of CD4 and CD8 CAR T cells made from pan-CD3 T cells, isolated CD4 T cells, or isolated CD8 T cells as starting material.

d, Declining representation of CD4 CAR T cells in co-culture with CD8 CAR T cells. Pan-CD3 T cells were used as starting material.

e, Puromycin titration to determine the optimal concentration (0.5 μg/ml) to select for T cells that have been successfully transduced with CROP-seq-CAR lentivirus.

f, Blasticidin titration to determine the optimal concentration (50 μg/ml) to select for T cells that were successfully electroporated with blasticidin resistance mRNA (BSD), which was co-delivered with the CRISPR editor mRNA.

g, Optimal programs for genome editing of human primary T cells on the Amaxa and MaxCyte electroporators used for small-scale experiments (up to 1.5 million cells per cuvette) and for large-scale screens (up to 100 million cells per cuvette), respectively. Results for CD4 and CD8 T cells from pan-CD3 T cell culture are shown.

h, T cell expansion after electroporation of synthetic Cas9 and BSD mRNA.

i, Lentivirus transduction rates after T cell stimulation with different reagents (4 independent T cell donors).

j, Effect of common supplements on T cell transduction rates (4 independent T cell donors).

k, T cell viability when using transduction supplements (4 independent T cell donors).

l, Quantification of lentivirus preparations based on RT-qPCR quantification of lentiviral RNA (3 technical replicates).

m, Lentivirus titration in CD4 and CD8 T cells based on RT-qPCR-based quantification of lentiviral RNA (shown are mean ± s.e.m of 3 technical replicates).

n, Human primary T cells were transduced with the CROP-seq-CAR lentiviral vector carrying the genome-wide Brunello gRNA library. To quantify the number of gRNAs per cell, we individually expanded 62 single-cell-derived T cell clones and performed gRNA sequencing. By plotting gRNA read counts, we determined the number of integrated gRNAs for each clone. Representative examples of T cell clones with 1, 2, or 3 gRNA integrations are shown.

o, Barplot showing the frequency of lentiviral integrations into the same cell across the 62 single-cell expanded T cell clones. The average number of gRNA integrations per cell was 1.5.

p, Robust CAR expression in CAR T cells engineered with the CROP-seq-CAR lentiviral vector. To detect the CAR, we used PE-labelled recombinant CD19 antigen.

q, Specific killing of $CD19^+$ cancer cells by CROP-seq-CAR engineered CAR T cells.

In panels i-l, the center line is the median, the box limits are the upper and lower quartiles, and the whiskers extend to 1.5 times the interquartile range.

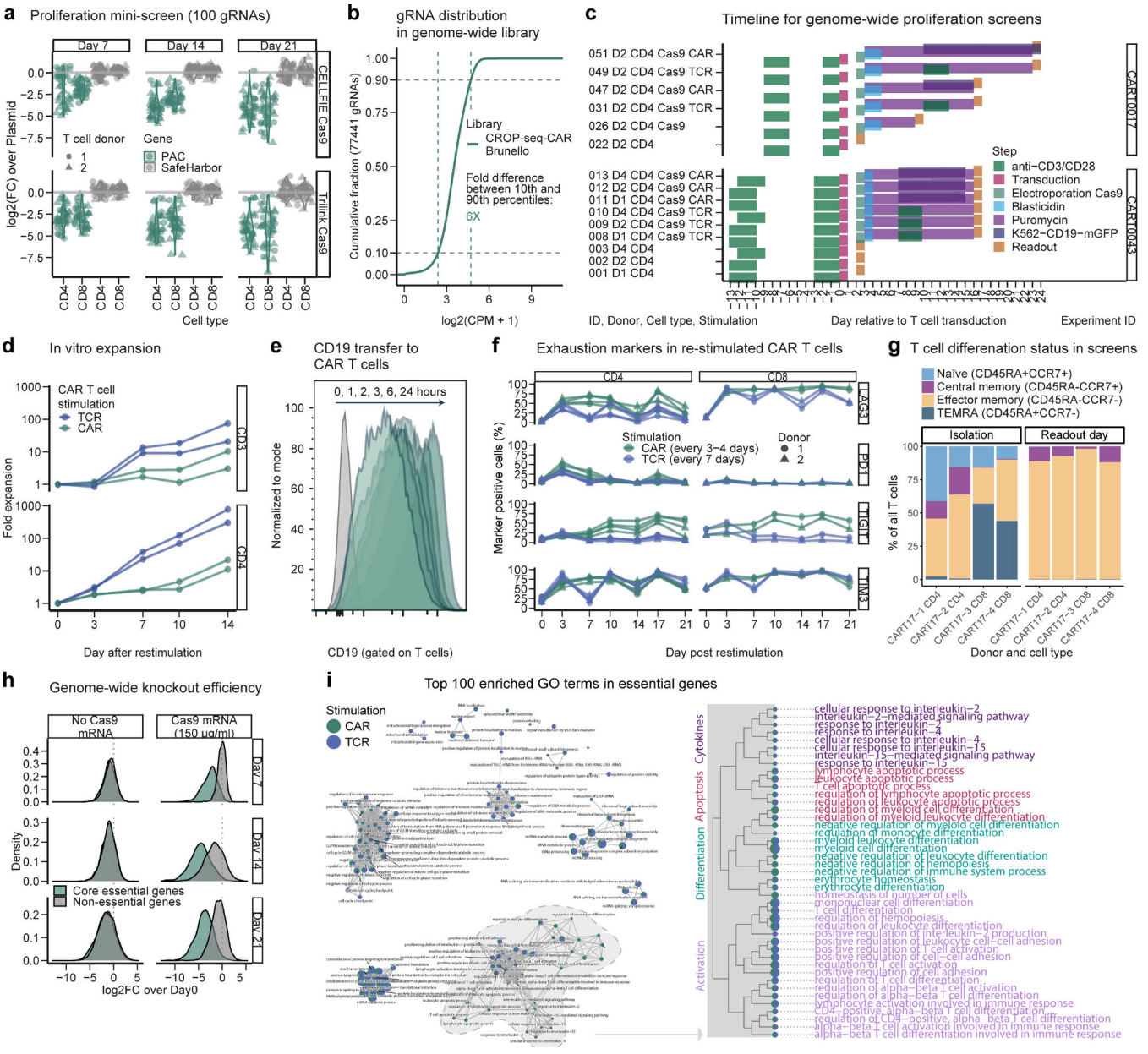

Fig. S3 | Optimizing genome-wide fitness screens in human primary CAR T cells.

a, The proof-of-concept fitness mini-screen. We delivered a focused gRNA library comprising 100 gRNAs using the CROP-seq-CAR lentiviral vector and electroporated custom-made or commercial Cas9 mRNA. Samples for gRNA sequencing were collected on days 7, 14, and 21. We observed the dropout of PAC (puromycin N-acetyl-transferase) gRNAs (n = 20) in comparison to safe harbor-targeting gRNAs (n = 20) over time. PAC mediates puromycin resistance and was used as the selection marker for CROP-seq-CAR lentiviral delivery.

b, gRNA representation after cloning the genome-wide Brunello library into the CROP-seq-CAR vector, plotted as a cumulative distribution function based on amplicon sequencing of the plasmid pool, with highlighted fold difference between the 10^{th} and 90^{th} percentiles as a measure of gRNA library balance.

c, Detailed experimental timeline for the genome-wide fitness screens. Screens were based on 4 blood donors and performed in 2 independent screening experiments. Key steps in the CELLFIE workflow are highlighted. Samples for gRNA sequencing were collected at day 0 before electroporation, and at day 7, 14, and 21 after electroporation.

d, Observed expansion of human primary CAR T cells upon repeated CAR or TCR stimulation (2 independent T cell donors).

e, CD19 accumulation on CAR T cells during co-culture with target cells as the result of trogocytosis.

f, Flow cytometry profiling of the T cell exhaustion markers PD1, LAG3, TIM3, and TIGIT during co-culture of CAR T cells with $CD19^{+}$ K562 cancer cells.

g, T cell subset profiling by flow cytometry at the isolation and readout time points of the genome-wide screens.

h, Specific dropout of known essential genes (n = 684, based on BAGEL2 predictions) relative to non-essential genes (n = 927) in genome-wide fitness screens with Cas9 mRNA (right), not seen without Cas9 mRNA (left).

i, Gene set enrichment analysis for genes that were essential in human primary CAR T cells under CAR and TCR stimulation, according to the fitness screens. We clustered the top-100 most enriched Gene Ontology (GO) terms from the Biological Process category. One cluster related to T cell functions is shown in detail as a tree plot.

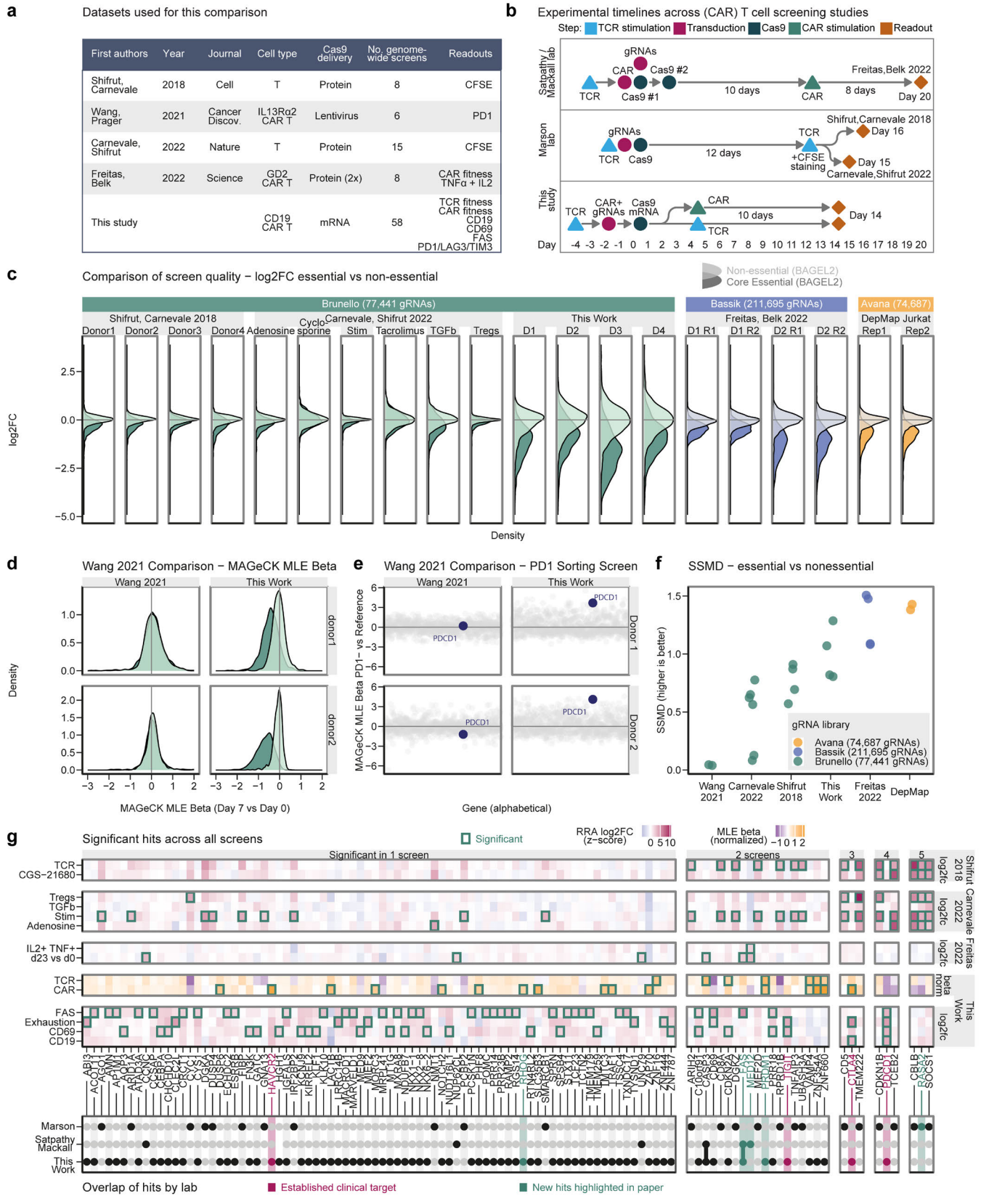

First authors	Year	Journal	Cell type	Cas9 delivery	No. genome-wide screens	Readouts
Shifrut, Carnevale	2018	Cell	T	Protein	8	CFSE
Wang, Prager	2021	Cancer Discov.	IL13Rα2 CAR T	Lentivirus	6	PD1
Carnevale, Shifrut	2022	Nature	T	Protein	15	CFSE
Freitas, Belk	2022	Science	GD2 CAR T	Protein (2x)	8	CAR fitness TNFα + IL2
This study			CD19 CAR T	mRNA	58	TCR fitness CAR fitness CD19 CD69 FAS PD1/LAG3/TIM3

Fig. S4 | Comparison of screening data quality and results with published (CAR) T cell screening datasets.

a, Published datasets of CRISPR screening in human T cells or CAR T cells used for the comparison.

b, T cell screening timelines compared across the studies listed in panel a.

c-d, Dropout of essential genes across studies based on gRNA $\log_2$ fold changes (**c**) or MAGeCK MLE Beta value (**d**) for known essential genes (n = 684, based on BAGEL2 predictions) relative to non-essential genes (n = 927) in genome-wide proliferation-based screens.

e, Comparison of PD1 (PDCD1) knockout enrichment in FACS-based screens enriching for PD1-negative cells.

f, Strength of the separation between the distributions of gRNA frequencies between essential and non-essential genes (panels c-d), quantified by the strictly standardized mean difference (SSMD). This comparison includes genome-wide screens in human primary T cells and in the Jurkat cell line.

g, Significant screening hits across all high-quality genome-wide screens in human (CAR) T cells (z-normalized $\log_2$ fold change of >2 and FDR < 0.05 for MAGeCK RRA results, normalized beta of >0.99 for MAGeCK MLE results). Genes highlighted by each study are shown in green; established clinical targets are shown in magenta.

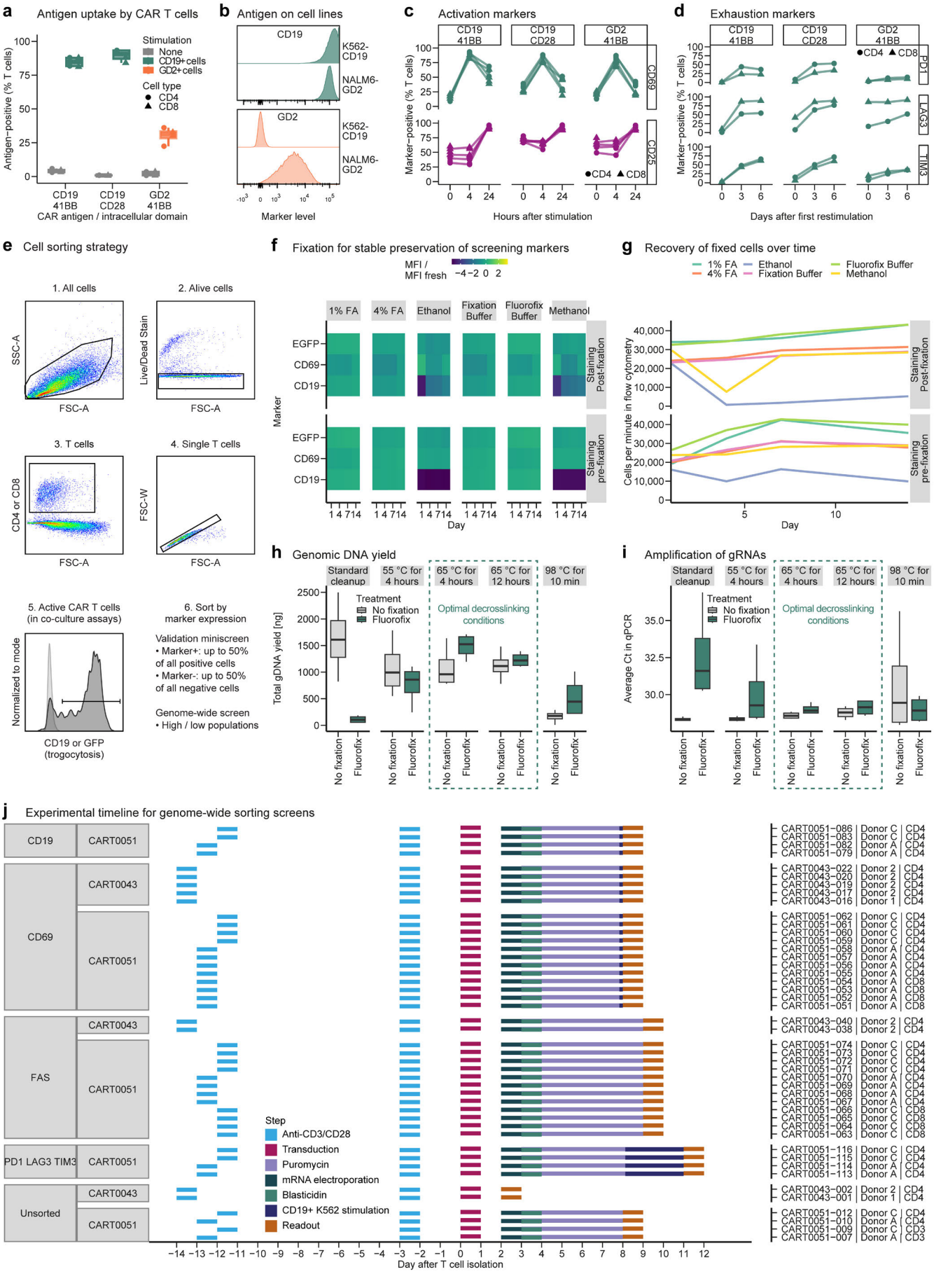
a
Antigen uptake by CAR T cells
Antigen−positive (% T cells)
Stimulation
None
CD19+cells
GD2+cells
Cell type
CD4
CD8
CD19 41BB
CD19 CD28
GD2 41BB
CAR antigen / intracellular domain
b
Antigen on cell lines
CD19
K562-CD19
NALM6-GD2
GD2
Marker level
c
Activation markers
Marker−positive (% T cells)
CD69
CD25
Hours after stimulation
d
Exhaustion markers
PD1
LAG3
TIM3
Days after first restimulation
e
Cell sorting strategy
1. All cells
2. Alive cells
3. T cells
4. Single T cells
5. Active CAR T cells (in co-culture assays)
6. Sort by marker expression
Validation miniscreen
• Marker+: up to 50% of all positive cells
• Marker-: up to 50% of all negative cells
Genome-wide screen
• High / low populations
CD19 or GFP (trogocytosis)
f
Fixation for stable preservation of screening markers
MFI / MFI fresh
1% FA
4% FA
Ethanol
Fixation Buffer
Fluorofix Buffer
Methanol
EGFP
CD69
CD19
Staining Post-fixation
Staining pre-fixation
Day
g
Recovery of fixed cells over time
Cells per minute in flow cytometry
h
Genomic DNA yield
Standard cleanup
55 °C for 4 hours
65 °C for 4 hours
65 °C for 12 hours
98 °C for 10 min
Treatment
No fixation
Fluorofix
Optimal decrosslinking conditions
Total gDNA yield [ng]
i
Amplification of gRNAs
Average Ct in qPCR
j
Experimental timeline for genome-wide sorting screens
CD19
CD69
FAS
PD1 LAG3 TIM3
Unsorted
CART0051
CART0043
Step
Anti-CD3/CD28
Transduction
Puromycin
mRNA electroporation
Blasticidin
CD19+ K562 stimulation
Readout
Day after T cell isolation

Fig. S5 | Optimizing FACS-based readouts for genome-wide screens in CAR T cells.

a–d, Evaluation of screening markers in T cells with different CARs. CAR T cells expressing anti-CD19 CARs (FMC63 scFv with 41BB or CD28 co-stimulatory domains) or anti-GD2 CARs (14g2a scFv with 41BB) were stimulated with K562-CD19 or NALM6-GD2 cells, respectively. Marker expression was profiled by flow cytometry at several time points, including those used in our genome-wide screens: (a) antigen uptake via trogocytosis, (b) antigen expression on target cell lines, (c) early activation markers CD69 and CD25, and (d) exhaustion markers PD1, LAG3, and TIM3. Data represent independent biological replicates from distinct T cell donors.

e, Outline of the FACS gating strategy. We selected viable T cells based on physical gates, live/dead stain, and CD4 or CD8 marker expression, and we excluded cell doublets. For screens involving co-culture with cancer cells, we selected active CAR T cells based on trogocytosis-acquired CD19 (except for the CD19 screen itself). In the focused validation screens, we sorted for the top and bottom 50% of marker expression. For the genome-wide screens, we sorted cell populations with stringent thresholds of marker expression (Fig. 2c).

f, Marker protein expression over time, profiled by flow cytometry. We tested six different methods for cell fixation, with antibody staining either before or after fixation. Mean fluorescent intensities (MFI) were normalized to the staining of fresh unfixed cells.

g, Recovery of fixed cells removed from storage at different days after cell fixation.

h, Genomic DNA yield of gRNA amplification from fresh and fixed cells for different de-crosslinking conditions.

i, qPCR quantification of gRNA amplification from fresh and fixed cells for different de-crosslinking conditions.

j, Experimental timelines for all 45 genome-wide FACS-based screens reported in this study.

The center line of boxplots indicates the median, the box limits represent the upper and lower quartiles, and the whiskers extend to 1.5 times the interquartile range.

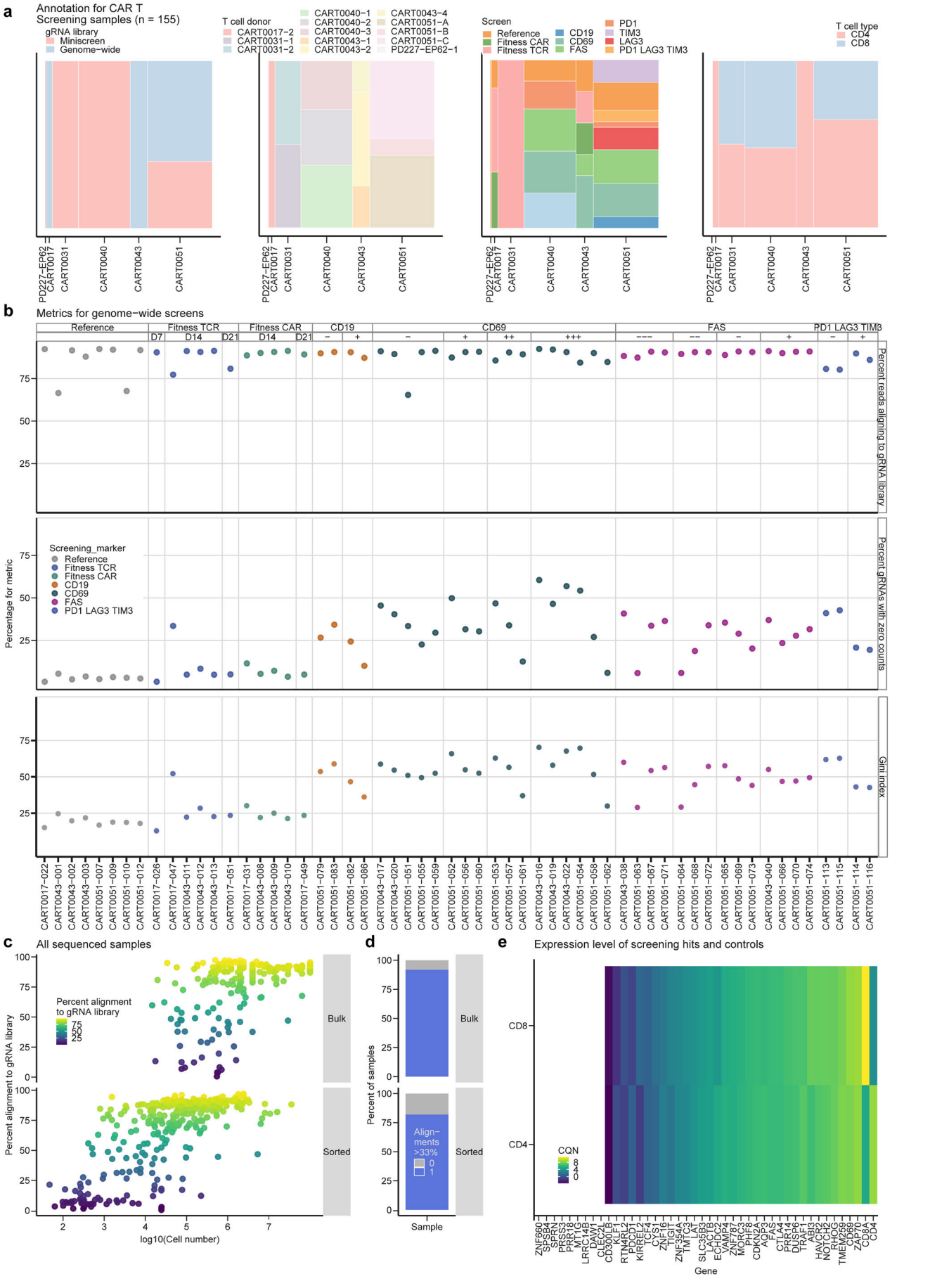
a
Annotation for CAR T Screening samples (n = 155)
gRNA library
Miniscreen
Genome−wide
T cell donor
CART0017−2
CART0031−1
CART0031−2
CART0040−1
CART0040−2
CART0040−3
CART0043−1
CART0043−2
CART0043−4
CART0051−A
CART0051−B
CART0051−C
PD227−EP62−1
Screen
Reference
Fitness CAR
Fitness TCR
CD19
CD69
FAS
PD1
TIM3
LAG3
PD1 LAG3 TIM3
T cell type
CD4
CD8
PD227−EP62
CART0017
CART0031
CART0040
CART0043
CART0051
b
Metrics for genome−wide screens
Reference
Fitness TCR
Fitness CAR
CD19
CD69
FAS
PD1 LAG3 TIM3
D7
D14
D21
Percent reads aligning to gRNA library
Percentage for metric
Screening_marker
Percent gRNAs with zero counts
Gini index
c
All sequenced samples
Percent alignment to gRNA library
Bulk
Sorted
log10(Cell number)
d
Percent of samples
Align−ments >33%
Sample
e
Expression level of screening hits and controls
CD8
CD4
CQN
Gene

Fig. S6 | Quality metrics for genome-wide screens in CAR T cells.

a, Mosaic plots showing details for the 155 CRISPR screening samples that were collected and analyzed in this study (including proof-of-concept mini-screens and genome-wide screens), with indicated gRNA library size, number of independent T cell donors, screening readouts, and included T cell subsets.

b, Quality control metrics for all 58 genome-wide CRISPR screening samples in this study. Shown are the percentage of reads aligning to the gRNA library (NGS library quality), the percentage of gRNAs with zero counts (stochastic dropout), and the Gini index (indicative of selective enrichment).

c, Scatterplot showing the percentage of reads aligning to the gRNA library as a function of the number of cells that were used as input for the gRNA amplification. We achieved good results with as few as 1000 sorted cells.

d, Barplot showing the percentage of all sequenced samples that achieved sufficient gRNA alignment rates.

e, RNA expression of top hits from our genome-wide screens (Fig. 2f) based on RNA-seq for the CAR T cells.

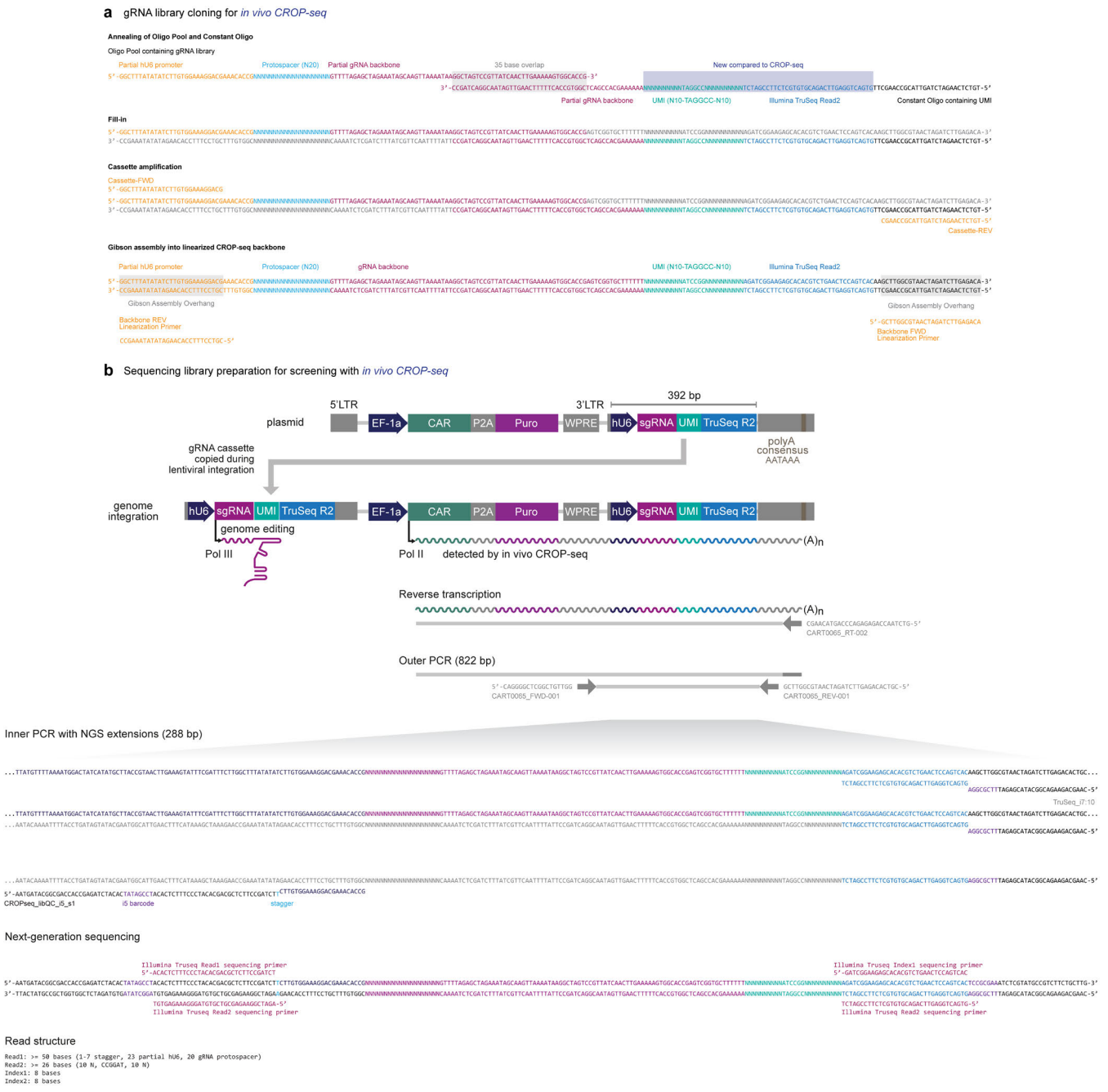

Fig. S7 | Design of the *in vivo* CROP-seq method for pooled screening in mice.

a, Cloning of gRNA libraries for *in vivo* CROP-seq. The gRNA library is synthesized as an oligo pool, where gRNA protospacers are flanked by a partial hU6 promoter and gRNA backbone. The UMI and Illumina Read2 primer are introduced by a separate oligonucleotide. The gRNA oligo pool and the UMI oligo are annealed via their 35-base overlap, extended by a fill-in reaction, and PCR-amplified. CROP-seq vectors are linearized by PCR and assembled with insert by Gibson's isothermal assembly.

b, Library preparation for *in vivo* CROP-seq, shown here with the CROP-seq-CAR vector. The gRNA expression cassette (consisting of hU6 promoter, sgRNA protospacer, UMI, and Illumina TruSeq read 2 primer binding site) is located inside the 3' LTR. During lentiviral integration, the gRNA cassette gets copied to the 5' LTR by viral mechanisms. From the 5' LTR, the gRNA is transcribed by polymerase III from the hU6 promoter for efficient genome editing. The 3' LTR copy is included in the highly expressed CAR-P2A-Puro mRNA. The *in vivo* CROP-seq method

detects gRNAs from this high-copy mRNA, rather than from the genomic DNA. It employs construct-specific reverse transcription followed by nested PCR amplification of the gRNA and the UMI. Details for gRNA sequencing on the Illumina NovaSeq 6000 platform are shown at the bottom of the diagram.

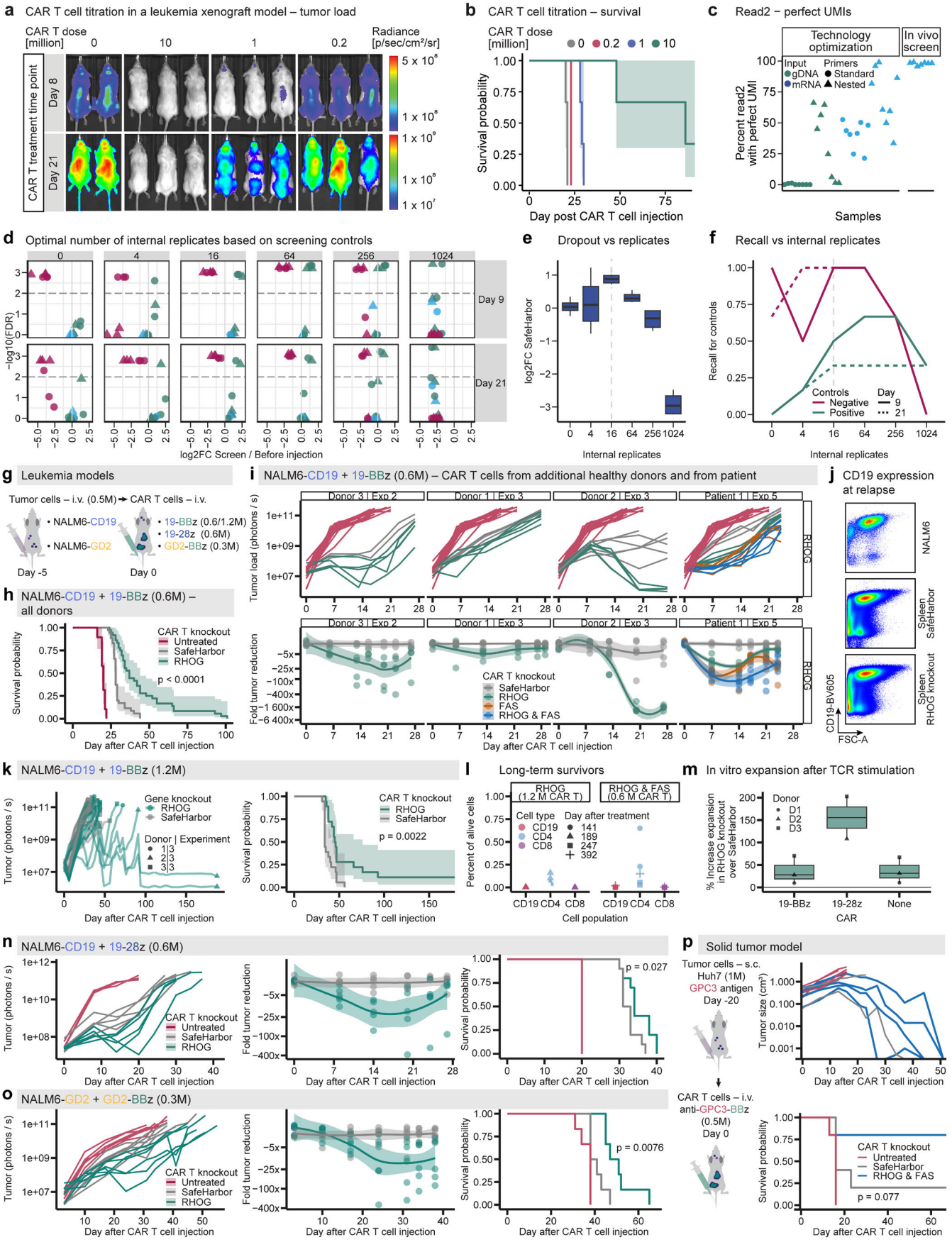
a
CAR T cell titration in a leukemia xenograft model – tumor load
CAR T dose [million]
0
10
1
0.2
Radiance [p/sec/cm²/sr]
CAR T treatment time point
Day 8
Day 21
b
CAR T cell titration – survival
CAR T dose [million]
0
0.2
1
10
Survival probability
Day post CAR T cell injection
c
Read2 – perfect UMIs
Technology optimization
In vivo screen
Input
gDNA
mRNA
Primers
Standard
Nested
Percent read2 with perfect UMI
Samples
d
Optimal number of internal replicates based on screening controls
Day 9
Day 21
−log10(FDR)
log2FC Screen / Before injection
e
Dropout vs replicates
log2FC SafeHarbor
Internal replicates
f
Recall vs internal replicates
Recall for controls
Controls
Negative
Positive
Day
9
21
Internal replicates
g
Leukemia models
Tumor cells – i.v. (0.5M) → CAR T cells – i.v.
• NALM6-CD19
• NALM6-GD2
• 19-BBz (0.6/1.2M)
• 19-28z (0.6M)
• GD2-BBz (0.3M)
Day -5
Day 0
h
NALM6-CD19 + 19-BBz (0.6M) – all donors
Survival probability
CAR T knockout
Untreated
SafeHarbor
RHOG
p < 0.0001
Day after CAR T cell injection
i
NALM6-CD19 + 19-BBz (0.6M) – CAR T cells from additional healthy donors and from patient
Donor 3 | Exp 2
Donor 1 | Exp 3
Donor 2 | Exp 3
Patient 1 | Exp 5
Tumor load (photons / s)
Fold tumor reduction
RHOG
CAR T knockout
SafeHarbor
RHOG
FAS
RHOG & FAS
Day after CAR T cell injection
j
CD19 expression at relapse
NALM6
Spleen SafeHarbor
Spleen RHOG knockout
CD19-BV605
FSC-A
k
NALM6-CD19 + 19-BBz (1.2M)
Tumor (photons / s)
Gene knockout
RHOG
SafeHarbor
Donor | Experiment
1|3
2|3
3|3
Day after CAR T cell injection
Survival probability
CAR T knockout
RHOG
SafeHarbor
p = 0.0022
Day after CAR T cell injection
l
Long-term survivors
RHOG (1.2 M CAR T)
RHOG & FAS (0.6 M CAR T)
Percent of alive cells
Cell type
CD19
CD4
CD8
Day after treatment
141
189
247
392
Cell population
m
In vitro expansion after TCR stimulation
% Increase expansion in RHOG knockout over SafeHarbor
Donor
D1
D2
D3
19-BBz
19-28z
None
CAR
n
NALM6-CD19 + 19-28z (0.6M)
Tumor (photons / s)
CAR T knockout
Untreated
SafeHarbor
RHOG
Day after CAR T cell injection
Fold tumor reduction
Survival probability
p = 0.027
Day after CAR T cell injection
o
NALM6-GD2 + GD2-BBz (0.3M)
Tumor (photons / s)
CAR T knockout
Untreated
SafeHarbor
RHOG
Day after CAR T cell injection
Fold tumor reduction
Survival probability
p = 0.0076
Day after CAR T cell injection
p
Solid tumor model
Tumor cells – s.c.
Huh7 (1M)
GPC3 antigen
Day -20
CAR T cells – i.v.
anti-GPC3-BBz
(0.5M)
Day 0
Tumor size (cm³)
Day after CAR T cell injection
Survival probability
CAR T knockout
Untreated
SafeHarbor
RHOG & FAS
p = 0.077
Day after CAR T cell injection

Fig. S8 | Optimizing the *in vivo* CROP-seq setup and validation of knockout CAR T cells in several models.

a, CAR T cell titration in a xenograft mouse model of human leukemia. Immunodeficient NSG mice were injected with 0.5 million NALM6 cells engineered to express firefly luciferase. On day 5, mice were treated with different doses of CAR T cells. Leukemic cell load over time was monitored using live bioluminescence imaging. When left untreated, mice succumb to the leukemia around day 21. To make the model most informative, we selected a low (and deliberately non-curative) dose of CAR T cells that leads to initial leukemic control followed by a quick relapse.

b, Survival analysis for the mice shown in panel a.

c, Percentage of UMI reads perfectly matching the reference sequence. We compared state-of-the-art pooled screening with gRNA amplification from genomic DNA and *in vivo* CROP-seq with gRNA amplification from mRNA, both tested with single PCR and nested PCR amplification.

d, Optimal number of UMI-based internal replicates for data analysis based on screening controls. Each random UMI base can be an A, C, G, or T. Using UMI bases 1 to 5, we created 4, 16, 64, 256, and 1024 internal replicates. Standard analysis is labeled as 0 internal replicates (left). Negative, neutral, and positive controls are color-coded.

e, Dropout of neutral control gRNAs targeting a safe harbor locus when the read number in the internal replicates gets too small for large numbers of internal replicates. The center line of the boxplots indicates the median, the box limits represent the upper and lower quartiles, and the whiskers extend to 1.5 times the interquartile range.

f, Number of internal replicates versus recall for negative and positive controls.

g, Overview of leukemia models used in this study, including different tumor cell lines, antigens, CAR designs, and CAR T cell doses.

h, Survival analysis for leukemic mice treated with 0.6 million 19-BBz CAR T cells. Data aggregated for all mice and healthy CAR T cell donors (n = 6).

i, Leukemic cell load (absolute values, top, and fold reduction, bottom) for leukemic mice treated with 0.6 million 19-BBz CAR T cells for 3 new healthy donors (in addition to the 3 healthy donors in Fig. 4), and from leukapheresis product of a patient with multiple myeloma scheduled to receive CAR T cell therapy (rightmost plots).

j, $CD19^+$ NALM6 tumor cells observed in mouse spleens at tumor relapse after RHOG knockout and standard (safe harbor locus-edited) CAR T cell treatment. NALM6 cells are shown as reference.

k, Leukemic cell load and survival data for leukemic mice treated with a higher dose of 1.2 million 19-BBz CAR T cells. Data aggregated for all mice and donors (3 independent donors).

l, Percentage of CAR T cells (CD4+ or CD8+) and NALM6 ($CD19^+$) cells in long-term survivor mice in the NALM6 model treated with RHOG or RHOG-FAS knockout CAR T cells. Blood (tail bleeds) and organs (at the end point) were analyzed by flow cytometry after erythrocyte lysis.

m, T cells were transduced with the CROP-seq-CAR vector with 19-BBz or 19-28z, or with the CROP-seq-mCherry vector (with no CAR), modified by RNP electroporation, and restimulated 5 days later with anti-CD3/CD28 reagent. Cells were counted on day 0 and day 6 after restimulation. Data are fold expansion normalized between RHOG knockout and standard (safe harbor locus-edited) CAR T cells for each donor (3 independent T cell donors).

n, Leukemic cell load (absolute values, left, and fold reduction, right) and survival analysis for leukemic mice treated with 0.6 million of 19-28z CAR T cells.

o, Leukemic cell load (absolute values, left, and fold reduction, right) and survival analysis for NALM6-GD2 leukemic mice treated with 0.3 million GD2-BBz CAR T cells.

p, Schematic of the Huh7 solid tumor xenograft model treated with 0.5 million GPC3-BBz CAR T cells, along with tumor growth over time (caliper measurements) and survival analysis.

Survival analysis includes log-rank test p-values comparing groups treated with modified versus standard (safe harbor-edited) CAR T cells.

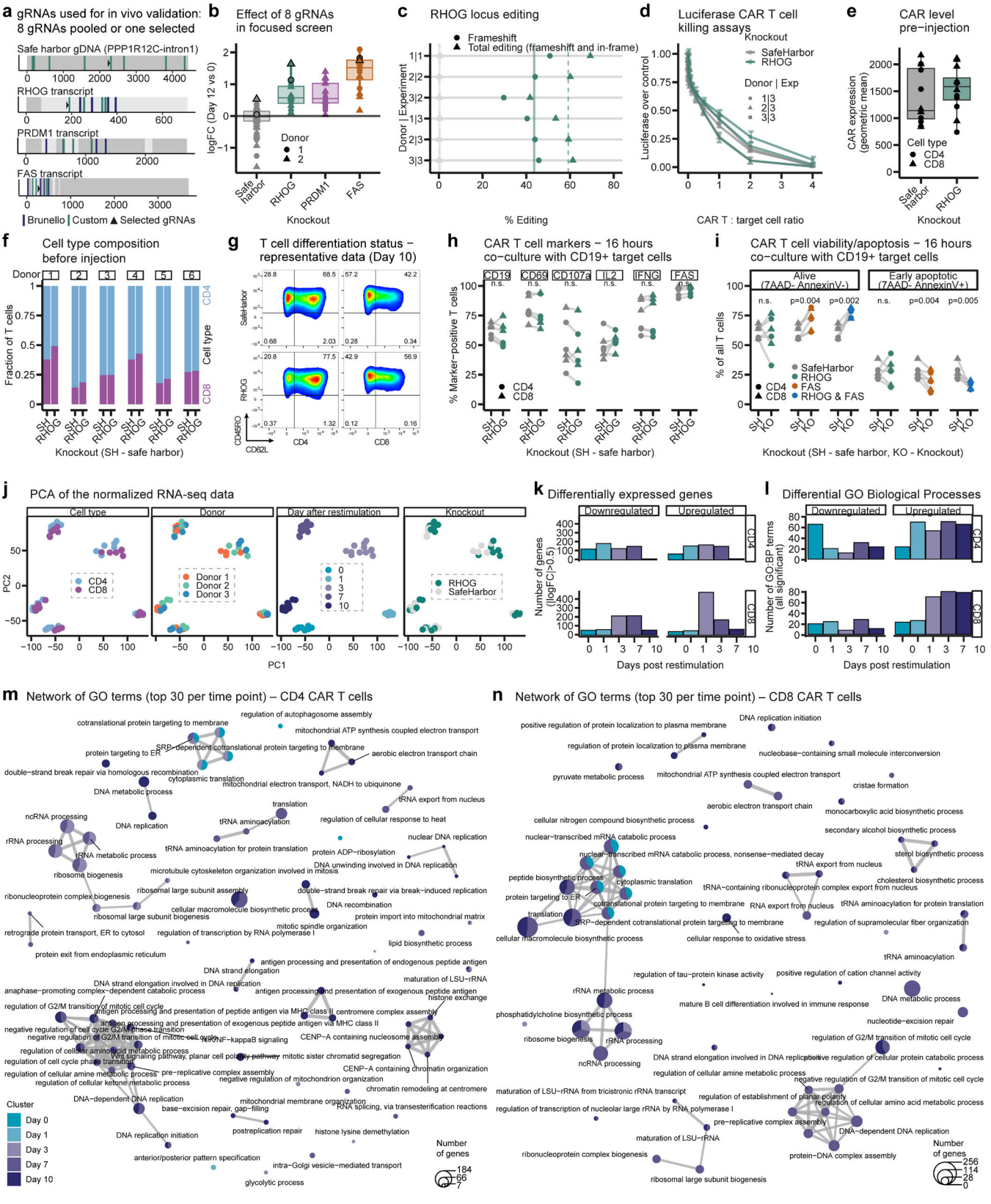
a gRNAs used for in vivo validation: 8 gRNAs pooled or one selected
Safe harbor gDNA (PPP1R12C-intron1)
RHOG transcript
PRDM1 transcript
FAS transcript
Brunello | Custom ▲ Selected gRNAs
b Effect of 8 gRNAs in focused screen
logFC (Day 12 vs 0)
Donor
Safe harbor
RHOG
PRDM1
FAS
Knockout
c RHOG locus editing
Frameshift
Total editing (frameshift and in-frame)
Donor | Experiment
% Editing
d Luciferase CAR T cell killing assays
Knockout
SafeHarbor
RHOG
Donor | Exp
Luciferase over control
CAR T : target cell ratio
e CAR level pre−injection
CAR expression (geometric mean)
Cell type
CD4
CD8
Knockout
f Cell type composition before injection
Donor
Fraction of T cells
Cell type
Knockout (SH - safe harbor)
g T cell differentiation status − representative data (Day 10)
SafeHarbor
RHOG
CD45RO
CD62L
CD4
CD8
h CAR T cell markers − 16 hours co−culture with CD19+ target cells
CD19
CD69
CD107a
IL2
IFNG
FAS
% Marker−positive T cells
Knockout (SH - safe harbor)
i CAR T cell viability/apoptosis − 16 hours co−culture with CD19+ target cells
Alive (7AAD- AnnexinV-)
Early apoptotic (7AAD- AnnexinV+)
% of all T cells
SafeHarbor
RHOG
FAS
RHOG & FAS
Knockout (SH - safe harbor, KO - Knockout)
j PCA of the normalized RNA-seq data
Cell type
Donor
Day after restimulation
Knockout
CD4
CD8
Donor 1
Donor 2
Donor 3
RHOG
SafeHarbor
PC1
PC2
k Differentially expressed genes
Downregulated
Upregulated
Number of genes (|logFC|>0.5)
Days post restimulation
l Differential GO Biological Processes
Number of GO:BP terms (all significant)
Days post restimulation
m Network of GO terms (top 30 per time point) – CD4 CAR T cells
Cluster
Day 0
Day 1
Day 3
Day 7
Day 10
Number of genes
n Network of GO terms (top 30 per time point) – CD8 CAR T cells
Number of genes

Fig. S9 | Further molecular characterization of RHOG knockout CAR T cells.

a, gRNAs selected for *in vivo* screens (8 gRNAs per gene) or individual validation (as pools of 8 or single gRNAs).

b, Individual effects of the 8 gRNAs per gene in the focused validation screen, with the single gRNAs highlighted that were used for individual validation. The center line is the median, the box limits are the upper and lower quartiles, and the whiskers extend to 1.5 times the interquartile range.

c, Percentage of successful RHOG editing determined by sequencing of the gene locus.

d, Killing of NALM6-Luc cancer cells by RHOG knockout CAR T cells, measured by luciferase assays at 18 hours of co-culture for different CAR T cell target cell ratios.

e, CAR expression on standard CAR T cells and RHOG knockout CAR T cells, determined by flow cytometry the day before injection into mice.

f, CD4 and CD8 cell composition among the standard CAR T cells and RHOG knockout CAR T cells, determined by flow cytometry the day before injection into the mice (independent T cell donors). Statistical comparison was performed using paired two-tailed Student's t-test.

g, T cell differentiation status was profiled after 10 days of co-culture of CAR T cells and cancer cells. Representative flow cytometry data are shown.

h-i, Cell surface markers (**h**) and viability as well as apoptosis (**i**) were assayed by flow cytometry after 16 hours of co-culture with K562-CD19 cells. Statistical comparison was performed using paired one-tailed Student's t-test.

j, Principal component analysis (PCA) of normalized RNA-seq data, with samples color-coded by CD4 versus CD8 expression, T cell donor, time point, and RHOG knockout versus standard CAR T cells.

k, Number of differentially expressed genes between RHOG knockout versus standard CAR T cells, shown separately for CD4 and CD8 CAR T cells ($|\log_2 FC| > 0.5$, adjusted p-value < 0.05).

l, Number of differential GO Biological Process terms (FDR < 0.05) in RNA-seq data comparing RHOG knockout to standard CAR T cells, shown separately for CD4 and CD8 CAR T cells.

m,**n**, Network visualization of upregulated GO Biological Process terms in RNA-seq data comparing RHOG knockout to standard CAR T cells, shown separately for CD4 (panel m) and CD8 (panel n) CAR T cells.

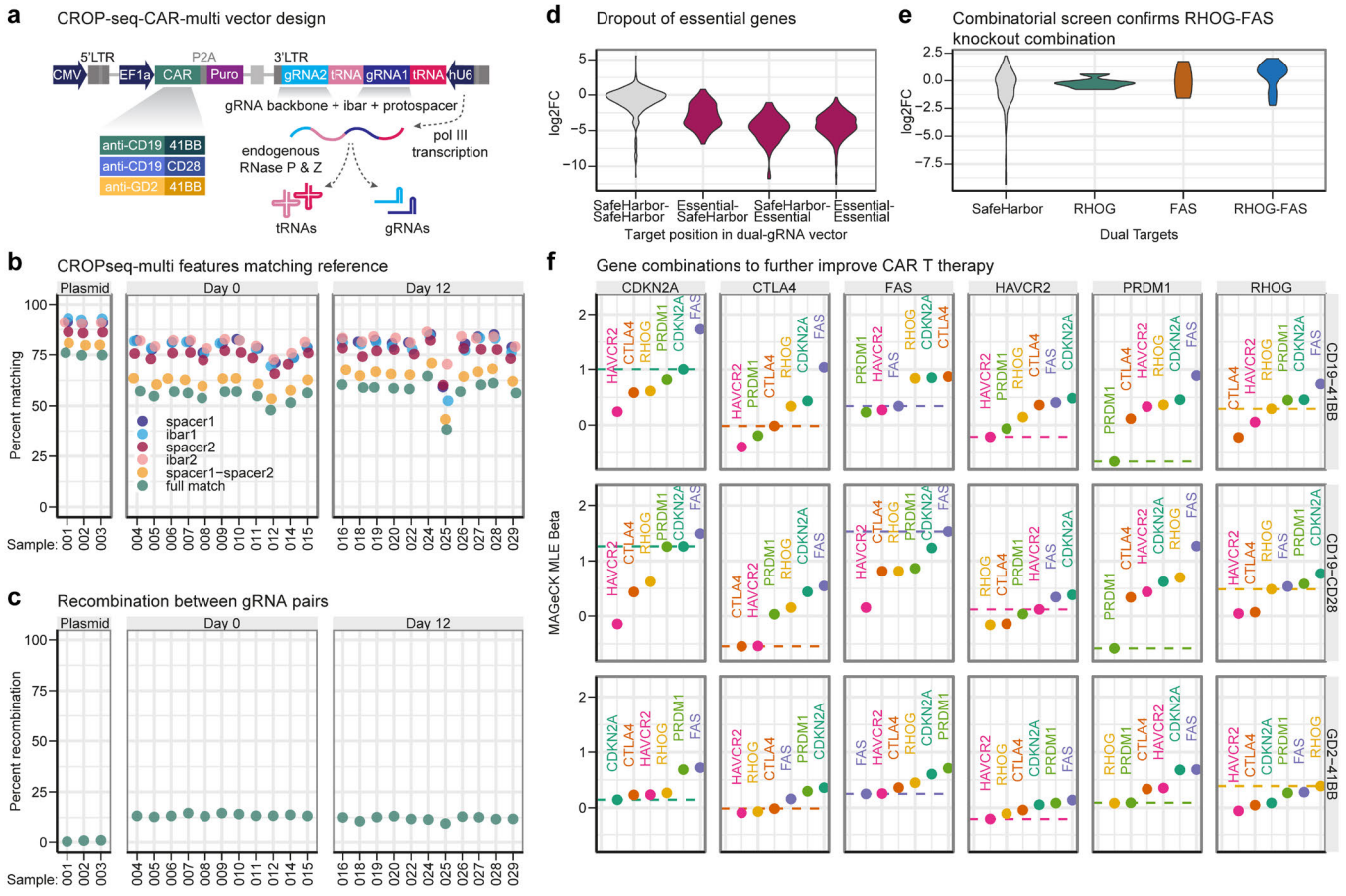

Fig. S10 | Optimizing combinatorial screens in human primary CAR T cells.

a, CROP-seq-CAR-multi vectors for double knockout screens in CAR T cells, with three CAR designs (CD19-BBz, CD19-28z, GD2-41BB). The construct expresses a dual-gRNA cassette separated by a tRNA sequence that is cleaved by cellular enzymes.

b, Percentage of reads fully matching the reference (spacer1-ibar1-spacer2-ibar2) or partially matching the indicated features in the combinatorial screening samples.

c, Percentage of reads showing evidence of recombination between the gRNA-iBAR pairs.

d, Dropout of essential genes for different gRNA configurations, shown by $\log_2$ fold changes between days 12 and 0 and aggregated for screens with all three CARs. Results are grouped for gRNA combinations targeting only the safe harbor locus ("SH-SH"), targeting essential genes only in position 1 ("essential-SH"), or position 2 ("SH-essential"), or both positions ("essential-essential").

e, Log_2 fold changes of gRNA combinations targeting RHOG-RHOG, FAS-FAS, or RHOG-FAS, between days 12 and 0 and aggregated for screens with all three CARs.

f, Combinatorial perturbations enhancing each of the single knockouts. Effect sizes are MAGeCK MLE beta values comparing day 12 and day 0. Dashed lines indicate the effect of the single knockout in the screen.

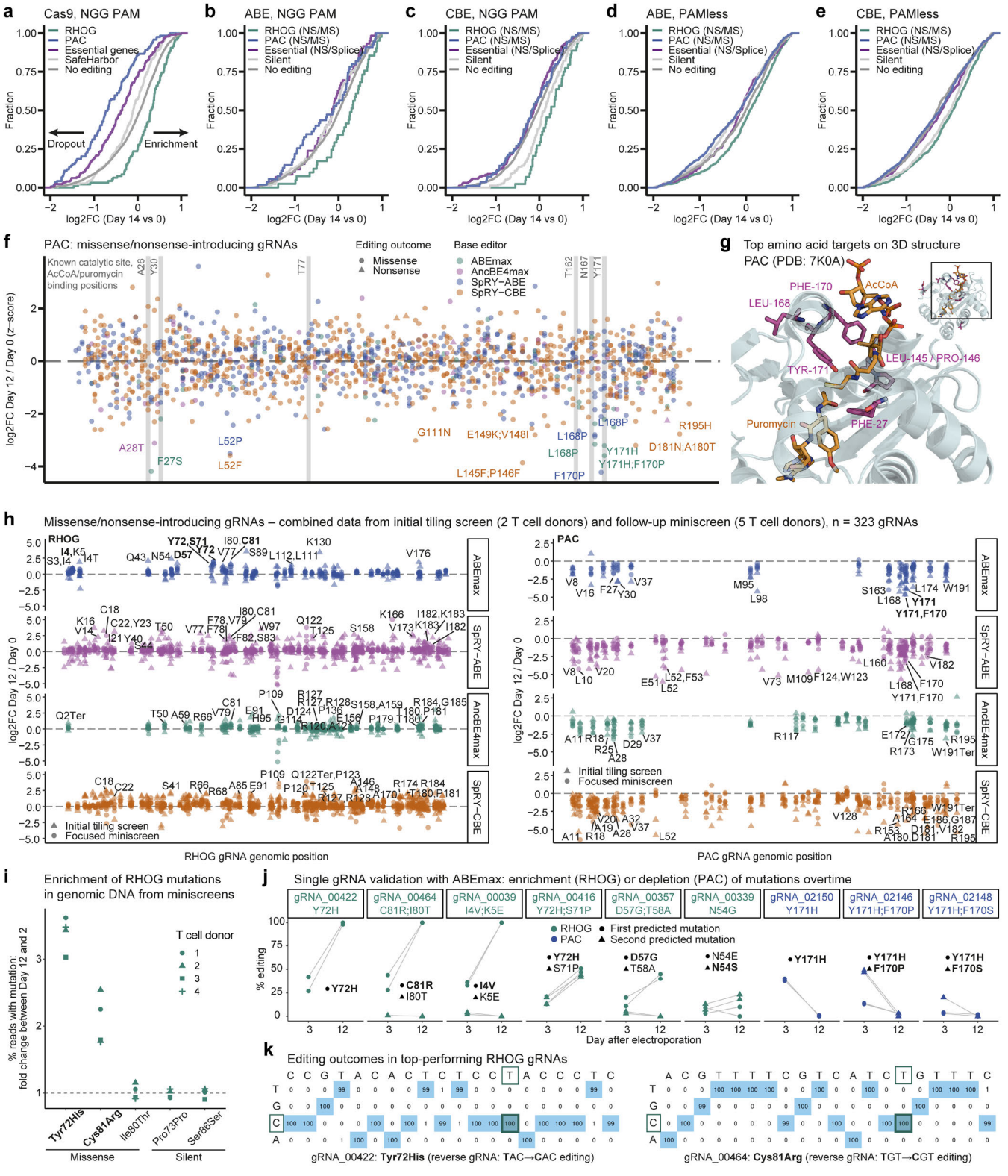

Fig. S11 | Optimizing base editing screens in human primary CAR T cells and validating single gRNAs.

a-e, Cumulative distribution plots showing the enrichment and depletion of gRNAs predicted to introduce specific mutation types for Cas9 and the four base editors. Abbreviations: NS (nonsense mutation), MS (missense mutation), Splice (splice-site mutation).

f, Mutagenesis map for PAC derived from the base editing screens. Log_2 fold changes of z-scores (y-axis) are shown for each gRNA throughout the gene body. The top-15 most depleted gRNAs are labeled with predicted amino acid changes, and key PAC amino acids are annotated.

g, Amino acids with the strongest mutagenesis effects for PAC overlaid on the protein structure.

h, Log_2 fold changes of base editing gRNAs selected for follow-up validation screens (n = 323, targeting RHOG, PAC, or safe harbor, Table S9), shown for each T cell donor (2 donors from the initial screen and 5 additional donors in the focused validation screens). The top-5 gRNAs per base editor and donor are annotated with target amino acids predicted to be mutated (missense or nonsense mutations).

i, Enrichment of specific RHOG mutations in CAR T cells over time, assessed by next-generation sequencing of the RHOG locus in base editing screens with the focused library (day 12 vs day 2 after mRNA electroporation, 4 T cell donors).

j, Quantification of ABEmax base editing by single gRNAs targeting RHOG or PAC, analyzed by Sanger sequencing with EditR. Editing efficiency was measured on day 3, and mutation enrichment or depletion was assessed on day 12 after electroporation.

k, Detailed editing outcomes for single gRNAs targeting RHOG, visualized with EditR. Highlighted in green are the base editing rates for target bases, whose substitutions introduce missense mutations.

Extended Data Tables

Table S1 | Plasmid vectors, gRNAs, synthetic oligos, and staining reagents used in this study.

a, Plasmid constructs used for CAR T cell and target cell line engineering.

b, Plasmid constructs used for synthetic mRNA production.

c, gRNAs used for single-locus targeting, and oligos used for single-locus amplification.

d, Primers used for amplicon sequencing of genomic loci.

e, Primers used for pooled CAR T cell screening.

f, Primers used for *in vivo* CROP-seq cloning, reverse transcription, and outer PCR amplification.

g, Primers used for *in vivo* CROP-seq NGS indexing PCR.

h, Staining reagents for flow cytometry and FACS.

i, Oligonucleotides and gBlocks used for cloning.

j, Primers used for combinatorial CAR T cell screening NGS indexing PCR.

Table S2 | Genome-wide screens for CAR T cell fitness.

a, Focused gRNA library for the technology validation fitness mini-screens.

b, Sample annotation for the technology validation fitness mini-screens.

c, Raw gRNA counts for the technology validation fitness mini-screens.

d, Genome-wide gRNA library, derived from the Brunello library and cloned into CROP-seq-CAR.

e, Sample annotation for the genome-wide fitness screens.

f, Raw gRNA counts for the genome-wide fitness screens.

g, Quality control metrics for the genome-wide fitness screens.

h, MAGeCK RRA results for the genome-wide fitness screens under TCR stimulation.

i, MAGeCK RRA results for the genome-wide fitness screens under CAR stimulation.

j, Design matrix for MAGeCK MLE analysis of the genome-wide fitness screens.

k, MAGeCK MLE results and beta values for the genome-wide fitness screens with TCR and CAR stimulation.

l, Cell numbers at T cell isolation, transduction, and electroporation.

Table S3 | Genome-wide screens with FACS-based readouts.

a, Focused gRNA library for the FACS-based mini-screens validating CD69 and FAS readouts.

b, Focused gRNA library for the FACS-based mini-screens validating PD1, LAG3, TIM3 readouts.

c, Sample annotation for the FACS-based mini-screens.

d, Raw gRNA counts for the FACS-based mini-screens validating CD69 and FAS readouts.

e, Raw gRNA counts for the FACS-based mini-screens validating PD1, LAG3, TIM3 readouts.

f, Genome-wide gRNA library, derived from the Brunello library and cloned into CROP-seq-CAR. This library and table are the same as Table S2d.

g, Sample annotation for the genome-wide FACS-based screens.

h, Raw gRNA counts for the genome-wide FACS-based screens.

i, MAGeCK RRA results for CD19 negative ($CD19^-$) versus unsorted CAR T cells.

j, MAGeCK RRA results for CD19 positive ($CD19^+$) versus unsorted CAR T cells.

k, MAGeCK RRA results for CD69 negative ($CD69^-$) versus unsorted CAR T cells.

l, MAGeCK RRA results for CD69 positive ($CD69^+$) versus unsorted CAR T cells.

m, MAGeCK RRA results for FAS strongly negative (FAS^{---}) versus unsorted CAR T cells.

n, MAGeCK RRA results for PD1, LAG3, TIM3 triple-negative versus unsorted CAR T cells.

o, MAGeCK RRA results for PD1, LAG3, TIM3 triple-positive versus unsorted CAR T cells.

p, Cell numbers at T cell isolation, transduction, and electroporation.

q, Quality control metrics for genome-wide FACS screens.

Table S4 | Comparison with published (CAR) T cell screening datasets

a, Overview of published genome-wide screens in human (CAR) T cells.

b, Comparison of screening quality based on the separation of essential and non-essential genes.

c, Log_2 fold changes of essential and non-essential genes compared across studies.

d, MLE beta values of essential and non-essential genes for fitness screens compared across studies.

e, MLE beta values for PD1 sorting screens compared across studies.

f, Overview of screening hits for each study.

g, Integration of screening hits across all high-quality datasets.

Table S5 | *In vivo* screens in a mouse model of systemic leukemia.

a, Development of *in vivo* CROP-seq and comparison to standard pooled screening

b, Focused gRNA library for the *in vivo* CROP-seq screens.

c, Sample annotation for the *in vivo* CROP-seq screens.

d, Raw gRNA counts for the *in vivo* CROP-seq screens.

e, Raw gRNA counts for the *in vivo* CROP-seq screens with 16 UMI-based internal replicates.

f, Results of the *in vivo* CROP-seq screens.

g, Number of T cell clones detected in each organ.

Table S6 | *In vivo* validation of single CAR T cell candidates in a mouse model of systemic leukemia.

a, Leukemic load (IVIS) for FAS, PRDM1, RHOG knockout and control (safe harbor locus-edited) CAR T cells.

b, Survival data for FAS, PRDM1, RHOG knockout and control CAR T cells.

c, Long-term evaluation of CAR T cell presence in mice remaining in remission.

Table S7 | RNA-seq analysis of RHOG versus control CAR T cells.

a, Sample annotation for the RNA-seq analysis.

b, Normalized and filtered RNA-seq read counts.

c, Differential gene expression for RHOG knockout versus control (safe harbor locus-edited) CAR T cells.

d, Gene set enrichment analysis (GSEA) for Gene Ontology (GO) Biological Process terms.

Table S8 | Combinatorial screens for CAR T cell fitness.

a, gRNA library for combinatorial screens with CROP-seq-CAR-multi.

b, Sample annotation for combinatorial screens.

c, Raw gRNA counts for combinatorial screens.

d, Quality control metrics for combinatorial screens.

e, MLE design matrix for analysis of combinatorial screens with MAGeCK MLE.

f, MAGeCK MLE results for combinatorial screens under CAR stimulation.

Table S9 | Base editing screen of RHOG and various controls.

a, gRNA library for the tiling base editing screen, with annotations of predicted mutations.

b, Sample annotation for the tiling base editing screen.

c, Raw gRNA counts for the tiling base editing screen.

d, MAGeCK RRA results for Day 12 versus Day 0 of the tiling base editing screen.

e, gRNA library for the validation base editing screen, with annotation of predicted mutations.

f, Sample annotation for the validation base editing screen.

g, Raw gRNA counts for the validation base editing screen.

References

1. Maude, S. L. *et al.* Tisagenlecleucel in Children and Young Adults with B-Cell Lymphoblastic Leukemia. *N Engl J Med* **378**, 439–448 (2018).
2. Neelapu, S. S. *et al.* Axicabtagene Ciloleucel CAR T-Cell Therapy in Refractory Large B-Cell Lymphoma. *N Engl J Med* **377**, 2531–2544 (2017).
3. Choi, B. D. *et al.* Intraventricular CARv3-TEAM-E T Cells in Recurrent Glioblastoma. *N Engl J Med* **390**, 1290–1298 (2024).
4. Bagley, S. J. *et al.* Intrathecal bivalent CAR T cells targeting EGFR and IL13Rα2 in recurrent glioblastoma: phase 1 trial interim results. *Nat Med* (2024) doi:10.1038/s41591-024-02893-z.
5. Müller, F. *et al.* CD19 CAR T-Cell Therapy in Autoimmune Disease - A Case Series with Follow-up. *N Engl J Med* **390**, 687–700 (2024).
6. Rurik, J. G. *et al.* CAR T cells produced in vivo to treat cardiac injury. *Science* **375**, 91–96 (2022).
7. Larson, R. C. & Maus, M. V. Recent advances and discoveries in the mechanisms and functions of CAR T cells. *Nat Rev Cancer* **21**, 145–161 (2021).
8. Hamieh, M. *et al.* CAR T cell trogocytosis and cooperative killing regulate tumour antigen escape. *Nature* **568**, 112–116 (2019).
9. Fraietta, J. A. *et al.* Disruption of TET2 promotes the therapeutic efficacy of CD19-targeted T cells. *Nature* **558**, 307–312 (2018).
10. Stadtmauer, E. A. *et al.* CRISPR-engineered T cells in patients with refractory cancer. *Science* **367**, eaba7365 (2020).
11. Agarwal, S. *et al.* Deletion of the inhibitory co-receptor CTLA-4 enhances and invigorates chimeric antigen receptor T cells. *Immunity* **56**, 2388-2407.e9 (2023).
12. Yoshikawa, T. *et al.* Genetic ablation of PRDM1 in antitumor T cells enhances therapeutic efficacy of adoptive immunotherapy. *Blood* **139**, 2156–2172 (2022).
13. Carnevale, J. *et al.* RASA2 ablation in T cells boosts antigen sensitivity and long-term function. *Nature* **609**, 174–182 (2022).
14. Freitas, K. A. *et al.* Enhanced T cell effector activity by targeting the Mediator kinase module. *Science* **378**, eabn5647 (2022).
15. Lynn, R. C. *et al.* c-Jun overexpression in CAR T cells induces exhaustion resistance. *Nature* **576**, 293–300 (2019).
16. Chan, J. D. *et al.* FOXO1 enhances CAR T cell stemness, metabolic fitness and efficacy. *Nature* **629**, 201–210 (2024).
17. Marchais, M. *et al.* FOXO1 Inhibition Generates Potent Nonactivated CAR T Cells against Solid Tumors. *Cancer Immunol Res* **11**, 1508–1523 (2023).
18. Wang, D. *et al.* CRISPR Screening of CAR T Cells and Cancer Stem Cells Reveals Critical Dependencies for Cell-Based Therapies. *Cancer Discov* **11**, 1192–1211 (2021).
19. Dai, X. *et al.* Massively parallel knock-in engineering of human T cells. *Nat Biotechnol* **41**, 1239–1255 (2023).
20. Shifrut, E. *et al.* Genome-wide CRISPR Screens in Primary Human T Cells Reveal Key Regulators of Immune Function. *Cell* **175**, 1958-1971.e15 (2018).
21. Schmidt, R. *et al.* CRISPR activation and interference screens decode stimulation responses in primary human T cells. *Science* **375**, eabj4008 (2022).

22. Walsh, Z. H. *et al.* Mapping variant effects on anti-tumor hallmarks of primary human T cells with base-editing screens. *Nat Biotechnol* (2024) doi:10.1038/s41587-024-02235-x.
23. Datlinger, P. *et al.* Pooled CRISPR screening with single-cell transcriptome read-out. *Nat Methods* **14**, 297–301 (2017).
24. Kalinichenko, A. *et al.* RhoG deficiency abrogates cytotoxicity of human lymphocytes and causes hemophagocytic lymphohistiocytosis. *Blood* **137**, 2033–2045 (2021).
25. Sahin, U. *et al.* BNT162b2 vaccine induces neutralizing antibodies and poly-specific T cells in humans. *Nature* **595**, 572–577 (2021).
26. Karikó, K., Buckstein, M., Ni, H. & Weissman, D. Suppression of RNA Recognition by Toll-like Receptors: The Impact of Nucleoside Modification and the Evolutionary Origin of RNA. *Immunity* **23**, 165–175 (2005).
27. Koblan, L. W. *et al.* Improving cytidine and adenine base editors by expression optimization and ancestral reconstruction. *Nat Biotechnol* **36**, 843–846 (2018).
28. Walton, R. T., Christie, K. A., Whittaker, M. N. & Kleinstiver, B. P. Unconstrained Genome Targeting with near-PAMless Engineered CRISPR-Cas9 Variants. *Science* **368**, 290–296 (2020).
29. Konermann, S. *et al.* Genome-scale transcriptional activation by an engineered CRISPR-Cas9 complex. *Nature* **517**, 583 (2015).
30. Doench, J. G. *et al.* Optimized sgRNA design to maximize activity and minimize off-target effects of CRISPR-Cas9. *Nat Biotechnol* **34**, 184–191 (2016).
31. Gudipati, V. *et al.* Inefficient CAR-proximal signaling blunts antigen sensitivity. *Nat Immunol* **21**, 848–856 (2020).
32. Fraietta, J. A. *et al.* Determinants of response and resistance to CD19 chimeric antigen receptor (CAR) T cell therapy of chronic lymphocytic leukemia. *Nat Med* **24**, 563–571 (2018).
33. DepMap, Broad (2024). DepMap 24Q4 Public. Figshare+. Dataset. https://doi.org/10.25452/figshare.plus.27993248.v1.
34. Schmierer, B. *et al.* CRISPR/Cas9 screening using unique molecular identifiers. *Mol Syst Biol* **13**, 945 (2017).
35. Yi, F. *et al.* CAR-engineered lymphocyte persistence is governed by a FAS ligand/FAS auto-regulatory circuit. 2024.02.26.582108 Preprint at https://doi.org/10.1101/2024.02.26.582108 (2024).
36. Ren, J. *et al.* A versatile system for rapid multiplex genome-edited CAR T cell generation. *Oncotarget* **8**, 17002–17011 (2017).
37. Tieu, V. *et al.* A versatile CRISPR-Cas13d platform for multiplexed transcriptomic regulation and metabolic engineering in primary human T cells. *Cell* **187**, 1278-1295.e20 (2024).
38. Menegatti, S. *et al.* Ablation of FAS confers allogeneic CD3– CAR T cells with resistance to rejection by T cells and natural killer cells. *Nat. Biomed. Eng* **8**, 1651–1664 (2024).
39. Ahmad Mokhtar, A. M. *et al.* RhoG's Role in T Cell Activation and Function. *Front. Immunol.* **13**, 845064 (2022).
40. Martínez-Martín, N. *et al.* T Cell Receptor Internalization from the Immunological Synapse Is Mediated by TC21 and RhoG GTPase-Dependent Phagocytosis. *Immunity* **35**, 208–222 (2011).
41. López-Cantillo, G., Urueña, C., Camacho, B. A. & Ramírez-Segura, C. CAR-T Cell Performance: How to Improve Their Persistence? *Front Immunol* **13**, 878209 (2022).
42. Walton, R. T., Qin, Y. & Blainey, P. C. CROPseq-multi: a versatile solution for multiplexed perturbation and decoding in pooled CRISPR screens. *bioRxiv* 2024.03.17.585235 (2024) doi:10.1101/2024.03.17.585235.

43. Chiesa, R. *et al.* Base-Edited CAR7 T Cells for Relapsed T-Cell Acute Lymphoblastic Leukemia. *N Engl J Med* **389**, 899–910 (2023).
44. Hanna, R. E. *et al.* Massively parallel assessment of human variants with base editor screens. *Cell* **184**, 1064-1080.e20 (2021).
45. Cuella-Martin, R. *et al.* Functional interrogation of DNA damage response variants with base editing screens. *Cell* **184**, 1081-1097.e19 (2021).
46. Coelho, M. A. *et al.* Base editing screens map mutations affecting interferon-γ signaling in cancer. *Cancer Cell* **41**, 288-303.e6 (2023).
47. Schmidt, R. *et al.* Base-editing mutagenesis maps alleles to tune human T cell functions. *Nature* 1–8 (2023) doi:10.1038/s41586-023-06835-6.
48. Bock, C. *et al.* High-content CRISPR screening. *Nat Rev Methods Primers* **2**, 9 (2022).
49. Michlits, G. *et al.* Multilayered VBC score predicts sgRNAs that efficiently generate loss-of-function alleles. *Nat Methods* **17**, 708–716 (2020).
50. Kim, E. & Hart, T. Improved analysis of CRISPR fitness screens and reduced off-target effects with the BAGEL2 gene essentiality classifier. *Genome Med* **13**, 2 (2021).
51. Wu, T. *et al.* clusterProfiler 4.0: A universal enrichment tool for interpreting omics data. *Innovation (Camb)* **2**, 100141 (2021).
52. Zhu, S. *et al.* Guide RNAs with embedded barcodes boost CRISPR-pooled screens. *Genome Biol* **20**, 20 (2019).
53. Köster, J. *et al.* snakemake-workflows/rna-seq-star-deseq2: Version 2.0.0. Zenodo https://doi.org/10.5281/zenodo.7885540 (2023).
54. Mölder, F. *et al.* Sustainable data analysis with Snakemake. *F1000Res* **10**, 33 (2021).
55. Reichl, S. & Bock, C. Workflow to Split, Filter, Normalize and Integrate Sequencing Data. Zenodo https://doi.org/10.5281/zenodo.8144220 (2023).
56. Robinson, M. D., McCarthy, D. J. & Smyth, G. K. edgeR: a Bioconductor package for differential expression analysis of digital gene expression data. *Bioinformatics* **26**, 139–140 (2010).
57. Hansen, K. D., Irizarry, R. A. & Wu, Z. Removing technical variability in RNA-seq data using conditional quantile normalization. *Biostatistics* **13**, 204–216 (2012).
58. Adamer, M. F. *et al.* reComBat: batch-effect removal in large-scale multi-source gene-expression data integration. *Bioinform Adv* **2**, vbac071 (2022).
59. Ritchie, M. E. *et al.* limma powers differential expression analyses for RNA-sequencing and microarray studies. *Nucleic Acids Res* **43**, e47 (2015).
60. Reichl, S., Folkman, L. & Bock, C. Differential Analysis & Visualization Workflow Using limma. Zenodo https://doi.org/10.5281/zenodo.7808680 (2023).
61. Reichl, S. & Bock, C. Genomic Region Set & (Ranked) Gene Set Enrichment Analysis & Visualization Workflow for Human and Mouse Genomes. Zenodo https://doi.org/10.5281/zenodo.7810622 (2023).
62. Fang, Z., Liu, X. & Peltz, G. GSEApy: a comprehensive package for performing gene set enrichment analysis in Python. *Bioinformatics* **39**, btac757 (2023).
63. Tirosh, I. *et al.* Dissecting the multicellular ecosystem of metastatic melanoma by single-cell RNA-seq. *Science* **352**, 189–196 (2016).
64. Kluesner, M. G. *et al.* EditR: A Method to Quantify Base Editing from Sanger Sequencing. *CRISPR J* **1**, 239–250 (2018).

3 Discussion

3.1 Scientific output and novelty

This study presents three key aspects that are discussed below:

(1) a broadly useful technology platform for CAR T cell optimization, which supports genome-wide discovery screens, *in vivo* pooled screens for hit validation, screens with multiplexed modifications to identify combinations of gene targets, and in-depth hit characterization by tiling base editing screens;

(2) a systematic collection of genome-wide CRISPR screens in human CAR T cells, providing a foundation for functional genetics characterization of CAR T cell biology; and

(3) a surprising and comprehensively validated way of enhancing CAR T cell performance by knocking out the small GTPase RHOG with the cell death receptor FAS.

1. Technology. Building on our CROP-seq technology (Datlinger et al. 2017b), the latest advances in synthetic mRNA production and delivery (Sahin et al. 2021), and the concept of high-content screening (Bock et al. 2022), we developed a versatile platform to enhance CAR T cells across multiple clinically relevant objectives. Named CELLFIE ("cell engineering for immunotherapy enhancement"), this platform enabled (1) genome-wide discovery screens in human primary CAR T cells, (2) *in vivo* validation screens with an innovative *in vivo* CROP-seq method, (3) combinatorial screens to identify promising dual knockout perturbations, and (4) tiling base editing screens to functionally characterize our top hit ("biochemistry by sequencing") and prioritize gene edits for clinical translation. Our technology comprises open-source reagents, thoroughly optimized protocols, and cost-effective workflows, creating a broadly useful technology platform that can make large-scale screening in human primary cells more accessible to many laboratories.

2. Dataset. Exploiting the versatility and scalability of our CELLFIE technology platform, we created a comprehensive functional genetics resource of human CAR T cell biology. The presented dataset comprises a total of 58 genome-wide screens covering multiple biological processes: CAR T cell fitness upon TCR and upon CAR stimulation, tumor cell recognition, T cell activation, apoptosis and fratricide, and T cell exhaustion. This is much larger than any published CRISPR screening study in human primary cells (Table 2) and represents a larger collection than all published genome-wide screens in human T cells and CAR T cells combined. With *in vivo* CROP-seq, we resolved the bottleneck of individual knockout validation in mice and tested 39 screening hits in a single experiment (20-fold reduction compared to 400

mice required for individual testing). All three top-ranked hits from the *in vivo* screen (RHOG, PRDM1, FAS) were validated in further in-depth experiments with leukemic mice, confirming the high quality of the dataset. Our combinatorial screens further identified dual knockouts enhancing CAR T cell persistence, including RHOG and FAS double knockout and other promising combinations.

Genome-scale CRISPR screening in T cells and CAR T cells												
First authors	Correspon-ding authors	Year	Journal	Screened cell types	# of ge-nome-scale screens	Screening readouts	Technology platform	Perturbation reagent	CRISPR modes	Number of CRISPR editors	*In vivo* / combinato-rial screen-ing	Knockouts validated *in vivo*
Shifrut, Carnevale	Marson	2018	Cell	T	4	Proliferation (CTFE)	SLICE	Cas9 protein	Knockout	1	-	-
Wang, Prager	Xie, Brown, Rich	2021	Cancer Discovery	CAR T	2	Exhaustion (PD1)	-	Double transduction	Knockout	1	-	TLE4 IKZF2
Carnevale, Shifrut	Marson	2022	Nature	T	15	Proliferation (CFSE)	SLICE	Cas9 protein	Knockout	1	-	RASA2
Freitas, Belk	Satpathy, Mackall	2022	Science	CAR T	6	CAR fitness (proliferation) Cytokines (TNF, IL2)	SLICE	Cas9 protein	Knockout	1	-	MED12
Schmidt, Steinhart	Marson	2022	Science	T	8	Cytokines (IFNγ, IL2)	-	Double transduction	Inhibition Activation	3	-	-
Schmidt, Ward	Schmidt, Ward, Marson	2024	Nature	T	8	Proliferation (CFSE)	-	Double transduction	Base editing	4	-	-
Present study				CAR T	58	Fitness (CAR stimulation) Fitness (TCR stimulation) Target recognition (CD19) T cell activation (CD69) Apoptosis/fratricide (FAS) T cell exhaustion (PD1, LAG3, TIM3)	CELLFIE	Synthetic mRNA	Knockout, Activation, Base editing	7	yes	RHOG FAS PRDM1 RHOG+FAS

Table 2. Progress in genome-scale CRISPR screening in T cells and CAR T cells compared to the current study (in the last row).

3. Discovery. Our screens identified established targets of immunotherapeutic drugs (CTLA4, PD1, TIM3, TIGIT) and promising new candidates for improving CAR T cell function. RHOG and FAS knockouts in CAR T cells strongly enhanced tumor clearance and survival in preclinical mouse models. Of all gene knockouts proposed to enhance CAR T cell efficacy, RHOG presents a particularly unexpected discovery, which underlines the value of genome-wide screening to optimize cell therapies. RHOG had no previous links to cancer immunotherapy and would have been an unlikely candidate given that monogenic RHOG deficiency causes an inborn error of immunity. We discovered a strong suppressive role of RHOG in CAR T cells and demonstrated enhanced fitness of RHOG knockout CAR T cells. Importantly, the beneficial effect of RHOG knockout was confirmed in CAR T cells containing CARs with multiple antigen recognition and intracellular signaling domains, indicating the translational potential of the RHOG knockout for a broad range of cell-based T cell therapies. We functionally characterized RHOG through tiling base editing screens, which identified the GTP binding site as a potential target for pharmacological inhibition of RHOG and established a dataset to prioritize gRNAs for RHOG ablation without double-strand breaks. We further nominated the dual knockout of RHOG and FAS genes as a strong candidate for clinical translation, acting through different biological axes by increasing proliferative capacity and survival of CAR T cells.

3.2 Limitations and future directions

Our work provides a technology platform for CAR T cell optimization as well as extensive biological insights on genetically modified CAR T cells. This section summarizes the limitations of the present study as well as potential future directions enabled by our research (Table 3).

Study aspects	Future directions
Technology development	• Other CRISPR applications • Single-cell screens
Screening findings	• New screening readouts to address challenges in CAR T cells • Combinatorial screens in T cells with different synthetic receptors
Biological mechanisms	• Further investigation of the role of RHOG in T and CAR T cells • Systematic analysis of other screening hits as CAR T cell regulators
Preclinical work and translation	• Testing modified CAR T cells in additional preclinical models • Potential first-in-human clinical trial using RHOG-deficient CAR T cells

Table 3. Future research directions enabled by the present study.

3.2.1 Technology

Our CELLFIE platform is differentiated from previous efforts by unprecedented versatility and scalability. One of the key decisions for the establishment of this platform was the mRNA-based delivery of CRISPR modifiers, which provided significant advantages in the flexibility and scale of its applications. We performed genome-scale and focused knockout and base editing screens. We envision that additional CRISPR applications can be easily adopted with this platform. For example, the CRISPRoff system (Nuñez et al. 2021) offers methylation-based heritable silencing of gene expression, which can be superior to knockouts, as CRISPR/Cas9-mediated leads to about 30% in-frame mutations with potentially lower effect on gene function. Prime editing (P. J. Chen et al. 2021) offers the opportunity to introduce large gene modifications such as the introduction of protein domains or synthetic sequences into the genome, which can further expand promising screening modalities. One limitation of the mRNA platform is the transient expression of the CRISPR modifier. This may affect the CRISPR applications that do not introduce permanent changes on genetic or epigenetic changes, including CRISPR activation. However, activation screens can still be performed when studying acute responses to increased gene expression. While our focus lies in CRISPR screens with gRNAs defining the gene perturbation in each cell, other screening modalities, for example integration and overexpression of libraries of artificially designed genes, could open exciting new paths in synthetic biology, which could benefit from our optimized platform.

Another key feature of the CELLFIE platform for screens in CAR T cells is the development of the CROP-seq-CAR vector, which allows flexible switching between different synthetic receptors and includes the advantages of the CROP-seq technology (Datlinger et al.

2017b). The CROP-seq design enables the expression of gRNA from the U6 promoter and as part of an mRNA transcript. Initially, CROP-seq was developed for CRISPR screens with a single-cell transcriptome readout using 3' mRNA detection protocols. Today, single-cell screens can also be performed using 5' chemistry and direct gRNA capture, making the screens compatible with other gRNA vectors (Replogle et al. 2020). Nevertheless, the gRNA expression as part of mRNA transcripts was key for our *in vivo* screens, where we isolated total cell RNA from whole organs, reducing the signal loss thanks to the high mRNA expression (in contrast to one copy integrated into the genomic DNA of each cell). Additionally, we adapted the recently developed CROPseq-multi design of dual-gRNA vectors (Russell T. Walton, Qin, and Blainey 2024) to establish combinatorial screens in CAR T cells. While we successfully utilized the features of CROP-seq-CAR for pooled *in vitro* and *in vivo* screens, this study does not include the originally intended for CROP-seq single-cell screening aspect. Future single-cell transcriptomic screens in CAR T cells screens could provide a high-resolution readout of the effects of genetic perturbation on cell states and account for cell heterogeneity.

3.2.2 Screening findings

CAR T cells are engineered to search and destroy their target cells and to induce a strong immune response. Compared to normal T cells, which need to maintain homeostasis and avoid autoimmune reactions over a human lifetime, CAR T cells have a focused short-term task. As CAR T cells are a human-engineered product which has not been optimized through evolution, the main hypothesis leading to our study was that genes with important roles in normal T cells may constitute obstacles to the therapeutic efficacy of CAR T cells. Our work has identified concrete examples. Through large-scale CRISPR screening in CAR T cells, we found both known and novel negative regulators of CAR T cell function. Using screens in mice, we prioritized gene knockouts and their combinations that enhance the therapeutic effect of CAR T cells *in vivo*. Among these hits were well established immunotherapy targets (such as PD1, CTLA4, TIGIT) and CAR T cell boosters (such as FAS) as well as new promising candidates (such as RHOG). These results support the hypothesis that CAR T cell performance can be improved by knocking out genes with important roles in T cell biology.

While systematic knockout screens enable unbiased discovery of CAR T cell boosters, such screens hold certain intrinsic limitations. When selecting hits from genome-wide screens, we used stringent significance cutoffs. This potentially results in false-negative hits (i.e., knockouts with beneficial effects but not selected for validation) due to low significance, which could be associated with technical noise in genome-wide screens or the inefficiencies of some of the gRNAs in the genome-wide library. Using a rank-based approach instead, commonly used in other CAR T cell screening studies, could expand the number of screening hits, some of which may also be validated in subsequent analysis. Thus, our genome-wide screening

dataset could be used for additional exploration. To further alleviate the differences in gRNA editing efficiencies, screens with increased numbers of gRNAs could be performed, for example using the Bassik library with 10 gRNAs per gene (total of 211,695 gRNAs) (Morgens et al. 2017) instead of the Brunello library with 4 gRNAs (total of 77,441 gRNAs) (Sanson et al. 2018) per gene. While a larger number of gRNAs would require an increased scale of screens, this could be circumvented by preselection of certain genes and by using genetic cassettes with multiple gRNAs expressed from a single vector.

An additional limitation specific to *in vivo* screens is that, due to the nature of dropout or enrichment pooled screens, they largely evaluate CAR T cell fitness and engraftment, and not necessarily the killing function. Therefore, the positive effects of certain knockouts might be missed unless they are tested individually, potentially resulting in false-negative results during knockout prioritization through the *in vivo* screens. An alternative possibility to predict enhanced therapeutic properties in a pooled fashion *in vivo* is to isolate CAR T cells from organs during the treatment and perform single-cell screening to profile transcriptomes or epigenomes of perturbed cells. Using this approach to profile screening hits from genome-wide screens could yield additional genetic modifications that enhance CAR T cell functions.

Our technology platform enabled high-throughput screening in human primary CAR T cells leading to the generation of a vast dataset with multiple readouts focusing on T cell fitness, tumor cell recognition, T cell activation, apoptosis and fratricide, and T cell exhaustion. In our analysis, we mainly focused on the knockouts enriched in cell populations with potentially beneficial properties of CAR T cells, such as increased fitness, higher level of CD19 uptake as a marker of tumor recognition, higher expression of T cell activation marker CD69, and lower expression of death receptor FAS and T cell exhaustion markers PD1, TIM3, and LAG3. However, we also provide the data for knockouts dropping out in the fitness screens, and we report the data for the knockout enrichment in opposite populations for FACS-based screens. This data can be used to further investigate the regulators of CAR T cell functions.

It is important to further acknowledge that improving the aspects of CAR T cell functionality selected in this work could only address some of the challenges associated with therapeutic outcomes. Other crucial limitations could be addressed by performing screens with alternative readouts in the future. For example, one promising direction could be to address challenges in T cell trafficking by performing *in vivo* screens in solid tumor models. In addition, other signaling properties of CAR T cells can be tweaked by using other readouts, such as degranulation, perforin and granzyme activity, or cytokine production. Fortunately, the scalability of the CELLFIE technology platform opens a wide range of possibilities for engineering next-generation T cell therapies through multi-readout genetic screens.

While the screening dataset generated in this study could serve as a substantial resource for further exploration, it is important to note that our genome-wide screens were

performed in CAR T cells containing an anti-CD19 scFv domain and a 41BBz intracellular signaling domain. Thus, some of the findings may be predominantly relevant for CAR T cells containing this specific CAR receptor, which resembles the clinically used tisagenlecleucel product. For example, our screens did not identify some of the known targets originally found to enhance CAR T cells with CD28z intracellular signaling domain. However, we demonstrated that certain findings from our screens could be translated across multiple synthetic receptors and T cell therapies, as illustrated by the example of the RHOG and FAS knockouts, thus providing a foundation for future studies. Moreover, as our CROP-seq-CAR vector design enables straightforward switching between different CAR constructs, the research community could leverage our platform to conduct screens customized to their CAR constructs of interest.

Single genetic perturbations might not constitute a complete solution to multiple challenges of CAR T cell therapy. This is demonstrated by our observation that a combination of identified hits, RHOG and FAS knockouts, result in an additive beneficial effect. Our unique extension of the CELLFIE platform enables combinatorial knockout screens in CAR T cells, establishing the workflow to identify dual gene targets to enhance T cell therapy. Furthermore, our study includes a comparative analysis of CAR T cell booster hits across published datasets, which we hope will serve as a foundation for future systematic combinatorial screens in engineered T cells.

3.2.3 Biological mechanisms

This study establishes the beneficial role of RHOG knockout in CAR T cells, as found through genome-wide screens and extensive validation experiments both *in vitro* and *in vivo*. We investigated the specific effects of the RHOG knockout in human primary CAR T cells and found that it leads to increased proliferative capacity, characterized by an elevated fraction of memory T cells, increased proliferation, and reduced T cell exhaustion. At the same time, the cytotoxic properties and survival of CAR T cells were unaltered by the RHOG knockout. Importantly, RHOG and FAS knockouts address two distinct obstacles to CAR T cell performance: RHOG – increased proliferative capacity; FAS – decreased apoptosis and fratricide. This explains the strong performance of the RHOG-FAS double knockout. While FAS ablation has already been reported to enhance CAR T cells in multiple studies (Ren et al. 2017; Tieu et al. 2024; Menegatti et al. 2024) and has been employed in clinical trials (NCT05617755), the RHOG knockout is a novel CAR T cell booster discovered in this work. Despite RhoG being a known regulator of multiple processes in human T cells, from T cell signaling to migration (Ahmad Mokhtar et al. 2022), our finding was surprising, given that RHOG ablation has been associated with immunodeficiency in patients (Kalinichenko et al. 2021). These results underscore the value of CRISPR screening, as it would have been nearly impossible to guess the beneficial role of RHOG knockout based on prior biological knowledge.

RHOG encodes a small GTPase, a member of the Rac subfamily of the Rho family of small G proteins (Ridley 2006). Like other small G proteins, RhoG cycles between active GTP-bound and inactive GDP-bound states, regulated by three protein classes: (1) guanine nucleotide exchange factors promote GTP binding to activate signaling; (2) GTPase-activating proteins enhance GTP hydrolysis to terminate signaling; (3) guanine nucleotide dissociation inhibitors block GDP dissociation and maintain the inactive state. Over a hundred Rho-family regulators from these three classes are involved in the regulation of RhoG activity in various cell types (Vigil et al. 2010). Upon activation, RhoG signals through multiple effectors, though only a few pathways are well characterized. The best-studied pathway involves RhoG-dependent Rac activation via DOCK-family guanine nucleotide exchange factors, which promote GTP-loading in brain cells (Côté and Vuori 2007). However, the signaling pathway of RhoG in T cells is understudied, and some RhoG functions in T cells appear to be redundant and shared with other proteins (Ahmad Mokhtar et al. 2022).

Based on our extensive flow cytometry data and bulk RNA-seq profiling of knockout versus standard CAR T cells, we hypothesize that the presence of RHOG may act as a brake on CAR T cell proliferation. Notably, the effects of RHOG knockout were largely consistent between CD4 and CD8 T cells, suggesting a broad effect of RHOG knockout on CAR T cells. However, the molecular mechanism and downstream signaling of RHOG in CAR T cells remain to be studied further, which requires additional research in T or CAR T cells with both deficient and intact RHOG.

Activated RHOG in T cells is known to mediate phosphorylation of NFAT (nuclear factor of activated T cells), resulting in its translocation to nucleus and activation of transcriptional programs leading to T cell anergy and exhaustion (Ahmad Mokhtar et al. 2022). However, the exact mediators of this process are unknown. Further experiments, such as NFAT phosphorylation profiling in RHOG knockout cells, are required to investigate whether it is involved in RHOG signaling in CAR T cells. Additional transcription factors could play a role in RHOG knockout effects in CAR T cells. Our RNA-seq dataset comparing knockout and standard CAR T cells could be used to analyze the enrichment of the known transcriptional regulators of differentially expressed genes, in order to systematically identify transcription factors involved in RHOG signaling. ATAC-seq studies in a similar setup could further aid the identification of key transcription factors by the enrichment analysis of their binding site motifs in differentially open or closed chromatin regions upon knockout.

The protein interactors of RHOG and its signaling regulators remain understudied in T cells. Our tiling base editing screens indicated the potential importance of GTPase activity of RHOG in CAR T cells. Future research could focus on investigating its function in more detail. Such studies could benefit from multiple molecular biology and biochemistry tools, including profiling protein-protein interactions of RHOG, since little is known about the state of RHOG

in T cells (GTP- vs GDP-bound), the proteins regulating this state, and mediators of signaling pathways that RHOG induces in its active form.

3.2.4 Translation

Given that CAR T cells are already genetically engineered, CRISPR screening constitutes a natural approach to optimize them as therapeutics. CRISPR-boosted CAR T cells could address key challenges faced by CAR T cell therapy. First, with currently available CAR T cell therapies for leukemia and lymphoma, many patients never achieve a complete response or eventually relapse (Cappell and Kochenderfer 2023). Second, the situation is even more challenging for most solid cancers, in part due to immunosuppressive microenvironments (Albelda 2024). Third, allogeneic “off-the-shelf” CAR T cells have so far had limited impact because they are too quickly rejected by host immunity. For all these challenges, more potent CAR T cells, including our CRISPR-boosted CAR T cell design, could be broadly beneficial.

T cell-based therapies enhanced by additional genetic modifications have already entered clinical trials (V. Wang et al. 2023b), for example CAR T cells with overexpression of interleukin 18 (NCT04684563), CAR T cells with PD1 knockout (NCT04213469, NCT03545815, NCT03525782) or FAS knockdown (NCT05617755), and TILs with a knockout of SOCS1 (NCT06237881). The latter examples showcase the use of CRISPR knockout-boosted T cell therapies in real clinical practice. Moreover, they highlight that not only T cells with synthetic receptors such as CAR or TCR T cells, but also TILs are ready for CRISPR-modifications to enhance their function, widely expanding their potential application.

Through the genetic screens in our study, we discovered the RHOG knockout, separately and in combination with FAS knockout, as an effective way to enhance clinically validated CAR T cell therapies. The double knockout of RHOG and FAS showed the strongest *in vitro* and *in vivo* results across multiple experiments, cell donors, models, readouts, and CAR designs. The double knockout not only promoted the therapeutic efficacy of CAR T cells in a widely established leukemia but also in a solid tumor model.

Our extensive data demonstrate the superior potency of our CRISPR-boosted CAR T cells, providing a rational for further preclinical and clinical development. In particular, our findings support the potential advantage of RHOG and FAS knockout CAR T cells in CD19+ leukemia models, providing a baseline scenario for potential clinical development. We envision that a well-suited population for a first-in-human clinical trial is represented by the patients who receive approved anti-CD19 CAR T cell therapy for B cell leukemia or lymphoma but achieve only a partial response or rapidly relapse. First, a partial response to an approved CAR T cell product would confirm the efficacy of this treatment modality and indicate that more potent CAR T cells may achieve a better response. Second, only patients lacking severe side effects to the approved anti-CD19 CAR T cell therapy would be included, increasing confidence

regarding the safety of another CAR T cell design targeting the same cancer antigen. Third, most of these patients would likely have few therapeutic options remaining, making it ethically justifiable to test an experimental therapy. Similar clinical trial setup has been already used to test CAR T cells boosted by IL18 overexpression (NCT04684563) (Svoboda et al. 2024). Thus, it could be a potential starting point for clinical trials using CAR T cells enhanced by genetic modifications discovered in this work.

The outlined approach of implementing CRISPR-boosted CAR T cells in established indications has certain weaknesses, including the concern that patients who have already failed one anti-CD19 CAR T cell therapy may be unlikely to respond to a second one. Therefore, further testing of knockout CAR T cells in multiple preclinical models could identify the best match and provide a broad basis of preclinical data supporting the choice of disease indication, target antigen, and treatment regimen for subsequent clinical development. Complementing our data in the xenograft model of hepatocellular carcinoma, other solid tumor models are required to determine the potential applicability of identified CRISPR targets to a wider range of indications. One expected challenge in such models is that they are typically based on cell line-derived xenografts. To more precisely mimic human cancer, we envision a wider use of patient-derived xenografts (Y. Liu et al. 2023b) in the future. Another key challenge of xenograft models is the requirement to use immunodeficient mice in order to let cancer cells engraft and not be immediately rejected by the host immune system. One solution is switching from human to murine CAR T cells, which can treat tumors in immunocompetent mice but would first require testing and successful results for mouse gene knockouts. Another possibility is offered by humanized mouse models (Alves da Costa et al. 2019), where human immune cells are implanted into immunocompromised mice enabling the use of human CAR T cells while preserving the tumor microenvironment component. Evaluation of our CRISPR-boosted CAR T cells in multiple preclinical tests, both for cancer and other models including autoimmune diseases, could broaden their applicability across different therapeutic settings.

Our work advances the discovery of CRISPR-boosters for CAR T cells, which could promote next-generation T cell-based therapies toward clinical testing. However, taking innovations from the lab to the clinic will require numerous steps prior to any envisioned first-in-human clinical trials. This includes establishing the production pipeline for genetically modified CAR T cells, evaluation of efficacy and safety profiles of the final product in a preclinical setting, and only then choosing the patient group that may benefit from enhanced CAR T cells. To use our CRISPR knockout CAR T cells in clinical trials, they need to be manufactured in a GMP-compliant manner, which is a labor-intensive and costly task that requires careful preparation. Fortunately, substantial progress has been made over the last years in terms of GMP-grade CAR T cell production in an academic setting (Stemer et al. 2024; Sánchez-Guijo et al. 2023; Le Guen et al. 2024; P. Fischer et al. 2023). For standard CAR T cells targeting

leukemia/lymphoma antigens such as CD19 and BCMA, GMP-compliant production based on lentiviral delivery of CAR is already established at many academic medical centers including the Medical University of Vienna. For CRISPR genome editing, it is necessary to additionally deliver the Cas9 editor and the targeting gRNAs into the CAR T cells. The effective and scalable method for synthetic RNA delivery used in our study could leverage the lower cost of GMP-grade RNA production compared to the commonly used lentiviral approach. In the context of multiple gene knockouts, the introduction of several CRISPR edits comes with a certain risk of genotoxicity, off-target effects (Malinin et al. 2021), chromosomal rearrangements (Turchiano et al. 2021), or other types of mutations, which need to be experimentally assessed and quantified. The level of genotoxicity will depend on the specific perturbations and the techniques chosen for gene modulation. To provide a clinically relevant multiplex gene editing approach, we established CRISPR base editing screens to prioritize gRNAs introducing functional amino acid mutations for potential clinical translation, since the base editing approach could reduce the chromosomal translocations associated with multiple CRISPR-Cas9 double-strand breaks (Webber et al. 2019; Chiesa et al. 2023).

While many steps lie ahead for the translation of CRISPR-boosted CAR T cells, there are multiple examples of the successful development of innovative CAR T cells by academic groups, resulting in the clinical application of CAR T cell therapy (V. Wang et al. 2023b). We therefore envision that our work provides a foundation for future efforts to translate lab innovations in cell therapies into clinical practice.

3.3 Conclusions

Presented in this study, our CELLFIE technology established a powerful platform for optimizing cell-based immunotherapy through CRISPR screening and a foundational dataset of CRISPR knockout effects for biological characterization and functional optimization of CAR T cells. On this basis, we identified RHOG and FAS single and double knockouts as boosters of CAR T cell performance *in vitro* and *in vivo*, followed by the comprehensive characterization of RHOG-deficient CAR T cells. As CAR T cells are genetically modified cell products, there is a path toward clinical translation of CRISPR-boosted CAR T cells.

4 Materials and methods

Materials and methods can be found in the “Methods” section of the accompanying manuscript, including experimental models and subject details, resource availability, experimental procedures, and computational analysis.

References

Abramson, Jeremy S., M. Lia Palomba, Leo I. Gordon, Matthew A. Lunning, Michael Wang, Jon Arnason, Amitkumar Mehta, et al. 2020. “Lisocabtagene Maraleucel for Patients with Relapsed or Refractory Large B-Cell Lymphomas (TRANSCEND NHL 001): A Multicentre Seamless Design Study.” *Lancet (London, England)* 396 (10254): 839–52. https://doi.org/10.1016/S0140-6736(20)31366-0.

Adamson, Britt, Thomas M. Norman, Marco Jost, Min Y. Cho, James K. Nuñez, Yuwen Chen, Jacqueline E. Villalta, et al. 2016. “A Multiplexed Single-Cell CRISPR Screening Platform Enables Systematic Dissection of the Unfolded Protein Response.” *Cell* 167 (7): 1867-1882.e21. https://doi.org/10.1016/j.cell.2016.11.048.

Aghajanian, Haig, Toru Kimura, Joel G. Rurik, Aidan S. Hancock, Michael S. Leibowitz, Li Li, John Scholler, et al. 2019. “Targeting Cardiac Fibrosis with Engineered T Cells.” *Nature* 573 (7774): 430–33. https://doi.org/10.1038/s41586-019-1546-z.

Ahmad Mokhtar, Ana Masara, Nor Hawani Salikin, Aminah Suhaila Haron, Syafinaz Amin-Nordin, Ilie Fadzilah Hashim, Muaz Mohd Zaini Makhtar, Siti Balqis Zulfigar, and Nurul Izza Ismail. 2022. “RhoG’s Role in T Cell Activation and Function.” *Frontiers in Immunology* 13 (February):845064. https://doi.org/10.3389/fimmu.2022.845064.

Albelda, Steven M. 2024. “CAR T Cell Therapy for Patients with Solid Tumours: Key Lessons to Learn and Unlearn.” *Nature Reviews Clinical Oncology* 21 (1): 47–66. https://doi.org/10.1038/s41571-023-00832-4.

Alda-Catalinas, Celia, Ximena Ibarra-Soria, Christina Flouri, Jorge Esparza Gordillo, Diana Cousminer, Anna Hutchinson, Bin Sun, et al. 2024. “Mapping the Functional Impact of Non-Coding Regulatory Elements in Primary T Cells through Single-Cell CRISPR Screens.” *Genome Biology* 25 (1): 42. https://doi.org/10.1186/s13059-024-03176-z.

Alves da Costa, Thiago, Julie Lang, Raul M. Torres, and Roberta Pelanda. 2019. “The Development of Human Immune System Mice and Their Use to Study Tolerance and Autoimmunity.” *Journal of Translational Autoimmunity* 2 (November):100021. https://doi.org/10.1016/j.jtauto.2019.100021.

Amini, Leila, Sara K. Silbert, Shannon L. Maude, Loretta J. Nastoupil, Carlos A. Ramos, Renier J. Brentjens, Craig S. Sauter, Nirali N. Shah, and Mohamed Abou-el-Enein. 2022. “Preparing for CAR T Cell Therapy: Patient Selection, Bridging Therapies and Lymphodepletion.” *Nature Reviews Clinical Oncology* 19 (5): 342–55. https://doi.org/10.1038/s41571-022-00607-3.

Amor, Corina, Inés Fernández-Maestre, Saria Chowdhury, Yu-Jui Ho, Sandeep Nadella, Courtenay Graham, Sebastian E. Carrasco, et al. 2024. “Prophylactic and Long-Lasting Efficacy of Senolytic CAR T Cells against Age-Related Metabolic Dysfunction.” *Nature Aging* 4 (3): 336–49. https://doi.org/10.1038/s43587-023-00560-5.

Anzalone, Andrew V., Peyton B. Randolph, Jessie R. Davis, Alexander A. Sousa, Luke W. Koblan, Jonathan M. Levy, Peter J. Chen, et al. 2019. “Search-and-Replace Genome Editing without Double-Strand Breaks or Donor DNA.” *Nature* 576 (7785): 149–57. https://doi.org/10.1038/s41586-019-1711-4.

Ayala Ceja, Melanie, Mobina Khericha, Caitlin M. Harris, Cristina Puig-Saus, and Yvonne Y. Chen. 2024. “CAR-T Cell Manufacturing: Major Process Parameters and next-Generation Strategies.” *The Journal of Experimental Medicine* 221 (2): e20230903. https://doi.org/10.1084/jem.20230903.

Barber, E K, J D Dasgupta, S F Schlossman, J M Trevillyan, and C E Rudd. 1989. “The CD4 and CD8 Antigens Are Coupled to a Protein-Tyrosine Kinase (P56lck) That Phosphorylates the CD3 Complex.” *Proceedings of the National Academy of Sciences of the United States of America* 86 (9): 3277–81.

Belk, Julia A., Winnie Yao, Nghi Ly, Katherine A. Freitas, Yan-Ting Chen, Quanming Shi, Alfredo M. Valencia, et al. 2022. “Genome-Wide CRISPR Screens of T Cell Exhaustion Identify Chromatin Remodeling Factors That Limit T Cell Persistence.” *Cancer Cell* 40 (7): 768-786.e7. https://doi.org/10.1016/j.ccell.2022.06.001.

Benmebarek, Mohamed-Reda, Clara Helke Karches, Bruno Loureiro Cadilha, Stefanie Lesch, Stefan Endres, and Sebastian Kobold. 2019. “Killing Mechanisms of Chimeric Antigen Receptor (CAR) T Cells.” *International Journal of Molecular Sciences* 20 (6): 1283. https://doi.org/10.3390/ijms20061283.

Blache, Ulrich, Georg Popp, Anna Dünkel, Ulrike Koehl, and Stephan Fricke. 2022. “Potential Solutions for Manufacture of CAR T Cells in Cancer Immunotherapy.” *Nature Communications* 13 (1): 5225. https://doi.org/10.1038/s41467-022-32866-0.

Bock, Christoph, Paul Datlinger, Florence Chardon, Matthew A. Coelho, Matthew B. Dong, Keith A. Lawson, Tian Lu, et al. 2022. “High-Content CRISPR Screening.” *Nature Reviews. Methods Primers* 2 (1): 9. https://doi.org/10.1038/s43586-022-00098-7.

Brown, Christine E., Darya Alizadeh, Renate Starr, Lihong Weng, Jamie R. Wagner, Araceli Naranjo, Julie R. Ostberg, et al. 2016. “Regression of Glioblastoma after Chimeric Antigen Receptor T-Cell Therapy.” *The New England Journal of Medicine* 375 (26): 2561–69. https://doi.org/10.1056/NEJMoa1610497.

Cappell, Kathryn M., and James N. Kochenderfer. 2021. “A Comparison of Chimeric Antigen Receptors Containing CD28 versus 4-1BB Costimulatory Domains.” *Nature Reviews Clinical Oncology* 18 (11): 715–27. https://doi.org/10.1038/s41571-021-00530-z.

Carnevale, Julia, Eric Shifrut, Nupura Kale, William A. Nyberg, Franziska Blaeschke, Yan Yi Chen, Zhongmei Li, et al. 2022. “RASA2 Ablation in T Cells Boosts Antigen Sensitivity and Long-Term Function.” *Nature* 609 (7925): 174–82. https://doi.org/10.1038/s41586-022-05126-w.

Carvalho, Thiago. 2023. “First Two Patients Receive CAR T Cell Therapy for HIV.” *Nature Medicine* 29 (6): 1290–91. https://doi.org/10.1038/d41591-023-00042-6.

Chan, Jack D., Christina M. Scheffler, Isabelle Munoz, Kevin Sek, Joel N. Lee, Yu-Kuan Huang, Kah Min Yap, et al. 2024. “FOXO1 Enhances CAR T Cell Stemness, Metabolic Fitness and Efficacy.” *Nature* 629 (8010): 201–10. https://doi.org/10.1038/s41586-024-07242-1.

Chen, Joyce, Isaac F. López-Moyado, Hyungseok Seo, Chan-Wang J. Lio, Laura J. Hempleman, Takashi Sekiya, Akihiko Yoshimura, James P. Scott-Browne, and Anjana Rao. 2019. “Nr4a Transcription Factors Limit CAR T Cell Function in Solid Tumors.” *Nature* 567 (7749): 530–34. https://doi.org/10.1038/s41586-019-0985-x.

Chen, Peter J., Jeffrey A. Hussmann, Jun Yan, Friederike Knipping, Purnima Ravisankar, Pin-Fang Chen, Cidi Chen, et al. 2021. “Enhanced Prime Editing Systems by Manipulating Cellular Determinants of Editing Outcomes.” *Cell* 184 (22): 5635-5652.e29. https://doi.org/10.1016/j.cell.2021.09.018.

Chen, Zeyu, Eri Arai, Omar Khan, Zhen Zhang, Shin Foong Ngiow, Yuan He, Hua Huang, et al. 2021. “In Vivo CD8+ T Cell CRISPR Screening Reveals Control by Fli1 in Infection and Cancer.” *Cell* 184 (5): 1262-1280.e22. https://doi.org/10.1016/j.cell.2021.02.019.

Chester, Cariad, Siddhant Ambulkar, and Holbrook E. Kohrt. 2016. “4-1BB Agonism: Adding the Accelerator to Cancer Immunotherapy.” *Cancer Immunology, Immunotherapy: CII* 65 (10): 1243–48. https://doi.org/10.1007/s00262-016-1829-2.

Chiesa, Robert, Christos Georgiadis, Farhatullah Syed, Hong Zhan, Annie Etuk, Soragia Athina Gkazi, Roland Preece, et al. 2023. “Base-Edited CAR7 T Cells for Relapsed T-Cell Acute Lymphoblastic Leukemia.” *The New England Journal of Medicine* 389 (10): 899–910. https://doi.org/10.1056/NEJMoa2300709.

Choi, Bryan D., Xiaoling Yu, Ana P. Castano, Amanda A. Bouffard, Andrea Schmidts, Rebecca C. Larson, Stefanie R. Bailey, et al. 2019. “CAR-T Cells Secreting BiTEs Circumvent Antigen Escape without Detectable Toxicity.” *Nature Biotechnology* 37 (9): 1049–58. https://doi.org/10.1038/s41587-019-0192-1.

Cong, Le, F. Ann Ran, David Cox, Shuailiang Lin, Robert Barretto, Naomi Habib, Patrick D. Hsu, et al. 2013. “Multiplex Genome Engineering Using CRISPR/Cas Systems.” *Science (New York, N.Y.)* 339 (6121): 819–23. https://doi.org/10.1126/science.1231143.

Copelan, Edward A. 2006. “Hematopoietic Stem-Cell Transplantation.” *New England Journal of Medicine* 354 (17): 1813–26. https://doi.org/10.1056/NEJMra052638.

Côté, Jean-François, and Kristiina Vuori. 2007. “GEF What? Dock180 and Related Proteins Help Rac to Polarize Cells in New Ways.” *Trends in Cell Biology* 17 (8): 383–93. https://doi.org/10.1016/j.tcb.2007.05.001.

Crabtree, Gerald R., and Eric N. Olson. 2002. “NFAT Signaling: Choreographing the Social Lives of Cells.” *Cell* 109 Suppl (April):S67-79. https://doi.org/10.1016/s0092-8674(02)00699-2.

Dai, Xiaoyun, Jonathan J. Park, Yaying Du, Zhenkun Na, Stanley Z. Lam, Ryan D. Chow, Paul A. Renauer, et al. 2023. “Massively Parallel Knock-in Engineering of Human T Cells.” *Nature Biotechnology* 41 (9): 1239–55. https://doi.org/10.1038/s41587-022-01639-x.

Datlinger, Paul, André F Rendeiro, Christian Schmidl, Thomas Krausgruber, Peter Traxler, Johanna Klughammer, Linda C Schuster, Amelie Kuchler, Donat Alpar, and Christoph Bock. 2017a. “Pooled CRISPR Screening with Single-Cell Transcriptome Read-Out.” *Nature Methods* 14 (3): 297–301. https://doi.org/10.1038/nmeth.4177.

De Castro, Valentine, Jeanne Galaine, Romain Loyon, and Yann Godet. 2024. “CRISPR-Cas Gene Knockouts to Optimize Engineered T Cells for Cancer Immunotherapy.” *Cancer Gene Therapy*, April, 1–11. https://doi.org/10.1038/s41417-024-00771-x.

Dekkers, Johanna F., Maria Alieva, Astrid Cleven, Farid Keramati, Amber K. L. Wezenaar, Esmée J. van Vliet, Jens Puschhof, et al. 2023. “Uncovering the Mode of Action of Engineered T Cells in Patient Cancer Organoids.” *Nature Biotechnology* 41 (1): 60–69. https://doi.org/10.1038/s41587-022-01397-w.

Del Bufalo, Francesca, Biagio De Angelis, Ignazio Caruana, Giada Del Baldo, Maria A. De Ioris, Annalisa Serra, Angela Mastronuzzi, et al. 2023. “GD2-CART01 for Relapsed or Refractory High-Risk Neuroblastoma.” *New England Journal of Medicine* 388 (14): 1284–95. https://doi.org/10.1056/NEJMoa2210859.

Delgoffe, Greg M., Chenqi Xu, Crystal L. Mackall, Michael R. Green, Stephen Gottschalk, Daniel E. Speiser, Dietmar Zehn, and Paul A. Beavis. 2021. “The Role of Exhaustion in CAR T Cell Therapy.” *Cancer Cell* 39 (7): 885–88. https://doi.org/10.1016/j.ccell.2021.06.012.

Deng, Qing, Guangchun Han, Nahum Puebla-Osorio, Man Chun John Ma, Paolo Strati, Beth Chasen, Enyu Dai, et al. 2020. “Characteristics of Anti-CD19 CAR T Cell Infusion Products Associated with Efficacy and Toxicity in Patients with Large B Cell Lymphomas.” *Nature Medicine* 26 (12): 1878–87. https://doi.org/10.1038/s41591-020-1061-7.

Depil, S., P. Duchateau, S. A. Grupp, G. Mufti, and L. Poirot. 2020. “‘Off-the-Shelf’ Allogeneic CAR T Cells: Development and Challenges.” *Nature Reviews Drug Discovery* 19 (3): 185–99. https://doi.org/10.1038/s41573-019-0051-2.

Dixit, Atray, Oren Parnas, Biyu Li, Jenny Chen, Charles P. Fulco, Livnat Jerby-Arnon, Nemanja D. Marjanovic, et al. 2016. “Perturb-Seq: Dissecting Molecular Circuits with Scalable Single-Cell RNA Profiling of Pooled Genetic Screens.” *Cell* 167 (7): 1853-1866.e17. https://doi.org/10.1016/j.cell.2016.11.038.

Doan, Alexander E., Katherine P. Mueller, Andy Y. Chen, Geoffrey T. Rouin, Yingshi Chen, Bence Daniel, John Lattin, et al. 2024. “FOXO1 Is a Master Regulator of Memory Programming in CAR T Cells.” *Nature* 629 (8010): 211–18. https://doi.org/10.1038/s41586-024-07300-8.

Doench, John G. 2018. “Am I Ready for CRISPR? A User’s Guide to Genetic Screens.” *Nature Reviews Genetics* 19 (2): 67–80. https://doi.org/10.1038/nrg.2017.97.

Dong, Matthew B., Guangchuan Wang, Ryan D. Chow, Lupeng Ye, Lvyun Zhu, Xiaoyun Dai, Jonathan J. Park, et al. 2019. “Systematic Immunotherapy Target Discovery Using Genome-Scale in Vivo CRISPR Screens in CD8 T Cells.” *Cell* 178 (5): 1189-1204.e23. https://doi.org/10.1016/j.cell.2019.07.044.

Drougkas, Konstantinos, Konstantinos Karampinos, Ioannis Karavolias, Ioannis-Alexios Koumprentziotis, Ioanna Ploumaki, Efthymios Triantafyllou, Ioannis Trontzas, and Elias Kotteas. 2023. “Comprehensive Clinical Evaluation of CAR-T Cell Immunotherapy for Solid Tumors: A Path Moving Forward or a Dead End?” *Journal of Cancer Research and Clinical Oncology* 149 (6): 2709–34. https://doi.org/10.1007/s00432-022-04547-4.

Duncan, Brynn B., Cynthia E. Dunbar, and Kazusa Ishii. 2022. “Applying a Clinical Lens to Animal Models of CAR-T Cell Therapies.” *Molecular Therapy. Methods & Clinical Development* 27 (December):17–31. https://doi.org/10.1016/j.omtm.2022.08.008.

Echeverri, Christophe J., and Norbert Perrimon. 2006. “High-Throughput RNAi Screening in Cultured Cells: A User’s Guide.” *Nature Reviews. Genetics* 7 (5): 373–84. https://doi.org/10.1038/nrg1836.

Eyquem, Justin, Jorge Mansilla-Soto, Theodoros Giavridis, Sjoukje J. C. van der Stegen, Mohamad Hamieh, Kristen M. Cunanan, Ashlesha Odak, Mithat Gönen, and Michel Sadelain. 2017. “Targeting a CAR to the TRAC Locus with CRISPR/Cas9 Enhances Tumour Rejection.” *Nature* 543 (7643): 113–17. https://doi.org/10.1038/nature21405.

FDA. 2024. “FDA Approves First Cellular Therapy to Treat Patients with Unresectable or Metastatic Melanoma.” FDA. FDA. February 21, 2024. https://www.fda.gov/news-events/press-announcements/fda-approves-first-cellular-therapy-treat-patients-unresectable-or-metastatic-melanoma.

FDA, Center for Biologics Evaluation and. 2023. “FDA Investigating Serious Risk of T-Cell Malignancy Following BCMA-Directed or CD19-Directed Autologous Chimeric Antigen Receptor (CAR) T Cell Immunotherapies.” *FDA*, November. https://www.fda.gov/vaccines-blood-biologics/safety-availability-biologics/fda-investigating-serious-risk-t-cell-malignancy-following-bcma-directed-or-cd19-directed-autologous.

Fischer, April M., Carol D. Katayama, Giles Pagès, Jacques Pouysségur, and Stephen M. Hedrick. 2005. “The Role of Erk1 and Erk2 in Multiple Stages of T Cell Development.” *Immunity* 23 (4): 431–43. https://doi.org/10.1016/j.immuni.2005.08.013.

Fischer, Piret, Thomas Reiss, Jörg Mahlich, Erwan Gicquel, Heike Aichinger, Liliya Pullmann, and Tanja Bratan. 2023. “Unlocking the Value of Innovative Medicines: Insights from the Advanced Therapy Medicinal Products (ATMP) Innovation Systems in Germany and Sweden.” *Health Policy and Technology* 12 (2): 100744. https://doi.org/10.1016/j.hlpt.2023.100744.

Flugel, Christian L., Robbie G. Majzner, Giedre Krenciute, Gianpietro Dotti, Stanley R. Riddell, Dimitrios L. Wagner, and Mohamed Abou-el-Enein. 2023. “Overcoming On-Target, off-Tumour Toxicity of CAR T Cell Therapy for Solid Tumours.” *Nature Reviews Clinical Oncology* 20 (1): 49–62. https://doi.org/10.1038/s41571-022-00704-3.

Fraietta, Joseph A., Simon F. Lacey, Elena J. Orlando, Iulian Pruteanu-Malinici, Mercy Gohil, Stefan Lundh, Alina C. Boesteanu, et al. 2018. “Determinants of Response and Resistance to CD19 Chimeric Antigen Receptor (CAR) T Cell Therapy of Chronic Lymphocytic Leukemia.” *Nature Medicine* 24 (5): 563–71. https://doi.org/10.1038/s41591-018-0010-1.

Fraietta, Joseph A., Christopher L. Nobles, Morgan A. Sammons, Stefan Lundh, Shannon A. Carty, Tyler J. Reich, Alexandria P. Cogdill, et al. 2018. “Disruption of TET2 Promotes the Therapeutic Efficacy of CD19-Targeted T Cells.” *Nature* 558 (7709): 307–12. https://doi.org/10.1038/s41586-018-0178-z.

Freitas, Katherine A., Julia A. Belk, Elena Sotillo, Patrick J. Quinn, Maria C. Ramello, Meena Malipatlolla, Bence Daniel, et al. 2022. “Enhanced T Cell Effector Activity by Targeting the Mediator Kinase Module.” *Science* 378 (6620): eabn5647. https://doi.org/10.1126/science.abn5647.

Georgiadis, Christos, Jane Rasaiyaah, Soragia Athina Gkazi, Roland Preece, Aniekan Etuk, Abraham Christi, and Waseem Qasim. 2021. “Base-Edited CAR T Cells for Combinational Therapy against T Cell Malignancies.” *Leukemia* 35 (12): 3466–81. https://doi.org/10.1038/s41375-021-01282-6.

Ghahri-Saremi, Navid, Behnia Akbari, Tahereh Soltantoyeh, Jamshid Hadjati, Saba Ghassemi, and Hamid Reza Mirzaei. 2021. “Genetic Modification of Cytokine Signaling to Enhance Efficacy of CAR T Cell Therapy in Solid Tumors.” *Frontiers in Immunology* 12 (October):738456. https://doi.org/10.3389/fimmu.2021.738456.

Giuffrida, Lauren, Kevin Sek, Melissa A. Henderson, Junyun Lai, Amanda X. Y. Chen, Deborah Meyran, Kirsten L. Todd, et al. 2021. “CRISPR/Cas9 Mediated Deletion of the

Adenosine A2A Receptor Enhances CAR T Cell Efficacy." *Nature Communications* 12 (1): 3236. https://doi.org/10.1038/s41467-021-23331-5.

Good, Charly R., M. Angela Aznar, Shunichiro Kuramitsu, Parisa Samareh, Sangya Agarwal, Greg Donahue, Kenichi Ishiyama, et al. 2021. "An NK-like CAR T Cell Transition in CAR T Cell Dysfunction." *Cell* 184 (25): 6081-6100.e26. https://doi.org/10.1016/j.cell.2021.11.016.

Gross, G, T Waks, and Z Eshhar. 1989. "Expression of Immunoglobulin-T-Cell Receptor Chimeric Molecules as Functional Receptors with Antibody-Type Specificity." *Proceedings of the National Academy of Sciences* 86 (24): 10024–28. https://doi.org/10.1073/pnas.86.24.10024.

Grosser, Rachel, Leonid Cherkassky, Navin Chintala, and Prasad S. Adusumilli. 2019. "Combination Immunotherapy with CAR T Cells and Checkpoint Blockade for the Treatment of Solid Tumors." *Cancer Cell* 36 (5): 471–82. https://doi.org/10.1016/j.ccell.2019.09.006.

Gudipati, Venugopal, Julian Rydzek, Iago Doel-Perez, Vasco Dos Reis Gonçalves, Lydia Scharf, Sebastian Königsberger, Elisabeth Lobner, et al. 2020. "Inefficient CAR-Proximal Signaling Blunts Antigen Sensitivity." *Nature Immunology* 21 (8): 848–56. https://doi.org/10.1038/s41590-020-0719-0.

Guedan, Sonia, Marco Ruella, and Carl H. June. 2019. "Emerging Cellular Therapies for Cancer." *Annual Review of Immunology* 37 (April):145–71. https://doi.org/10.1146/annurev-immunol-042718-041407.

Hamieh, Mohamad, Anton Dobrin, Annalisa Cabriolu, Sjoukje J. C. van der Stegen, Theodoros Giavridis, Jorge Mansilla-Soto, Justin Eyquem, et al. 2019. "CAR T Cell Trogocytosis and Cooperative Killing Regulate Tumour Antigen Escape." *Nature* 568 (7750): 112–16. https://doi.org/10.1038/s41586-019-1054-1.

Hayden, Matthew S., and Sankar Ghosh. 2008. "Shared Principles in NF-kappaB Signaling." *Cell* 132 (3): 344–62. https://doi.org/10.1016/j.cell.2008.01.020.

Hombach, Andreas A., Johannes Heiders, Marcel Foppe, Markus Chmielewski, and Hinrich Abken. 2012. "OX40 Costimulation by a Chimeric Antigen Receptor Abrogates CD28 and IL-2 Induced IL-10 Secretion by Redirected CD4+ T Cells." *Oncoimmunology* 1 (4): 458–66.

Hong, Mingye, Shuang Tao, Ling Zhang, Li-Ting Diao, Xuanmei Huang, Shaohui Huang, Shu-Juan Xie, Zhen-Dong Xiao, and Hua Zhang. 2020. "RNA Sequencing: New Technologies and Applications in Cancer Research." *Journal of Hematology & Oncology* 13 (1): 166. https://doi.org/10.1186/s13045-020-01005-x.

Hou, Andrew J., Laurence C. Chen, and Yvonne Y. Chen. 2021. "Navigating CAR-T Cells through the Solid-Tumour Microenvironment." *Nature Reviews Drug Discovery* 20 (7): 531–50. https://doi.org/10.1038/s41573-021-00189-2.

Huang, Tony P., Gregory A. Newby, and David R. Liu. 2021. "Precision Genome Editing Using Cytosine and Adenine Base Editors in Mammalian Cells." *Nature Protocols* 16 (2): 1089–1128. https://doi.org/10.1038/s41596-020-00450-9.

Imai, C., K. Mihara, M. Andreansky, I. C. Nicholson, C.-H. Pui, T. L. Geiger, and D. Campana. 2004. "Chimeric Receptors with 4-1BB Signaling Capacity Provoke Potent Cytotoxicity against Acute Lymphoblastic Leukemia." *Leukemia* 18 (4): 676–84. https://doi.org/10.1038/sj.leu.2403302.

Jaitin, Diego Adhemar, Assaf Weiner, Ido Yofe, David Lara-Astiaso, Hadas Keren-Shaul, Eyal David, Tomer Meir Salame, Amos Tanay, Alexander van Oudenaarden, and Ido Amit. 2016. "Dissecting Immune Circuits by Linking CRISPR-Pooled Screens with Single-Cell RNA-Seq." *Cell* 167 (7): 1883-1896.e15. https://doi.org/10.1016/j.cell.2016.11.039.

Jinek, Martin, Krzysztof Chylinski, Ines Fonfara, Michael Hauer, Jennifer A. Doudna, and Emmanuelle Charpentier. 2012. "A Programmable Dual RNA-Guided DNA Endonuclease in Adaptive Bacterial Immunity." *Science (New York, N.Y.)* 337 (6096): 816–21. https://doi.org/10.1126/science.1225829.

Jones, Benjamin S., Lawrence S. Lamb, Frederick Goldman, and Antonio Di Stasi. 2014. “Improving the Safety of Cell Therapy Products by Suicide Gene Transfer.” *Frontiers in Pharmacology* 5:254. https://doi.org/10.3389/fphar.2014.00254.

June, Carl H., Roddy S. O’Connor, Omkar U. Kawalekar, Saba Ghassemi, and Michael C. Milone. 2018. “CAR T Cell Immunotherapy for Human Cancer.” *Science (New York, N.Y.)* 359 (6382): 1361–65. https://doi.org/10.1126/science.aar6711.

June, Carl H., and Michel Sadelain. 2018. “Chimeric Antigen Receptor Therapy.” *The New England Journal of Medicine* 379 (1): 64–73. https://doi.org/10.1056/NEJMra1706169.

Jung, In-Young, Vivek Narayan, Sierra McDonald, Andrew J. Rech, Robert Bartoszek, Gwanui Hong, Megan M. Davis, et al. 2022. “BLIMP1 and NR4A3 Transcription Factors Reciprocally Regulate Antitumor CAR T Cell Stemness and Exhaustion.” *Science Translational Medicine* 14 (670): eabn7336. https://doi.org/10.1126/scitranslmed.abn7336.

Kagoya, Yuki, Shinya Tanaka, Tingxi Guo, Mark Anczurowski, Chung-Hsi Wang, Kayoko Saso, Marcus O. Butler, Mark D. Minden, and Naoto Hirano. 2018. “A Novel Chimeric Antigen Receptor Containing a JAK-STAT Signaling Domain Mediates Superior Antitumor Effects.” *Nature Medicine* 24 (3): 352–59. https://doi.org/10.1038/nm.4478.

Kalinichenko, Artem, Giovanna Perinetti Casoni, Loïc Dupré, Luca Trotta, Jakob Huemer, Donatella Galgano, Yolla German, et al. 2021. “RhoG Deficiency Abrogates Cytotoxicity of Human Lymphocytes and Causes Hemophagocytic Lymphohistiocytosis.” *Blood* 137 (15): 2033–45. https://doi.org/10.1182/blood.2020008738.

Karin, Michael. 1995. “The Regulation of AP-1 Activity by Mitogen-Activated Protein Kinases *.” *Journal of Biological Chemistry* 270 (28): 16483–86. https://doi.org/10.1074/jbc.270.28.16483.

Karsten, Hendrik, Ludwig Matrisch, Sophia Cichutek, Walter Fiedler, Winfried Alsdorf, and Andreas Block. 2023. “Broadening the Horizon: Potential Applications of CAR-T Cells beyond Current Indications.” *Frontiers in Immunology* 14:1285406. https://doi.org/10.3389/fimmu.2023.1285406.

Khan, Afreen, and Esha Sarkar. 2022. “CRISPR/Cas9 Encouraged CAR-T Cell Immunotherapy Reporting Efficient and Safe Clinical Results towards Cancer.” *Cancer Treatment and Research Communications* 33:100641. https://doi.org/10.1016/j.ctarc.2022.100641.

Klysz, Dorota D., Carley Fowler, Meena Malipatlolla, Lucille Stuani, Katherine A. Freitas, Yiyun Chen, Stefanie Meier, et al. 2024. “Inosine Induces Stemness Features in CAR-T Cells and Enhances Potency.” *Cancer Cell*, January, S1535610824000084. https://doi.org/10.1016/j.ccell.2024.01.002.

Konermann, Silvana, Mark D. Brigham, Alexandro E. Trevino, Julia Joung, Omar O. Abudayyeh, Clea Barcena, Patrick D. Hsu, et al. 2015. “Genome-Scale Transcriptional Activation by an Engineered CRISPR-Cas9 Complex.” *Nature* 517 (7536): 583. https://doi.org/10.1038/nature14136.

Korell, Felix, Nelson H. Knudsen, Tamina Kienka, Giulia Escobar, Celeste Nobrega, Seth Anderson, Andrew Y. Cheng, et al. 2024. “In Vivo CRISPR Screens Identify Key Modifiers of CAR T Cell Function in Myeloma.” bioRxiv. https://doi.org/10.1101/2024.11.19.624352.

Kuwana, Yoshihisa, Yoshihiro Asakura, Naoko Utsunomiya, Mamoru Nakanishi, Yohji Arata, Seiga Itoh, Fumihiko Nagase, and Yoshikazu Kurosawa. 1987. “Expression of Chimeric Receptor Composed of Immunoglobulin-Derived V Resions and T-Cell Receptor-Derived C Regions.” *Biochemical and Biophysical Research Communications* 149 (3): 960–68. https://doi.org/10.1016/0006-291X(87)90502-X.

Labanieh, Louai, and Crystal L. Mackall. 2023. “CAR Immune Cells: Design Principles, Resistance and the next Generation.” *Nature* 614 (7949): 635–48. https://doi.org/10.1038/s41586-023-05707-3.

Lamble, Adam J., Regina M. Myers, Agne Taraseviciute, Samuel John, Bonnie Yates, Seth M. Steinberg, Jennifer Sheppard, et al. 2023. “Preinfusion Factors Impacting Relapse Immunophenotype Following CD19 CAR T Cells.” *Blood Advances* 7 (4): 575–85. https://doi.org/10.1182/bloodadvances.2022007423.

Le Guen, Camille, Audrey Grain, Baptiste Le Calvez, Soraya Saiagh, Florence Vrignaud, Marion Eveillard, Béatrice Clémenceau, and Mina Benjelloun Zahar. 2024. “[Can academic structures improve access to CAR-T cells?].” *Bulletin Du Cancer* 111 (1): 62–72. https://doi.org/10.1016/j.bulcan.2023.10.005.

Lindner, S. E., S. M. Johnson, C. E. Brown, and L. D. Wang. 2020. “Chimeric Antigen Receptor Signaling: Functional Consequences and Design Implications.” *Science Advances* 6 (21): eaaz3223. https://doi.org/10.1126/sciadv.aaz3223.

Liscovitch-Brauer, Noa, Antonino Montalbano, Jiale Deng, Alejandro Méndez-Mancilla, Hans-Hermann Wessels, Nicholas G. Moss, Chia-Yu Kung, et al. 2021. “Profiling the Genetic Determinants of Chromatin Accessibility with Scalable Single-Cell CRISPR Screens.” *Nature Biotechnology* 39 (10): 1270–77. https://doi.org/10.1038/s41587-021-00902-x.

Liu, Ming, Linlin Zhang, Mingtian Zhong, Yihao Long, Wenhui Yang, Ting Liu, Xingxu Huang, and Xiaodong Ma. 2023. “CRISPR/Cas9-Mediated Knockout of Intracellular Molecule SHP-1 Enhances Tumor-Killing Ability of CD133-Targeted CAR T Cells in Vitro.” *Experimental Hematology & Oncology* 12 (1): 88. https://doi.org/10.1186/s40164-023-00450-x.

Liu, Yihan, Wantao Wu, Changjing Cai, Hao Zhang, Hong Shen, and Ying Han. 2023a. “Patient-Derived Xenograft Models in Cancer Therapy: Technologies and Applications.” *Signal Transduction and Targeted Therapy* 8 (1): 1–24. https://doi.org/10.1038/s41392-023-01419-2.

Locke, Frederick L., David B. Miklos, Caron A. Jacobson, Miguel-Angel Perales, Marie-José Kersten, Olalekan O. Oluwole, Armin Ghobadi, et al. 2022. “Axicabtagene Ciloleucel as Second-Line Therapy for Large B-Cell Lymphoma.” *New England Journal of Medicine* 386 (7): 640–54. https://doi.org/10.1056/NEJMoa2116133.

López-Cantillo, Gina, Claudia Urueña, Bernardo Armando Camacho, and Cesar Ramírez-Segura. 2022. “CAR-T Cell Performance: How to Improve Their Persistence?” *Frontiers in Immunology* 13 (April):878209. https://doi.org/10.3389/fimmu.2022.878209.

Lu, You, Jianxin Xue, Tao Deng, Xiaojuan Zhou, Kun Yu, Lei Deng, Meijuan Huang, et al. 2020. “Safety and Feasibility of CRISPR-Edited T Cells in Patients with Refractory Non-Small-Cell Lung Cancer.” *Nature Medicine* 26 (5): 732–40. https://doi.org/10.1038/s41591-020-0840-5.

Lynn, Rachel C., Evan W. Weber, Elena Sotillo, David Gennert, Peng Xu, Zinaida Good, Hima Anbunathan, et al. 2019. “C-Jun Overexpression in CAR T Cells Induces Exhaustion Resistance.” *Nature* 576 (7786): 293–300. https://doi.org/10.1038/s41586-019-1805-z.

MacKay, Matthew, Ebrahim Afshinnekoo, Jonathan Rub, Ciaran Hassan, Mihir Khunte, Nithyashri Baskaran, Bryan Owens, et al. 2020. “The Therapeutic Landscape for Cells Engineered with Chimeric Antigen Receptors.” *Nature Biotechnology* 38 (2): 233–44. https://doi.org/10.1038/s41587-019-0329-2.

Mackensen, Andreas, John B. A. G. Haanen, Christian Koenecke, Winfried Alsdorf, Eva Wagner-Drouet, Peter Borchmann, Daniel Heudobler, et al. 2023. “CLDN6-Specific CAR-T Cells plus Amplifying RNA Vaccine in Relapsed or Refractory Solid Tumors: The Phase 1 BNT211-01 Trial.” *Nature Medicine* 29 (11): 2844–53. https://doi.org/10.1038/s41591-023-02612-0.

Mackensen, Andreas, Fabian Müller, Dimitrios Mougiakakos, Sebastian Böltz, Artur Wilhelm, Michael Aigner, Simon Völkl, et al. 2022. “Anti-CD19 CAR T Cell Therapy for Refractory Systemic Lupus Erythematosus.” *Nature Medicine* 28 (10): 2124–32. https://doi.org/10.1038/s41591-022-02017-5.

Maher, John, Renier J. Brentjens, Gertrude Gunset, Isabelle Rivière, and Michel Sadelain. 2002. “Human T-Lymphocyte Cytotoxicity and Proliferation Directed by a Single Chimeric TCRzeta /CD28 Receptor.” *Nature Biotechnology* 20 (1): 70–75. https://doi.org/10.1038/nbt0102-70.

Mali, Prashant, Luhan Yang, Kevin M. Esvelt, John Aach, Marc Guell, James E. DiCarlo, Julie E. Norville, and George M. Church. 2013. “RNA-Guided Human Genome Engineering

via Cas9." *Science (New York, N.Y.)* 339 (6121): 823–26. https://doi.org/10.1126/science.1232033.
Malinin, Nikolay L., GaHyun Lee, Cicera R. Lazzarotto, Yichao Li, Zongli Zheng, Nhu T. Nguyen, Matthew Liebers, et al. 2021. "Defining Genome-Wide CRISPR–Cas Genome-Editing Nuclease Activity with GUIDE-Seq." *Nature Protocols* 16 (12): 5592–5615. https://doi.org/10.1038/s41596-021-00626-x.
Manguso, Robert T., Hans W. Pope, Margaret D. Zimmer, Flavian D. Brown, Kathleen B. Yates, Brian C. Miller, Natalie B. Collins, et al. 2017. "In Vivo CRISPR Screening Identifies Ptpn2 as a Cancer Immunotherapy Target." *Nature* 547 (7664): 413–18. https://doi.org/10.1038/nature23270.
Martin, Thomas, Saad Z. Usmani, Jesus G. Berdeja, Mounzer Agha, Adam D. Cohen, Parameswaran Hari, David Avigan, et al. 2023a. "Ciltacabtagene Autoleucel, an Anti-B-Cell Maturation Antigen Chimeric Antigen Receptor T-Cell Therapy, for Relapsed/Refractory Multiple Myeloma: CARTITUDE-1 2-Year Follow-Up." *Journal of Clinical Oncology: Official Journal of the American Society of Clinical Oncology* 41 (6): 1265–74. https://doi.org/10.1200/JCO.22.00842.
Maude, Shannon L., Theodore W. Laetsch, Jochen Buechner, Susana Rives, Michael Boyer, Henrique Bittencourt, Peter Bader, et al. 2018. "Tisagenlecleucel in Children and Young Adults with B-Cell Lymphoblastic Leukemia." *The New England Journal of Medicine* 378 (5): 439–48. https://doi.org/10.1056/NEJMoa1709866.
McCutcheon, Sean R., Adam M. Swartz, Michael C. Brown, Alejandro Barrera, Christian McRoberts Amador, Keith Siklenka, Lucas Humayun, et al. 2023. "Transcriptional and Epigenetic Regulators of Human CD8+ T Cell Function Identified through Orthogonal CRISPR Screens." *Nature Genetics* 55 (12): 2211–23. https://doi.org/10.1038/s41588-023-01554-0.
Menegatti, Silvia, Sheila Lopez-Cobo, Aurelien Sutra Del Galy, Jaime Fuentealba, Lisseth Silva, Laetitia Perrin, Sandrine Heurtebise-Chrétien, et al. 2024. "Ablation of FAS Confers Allogeneic CD3– CAR T Cells with Resistance to Rejection by T Cells and Natural Killer Cells." *Nature Biomedical Engineering* 8 (12): 1651–64. https://doi.org/10.1038/s41551-024-01282-8.
Milone, Michael C., and Una O'Doherty. 2018. "Clinical Use of Lentiviral Vectors." *Leukemia* 32 (7): 1529–41. https://doi.org/10.1038/s41375-018-0106-0.
Mirzaei, Hamid Reza, Hossein Pourghadamyari, Majid Rahmati, Abbas Mohammadi, Javid Sadri Nahand, Abbas Rezaei, Hamed Mirzaei, and Jamshid Hadjati. 2018. "Gene-Knocked out Chimeric Antigen Receptor (CAR) T Cells: Tuning up for the next Generation Cancer Immunotherapy." *Cancer Letters* 423 (June):95–104. https://doi.org/10.1016/j.canlet.2018.03.010.
Mitra, Aroshi, Amrita Barua, Luping Huang, Siddhartha Ganguly, Qin Feng, and Bin He. 2023. "From Bench to Bedside: The History and Progress of CAR T Cell Therapy." *Frontiers in Immunology* 14 (May). https://doi.org/10.3389/fimmu.2023.1188049.
Morgens, David W., Michael Wainberg, Evan A. Boyle, Oana Ursu, Carlos L. Araya, C. Kimberly Tsui, Michael S. Haney, et al. 2017. "Genome-Scale Measurement of off-Target Activity Using Cas9 Toxicity in High-Throughput Screens." *Nature Communications* 8 (May):15178. https://doi.org/10.1038/ncomms15178.
Mougiakakos, Dimitrios, Gerhard Krönke, Simon Völkl, Sascha Kretschmann, Michael Aigner, Soraya Kharboutli, Sebastian Böltz, Bernhard Manger, Andreas Mackensen, and Georg Schett. 2021. "CD19-Targeted CAR T Cells in Refractory Systemic Lupus Erythematosus." *The New England Journal of Medicine* 385 (6): 567–69. https://doi.org/10.1056/NEJMc2107725.
Müller, Fabian, Jule Taubmann, Laura Bucci, Artur Wilhelm, Christina Bergmann, Simon Völkl, Michael Aigner, et al. 2024. "CD19 CAR T-Cell Therapy in Autoimmune Disease - A Case Series with Follow-Up." *The New England Journal of Medicine* 390 (8): 687–700. https://doi.org/10.1056/NEJMoa2308917.
Munshi, Nikhil C., Larry D. Anderson, Nina Shah, Deepu Madduri, Jesús Berdeja, Sagar Lonial, Noopur Raje, et al. 2021a. "Idecabtagene Vicleucel in Relapsed and Refractory

Multiple Myeloma." *The New England Journal of Medicine* 384 (8): 705–16. https://doi.org/10.1056/NEJMoa2024850.

Neelapu, Sattva S., Frederick L. Locke, Nancy L. Bartlett, Lazaros J. Lekakis, David B. Miklos, Caron A. Jacobson, Ira Braunschweig, et al. 2017. "Axicabtagene Ciloleucel CAR T-Cell Therapy in Refractory Large B-Cell Lymphoma." *New England Journal of Medicine* 377 (26): 2531–44. https://doi.org/10.1056/NEJMoa1707447.

Nuñez, James K., Jin Chen, Greg C. Pommier, J. Zachery Cogan, Joseph M. Replogle, Carmen Adriaens, Gokul N. Ramadoss, et al. 2021. "Genome-Wide Programmable Transcriptional Memory by CRISPR-Based Epigenome Editing." *Cell* 184 (9): 2503-2519.e17. https://doi.org/10.1016/j.cell.2021.03.025.

Pacesa, Martin, Oana Pelea, and Martin Jinek. 2024. "Past, Present, and Future of CRISPR Genome Editing Technologies." *Cell* 187 (5): 1076–1100. https://doi.org/10.1016/j.cell.2024.01.042.

Pan, Deng, Aya Kobayashi, Peng Jiang, Lucas Ferrari de Andrade, Rong En Tay, Adrienne M. Luoma, Daphne Tsoucas, et al. 2018. "A Major Chromatin Regulator Determines Resistance of Tumor Cells to T Cell-Mediated Killing." *Science (New York, N.Y.)* 359 (6377): 770–75. https://doi.org/10.1126/science.aao1710.

Parker, Kevin R., Denis Migliorini, Eric Perkey, Kathryn E. Yost, Aparna Bhaduri, Puneet Bagga, Mohammad Haris, et al. 2020. "Single-Cell Analyses Identify Brain Mural Cells Expressing CD19 as Potential Off-Tumor Targets for CAR-T Immunotherapies." *Cell* 183 (1): 126-142.e17. https://doi.org/10.1016/j.cell.2020.08.022.

Patel, Shashank J., Neville E. Sanjana, Rigel J. Kishton, Arash Eidizadeh, Suman K. Vodnala, Maggie Cam, Jared J. Gartner, et al. 2017. "Identification of Essential Genes for Cancer Immunotherapy." *Nature* 548 (7669): 537–42. https://doi.org/10.1038/nature23477.

Perez, Caleb R., Andrea Garmilla, Avlant Nilsson, Hratch M. Baghdassarian, Khloe S. Gordon, Louise G. Lima, Blake E. Smith, Marcela V. Maus, Douglas A. Lauffenburger, and Michael E. Birnbaum. 2024. "Library-Based Single-Cell Analysis of CAR Signaling Reveals Drivers of in Vivo Persistence." bioRxiv. https://doi.org/10.1101/2024.04.29.591541.

Pierce, Sarah E., Jeffrey M. Granja, and William J. Greenleaf. 2021. "High-Throughput Single-Cell Chromatin Accessibility CRISPR Screens Enable Unbiased Identification of Regulatory Networks in Cancer." *Nature Communications* 12 (1): 2969. https://doi.org/10.1038/s41467-021-23213-w.

Prinzing, Brooke, Caitlin C. Zebley, Christopher T. Petersen, Yiping Fan, Alejandro Allo Anido, Zhongzhen Yi, Phuong Nguyen, et al. 2021. "Deleting DNMT3A in CAR T Cells Prevents Exhaustion and Enhances Antitumor Activity." *Science Translational Medicine* 13 (620): eabh0272. https://doi.org/10.1126/scitranslmed.abh0272.

Prommersberger, Sabrina, Michael Reiser, Julia Beckmann, Sophia Danhof, Maximilian Amberger, Patricia Quade-Lyssy, Hermann Einsele, Michael Hudecek, Halvard Bonig, and Zoltán Ivics. 2021. "CARAMBA: A First-in-Human Clinical Trial with SLAMF7 CAR-T Cells Prepared by Virus-Free Sleeping Beauty Gene Transfer to Treat Multiple Myeloma." *Gene Therapy* 28 (9): 560–71. https://doi.org/10.1038/s41434-021-00254-w.

Qi, Changsong, Jifang Gong, Jian Li, Dan Liu, Yanru Qin, Sai Ge, Miao Zhang, et al. 2022. "Claudin18.2-Specific CAR T Cells in Gastrointestinal Cancers: Phase 1 Trial Interim Results." *Nature Medicine* 28 (6): 1189–98. https://doi.org/10.1038/s41591-022-01800-8.

Rafiq, Sarwish, Christopher S. Hackett, and Renier J. Brentjens. 2020. "Engineering Strategies to Overcome the Current Roadblocks in CAR T Cell Therapy." *Nature Reviews. Clinical Oncology* 17 (3): 147–67. https://doi.org/10.1038/s41571-019-0297-y.

Rafiq, Sarwish, Oladapo O Yeku, Hollie J Jackson, Terence J Purdon, Dayenne G van Leeuwen, Dylan J Drakes, Mei Song, et al. 2018. "Targeted Delivery of a PD-1-Blocking scFv by CAR-T Cells Enhances Anti-Tumor Efficacy in Vivo." *Nature Biotechnology* 36 (9): 847–56. https://doi.org/10.1038/nbt.4195.

Ren, Jiangtao, Xuhua Zhang, Xiaojun Liu, Chongyun Fang, Shuguang Jiang, Carl H. June, and Yangbing Zhao. 2017. “A Versatile System for Rapid Multiplex Genome-Edited CAR T Cell Generation.” *Oncotarget* 8 (10): 17002–11. https://doi.org/10.18632/oncotarget.15218.

Replogle, Joseph M., Thomas M. Norman, Albert Xu, Jeffrey A. Hussmann, Jin Chen, J. Zachary Cogan, Elliott J. Meer, et al. 2020. “Combinatorial Single-Cell CRISPR Screens by Direct Guide RNA Capture and Targeted Sequencing.” *Nature Biotechnology* 38 (8): 954–61. https://doi.org/10.1038/s41587-020-0470-y.

Ridley, Anne J. 2006. “Rho GTPases and Actin Dynamics in Membrane Protrusions and Vesicle Trafficking.” *Trends in Cell Biology*, Membrane Dynamics, 16 (10): 522–29. https://doi.org/10.1016/j.tcb.2006.08.006.

Roddie, Claire, Karamjeet S. Sandhu, Eleni Tholouli, Aaron C. Logan, Paul Shaughnessy, Pere Barba, Armin Ghobadi, et al. 2024. “Obecabtagene Autoleucel in Adults with B-Cell Acute Lymphoblastic Leukemia.” *New England Journal of Medicine* 391 (23): 2219–30. https://doi.org/10.1056/NEJMoa2406526.

Rosenberg, S. A., B. S. Packard, P. M. Aebersold, D. Solomon, S. L. Topalian, S. T. Toy, P. Simon, M. T. Lotze, J. C. Yang, and C. A. Seipp. 1988. “Use of Tumor-Infiltrating Lymphocytes and Interleukin-2 in the Immunotherapy of Patients with Metastatic Melanoma. A Preliminary Report.” *The New England Journal of Medicine* 319 (25): 1676–80. https://doi.org/10.1056/NEJM198812223192527.

Rosenberg, S. A., P. Spiess, and R. Lafreniere. 1986. “A New Approach to the Adoptive Immunotherapy of Cancer with Tumor-Infiltrating Lymphocytes.” *Science (New York, N.Y.)* 233 (4770): 1318–21. https://doi.org/10.1126/science.3489291.

Rosenberg, Steven A., and Nicholas P. Restifo. 2015. “Adoptive Cell Transfer as Personalized Immunotherapy for Human Cancer.” *Science (New York, N.Y.)* 348 (6230): 62–68. https://doi.org/10.1126/science.aaa4967.

Roybal, Kole T., Levi J. Rupp, Leonardo Morsut, Whitney J. Walker, Krista A. McNally, Jason S. Park, and Wendell A. Lim. 2016. “Precision Tumor Recognition by T Cells With Combinatorial Antigen-Sensing Circuits.” *Cell* 164 (4): 770–79. https://doi.org/10.1016/j.cell.2016.01.011.

Rudd, C E, J M Trevillyan, J D Dasgupta, L L Wong, and S F Schlossman. 1988. “The CD4 Receptor Is Complexed in Detergent Lysates to a Protein-Tyrosine Kinase (Pp58) from Human T Lymphocytes.” *Proceedings of the National Academy of Sciences of the United States of America* 85 (14): 5190–94.

Rurik, Joel G., István Tombácz, Amir Yadegari, Pedro O. Méndez Fernández, Swapnil V. Shewale, Li Li, Toru Kimura, et al. 2022. “CAR T Cells Produced in Vivo to Treat Cardiac Injury.” *Science* 375 (6576): 91–96. https://doi.org/10.1126/science.abm0594.

Sadelain, Michel, Renier Brentjens, and Isabelle Rivière. 2013. “The Basic Principles of Chimeric Antigen Receptor Design.” *Cancer Discovery* 3 (4): 388–98. https://doi.org/10.1158/2159-8290.CD-12-0548.

Sahin, Ugur, Alexander Muik, Isabel Vogler, Evelyna Derhovanessian, Lena M. Kranz, Mathias Vormehr, Jasmin Quandt, et al. 2021. “BNT162b2 Vaccine Induces Neutralizing Antibodies and Poly-Specific T Cells in Humans.” *Nature* 595 (7868): 572–77. https://doi.org/10.1038/s41586-021-03653-6.

Salvador, Jesus M., Paul R. Mittelstadt, Tad Guszczynski, Terry D. Copeland, Hiroshi Yamaguchi, Ettore Appella, Albert J. Fornace, and Jonathan D. Ashwell. 2005. “Alternative P38 Activation Pathway Mediated by T Cell Receptor-Proximal Tyrosine Kinases.” *Nature Immunology* 6 (4): 390–95. https://doi.org/10.1038/ni1177.

Sánchez-Guijo, Fermín, Cristina Avendaño-Solá, Lina Badimón, Juan A. Bueren, Josep M. Canals, Joaquim Delgadillo, Julio Delgado, et al. 2023. “Role of Hospital Exemption in Europe: Position Paper from the Spanish Advanced Therapy Network (TERAV).” *Bone Marrow Transplantation* 58 (6): 727–28. https://doi.org/10.1038/s41409-023-01962-0.

Sanson, Kendall R., Ruth E. Hanna, Mudra Hegde, Katherine F. Donovan, Christine Strand, Meagan E. Sullender, Emma W. Vaimberg, et al. 2018. “Optimized Libraries for

CRISPR-Cas9 Genetic Screens with Multiple Modalities." *Nature Communications* 9 (1): 5416. https://doi.org/10.1038/s41467-018-07901-8.
Schmidt, Ralf, Zachary Steinhart, Madeline Layeghi, Jacob W. Freimer, Raymund Bueno, Vinh Q. Nguyen, Franziska Blaeschke, Chun Jimmie Ye, and Alexander Marson. 2022. "CRISPR Activation and Interference Screens Decode Stimulation Responses in Primary Human T Cells." *Science* 375 (6580): eabj4008. https://doi.org/10.1126/science.abj4008.
Schmidt, Ralf, Carl C. Ward, Rama Dajani, Zev Armour-Garb, Mineto Ota, Vincent Allain, Rosmely Hernandez, et al. 2023. "Base-Editing Mutagenesis Maps Alleles to Tune Human T Cell Functions." *Nature*, December, 1–8. https://doi.org/10.1038/s41586-023-06835-6.
Schumann, Kathrin, Steven Lin, Eric Boyer, Dimitre R. Simeonov, Meena Subramaniam, Rachel E. Gate, Genevieve E. Haliburton, et al. 2015. "Generation of Knock-in Primary Human T Cells Using Cas9 Ribonucleoproteins." *Proceedings of the National Academy of Sciences of the United States of America* 112 (33): 10437–42. https://doi.org/10.1073/pnas.1512503112.
Schuster, Stephen J., Michael R. Bishop, Constantine S. Tam, Edmund K. Waller, Peter Borchmann, Joseph P. McGuirk, Ulrich Jäger, et al. 2019. "Tisagenlecleucel in Adult Relapsed or Refractory Diffuse Large B-Cell Lymphoma." *The New England Journal of Medicine* 380 (1): 45–56. https://doi.org/10.1056/NEJMoa1804980.
Shah, Bijal D., Armin Ghobadi, Olalekan O. Oluwole, Aaron C. Logan, Nicolas Boissel, Ryan D. Cassaday, Thibaut Leguay, et al. 2021. "KTE-X19 for Relapsed or Refractory Adult B-Cell Acute Lymphoblastic Leukaemia: Phase 2 Results of the Single-Arm, Open-Label, Multicentre ZUMA-3 Study." *Lancet (London, England)* 398 (10299): 491–502. https://doi.org/10.1016/S0140-6736(21)01222-8.
Shah, Nirali N., and Terry J. Fry. 2019. "Mechanisms of Resistance to CAR T Cell Therapy." *Nature Reviews Clinical Oncology*, March. https://doi.org/10.1038/s41571-019-0184-6.
Shalem, Ophir, Neville E. Sanjana, and Feng Zhang. 2015. "High-Throughput Functional Genomics Using CRISPR-Cas9." *Nature Reviews. Genetics* 16 (5): 299–311. https://doi.org/10.1038/nrg3899.
Shi, Long, Tongyu Meng, Zhilong Zhao, Jinsheng Han, Wei Zhang, Fei Gao, and Jianhui Cai. 2017. "CRISPR Knock out CTLA-4 Enhances the Anti-Tumor Activity of Cytotoxic T Lymphocytes." *Gene* 636 (December):36–41. https://doi.org/10.1016/j.gene.2017.09.010.
Shifrut, Eric, Julia Carnevale, Victoria Tobin, Theodore L. Roth, Jonathan M. Woo, Christina T. Bui, P. Jonathan Li, Morgan E. Diolaiti, Alan Ashworth, and Alexander Marson. 2018. "Genome-Wide CRISPR Screens in Primary Human T Cells Reveal Key Regulators of Immune Function." *Cell* 175 (7): 1958-1971.e15. https://doi.org/10.1016/j.cell.2018.10.024.
Short, Lauralie, Robert A. Holt, Pieter R. Cullis, and Laura Evgin. 2024. "Direct in Vivo CAR T Cell Engineering." *Trends in Pharmacological Sciences* 45 (5): 406–18. https://doi.org/10.1016/j.tips.2024.03.004.
Si, Xiaohui, Lu Xiao, Christine E. Brown, and Dongrui Wang. 2022. "Preclinical Evaluation of CAR T Cell Function: In Vitro and In Vivo Models." *International Journal of Molecular Sciences* 23 (6): 3154. https://doi.org/10.3390/ijms23063154.
Smith-Garvin, Jennifer E., Gary A. Koretzky, and Martha S. Jordan. 2009. "T Cell Activation." *Annual Review of Immunology* 27:591–619. https://doi.org/10.1146/annurev.immunol.021908.132706.
Srivastava, Shivani, and Stanley R. Riddell. 2015. "Engineering CAR-T Cells: Design Concepts." *Trends in Immunology* 36 (8): 494–502. https://doi.org/10.1016/j.it.2015.06.004.
Stadtmauer, Edward A., Joseph A. Fraietta, Megan M. Davis, Adam D. Cohen, Kristy L. Weber, Eric Lancaster, Patricia A. Mangan, et al. 2020. "CRISPR-Engineered T Cells in

Patients with Refractory Cancer." *Science* 367 (6481): eaba7365. https://doi.org/10.1126/science.aba7365.

Stemer, Gunar, Tarquin Mittermayr, Petra Schnell-Inderst, and Claudia Wild. 2024. "Costs, Challenges and Opportunities of Decentralised Chimeric Antigen Receptor T-Cell Production: A Literature Review and Clinical Experts' Interviews." *European Journal of Hospital Pharmacy: Science and Practice*, August, ejhpharm-2024-004130. https://doi.org/10.1136/ejhpharm-2024-004130.

Sterner, Robert C., and Rosalie M. Sterner. 2021. "CAR-T Cell Therapy: Current Limitations and Potential Strategies." *Blood Cancer Journal* 11 (4): 1–11. https://doi.org/10.1038/s41408-021-00459-7.

Sutra Del Galy, Aurélien, Silvia Menegatti, Jaime Fuentealba, Francesca Lucibello, Laetitia Perrin, Julie Helft, Aurélie Darbois, et al. 2021. "In Vivo Genome-Wide CRISPR Screens Identify SOCS1 as Intrinsic Checkpoint of CD4+ TH1 Cell Response." *Science Immunology* 6 (66): eabe8219. https://doi.org/10.1126/sciimmunol.abe8219.

Svoboda, Jakub, Daniel J Landsburg, Sunita Dwivedy Nasta, Stefan K. Barta, Elise A. Chong, Michael J. Lariviere, Joanne Shea, et al. 2024. "Safety and Efficacy of Armored huCART19-IL18 in Patients with Relapsed/Refractory Lymphomas That Progressed after Anti-CD19 CAR T Cells." *Journal of Clinical Oncology* 42 (16_suppl): 7004–7004. https://doi.org/10.1200/JCO.2024.42.16_suppl.7004.

Tang, Na, Chen Cheng, Xingying Zhang, Miaomiao Qiao, Na Li, Wei Mu, Xiao-Fei Wei, Weidong Han, and Haoyi Wang. 2020. "TGF-β Inhibition via CRISPR Promotes the Long-Term Efficacy of CAR T Cells against Solid Tumors." *JCI Insight* 5 (4): e133977, 133977. https://doi.org/10.1172/jci.insight.133977.

Thomas, E. D., H. L. Lochte, W. C. Lu, and J. W. Ferrebee. 1957. "Intravenous Infusion of Bone Marrow in Patients Receiving Radiation and Chemotherapy." *The New England Journal of Medicine* 257 (11): 491–96. https://doi.org/10.1056/NEJM195709122571102.

Tieu, Victor, Elena Sotillo, Jeremy R. Bjelajac, Crystal Chen, Meena Malipatlolla, Justin A. Guerrero, Peng Xu, et al. 2024. "A Versatile CRISPR-Cas13d Platform for Multiplexed Transcriptomic Regulation and Metabolic Engineering in Primary Human T Cells." *Cell* 187 (5): 1278-1295.e20. https://doi.org/10.1016/j.cell.2024.01.035.

Tiriveedhi, Venkataswarup, Michael T. Ivy, Elbert L. Myles, Roy Zent, Jeffrey C. Rathmell, and Jens Titze. 2021. "Ex Vivo High Salt Activated Tumor-Primed CD4+T Lymphocytes Exert a Potent Anti-Cancer Response." *Cancers* 13 (7): 1690. https://doi.org/10.3390/cancers13071690.

Tokarew, Nicholas, Justyna Ogonek, Stefan Endres, Michael von Bergwelt-Baildon, and Sebastian Kobold. 2019. "Teaching an Old Dog New Tricks: Next-Generation CAR T Cells." *British Journal of Cancer* 120 (1): 26–37. https://doi.org/10.1038/s41416-018-0325-1.

Tsimberidou, Apostolia-Maria, Karlyle Van Morris, Henry Hiep Vo, Stephen Eck, Yu-Feng Lin, Jorge Mauricio Rivas, and Borje S. Andersson. 2021. "T-Cell Receptor-Based Therapy: An Innovative Therapeutic Approach for Solid Tumors." *Journal of Hematology & Oncology* 14 (1): 102. https://doi.org/10.1186/s13045-021-01115-0.

Turchiano, Giandomenico, Geoffroy Andrieux, Julia Klermund, Georges Blattner, Valentina Pennucci, Melina el Gaz, Gianni Monaco, et al. 2021. "Quantitative Evaluation of Chromosomal Rearrangements in Gene-Edited Human Stem Cells by CAST-Seq." *Cell Stem Cell* 28 (6): 1136-1147.e5. https://doi.org/10.1016/j.stem.2021.02.002.

Ureña-Bailén, Guillermo, Andrés Lamsfus-Calle, Alberto Daniel-Moreno, Janani Raju, Patrick Schlegel, Christian Seitz, Daniel Atar, Justin S Antony, Rupert Handgretinger, and Markus Mezger. 2020. "CRISPR/Cas9 Technology: Towards a New Generation of Improved CAR-T Cells for Anticancer Therapies." *Briefings in Functional Genomics* 19 (3): 191–200. https://doi.org/10.1093/bfgp/elz039.

Vigil, Dominico, Jacqueline Cherfils, Kent L. Rossman, and Channing J. Der. 2010. "Ras Superfamily GEFs and GAPs: Validated and Tractable Targets for Cancer Therapy?" *Nature Reviews. Cancer* 10 (12): 842–57. https://doi.org/10.1038/nrc2960.

Waldman, Alex D., Jill M. Fritz, and Michael J. Lenardo. 2020. “A Guide to Cancer Immunotherapy: From T Cell Basic Science to Clinical Practice.” *Nature Reviews Immunology* 20 (11): 651–68. https://doi.org/10.1038/s41577-020-0306-5.

Walsh, Zachary H., Parin Shah, Neeharika Kothapalli, Shivem B. Shah, Gergo Nikolenyi, D. Zack Brodtman, Giuseppe Leuzzi, et al. 2024. “Mapping Variant Effects on Anti-Tumor Hallmarks of Primary Human T Cells with Base-Editing Screens.” *Nature Biotechnology*, May. https://doi.org/10.1038/s41587-024-02235-x.

Walton, R. T., K. A. Christie, Madelynn N. Whittaker, and B. P. Kleinstiver. 2020. “Unconstrained Genome Targeting with Near-PAMless Engineered CRISPR-Cas9 Variants.” *Science (New York, N.Y.)* 368 (6488): 290–96. https://doi.org/10.1126/science.aba8853.

Walton, Russell T., Yue Qin, and Paul C. Blainey. 2024. “CROPseq-Multi: A Versatile Solution for Multiplexed Perturbation and Decoding in Pooled CRISPR Screens.” *bioRxiv: The Preprint Server for Biology*, March, 2024.03.17.585235. https://doi.org/10.1101/2024.03.17.585235.

Wang, Dongrui, Briana C. Prager, Ryan C. Gimple, Brenda Aguilar, Darya Alizadeh, Hongzhen Tang, Deguan Lv, et al. 2021. “CRISPR Screening of CAR T Cells and Cancer Stem Cells Reveals Critical Dependencies for Cell-Based Therapies.” *Cancer Discovery* 11 (5): 1192–1211. https://doi.org/10.1158/2159-8290.CD-20-1243.

Wang, Tim, Jenny J. Wei, David M. Sabatini, and Eric S. Lander. 2014. “Genetic Screens in Human Cells Using the CRISPR/Cas9 System.” *Science (New York, N.Y.)* 343 (6166): 80–84. https://doi.org/10.1126/science.1246981.

Wang, Valentine, Mélanie Gauthier, Véronique Decot, Loïc Reppel, and Danièle Bensoussan. 2023a. “Systematic Review on CAR-T Cell Clinical Trials Up to 2022: Academic Center Input.” *Cancers* 15 (4): 1003. https://doi.org/10.3390/cancers15041003.

Wang, Xiuyan, and Isabelle Rivière. 2016. “Clinical Manufacturing of CAR T Cells: Foundation of a Promising Therapy.” *Molecular Therapy - Oncolytics* 3 (January). https://doi.org/10.1038/mto.2016.15.

Ward, S. G., and D. A. Cantrell. 2001. “Phosphoinositide 3-Kinases in T Lymphocyte Activation.” *Current Opinion in Immunology* 13 (3): 332–38. https://doi.org/10.1016/s0952-7915(00)00223-5.

Webber, Beau R., Cara-lin Lonetree, Mitchell G. Kluesner, Matthew J. Johnson, Emily J. Pomeroy, Miechaleen D. Diers, Walker S. Lahr, et al. 2019. “Highly Efficient Multiplex Human T Cell Engineering without Double-Strand Breaks Using Cas9 Base Editors.” *Nature Communications* 10 (1): 5222. https://doi.org/10.1038/s41467-019-13007-6.

Weber, Evan W., Kevin R. Parker, Elena Sotillo, Rachel C. Lynn, Hima Anbunathan, John Lattin, Zinaida Good, et al. 2021. “Transient ‘Rest’ Restores Functionality in Exhausted CAR-T Cells via Epigenetic Remodeling.” *Science (New York, N.Y.)* 372 (6537): eaba1786. https://doi.org/10.1126/science.aba1786.

Wiede, Florian, Kun-Hui Lu, Xin Du, Shuwei Liang, Katharina Hochheiser, Garron T. Dodd, Pei K. Goh, et al. 2020. “PTPN2 Phosphatase Deletion in T Cells Promotes Anti-Tumour Immunity and CAR T-Cell Efficacy in Solid Tumours.” *The EMBO Journal* 39 (2): e103637. https://doi.org/10.15252/embj.2019103637.

Xiang, Minghua, Huayi Li, Yuanyuan Zhan, Ding Ma, Qinglei Gao, and Yong Fang. 2024. “Functional CRISPR Screens in T Cells Reveal New Opportunities for Cancer Immunotherapies.” *Molecular Cancer* 23 (1): 73. https://doi.org/10.1186/s12943-024-01987-z.

Ye, Lupeng, Jonathan J. Park, Matthew B. Dong, Quanjun Yang, Ryan D. Chow, Lei Peng, Yaying Du, et al. 2019. “In Vivo CRISPR Screening in CD8 T Cells with AAV–Sleeping Beauty Hybrid Vectors Identifies Membrane Targets for Improving Immunotherapy for Glioblastoma.” *Nature Biotechnology* 37 (11): 1302–13. https://doi.org/10.1038/s41587-019-0246-4.

Ye, Lupeng, Jonathan J. Park, Lei Peng, Quanjun Yang, Ryan D. Chow, Matthew B. Dong, Stanley Z. Lam, et al. 2022. “A Genome-Scale Gain-of-Function CRISPR Screen in CD8 T Cells Identifies Proline Metabolism as a Means to Enhance CAR-T Therapy.”

Cell Metabolism, March, S1550413122000535. https://doi.org/10.1016/j.cmet.2022.02.009.

Yi, Fei, Tal Cohen, Natalie Zimmerman, Friederike Dündar, Paul Zumbo, Razan Eltilib, Erica J. Brophy, et al. 2024. “CAR-Engineered Lymphocyte Persistence Is Governed by a FAS Ligand/FAS Auto-Regulatory Circuit.” bioRxiv. https://doi.org/10.1101/2024.02.26.582108.

Yong, Carmen S. M., Valerie Dardalhon, Christel Devaud, Naomi Taylor, Phillip K. Darcy, and Michael H. Kershaw. 2017. “CAR T-Cell Therapy of Solid Tumors.” *Immunology and Cell Biology* 95 (4): 356–63. https://doi.org/10.1038/icb.2016.128.

Yoshikawa, Toshiaki, Zhiwen Wu, Satoshi Inoue, Hitomi Kasuya, Hirokazu Matsushita, Yusuke Takahashi, Hiroaki Kuroda, Waki Hosoda, Shiro Suzuki, and Yuki Kagoya. 2022. “Genetic Ablation of PRDM1 in Antitumor T Cells Enhances Therapeutic Efficacy of Adoptive Immunotherapy.” *Blood* 139 (14): 2156–72. https://doi.org/10.1182/blood.2021012714.

Zhang, W., J. Sloan-Lancaster, J. Kitchen, R. P. Trible, and L. E. Samelson. 1998. “LAT: The ZAP-70 Tyrosine Kinase Substrate That Links T Cell Receptor to Cellular Activation.” *Cell* 92 (1): 83–92. https://doi.org/10.1016/s0092-8674(00)80901-0.

Zhang, Xingying, Chenze Zhang, Miaomiao Qiao, Chen Cheng, Na Tang, Shan Lu, Wen Sun, et al. 2022. “Depletion of BATF in CAR-T Cells Enhances Antitumor Activity by Inducing Resistance against Exhaustion and Formation of Central Memory Cells.” *Cancer Cell* 40 (11): 1407-1422.e7. https://doi.org/10.1016/j.ccell.2022.09.013.

Zhang, Yongping, Xingying Zhang, Chen Cheng, Wei Mu, Xiaojuan Liu, Na Li, Xiaofei Wei, Xiang Liu, Changqing Xia, and Haoyi Wang. 2017. “CRISPR-Cas9 Mediated LAG-3 Disruption in CAR-T Cells.” *Frontiers of Medicine* 11 (4): 554–62. https://doi.org/10.1007/s11684-017-0543-6.

Zhou, Peipei, Hao Shi, Hongling Huang, Xiang Sun, Sujing Yuan, Nicole M. Chapman, Jon P. Connelly, et al. 2023. “Single-Cell CRISPR Screens in Vivo Map T Cell Fate Regulomes in Cancer.” *Nature* 624 (7990): 154–63. https://doi.org/10.1038/s41586-023-06733-x.

Zou, Fan, Lijuan Lu, Jun Liu, Baijin Xia, Wanying Zhang, Qifei Hu, Weiwei Liu, et al. 2019. “Engineered Triple Inhibitory Receptor Resistance Improves Anti-Tumor CAR-T Cell Performance via CD56.” *Nature Communications* 10 (1): 4109. https://doi.org/10.1038/s41467-019-11893-4.

EUGENIA PANKEVICH

Scientist | Technology developer

epankevich @ outlook.com
https://www.linkedin.com/in/eugeniapankevich/

HARD SKILLS

Wet-lab skills

Cell culture: cell lines and primary cells (T cells, astrocytes), **10** engineered cell lines with knockouts and integrations, maintaining up to **100** billion cells in up to **40** liters of culture medium simultaneously; multicolor flow cytometry with up to **14** colors; sorted **50** billion cells. Animal handling: **3** mouse models of leukemia and solid tumors. Molecular biology: nucleic acids extraction, PCR, large-scale cloning: **224** ORFs of human genes, **176** single gRNAs, libraries of >**75000** gRNAs. Next-generation sequencing: >**900** CRISPR screening libraries, **127** bulk and single-cell RNA-seq samples. Gene engineering; lentiviral vector construction, CRISPR-mediated knockout and base editing, genome-wide screens, RNA interference.

Programming & Bioinformatics

R, Python, bash, git
Analysis of CRISPR gene editing, CRISPR screens, RNA-sequencing, tumor clonal structure

Selected software

Molecular cloning Geneious, SnapGene
Flow cytometry FlowJo
Graphics ggplot2, matplotlib, Adobe Illustrator

PATENTS

Inventor: co-developed a patent on optimized T cell immunotherapy (WO2024121426A1)

SOFT SKILLS

Project management Notion, Jira
Teamwork in project-based and matrixed structure
Training of **2** students, **6** technicians, **1** staff scientist

ADDITIONAL EDUCATION

- LBG **Leadership** Development Program for Junior Group Leaders
- **Entrepreneurship** courses: LBG Innovator's Road Program, XBIO Biotech business course

FORMAL EDUCATION

2019 – present: **PhD Student – Malignant Diseases**
CeMM Research Center for Molecular Medicine of the Austrian Academy of Sciences; Medical University of Vienna, Austria

2012 – 2018: **Master of Science – Bioengineering and Bioinformatics**
Faculty of Bioengineering and Bioinformatics at Lomonosov Moscow State University, Russia (*magna cum laude*)

2008 – 2012: **High school – Chemistry and Biology**
Specialized Educational Scientific Center of the Ural Federal University, Russia

EXPERIENCE

2019 – present. **Predoctoral Fellow** | **Bock Lab, CeMM**, Vienna, Austria
Engineering next-generation T cell therapies through CRISPR screens.
Novel platform for genome engineering in primary cells. Systematic identification of genetic perturbations to enhance CAR T cells using *in vitro* and *in vivo* screens

2018 – 2019. **Guest Scientist** | **Bock Lab, CeMM**, Vienna, Austria

2017 – 2018. **Diploma Student** | **Deplancke Lab, EPFL**, Lausanne, Switzerland
Development of SMILE-seq (microfluidics-based method to map protein-DNA binding sites) to test methylation specificity of human transcription factors

2016 – 2017. **Bioinformatician | BostonGene**, USA (remote)
Integration of methods for copy number alterations and clonal structure analysis in tumor into the pipeline to develop therapy strategies

2017 (3 months). **Intern | Stark Lab, IMP Vienna BioCenter**, Vienna, Austria
Assessing the role of human cofactors in transcription genome-wide; optimization of STAP-seq protocol in human cells

2012 – 2016. **Student Researcher** | **Belozersky Institute**, Moscow, Russia
Sergeeva Group of system biology of lipids: mRNA degradation in glial cells
Evstafieva Lab of molecular biology of gene: TP53I3 function in apoptosis

SELECTED PUBLICATIONS

Datlinger P & Pankevich EV & Arnold C (shared first authors), … , Bock C. **Systematic discovery of CRISPR-boosted CAR T cell immunotherapies** (in revision)
Pankevich EV, Bock C. **Single-cell CRISPR screening in mouse brain**. *Nature Protocols (News & Views)* 2025. doi:10.1038/s41596-024-01128-2
Hanzl A, …, Pankevich EV, … , Winter GE. **E3-Specific Degrader Discovery by Dynamic Tracing of Substrate Receptor Abundance**. *J Am Chem Soc* 2023. doi:10.1021/jacs.2c10784
Turelli P, … , Pankevich EV, Deplancke B, Busskamp V, Trono D. **Primate-restricted KRAB zinc finger proteins and target retrotransposons control gene expression in human neurons.** *Science Advances* 2020. doi:10.1126/sciadv.aba3200
Chen W & Schwalie PC, Pankevich EV, … , Deplancke B. **ZFP30 promotes adipogenesis through KAP1-mediated Pparg activation.** *Nature Communications* 2019. doi: 10.1038/s41467-019-09803-9

CONFERENCES

2025 SITC Cell Therapy for Solid Tumors, San Diego, USA | Selected talk
2024 European CAR T cell meeting, Valencia, Spain | Poster
2024 CAR-TCR Summit London, London, UK | Poster
2016 EPFL Summer School Conference, Lausanne, Switzerland | Poster
2015 LUMC Bioinformatics School, Leiden, Netherlands | Talk
2015 Basel Life Science Week, Basel, Switzerland | Poster